frontiers | Research Topics

Abiotic stress and physiological adaptive strategies of insects

Edited by
Seema Ramniwas, Divya Singh, Girish Kumar and Pankaj Kumar Tyagi

Published in
Frontiers in Physiology

ISSN 1664-8714
ISBN 978-2-8325-2462-6
DOI 10.3389/978-2-8325-2462-6

About Frontiers

Frontiers is more than just an open access publisher of scholarly articles: it is a pioneering approach to the world of academia, radically improving the way scholarly research is managed. The grand vision of Frontiers is a world where all people have an equal opportunity to seek, share and generate knowledge. Frontiers provides immediate and permanent online open access to all its publications, but this alone is not enough to realize our grand goals.

Frontiers journal series

The Frontiers journal series is a multi-tier and interdisciplinary set of open-access, online journals, promising a paradigm shift from the current review, selection and dissemination processes in academic publishing. All Frontiers journals are driven by researchers for researchers; therefore, they constitute a service to the scholarly community. At the same time, the *Frontiers journal series* operates on a revolutionary invention, the tiered publishing system, initially addressing specific communities of scholars, and gradually climbing up to broader public understanding, thus serving the interests of the lay society, too.

Dedication to quality

Each Frontiers article is a landmark of the highest quality, thanks to genuinely collaborative interactions between authors and review editors, who include some of the world's best academicians. Research must be certified by peers before entering a stream of knowledge that may eventually reach the public - and shape society; therefore, Frontiers only applies the most rigorous and unbiased reviews. Frontiers revolutionizes research publishing by freely delivering the most outstanding research, evaluated with no bias from both the academic and social point of view. By applying the most advanced information technologies, Frontiers is catapulting scholarly publishing into a new generation.

What are Frontiers Research Topics?

Frontiers Research Topics are very popular trademarks of the *Frontiers journals series*: they are collections of at least ten articles, all centered on a particular subject. With their unique mix of varied contributions from Original Research to Review Articles, Frontiers Research Topics unify the most influential researchers, the latest key findings and historical advances in a hot research area.

Find out more on how to host your own Frontiers Research Topic or contribute to one as an author by contacting the Frontiers editorial office: frontiersin.org/about/contact

Abiotic stress and physiological adaptive strategies of insects

Topic editors

Seema Ramniwas — Chandigarh University, India

Divya Singh — Chandigarh University, India

Girish Kumar — Rochester Institute of Technology, United States

Pankaj Kumar Tyagi — Noida Institute of Engineering and Technology (NIET), India

Citation

Ramniwas, S., Singh, D., Kumar, G., Tyagi, P. K., eds. (2023). *Abiotic stress and physiological adaptive strategies of insects*. Lausanne: Frontiers Media SA.

doi: 10.3389/978-2-8325-2462-6

Table of contents

frontiers | Frontiers in Physiology

TYPE Editorial
PUBLISHED 04 May 2023
DOI 10.3389/fphys.2023.1210052

OPEN ACCESS

EDITED AND REVIEWED BY
Sylvia Anton,
Institut National de Recherche pour l'Agriculture, l'Alimentation et l'Environnement (INRAE), France

*CORRESPONDENCE
Girish Kumar,
girishkumar.nio@gmail.com

RECEIVED 21 April 2023
ACCEPTED 28 April 2023
PUBLISHED 04 May 2023

CITATION
Ramniwas S, Tyagi PK, Sharma A and Kumar G (2023), Editorial: Abiotic stress and physiological adaptive strategies of insects.
Front. Physiol. 14:1210052.
doi: 10.3389/fphys.2023.1210052

Editorial: Abiotic stress and physiological adaptive strategies of insects

Seema Ramniwas[1], Pankaj Kumar Tyagi[2], Aanchal Sharma[1] and Girish Kumar[3]*

[1]University Center for Research and Development, Chandigarh University, Mohali, India, [2]Noida Institute of Engineering and Technology (NIET), Noida, India, [3]The Gosnell School of Life Sciences, Rochester Institute of Technology, Rochester, NY, United States

KEYWORDS

abiotic stress, insect, physiology, climate change, adaptation

Editorial on the Research Topic
Abiotic stress and physiological adaptive strategies of insects

Abiotic stress, such as extreme temperatures, hypoxia, or nutrient deficiencies, is an inherent part of every ecosystem and can have a range of impacts on insects. These stresses can affect the behavior, development, reproduction, and survival of insect populations, potentially altering the balance of predator-prey relationships and disrupting ecosystem functions. In response to threseese stresses, insects may exhibit physiological, biochemical, or behavioral adaptations to cope with adverse conditions, but if the stress is severe or prolonged, it can lead to population declines or even extinctions. Therefore, understanding the strategies employed by insects to respond to these challenges is crucial to predict and mitigate the impact of climate change on insect populations and the ecosystems they inhabit. By gaining insight into how insects respond to diverse abiotic stresses, we can develop effective conservation strategies to protect insect populations and maintain ecosystem health.

This Research Topic features ten research articles resulting from studies conducted in four different countries (China, India, Mexico, and United States), demonstrating the significance of collaborative science. The published articles add to the expanding literature on the physiological adaptations of insects in response to diverse abiotic stresses and provides valuable insights and knowledge that can inform future research in this area and help develop effective strategies for the conservation of insect populations in the face of climate change.

Temperature is one of the most stressful abiotic pressures. Exposure to elevated temperatures have been observed to negatively affect insect growth and development, leading to reduced fecundity, longevity, and dispersal (Ramniwas and Kumar, 2019). The study investigating the fruit fly genus *Anastrepha*, including species such as *A. ludens*, *A. obliqua*, *A. striata*, and *A. serpentine*, has revealed that lifespan can vary among different species even when exposed to the same constant temperature Guillén et al. Interestingly, the study discovered that *A. obliqua*, which typically thrives in hot environments, exhibited an unexpected cold hardiness. Furthermore, the study found that thermal stress could affect the lifespan of male and female insects differently.

Even brief periods of heat exposure can significantly impact reproductive processes and fertility, as reported by Walsh et al. (2021). This assertion is reinforced by the work

of Li et al. in their examination of the fruit fly *Zeugodacus tau*. Their research revealed that short-term exposure to high temperatures (34°C–44°C) for only 12 h led to changes in the mating behavior, antioxidant defence, and detoxifying enzymes of fruit flies in a sex-specific manner. These findings could have significant ecological implications for the survival, reproduction, and operational sex ratio of populations experiencing heat stress.

The impact of artificial light at night (ALAN) on biodiversity and ecosystem processes is gaining recognition as a significant threat apart from thermal stress (Sanders et al., 2021). ALAN has been suggested as a driver of insect declines (Grubisic et al., 2018; Owens et al., 2020), as it has diverse negative effects on insects throughout their life-cycles, including reduced adult activity, increased predation, and disrupted reproduction (Owens and Lewis, 2018; Boyes et al., 2021). Jiang et al. investigated the effects of ALAN on the locomotion and oviposition of *Dastarcus helophoroides*. The study revealed a decrease in the egg-laying capacity and locomotor activity of *D. helophoroides* under bright artificial light exposure (1–100 lx) at night.

Heat shock proteins (Hsps) act as molecular chaperones that respond to both biotic and abiotic stressors. Investigating the correlation between thermal acclimation and the expression of specific Hsps is crucial for gaining a deeper understanding of the molecular mechanisms involved in the heat response. Quan et al. conducted a study where they subjected *Ostrinia furnacalis*, the Asian corn borer, to temperatures of 33°C and 43°C to evaluate the expression of particular Hsps. They observed a significant upregulation of Hsp70 and Hsp90 transcripts within one to 2 h of sustained heat stress at 43°C, indicating a quick onset of these Hsps under extreme thermal stress. In a separate study, Barman et al. examined how *Bemisia tabaci*, the whitefly, expresses Hsps when exposed to different temperature conditions. The study showed that Hsp70 expression was induced by both cold (12°C) and hot (44°C) temperatures, suggesting its role in adapting to both heat and cold. Moreover, Hsp40 transcript levels were significantly upregulated under extreme temperature conditions, with a higher expression at 44°C, indicating a possible role in heat adaptation for *B. tabaci*.

Several studies have found a positive association between higher levels of Hsps and an increase in thermotolerance in organisms. However, Bowler (2005) has noted that the expression of Hsps varies between populations acclimated to different thermal histories. King and Stillman conducted a study on larval caddisflies (*Dicosmoecus gilvipes*) from three different eco-regions (mountain, valley, and coast) and exposed them to current and future summertime temperatures. The results indicated that there were population-specific patterns of gene expression in response to controlled and daily warming conditions, which suggests that local acclimatization or adaptation may differentiate populations. Nevertheless, the similarity in responses to extreme temperatures across populations indicates that the response to thermal stress is constrained or channeled, as highlighted in King and Stillman's study.

Despite the potential for adverse effects such as environmental contamination, insecticide resistance, and threats to human health, the primary method for managing insect pests is the use of synthetic chemical insecticides. Insects adapt to insecticides by modulating their gene expression, emphasizing the need to investigate the molecular basis of this adaptation to develop alternative control methods. Li et al. explored the expression of five chitinase-like proteins (ApIDGF, ApCht3, ApCht7, ApCht10, and ApENGase) in pea aphids (*Acyrthosiphon pisum*) exposed to various abiotic stresses, including temperature, insecticides, and 20-hydroxyecdysone (20E) stress. The study found that the expression of these five genes was differentially regulated by different stresses. For instance, ApCht7 expression was upregulated at low temperatures (10°C), while insecticide exposure (imidacloprid) downregulated the expression of all five genes. These findings provide insight into the role of chitinase-like proteins in abiotic stress management and can be beneficial in managing pea aphids under multiple stresses. In another study, Khalid et al. investigated the effect of cyromazine, a bio-rational insecticide, on the germ cells of *Drosophila*. The study suggested that cyromazine impacts the ecdysone signaling pathway, leading to a decrease in the number of germ cells. This highlights the ability of chemical insecticides to interfere with the biochemical and reproductive pathways of insects. In an effort to replace or decrease the use of chemical insecticides, recent research has focused on developing alternative control methods. Asad et al. examined the efficacy of a CRISPR/Cas9-mediated gene-drive construct for *Plutella xylostella*, a highly-destructive lepidopteran pest. The genetically modified construct had high gene-drive efficiency and could transmit desired traits to the pest's offspring, effectively controlling pests of cruciferous crops. The study suggests that it is possible to develop highly effective gene-edited constructs for other destructive pest species related to *P. xylostella*.

Fish often encounter hypoxia, a condition of insufficient oxygen in the cell, which can have adverse effects on their survival. To cope with this challenge, fishes have developed versatile mechanisms to acclimate to oxygen deficiency in their habitats (Mandic et al., 2009). Chang et al. investigated the molecular mechanism underlying the acclimation response to hypoxia in *Litopenaeus vannamei*, which is one of the most widely cultivated shrimp species worldwide. Their study used quantitative real-time PCR analysis and revealed differential expression of hemocyanin, chitinase, heat shock protein 90 (Hsp90), programmed death protein, and glycogen Phosphorylase, suggesting their role in hypoxia acclimation. The findings of this study can enhance the overall understanding of hypoxic stress in *L. vannamei* and the identified differentially expressed proteins could be utilized to support breeding programs for developing new strains of *L. vannamei* with enhanced tolerance to hypoxia.

In conclusion, Abiotic factors like temperature and artificial light impact insects' physiology and behavior, including survival, reproduction, and fitness. They can trigger stress responses, including heat shock protein expression, which varies across populations and species. Insects have developed resistance to chemical insecticides by modulating gene expression. Understanding the molecular mechanisms behind insect responses to stress can aid in developing sustainable pest control methods. More research is needed to comprehend the ecological implications of abiotic stressors on insect populations.

Author contributions

This editorial was led in drafting by SR and GK, who then revised and finalized the document for submission. PT and AS offered feedback and input by reviewing the draft. All authors contributed to this editorial, approving the final version for submission.

Acknowledgments

We extend our gratitude to the reviewers for generously dedicating their time and providing invaluable scientific feedback on the submissions. Additionally, we appreciate the editorial staff for their unwavering support.

Conflict of interest

The authors declare that the research was conducted in the absence of any commercial or financial relationships that could be construed as a potential conflict of interest.

Publisher's note

References

Bowler, K. (2005). Acclimation, heat shock and hardening. *J. Therm. Biol.* 30, 125–130. doi:10.1016/j.jtherbio.2004.09.001

Boyes, D. H., Evans, D. M., Fox, R., Parsons, M. S., and Pocock, M. J. (2021). Is light pollution driving moth population declines? A review of causal mechanisms across the life cycle. *Insect Conserv. divers.* 14 (2), 167–187. doi:10.1111/icad.12447

Grubisic, M., van Grunsven, R. H., Kyba, C. C., Manfrin, A., and Hölker, F. (2018). Insect declines and agroecosystems: Does light pollution matter? *Ann. Appl. Biol.* 173 (2), 180–189. doi:10.1111/aab.12440

Mandic, M., Todgham, A. E., and Richards, J. G. (2009). Mechanisms and evolution of hypoxia tolerance in fish. *Proc. R. Soc. B P Roy. Soc. B-BIOL Sci.* 276 (1657), 735–744. doi:10.1098/rspb.2008.1235

Owens, A. C., Cochard, P., Durrant, J., Farnworth, B., Perkin, E. K., and Seymoure, B. (2020). Light pollution is a driver of insect declines. *Biol. Conserv.* 241, 108259. doi:10.1016/j.biocon.2019.108259

Owens, A. C., and Lewis, S. M. (2018). The impact of artificial light at night on nocturnal insects: A review and synthesis. *Ecol. Evol.* 8 (22), 11337–11358. doi:10.1002/ece3.4557

Ramniwas, S., and Kumar, G. (2019). Pupation site preference selection in *Drosophila jambulina*. *Ethol. Ecol. Evol.* 31 (4), 301–312. doi:10.1080/03949370.2019.1592230

Sanders, D., Frago, E., Kehoe, R., Patterson, C., and Gaston, K. J. (2021). A meta-analysis of biological impacts of artificial light at night. *Nat. Ecol. Evol.* 5 (1), 74–81. doi:10.1038/s41559-020-01322-x

Walsh, B. S., Parratt, S. R., Mannion, N. L., Snook, R. R., Bretman, A., and Price, T. A. (2021). Plastic responses of survival and fertility following heat stress in pupal and adult *Drosophila virilis*. *Ecol. Evol.* 11 (24), 18238–18247. doi:10.1002/ece3.8418

frontiers | Frontiers in Physiology

ORIGINAL RESEARCH
published: 29 June 2022
doi: 10.3389/fphys.2022.938621

Development of CRISPR/Cas9-Mediated Gene-Drive Construct Targeting the Phenotypic Gene in *Plutella xylostella*

Muhammad Asad[1,2,3,4], *Dan Liu*[1,2,3,4], *Jianwen Li*[1,2,3,4], *Jing Chen*[1,2,3,4] *and Guang Yang*[1,2,3,4,5]*

[1]State Key Laboratory of Ecological Pest Control for Fujian and Taiwan Crops, Institute of Applied Ecology, Fujian Agriculture and Forestry University, Fuzhou, China, [2]Joint International Research Laboratory of Ecological Pest Control, Ministry of Education, Fuzhou, China, [3]Key Laboratory of Integrated Pest Management for Fujian-Taiwan Crops, Ministry of Agriculture, Fuzhou, China, [4]Key Laboratory of Green Pest Control, Fujian Province University, Fuzhou, China, [5]Ministerial and Provincial Joint Innovation Centre for Safety Production of Cross-Strait Crops, Fujian Agriculture and Forestry University, Fuzhou, China

OPEN ACCESS

Edited by:
Divya Singh,
Chandigarh University, India

Reviewed by:
Junaid Ali Siddiqui,
South China Agricultural University, China
Muhammad Fahad Raza,
Uludağ University, Turkey
Jaipal S. Choudhary,
ICAR-Research Complex for Eastern Region, India
Seema Ramniwas,
Chandigarh University, India

***Correspondence:**
Guang Yang
yxg@fafu.edu.cn

Specialty section:
This article was submitted to Invertebrate Physiology, a section of the journal Frontiers in Physiology

Received: 07 May 2022
Accepted: 01 June 2022
Published: 29 June 2022

Citation:
Asad M, Liu D, Li J, Chen J and Yang G (2022) Development of CRISPR/Cas9-Mediated Gene-Drive Construct Targeting the Phenotypic Gene in Plutella xylostella. Front. Physiol. 13:938621. doi: 10.3389/fphys.2022.938621

The gene-drive system can ensure that desirable traits are transmitted to the progeny more than the normal Mendelian segregation. The clustered regularly interspersed palindromic repeats (CRISPR)/CRISPR-associated protein 9 (Cas9) mediated gene-drive system has been demonstrated in dipteran insect species, including *Drosophila* and *Anopheles*, not yet in other insect species. Here, we have developed a single CRISPR/Cas9-mediated gene-drive construct for *Plutella xylostella,* a highly-destructive lepidopteran pest of cruciferous crops. The gene-drive construct was developed containing a Cas9 gene, a marker gene (*EGFP*) and a gRNA sequence targeting the phenotypic marker gene (*Pxyellow*) and site-specifically inserted into the *P. xylostella* genome. This homing-based gene-drive copied ~12 kb of a fragment containing *Cas9* gene, gRNA, and *EGFP* gene along with their promoters to the target site. Overall, 6.67%–12.59% gene-drive efficiency due to homology-directed repair (HDR), and 80.93%–86.77% resistant-allele formation due to non-homologous-end joining (NHEJ) were observed. Furthermore, the transgenic progeny derived from male parents showed a higher gene-drive efficiency compared with transgenic progeny derived from female parents. This study demonstrates the feasibility of the CRISPR/Cas9-mediated gene-drive construct in *P. xylostella* that inherits the desired traits to the progeny. The finding of this study provides a foundation to develop an effective CRISPR/Cas9-mediated gene-drive system for pest control.

Keywords: homology-directed repair, non-homologous-end joining, pxyellow, gene-drive efficiency, resistant-allele formation, diamondback moth

INTRODUCTION

During the Mendelian segregation, alleles generally have an equal chance (50:50) of being transmitted to progeny. Gene drives are selfish genetic elements that promote the spread of desirable traits across the populations by assuring that they are more often inherited than the Mendelian segregation (Akbari et al., 2015; Kandul et al., 2020). There are many examples of selfish genetic elements, either naturally occurring or synthetic, that can bypass the Mendelian segregation

(Werren et al., 1988; Werren, 2011). The meiotic drive, sex-ratio distortion, and replicative transposition are typical examples of naturally occurring gene-drive elements (Ågren, 2016). The synthetic *Medea* drive system (Chen et al., 2007; Akbari et al., 2014), engineered underdominance systems (Buchman et al., 2018), and homing endonuclease gene-drive (HEGD) (Marshall and Hay, 2012; Esvelt et al., 2014; Gantz and Bier, 2015; Gantz et al., 2015; Champer et al., 2016) are included in synthetic gene-drive systems. The development of HEGD is accelerated by discovering the CRISPR/Cas9 system (Jinek et al., 2012; Cong et al., 2013; Mali et al., 2013).

Theoretical and practical use of CRISPR/Cas9 systems as a HEGD to change the genotype of insect species has been demonstrated (Esvelt et al., 2014; Unckless et al., 2015), which can potentially transmit the desired phenotype into a wild-type population of target species (Deredec et al., 2008; Unckless et al., 2017). In the CRISPR/Cas9-based gene drive (CCGD), the CRISPR/Cas9 construct contains the coding sequence of Cas9 endonuclease and a 20-bp gRNA targeting the specific site of the host genome. RNA-guided Cas9 causes a break of double-stranded DNA in the wild-type allele, which is repaired through either HDR or NHEJ (Karaminejadranjbar et al., 2018). The HDR-mediated repair drives the desired components into the next generation, while NHEJ mediated repair leads to the formation of resistant allele without transferring the desirable traits into the next generation (Champer et al., 2017; Champer et al., 2018). The consequences of resistant alleles depend on several factors, including the fitness cost associated with the drive and the type of gene-drive approach.

The CCGD system has been successfully developed in different organisms including bacteria (Valderrama et al., 2019), yeast (Dicarlo et al., 2015; Roggenkamp et al., 2018; Shapiro et al., 2018), mammals (Grunwald et al., 2019), and insects (Gantz and Bier, 2015; Gantz et al., 2015; Champer et al., 2017; Karaminejadranjbar et al., 2018; Kyrou et al., 2018; Champer et al., 2020; Li et al., 2020). These studies show extremely-variable gene-drive efficiency, close to 100% in *Saccharomyces cerevisiae*, 19%–62% in *Drosophila melanogaster* and 87%–99% in *Anopheles*. The variability in gene-drive efficiency depends on the timing and level of Cas9 expression, organism-specific factors, and the genomic targets (Champer et al., 2019). The CCGD has recently been used to control the pest population through a population-modification and population-suppression drives. In a population-modification drive, the release of transgenic mosquitoes in which the CCGD contains effector genes inhibiting the mosquito pathogen transmission results in the replacement of disease-sensitive mosquitoes with disease-resistant mosquitoes, which decreases the pathogen transmission (Buchman et al., 2018; Buchman et al., 2020). In the population-suppression drive, the homing-based gene-drive is developed to target the conserved sex-specific genes (Kyrou et al., 2018). Given these characteristics, both alteration and suppression drives can be used to control the pest population.

The germline-specific promoters and phenotypic marker genes play a significant role in the development of CCGD. The germline-specific promoters, including *nanos* promoter and *vasa* promoter to drive germline-specific *Cas9* expression, have shown great potential to develop the CCGD in insects (Gantz and Bier, 2015; Gantz et al., 2015; Champer et al., 2017; Karaminejadranjbar et al., 2018; Kyrou et al., 2018; Champer et al., 2020; Li et al., 2020). Similarly, the phenotypic marker genes such as *yellow* and *white* are used as the target sites to assess and minimize the fitness cost caused by the CCGD. Furthermore, the phenotypic genes also provide an easy way to screen the progeny with resistant alleles through NHEJ (Gantz and Bier, 2015; Gantz et al., 2015; Champer et al., 2017; Champer et al., 2018). Therefore, we selected *PxnanosO* promoter to drive *Cas9* and *yellow* gene as the target site for CCGD.

The diamondback moth (*Plutella xylostella*) is a globally-distributed lepidopteran pest that mainly attacks cruciferous crops and has developed resistance to all classes of insecticides, making it difficult to control (Furlong et al., 2013). Genetic-based approaches, especially CCGD for population suppression and modification, have only been developed in dipteran insect species (Gantz and Bier, 2015; Gantz et al., 2015; Champer et al., 2017; Karaminejadranjbar et al., 2018; Kyrou et al., 2018; Li et al., 2020), not yet in other insect species. Previously, a CRISPR/Cas9-based split drive system has been successfully developed in *Plutella xylostella*. However, this split drive system failed to produce homing-based progeny (Xu et al., 2022). No homing-based progeny in the split-drive system might be because the two different transgenic lines (gRNA line and Cas9 line) cross each other. Keeping in view of these results, we developed a single CCGD construct for the first time in *P. xylostella* and evaluated its efficiency. The results provide a foundation for developing a CCGD system for population suppression or modification of *P. xylostella*.

MATERIALS AND METHODS

Rearing of *P. xylostella* Strain

The insecticide-susceptible strain Geneva 88 (G88) of *P. xylostella* used in this study was obtained from Cornell University in 2016 and subsequently established as a colony at the Institute of Applied Ecology, Fujian Agriculture and Forestry University. This strain was reared using a prepared artificial diet at 35%–50% RH, 16 h: 8 h (L:D) photoperiod, and 25 C in the growth chamber. After the larvae developed into pupae, the pupae were collected and transferred into the box for eclosion and mating. The adults were kept at 25 C and 80% RH and fed with 10% honey solution.

Amplification and Cloning of *Pxyellow* Gene Target Site

The genomic DNA of fourth instar larvae of *P. xylostella* was extracted using the MEGA Bio-Tek Tissue DNA kit (Omega, Norcross, United States), followed by purification after RNase treatment. The sequence of the candidate *Pxyellow* gene was obtained from *P. xylostella* genomic database (http://iae.fafu.edu.

cn/DBM/index.php). The specific primers for PCR amplification were designed by using the NCBI database's primer tool (https://www.ncbi.nlm.nih.gov/tools/primer-blast/). The 2.3-kb fragment of the *Pxyellow* gene, including the gRNA target site, was PCR amplified with designed primer Yts-F and Yts-R (**Supplementary Table S1**). The PCR reaction was prepared by using the Max Super-Fidelity DNA Polymerase (Vazyme, Nanjing, China) and carried out with the following conditions of 95 C for 3 min; 32 cycles of 95 C for 10 s, 62 C for 20 s, 72 C for 2 min; then 72 C for 5 min; and 4 C forever. The PCR amplified products were purified with the Omega Gel Purification Kit (Omega, Norcross, United States) following its protocol. The purified PCR product was sub-cloned into the PJET1.2 blunt-end vector (Thermo Scientific, Waltham, MA, United States) and confirmed through Sanger sequencing.

Design and *in vitro* Transcription of sgRNA

The DNA fragment at exon 3 of *Pxyellow* gene was selected as the target site of gRNA based on the 5′-GG-(N)18-NGG-3′ principle (Hwang et al., 2013) by using the CRISPR gRNA Design tool-ATUM (https://www.atum.bio/eCommerce/cas9/input). The GG bases were added at the 5′ end of the gRNA target site to ensure the *in vitro* transcription stability by T7 RNA polymerase. A pair of long oligonucleotides were used to produce a DNA template of sgRNA for *in vitro* transcription (Bassett et al., 2013). The sgRNA-F oligonucleotide contained a T7 RNA polymerase binding site and the sgRNA target site, and the sgRNA-R oligonucleotide contained gRNA scaffold and overlap region of forward primer (**Supplementary Table S1**). PCR reaction was carried out by using the PrimeSTAR HS DNA Polymerase (TaKara Biomedical Technology, Beijing, China) at the following conditions: 98 C for 3 min; 32 cycles of 98 C for 10 s, 55 C for 20 s, 72 C for 30 s; then 72 C for 5 min and 4 C forever. This PCR product was purified with the Omega universal DNA Purification Kit (Omega, Norcross, United States) by following its protocol. The purified PCR product was used for *in vitro* transcription of sgRNA with the HiScribe T7 Quick High Yield RNA Synthesis Kit (New England Biolabs, Ipswich, United States) by following its protocol.

Construction of PJET-Cas9 Cassette

Firstly, we obtained the germline-specific *nanos* gene sequence of *Bombyx mori* (NP_001093314) (Xu et al., 2019) from the NCBI (National Center for Biotechnology Information) (https://www.ncbi.nlm.nih.gov/) and blasted it against the *P. xylostella* genomic database (http://iae.fafu.edu.cn/DBM/index.php) (You et al., 2013). The highly-similar gene *PxnanosO* (gene id: Px008918) was identified and selected. The *PxnanosO* promoter (PxnanosP) was amplified by using Nanos-F and Nanos-R primers (**Supplementary Table S1**). The PCR reaction was prepared by using the Super-Fidelity DNA Polymerase (Vazyme, China) and carried out with the following PCR conditions: 95 C for 3 min; 32 cycles of 95 C for 15 s, 60 C for 20 s, 72 C for 1 min; 72 C for 5 min; and then 4 C forever. This amplified PCR product was further purified with the Omega Gel Purification Kit (Omega, Norcross, United States). The purified PCR product was sub-cloned into the PJET1.2 blunt-end vector (ThermoFisher Scientific, Waltham, MA, United States) and confirmed through sequencing. After sequence confirmation, we amplified PxnanosP from the PJET1.2 blunt-end vector with the same primers and conditions mentioned above.

The 4-kb Cas9 fragment was amplified from the plasmid PTD-T7-Cas9 (Huang et al., 2016) by using a pair of primers of Cas9-F and Cas9-R (SI, **Supplementary Table S1**) with the overlapping region of PxnanosP and SV40 PolyA tail. The PCR reaction was carried out with the Super-Fidelity DNA Polymerase (Vazyme, China) at the following conditions: 95 C for 3 min; 32 cycles of 95 C for 15 s, 58 C for 15 s, 72 C for 3 min; 72 C for 10 min; and then 4 C forever. The 4-kb amplified Cas9 product was further purified with the Omega Gel Purification Kit (Omega, Norcross, United States).

The 250-bp Sv40 PolyA tail fragment was amplified from the GPXL-BacII-IE1-EGFP-SV40 vector (Asad et al., 2020) by using primers of Sv40-F and Sv40-R (**Supplementary Table S1**) with the overlapping region of Cas9 fragment and PJET1.2 vector. The PCR reaction was carried out with the Super-Fidelity DNA Polymerase (Vazyme, China) at the following conditions: 95 C for 3 min; 32 cycles of 95 C for 15 s, 58 C for 15 s, 72 C for 3 min; 72 C for 10 min; and then 4 C forever. The PCR amplified product of 250-bp Sv40 PolyA tail was further purified with the Omega Gel Purification Kit.

These three fragments were assembled and cloned into the PJET1.2 blunt-end vector by using the HiFi DNA Assembly Master Mix (New England Biolabs, #E5510) by following its protocol to obtain the PJET-Cas9 vector (**Supplementary Figure S1**).

All oligonucleotides containing overlapping regions for assembling fragments into vectors were designed by using the NEB Builder Assembling Tool of New England Bio Lab (http://nebuilder.neb.com/). The vector and insert fragment concentrations were calculated by using the New England Bio Lab tool NEBio Calculator (https://nebiocalculator.neb.com/#!/ligation). The mixture concentrations of all digestion reactions were calculated by using the New England Bio Lab tool, NEB Cloner (http://nebcloner.neb.com/#!/).

Insertion of Hr5IE1-EGFP-Sv40 Fragment to PJET-Cas9 Vector

The Hr5IE1-EGFP-Sv40 fragment was amplified from the previously constructed vector GPXL-BacII-IE1-EGFP-SV40 (Asad et al., 2020). Two oligonucleotides (IE1-F and IE1-R) were used to amplify the Hr5IE1-EGFP fragment (**Supplementary Table S1**), which contains an overlapping region for insertion of this fragment at *Abs*I cutting site of PJET-Cas9 vector (**Supplementary Figure S1**). The PCR reaction was carried out with the Super-Fidelity DNA Polymerase (Vazyme, China) at the following conditions: 95 C for 3 min; 30 cycles of 95 C for 30 s, 58 C for 30 s, 72 C for 2 min; 72 C for 5 min and then 4 C forever. The amplified product of the Hr5IE1-EGFP-Sv40 fragment was further purified with the Omega Gel Purification Kit (Omega, Norcross, United States). The PJET-Cas9 vector was linearized with the digestion of *Abs*I (SibEnzyme, Russia). This digested product was purified by using

the Omega Gel Purification Kit (Omega, Norcross, United States). These two purified fragments (Hr5IE1-EGFP-Sv40 fragment and linearized PJET-Cas9 vector) were assembled with the HiFi DNA Assembly Master Mix (New England Biolabs, Ipswich, United States) by following the instruction of the manufacturer to obtain the PJET-Cas9-EGFP vector (**Supplementary Figure S2**). The insertion of Hr5IE1-EGFP-Sv40 fragment into the PJET-Cas9 vector was confirmed through colony PCR. The plasmid of positive clones was extracted with the Omega Mini Plasmid Extraction Kit (Omega, Norcross, United States) by following its protocol. The extracted plasmids of PJET-Cas9-EGFP vector were further used in double digestion with HF *Not*I (New England Biolabs, Ipswich, United States) and HF *Age*I (New England Biolabs, Ipswich, United States).

Insertion of PxU6-gRNA Cassette to PJET-Cas9-EGFP Vector

The PxU6 promoter was amplified from the previously-used U6: sgRNA expression vector (Huang et al., 2017). To link the gRNA sequence with U6, 20-bp gRNA and a sequence of terminal signals for the *PxU6* gene were added to the reverse primer U6-R (**Supplementary Table S1**). The PCR reaction mixture was prepared with the Super-Fidelity DNA Polymerase (Vazyme, China) by using two designed primers (U6-F and U6-R). The PCR reaction was carried out with following conditions: 95 C for 4 min; 35 cycles of 95 C for 30 s, 61 C for 30 s, 72 C for 1 min; 72 C for 5 min and then 4 C forever. Another PCR reaction was performed with two oligonucleotides (gRNA-F and gRNA-R) containing the overlapping sequence for insertion of this fragment to the PJET-Cas9-EGEP vector. The PCR reaction was carried out with the Super-Fidelity DNA Polymerase (Vazyme, China) at the same conditions used to amplify PxU6 promoter. This amplified product was further purified with the Omega Gel Purification Kit (Omega, Norcross, United States). The PJET-Cas9-EGFP vector was digested with *Age*I (New England Biolabs). The digested product was purified with the Omega Gel Purification Kit (Omega, Norcross, United States). The two fragments (PJET-Cas9-EGFP vector and PxU6-gRNA) were assembled with the HiFi DNA Assembly Master Mix (New England Biolabs, #E5510) by following the manufacturer's instruction to obtain the PJET-Cas9-EGFP-gRNA vector (**Supplementary Figure S3**). The plasmid of positive clones was extracted with the Omega Mini Plasmid Extraction Kit (Omega, Norcross, United States). The extracted plasmids were further used in double digestion with *Spe*I and *Age*I enzymes (New England Biolabs, Ipswich, United States).

Cloning of Homologous Arms

The 1-kb left and right regions from the gRNA target site of *Pxyellow* gene were selected as homologous arms. These two homologous arms were PCR amplified from the cloned *Pxyellow* gene with a pair of primers (LH-F & LH-R, RH-F & RH-R). The PCR reactions were carried out with the Super-Fidelity DNA Polymerase (Vazyme, China) at the following conditions: 95 C for 3 min; 35 cycles of 95 C for 15 s, 61 and 58 C for 30 s, 72 C for 1 min; 72 C for 5 min and then 4 C forever. These two amplified products were purified by gel electrophoresis and separately ligated into the PJET1.2 blunt vector. The ligated vector was confirmed through Sanger sequencing.

Insertion of Left and Right Homologous Arms to PJET-Cas9-EGFP-gRNA Vector

The left homologous arm (LHA) was PCR amplified by using the cloned fragment with two oligonucleotides (LHA-F and LHA-R) containing overlapping regions for assembling with the PJET-Cas9-EGFP-gRNA vector (**Supplementary Table S1**). The PCR reaction was carried out with the Super-Fidelity DNA Polymerase (Vazyme, China) at the following conditions: 95 C for 3 min; 35 cycles of 95 C for 15 s, 58 C for 30 s, 72 C for 1 min; 72 C for 5 min and then 4 C forever. The PJET-Cas9-EGFP-gRNA vector was digested with *Spe*I and then purified with the Omega Gel Purification Kit (Omega, Norcross, United States). The digested vector PJET-Cas9-EGFP-gRNA and amplified left homologous arm were assembled with the HiFi DNA Assembly Master Mix (New England Biolabs, #E5510). The insertion of LHA into PJET-Cas9-EGFP-gRNA was confirmed through colony PCR. The plasmid of positive clones was extracted with the Omega Mini Plasmid Extraction Kit (Omega, Norcross, United States)

The confirmed vector containing LHA was further digested with the *Age*I (New England Biolabs, Ipswich, United States) followed by purification with the Omega Gel Purification Kit (Omega, Norcross, United States). The right homologous arm (RHA) was PCR amplified by using the cloned fragment with two oligonucleotides (RHA-F and RHA-R) containing overlapping regions for assembling with the digested vector (**Supplementary Table S1**). The PCR reaction was carried out with the Super-Fidelity DNA Polymerase (Vazyme, China) at the following conditions: 95 C for 3 min; 32 cycles of 95 C for 15 s, 60 C for 15 s, 72 C for 1 min; 72 C for 5 min and then 4 C forever. The right homologous arm and digested vector were again assembled with the HiFi DNA Assembly Master Mix (New England Biolabs, #E5510) to obtain the PJET-Ca9-EGFP-gRNA-LRH vector (SI **Supplementary Figure S4**). The insertion of RHA was confirmed through colony PCR. The final gene-drive construct was named LHA-Ca9-EGFP-gRNA-RHA. The plasmid of positive clones was extracted with the Omega Mini Plasmid Extraction kit (Omega, Norcross, United States). The extracted plasmids were digested with HF *Not*I (New England Biolabs, Ipswich, United States) and HF *Age*I (New England Biolabs, Ipswich, United States) to confirm the insertion of LHA and RHA fragments into the PJET-Cas9-EGFP-gRNA vector.

Generation of Double-Stranded RNA to Target *Pxku70*

The putative sequence of *Pxku70* gene was obtained by blasting the X-ray repair protein 5-like mRNA (LOC101736121) sequence of *Bombyx mori* in the DBM genomic database (http://iae.fafu.edu.cn/DBM/index.php). The primers (Ku70-F and Ku70-R) were designed to amplify 610-bp fragment based on the

obtained sequence (**Supplementary Table S1**). PCR reaction was carried out with the Super-Fidelity DNA Polymerase (Vazyme, China) at the following conditions: 95 C for 3 min; 28 cycles of 95 C for 15 s, 60 C for 15 s, 72 C for 1 min; 72 C for 5 min and then 4 C forever. Furthermore, a pair of primers of T7Ku70-F and T7Ku70-R were designed to contain a T7 promoter in both primers (**Supplementary Table S1**). The PCR reaction was carried out with the Super-Fidelity DNA Polymerase (Vazyme, China) by using the previously-amplified product as the template at the same conditions explained above. The amplified product was used as the template for dsRNA synthesis with the T7 RiboMAX™ Express RNAi Kit (Promega) by following its protocol.

Microinjection

The injection mixture was prepared by mixing Cas9-N-NLS Nuclease (GenScript, United States), gRNA targeting *Pxyellow*, dsRNA targeting *Pxku70,* LHA-Cas9-EGFP-gRNA-RHA vector with the injection buffer as previously described (Asad et al., 2020). The parafilm sheets of 12 cm^2 coated with the cabbage leave extract were used to collect eggs, and the sheets were replaced every 30 min by new ones during the oviposition of female adults. The injections were performed within 1 h after oviposition by using the Olympus SZX16 microinjection system (Olympus, Japan). The injected embryos were placed in the hatching chamber at 25 ± 1 C, 60 ± 10% RH.

Crossing and Screening

The hatched larvae from the injected eggs were maintained on the freshly-prepared diet. The G_0 females and males were separated and outcrossed with wild-type adults of 1 G_0 female with 2 wild-type males and 1 G_0 male with 2 wild-type females. However, An equal number of transgenic and wild-type individuals (one transgenic cross with one wild-type individual) were used for the subsequent crosses of F_2, F_3, and F_4 generations. The larval progeny of F_1, F_2, F_3, and F_4 were screened by the EGFP fluorescence under the fluorescent microscope equipped with an EGFP filter and stereoscope. The homozygous larvae exhibited a strong EGFP signal, and the heterozygous larvae showed a patchy EGFP signal (Chen et al., 2021).

Confirmation of Gene Drive

The genomic DNA was extracted from adults of F_1 generation after oviposition with the Omega Genomic DNA Extraction Kit (Omega, Norcross, United States). A pair of primers (gTS-F and gTS-R) were used to amplify the gRNA target site (**Supplementary Table S1**). The amplified products were confirmed through Sanger sequencing. The insertion of the gene-drive cassette into the *Pxyellow* gene was confirmed through PCR by using the designed primers (**Supplementary Table S1**). PCR reaction was carried out with the Super-Fidelity DNA Polymerase (Vazyme, China) and the extracted DNA of F_1 EGFP-positive adults at the conditions: 95 C for 3 min; 32 cycles of 95 C for 15 s, 60 C for 15 s, 72 C for 1 min; 72 C for 5 min and then 4 C forever. The amplified products were confirmed through Sanger sequencing.

Statistical Analysis

The Chi-square (χ^2) analysis was performed by using the Graphpad 8.02 (GraphPad Software, La Jolla, San Diego, CA, United States) to determine the significant difference between the gene-drive efficiency in different generations of transgenic *P. xylostella* and $EGFP^+$ progeny derived from different parents at $p < 0.05$. The *Z* test was used to compare the NHEJ and HDR mutation rates in the progeny of different crosses at $p < 0.05$.

RESULTS

Confirmation of the Target Site *Pxyellow* Gene

The *Pxyellow* gene (gene ID: *Px007091*) is body pigmentation gene and disruption of *Pxyellow* gene only leads to a change in body color (Wang et al., 2020). Therefore, the *Pxyellow* gene is a suitable target site for screening the mutant progeny in the CRISPR/Cas9-based gene-drive system in *P. xylostella*. The *Pxyellow* gene is located at scaffold 25, containing four exons and five introns. The sgRNA was designed and synthesized to target the Exon 3 of *Pxyellow* (**Figure 1A**). A total of 150 preblastoderm embryos were injected with the mixture of sgRNA and Cas9 protein, and 90 hatched (the hatching rate of 60%). The 60 G_0 larvae showed yellow head compared with wild-type larvae, which was clearly observed at second and third instar larvae (**Figure 1B**), making the mutation rate 40% (60/150) in G_0 individuals. The 439-bp DNA fragment flanking the target site was amplified from these mosaic G_0 adults and sequenced.

Out of these 60 G_0 mutant individuals, 43 individuals showed indels at the target site (**Supplementary Appendix Table S1**). Four types of deletions (-2 bp, -4 bp. -3 bp and -9 bp) and two types of insertions (+11 bp and +14 bp) were observed in 43 individuals (**Figure 1C**).

Construct Design and Development of Transgenic *P. xylostella*

The 1.8-kb upstream sequence of the *Pxnanos*O gene was cloned and used as a putative promoter. The immediate-early-stage 1 promoter with an enhancer 5 (HR5IE1) was used to drive the EGFP marker gene. This promoter has been successfully used as a transformation marker in different insect species, including *P. xylostella* (Grossman et al., 2001; Gong et al., 2005; Martins et al., 2012). The PxU6:3 promoter has been used to drive gRNA in *P. xylostella* (Huang et al., 2017). The LHA-Cas9-EGFP-gRNA-RHA construct contained a *Cas9* gene driven by Pxnanos promoter, an *EGFP* marker gene-driven by HR5IE1 promoter and a gRNA sequence (targeting the phenotypic marker gene *Pxyellow*) driven by PxU6 promoter (**Figure 2A**). The details about the construction and verification of LHA-Cas9-EGFP-gRNA-RHA construct are listed in Supplementary information (**Supplementary Figure S5**). The detailed sequences

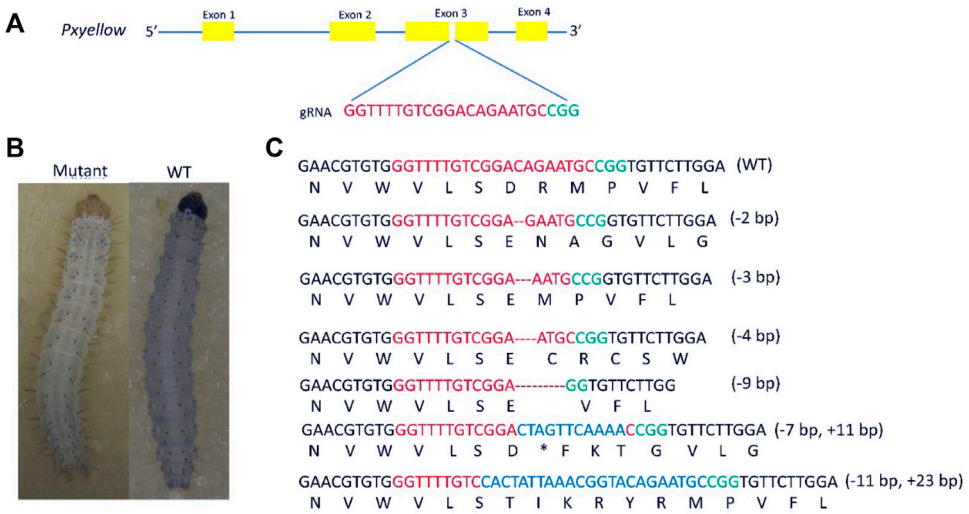

FIGURE 1 | Knockout of *Pxyellow* gene at the target site. **(A)**, the schematic representation of *Pxyellow* gene. The orange boxes indicate the exon of *Pxyellow* gene, and blue lines indicate the introns. **(B)**, phenotypic difference between *Pxyellow* mutant and wild type. **(C)**, types of deletions and insertions at the target site. Red base pairs indicate the gRNA sequence and green indicate the PAM, sequence; the deletions are highlighted with dashes (--), and the inserted base pairs are highlighted with blue colors.

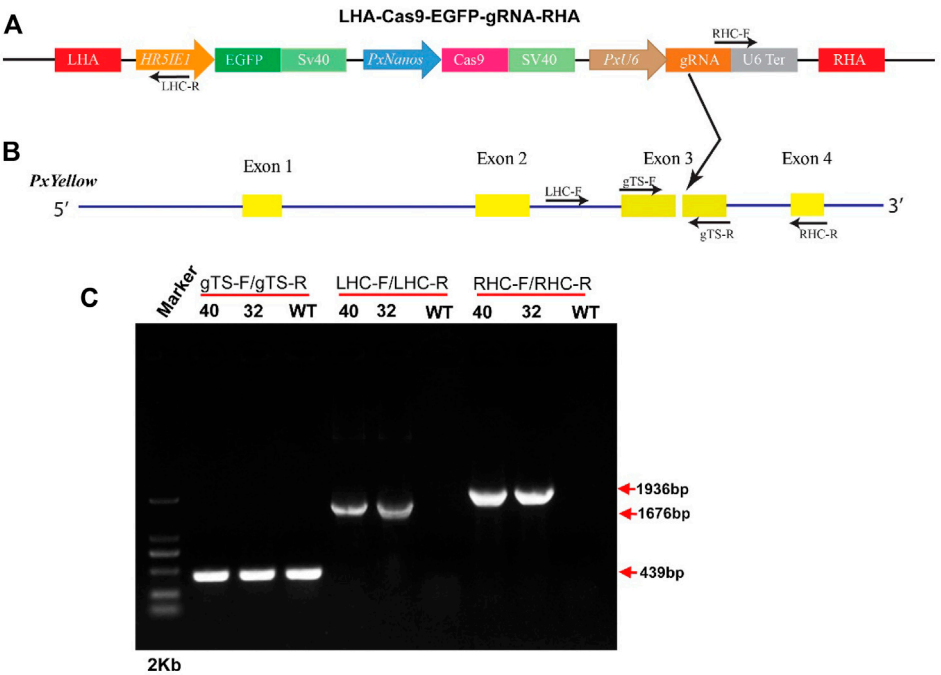

FIGURE 2 | Site-specific insertion of gene-drive construct. **(A)**, schematic representation of gene-drive cassette (LHA-Cas9-EGFP-gRNA-RHA). **(B)**, schematic representation of *Pxyellow* gene. The small arrow with the label represents the position, orientation and name of primers used to confirm the integration of the gene-drive cassette into the *Pxyellow* target site. The red boxes represent the left homologous arm (LHA) and right homologous arm (RHA). The other components of plasmid LHA-Cas9-EGFP-gRNA-RHA have been highlighted and labeled with different colors. The yellow boxes represent the 4 exons of *Pxyellow* gene. The dark gray lines represent the introns of *Pxyellow* gene. The black arrow represents the gRNA target site in *Pxyellow* locus. **(C)**, Verification of the site-specific insertion of LHA-Cas9-EGFP-gRNA-RHA construct by PCR.

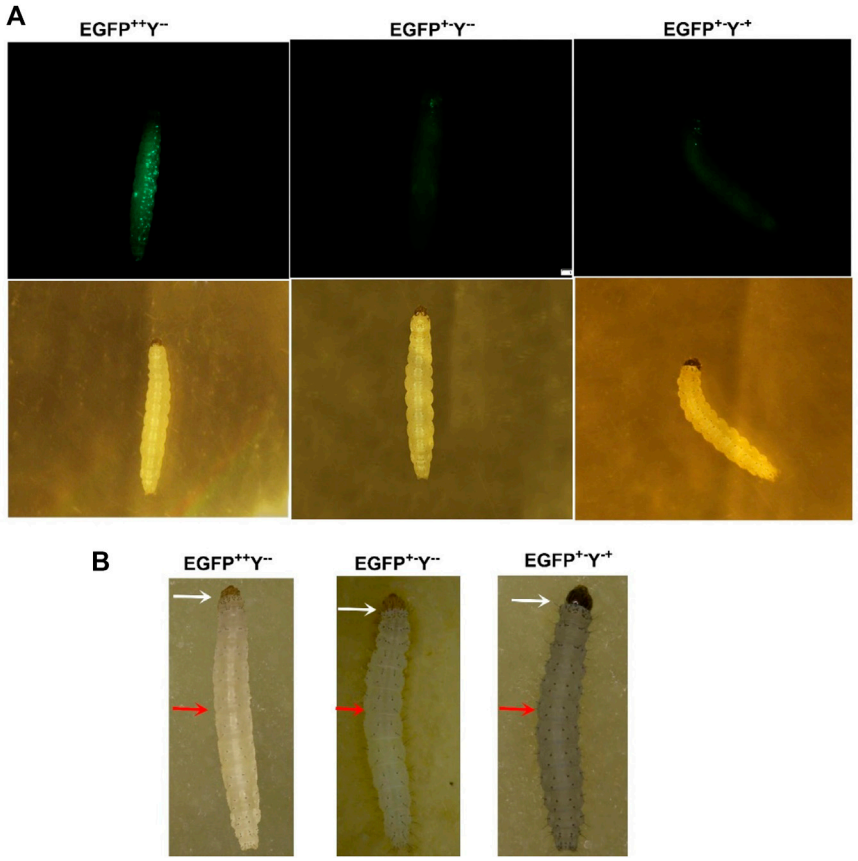

FIGURE 3 | Larval phenotypes of transgenic *P. xylostella* harboring the gene-drive cassette. **(A)**, larval images in the upper row taken in the presence of EGFP filter and larval images in the lower row taken with a bright-light filter. **(B)**, larval images taken by a stereoscope. The white arrows indicate the head color, and the red arrows indicate the body color.

of Pxnanos promoter, HR5IE1 promoter, *EGFP* marker gene, Cas9, PxU6 promoter gRNA, left and right homologous arms are also listed in (**Supplementary Appendix Table S2**).

The transgenic *P. xylostella* was developed by injecting the mixture of plasmid LHA-Cas9-EGFP-gRNA-RHA, Cas9 protein, sgRNA, and *Pxku70* dsRNA into embryos to insert the gene-drive cassette Cas9-EGFP-gRNA into the target site of *Pxyellow* (**Figure 2B**). A total of 5930 *P. xylostella* embryos were injected in five attempts, of which the mean G_0 survival rate was 22.02% (**Supplementary Table S2**). The survived G_0 male and female were individually outcrossed with wild-type to produce the F_1 progeny. The integration of drive cassette in F_1 was verified by the PCR products a 439-bp fragment amplified with primers gTS-F and gTS-R, a 1676-bp fragment amplified with primers LHC-F and LHC-R, and a 1936-bp fragment amplified with primers RHC-F and RHC-R (**Figure 2C**). The second and third instar larvae of the F_1 generation were screened for green fluorescence ($EGFP^+$) (**Figure 3A**) and abnormal yellow body and head pigmentation (Y^-) (**Figure 3B**). One EGFP-positive female and one EGFP-positive male with yellow mutant phenotype were subsequently obtained from 28200 F_1 individuals and named founder 32 and founder 40, respectively (**Supplementary Table S3**).

Furthermore, we scored three kinds of phenotypes with corresponding genotypes such as strong EGFP fluorescence and yellowish body ($EGFP^{++}Y^{--}$), patchy EGFP fluorescence and yellowish body ($EGFP^{+-}Y^{--}$), and patchy EGFP fluorescence and wild-type body color ($EGFP^{+-}Y^{-+}$) due to non-mendelian segregation after crossing of homozygous $EGFP^{++}Y^{--}$individuals with wild type ($EGFP^{--}Y^{++}$) in different generations of both founders (**Figure 3**). According to the Mendelian segregation, all F_1 progeny should be heterozygote with EGFP-positive and wild-type body color because *yellow* gene is recessive. The conversion of heterozygote to homozygote progeny indicates the homing of Cas9-EGFP-gRNA component to neighboring allele.

The target-specific insertion of the gene-drive cassette at *Pxyellow* locus was confirmed in both F_1 founders through PCR amplification (**Figure 2C**). The sequencing of both diagnostic amplicons containing the left and right homologous regions and their adjacent sequences in the gene-drive cassette showed cassette insertion at the *Pxyellow* target site (**Figure 4** and **Supplementary Appendix Table S3**).

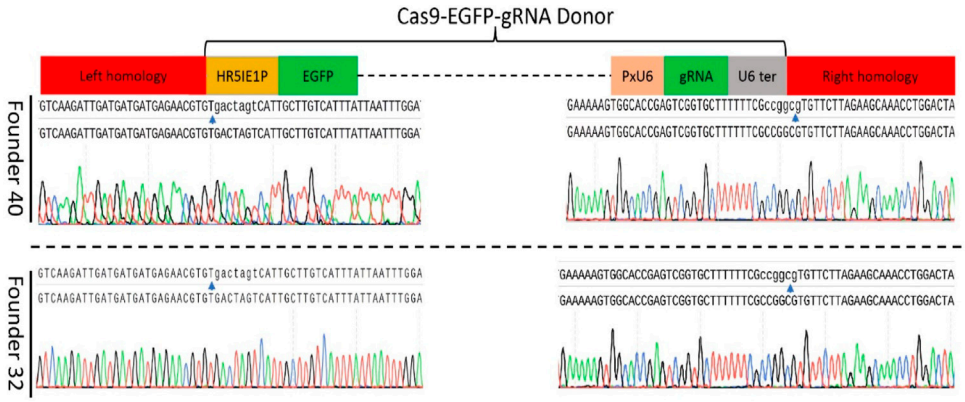

FIGURE 4 | Sequence confirmation of the precise insertion of the gene-drive construct into the *Pxyellow* locus. The PCR amplification and genomic DNA sequencing were performed to verify the precise insertion of gene-drive components at *Pxyellow* locus in two F_1 founders (40 and 32). Sequence of 5′-end fragment amplified by LH-F and LH-R is presented at the left side, and sequence of 3′-end fragment amplified by RH-F and RH-R is presented at the right side in both founders. The blue arrows represent the junction between the *Pxyellow* coding sequence and gene-drive construct.

Gene-Drive Efficiency in Different Generations of Transgenic *P. xylostella*

Under ideal homing endonuclease-based gene-drive conditions (100%), all progenies should show stable EGFP and yellowish phenotype (**Figure 5A**). Based on the above-mentioned genotypes, there were 13.19% individuals of $EGFP^{++}Y^{--}$ in F_2 generation, 9.40% in F_3 generation and 8.32% in F_4 generation for founder 40. Similarly, for founder 32, there were only 8.25% individuals of $EGFP^{++}Y^{--}$genotype in F_2 generation, 8.91% in F_3 generation and 7.82% in F_4 (**Figure 5B**). These individuals of genotype $EGFP^{++}Y^{--}$indicated the homing (gene-drive) of one inherited allele to neighboring wild-type allele through the HDR process. However, more than 85% of alleles were either mutated through the NHEJ process (**Figure 5C**) or uncut in F_2, F_3 and F_4 generations from both founders (**Figure 5D**).

There was no difference in the homing efficiency among the different generations of both founders (founder 32, χ^2 = 2.872, df = 2, p = 0.237; founder 40, χ^2 = 0.232, df = 2, p = 0.891) or between the two founders (χ^2 = 0.073, df = 1, p = 0.7870). These results indicated that all progeny derived from parent crosses contained the drive allele, from which only 7.82%–13.19% were converted into homozygous drive allele ($EGFP^{++}Y^{--}$) due to HDR and the rest were converted into resistance allele ($EGFP^{+-}Y^{--}$, $EGFP^{+-}Y^{-+}$) due to NHEJ (**Figure 5** C and D). This situation indicated that cleavage of the target site with Cas9 happened in somatic tissues rather than in the germline tissues, which caused the formation of resistance allele.

There was no difference in the Cas9/sgRNA cleavage efficiency of negibouring alleles between two founders (χ^2 = 1.869, df = 1, p = 0.1715) or among different generations of both founders (founder 32, χ^2 = 2.864, df = 2, p = 0.239; founder 40, χ^2 = 3.473, df = 2, p = 0.176), which all showed the cleavage efficiency of above 88% in *P. xylostella* (**Figure 6**).

Furthermore, the individuals with heterozygous $EGFP^{+-}Y^{--}$ phenotype were randomly selected for genotype confirmation through PCR amplification. The PCR results showed the deletion of base pairs at the *Pxyellow* target site in heterozygote $EGFP^{+-}Y^{--}$ mutants from both founders (**Supplementary Figure S6**). After cutting of genomic DNA by Cas9, $EGFP^{+-}Y^{--}$caused by NHEJ happened more frequently than $EGFP^{++}Y^{--}$caused by HDR in F_2 progeny (Z = -3.211, p = 0.001), in F_3 progeny (Z = -2.521, p = 0.012) and in F_4 progeny (Z = -2.521, p = 0.012).

Effects of Parents on Gene-Drive Efficiency in Progeny

The cross between founder 40 (F_1 $EGFP^{++}Y^{--}$male) and wild-type female produced less progeny (125 adult/cross) than the cross between founder 32 (F_1 $EGFP^{++}Y^{--}$female) and wild-type male (194 adult/cross) (χ^2 = 7.402, df = 1, p = 0.006) (**Table 1**).

For founder 40, crosses between F_2 $EGFP^{++}Y^{--}$female and wild-type male produced less progeny (147.1 adult/cross) than crosses between F_2 $EGFP^{++}Y^{--}$male and wild-type female (240.28 adult/cross) (χ^2 = 46.794, df = 1, p = 0.000); for founder 32, crosses between F_2 $EGFP^{++}Y^{--}$female and wild-type male (196.6 adult/cross) produced less progeny than crosses between F_2 $EGFP^{++}Y^{--}$ female and wild-type male (215 adult/cross) (χ^2 = 46.581, df = 1, p = 0.000) (**Table 2**.

For founder 40, crosses between F_3 $EGFP^{++}Y^{--}$female and wild-type male produced less progeny (188.16 adult/cross) than crosses between F_3 $EGFP^{++}Y^{--}$male and wild-type female (257.4 adult/cross) (χ^2 = 47.342, df = 1, p = 0.000); for founder 32, crosses between F_3 $EGFP^{++}Y^{--}$female and wild-type male produced less progeny (182.5 adult/cross) than crosses between F_3 $EGFP^{++}Y^{--}$ and wild-type female (264.7 adult/cross) (χ^2 = 519.35, df = 1, p = 0.000) (**Table 3**).

The cross between wild-type male and female produced more progeny than the cross between $EGFP^{++}Y^{--}$male and wild-type female (χ^2 = 7.33, df = 1, p = 0.003); the cross between $EGFP^{+}Y^{-}$ male produced more progeny than the cross between $EGFP^{++}Y^{--}$female and wild-type male

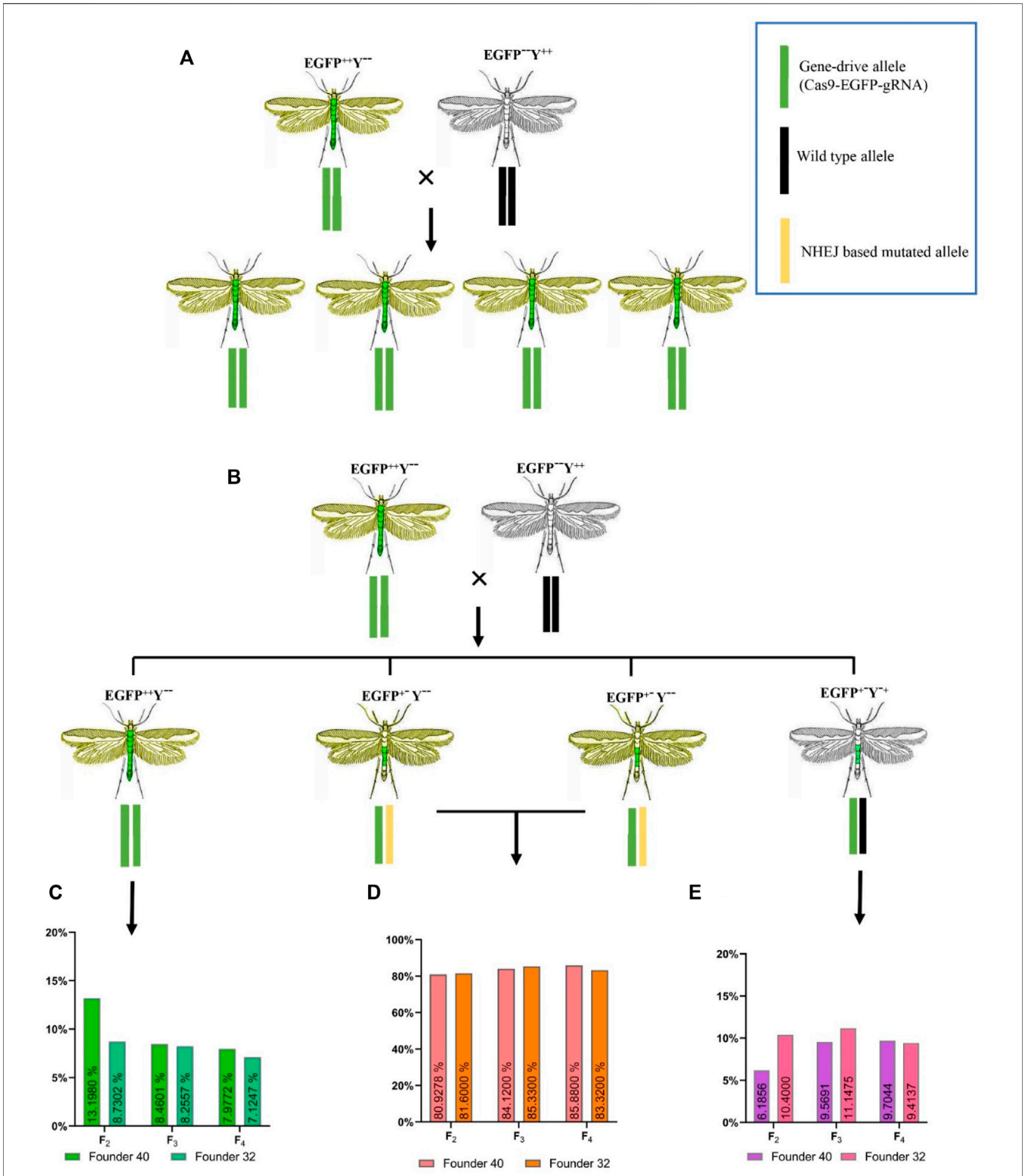

FIGURE 5 | Expected and obtained phenotypes with different genotypes. **(A)**, expected genotypes and phenotypes for an ideal homing endonuclease-based gene-drive system; **(B)**, obtained genotypes and phenotypes during this study; **(C)**, the homing efficiency in different generations; **(D)**, the resistant allele formation with one allele inherited and the second allele mutated without homing; **(E)**, the resistant-allele formation with one allele inherited and the second allele uncut.

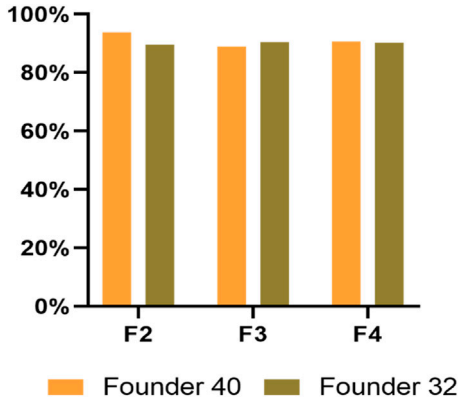

FIGURE 6 | The cleavage efficiency of *Pxyellow* target site in different generations from both founders.

(χ^2 = 16.34, *df* = 1, p = 0.000) (**Figure 7**). Therefore, the above results indicated that knock-in of gene-drive cassette reduced the fecundity of females.

Crosses between EGFP^{++}Y^{--}female and wild-type male produced less EGFP^{++}Y^{--}progeny than crosses between EGFP^{++}Y^{--}male and wild-type female (F_2, χ^2 = 7.994, *df* = 1, p = 0.004; F_3, χ^2 = 62.684, *df* = 1, p = 0.000; F_4, χ^2 = 104.791, *df* = 1, p = 0.000) (**Figure 8A**). Crosses between EGFP^{++}Y^{--} and wild type produced less EGFP^{++}Y^{--}females than EGFP^{++}Y^{--}males (F_2, χ^2 = 7.641, *df* = 1, p = 0.005; F_3, χ^2 = 112.035, *df* = 1, p = 0.000; F_4, χ^2 = 939.138, *df* = 1, p = 0.000) (**Figure 8B**). Therefore, the gene-drive efficiency caused by parent males was much higher than that caused by parent females. The gene-drive efficiency was much higher in male progeny than in female progeny in *P. xylostella*.

DISCUSSION

The *Pxyellow* gene was selected as the target site for the confirmation of phenotypic changes in *P. xylostella*. The CRISPR/Cas9-mediated knockout of *Pxyellow* gene demonstrated the change of body and head capsule color from black to yellowish. The change in body and head capsule color was quite apparent in the second and third instar larvae. A similar kind of results are previously reported, in which the *Pxyellow* gene plays an essential role in body pigmentations in *P. xylostella* (Wang et al., 2020). To develop an effective gene-drive system to evaluate drive efficiency and fitness cost, it is an appropriate way to target endogenous phenotypic marker genes, which help in screening mutant progeny. A CCGD system has previously been developed in *Drosophila melanogaster*, in which phenotypic marker *yellow* and *white* genes are used as the target sites (Champer et al., 2017; Champer et al., 2018; Champer et al., 2019). Similarly, this system has been developed in mosquitos (*Anopheles* and *Aedes*), in which the *white-eye* phenotypic marker gene is used as the target site (Gantz et al., 2015;

TABLE 1 | Genotypes of F_2 progeny of crosses between F_1 EGFP^{++}Y^{--}and wild type.

Cross			Genotype of progeny					
Founder (F_1 EGFP^{++}Y^{--})	WT	Number	Female			Male		
			EGFP^{++}Y^{--}	EGFP^{+-}Y^{--}	EGFP^{+-}Y^{-+}	EGFP^{++}Y^{--}	EGFP^{+-}Y^{--}	EGFP^{+-}Y^{-+}
40 (♂)	♀	1	7	84	7	18	73	5
32 (♀)	♂	1	3	67	6	7	35	7
Total			10	151	13	25	108	12

TABLE 2 | Genotypes of F_3 progeny of crosses between F_2 EGFP^{++}Y^{--} and wild type.

Cross			Genotype of progeny					
EGFP^{++}Y^{--}parent		Number	Female			Male		
Founder	Sex		EGFP^{++}Y^{--}	EGFP^{+-}Y^{--}	EGFP^{+-}Y^{-+}	EGFP^{++}Y^{--}	EGFP^{+-}Y^{--}	EGFP^{+-}Y^{-+}
40	♀	7		472	78	30	401	35
			14					
	♂	7		765	87	121	592	53
			64					
	Total			1237	165	151	993	88
			78					
32	♀	3		291	50	21	190	32
			6					
	♂	4		412	57	79	264	22
			26					
	Total			703	107	100	454	54
			32					

TABLE 3 | Genotypes of F_4 progeny of crosses between F_3 $EGFP^{++}Y^{--}$and wild type.

Cross			Genotype of progeny					
$EGFP^{++}Y^{--}$ parent		Number	Female			Male		
Founder	Sex		$EGFP^{++}Y^{--}$	$EGFP^{+-}Y^{--}$	$EGFP^{+-}Y^{++}$	$EGFP^{++}Y^{--}$	$EGFP^{+-}Y^{--}$	$EGFP^{+-}Y^{++}$
40	♀	6	2	672	66	30	313	46
	♂	10	5	1575	63	210	678	43
	Total		7	2247	129	240	991	89
32	♀	6	0	548	53	34	419	41
	♂	10	12	1430	70	223	850	62
	Total		12	1978	123	257	1269	103

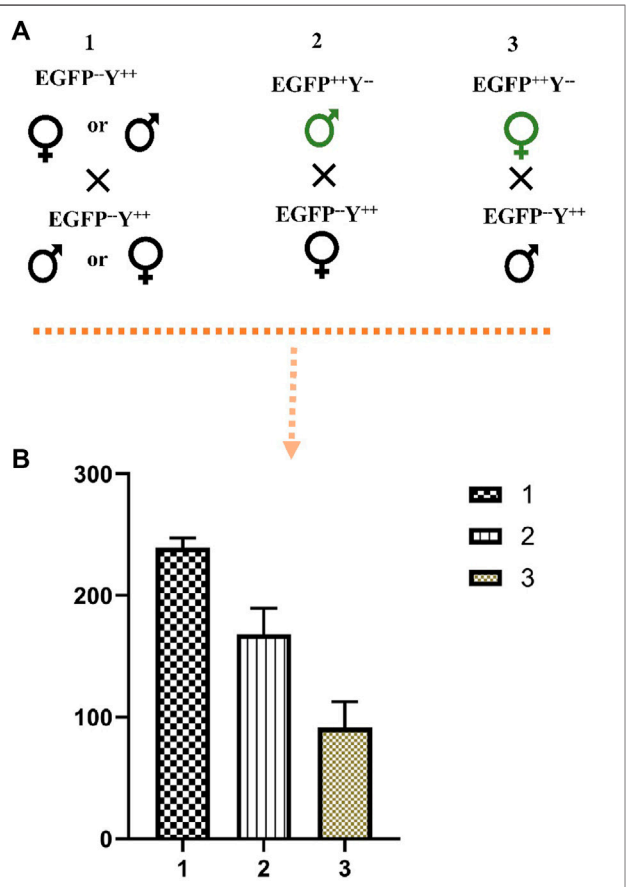

FIGURE 7 | The effect of $EGFP^{++}Y^{--}$parents on the number of progenies. **(A)**, schematic representation of crosses, **(B)**, the number of progenies produced from crosses of different parents; 1, cross between wild-type male and female; 2, cross between $EGFP^{++}Y^{--}$male and wild-type female; 3, cross between $EGFP^{++}Y^{--}$female and wild-type male.

Li et al., 2020). The selection of the phenotypic marker gene provides an easy way to screen the mutant progeny.

The gene-drive cassette worked in lepidopteran pest, *P. xylostella*. The approximately 12-kb long construct could effectively create site-specific mutation. These results are consistent with the previous study conducted in *An. gambiae*, in which approximately 17-kb construct shows its feasibility to create site-specific cleavage (Gantz et al., 2015). Additionally, the overall cleavage efficiency of neighboring allele of 88.86–93.82%, gene-drive of 6.67%–12.59%, and resistant-allele formation of 80.93%–86.77% were observed. Surprisingly, the gene-drive efficiency was much lower than other insects. Certain factors might be involved in the low gene-drive efficiency, either gene-drive component or the target site, associated with the fitness cost. The differences in the gene-drive efficiency depend upon numerous factors, such as species-specific factors, variations in the *Cas9* expression, and the genomic target site. The species-specific factor might contribute to the low gene-drive efficiency in *P. xylostella* because the enormous variations across the species were observed, such as close to 100% in yeast *Saccharomyces cerevisiae* (Dicarlo et al., 2015; Roggenkamp et al., 2018; Shapiro et al., 2018), 19%–62% in *D. melanogaster* (Champer et al., 2017; Champer et al., 2018; Karaminejadranjbar et al., 2018; Champer et al., 2019) and 87%–99% in *An. gambiae* (Gantz et al., 2015; Kyrou et al., 2018; Li et al., 2020). Therefore, different species may have different gene-drive efficiencies.

The expression of Cas9 in somatic and germline tissues also plays a crucial role in gene-drive efficiency. In *D. melanogaster*, the germline-specific *nanos* and *vasa* promoters were used to drive *Cas9* gene expression for the development of the CCGD system. The *nanos* promoter construct to drive *Cas9* exhibits a high gene-drive efficiency and a low resistant-allele formation due to the low *Cas9* expression in somatic tissues. In contrast, the construct containing *vasa* promoter to drive *Cas9* exhibits a high resistant-allele formation and a low gene-drive efficiency due to the high *Cas9* expression in somatic tissues (Champer et al., 2018). In *An. stephensi,* the *vasa* promoter used to drive the Cas9 expressions results in a high germline gene conversion through HDR-mediated repair (99%) (Gantz et al., 2015). Recently, the different germline-specific promoters of *P. xylostella* have been tested in the CRISPR/Cas9-mediated split-drive system. All these tested promoters show a high somatic cleavage with limited germline cleavage. However, no homing is observed in this CRISPR/Cas9 split drive (Xu et al., 2022). Therefore, the selection of germline-specific promoters to drive the *Cas9* expression is critical. In our study, the PxnanosP showed a high frequency of resistant-allele formation rather than gene-drive in *P. xylostella*, which might be due to a high *Cas9* expression driven by PxnanosP in somatic tissues.

Another factor that may contribute to the gene-drive efficiency is the genomic target site of gRNA. In *D. melanogaster*, the *nanos* promoter-based gene-drive construct targeting the two different

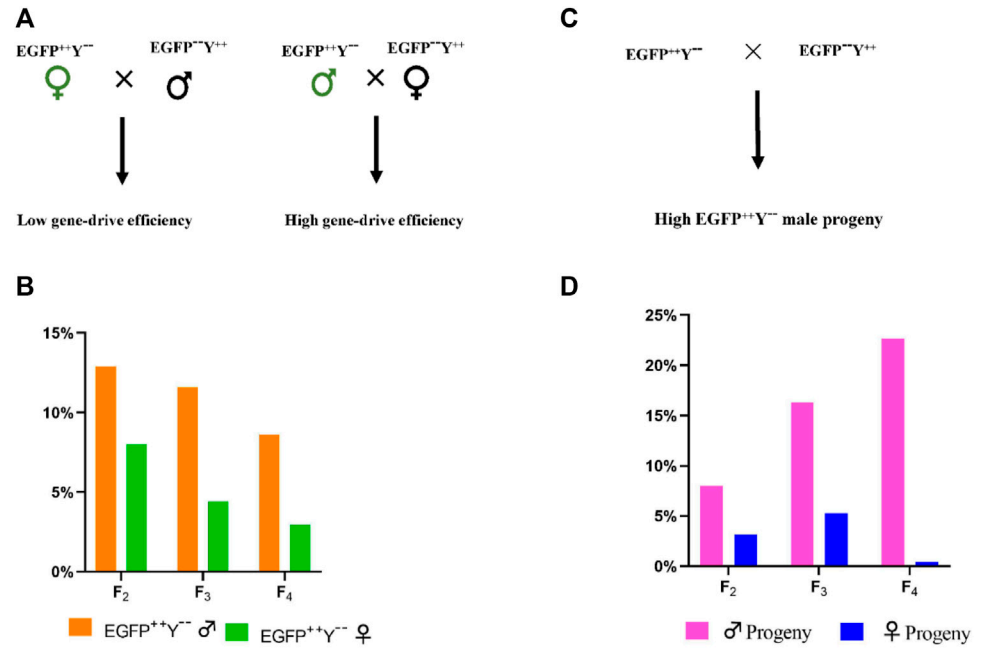

FIGURE 8 | The difference in gene-drive efficiency caused by the male and female parents. **(A)**, schematic representation of $EGFP^{++}Y^{--}$parents cross with wild-type parents, **(B)**, the gene-drive percentage caused by $EGFP^{++}Y^{--}$male and female parents; **(C)**, representation of crosses, **(D)**, percentage of male and female progeny with $EGFP^{++}Y^{--}$genotype.

genomic target sites, such as the *white* gene and *cinnabar* gene, exhibits different gene-drive efficiency (59% and 38%) (Champer et al., 2018; Champer et al., 2019). Similarly, the *vasa* promoter-based gene-drive construct targeting the two different genomic target sites, such as *yellow* gene and *yellow* gene promoter, showed 55% and 37% gene-drive efficiency, respectively (Champer et al., 2017). Hence, the different genomic target sites cause different gene-drive efficiencies. In our study, the *yellow* gene was targeted, which might contribute to a low gene-drive efficiency. Therefore, more targets should be identified and tested to achieve a high gene-drive efficiency.

The gene-drive efficiency caused by the parent male was much higher than that caused by parent female, and the gene-drive efficiency was much higher in male progeny than in female progeny in *P. xylostella*. Previous studies exhibit that the maternally-deposited *Cas9* contributes to the development of resistant alleles in *An. stephensi* (Gantz et al., 2015). Similarly, in *D. melanogaster,* resistant-allele formation is due to the high maternal-deposition of *Cas9* in eggs before fertilization or embryo development (Champer et al., 2017; Champer et al., 2018; Champer et al., 2019; Kandul et al., 2020). Therefore, the low gene-drive efficiency and high resistant-allele formation in progeny derived from transgenic females are due to the high level of maternally-deposited Cas9. The knock-in of gene-drive construct reduced the fecundity of transgenic females. The high Cas9 expression may have some side effects, reducing fecundity. Further studies are required to answer this question.

Toward the success of CRISPR/Cas9-mediated gene drive for pest control, it is essential to increase the gene-drive efficiency. The gene-drive efficiency is much lower in *P. xylostella* than in other insects. The problem of low gene-drive efficiency can be tackled with different approaches. The selection of suitable germline promoters can effectively drive Cas9 expression in germ cells and cause DSB followed by homing during gametogenesis (Hammond et al., 2016). Multiplex gRNAs targeting the different locus of a gene may increase the gene-drive efficiency (Champer et al., 2018). Suppression of NHEJ pathway genes may increase the rate of HDR (Zhu et al., 2015). As in *B. mori*, it has been described that the suppression of NHEJ-pathway genes, such as *BmKu70* and *BmKu80*, increases the HDR-mediated repair (Zhu et al., 2015). Since the gene-drive efficiency is low, further studies are required to understand the mechanism of resistant-allele formation for increasing the gene-drive efficiency.

CONCLUSION

In general, our data demonstrated that the CRISPR/Cas9-mediated gene-drive construct worked in *P. xylostella* through effectively copying the gene-drive components to the target site, and the NHEJ event happened more than the HDR. The progeny derived from mutant male parents showed a relatively-high gene-drive efficiency than those from mutant female parents. These results provided a foundation for further development of the CCGD system in *P. xylostella,* especially for the pest management program. Our results also provide a valuable information for future construction of highly improved and optimized CRISPR/Cas9-mediated

gene-drive for genetic control of globally-distributed pest *P. xylostella*.

DATA AVAILABILITY STATEMENT

The original contributions presented in the study are included in the article/**Supplementary Material**, further inquiries can be directed to the corresponding author.

AUTHOR CONTRIBUTIONS

Conceptualization, MA, and GY; methodology, MA; formal analysis, MA, and DL; investigation, MA, DL, and JL, data curation, MA, DL, and JC writing—original draft preparation, MA; writing—review and editing, MA, DL, and GY; supervision, GY; funding acquisition, GY. All authors have read and agreed to the published version of the manuscript.

FUNDING

This work was supported by the project of National Natural Science Foundation of China (3172237), the Special Key Project of Fujian Province (2018NZ01010013); and "111" program (KRA16001A).

ACKNOWLEDGMENTS

Authors are thankful to all lab members for their support to conduct the study.

SUPPLEMENTARY MATERIAL

The Supplementary Material for this article can be found online at: https://www.frontiersin.org/articles/10.3389/fphys.2022.938621/full#supplementary-material

REFERENCES

Ågren, J. A. (2016). Selfish Genetic Elements and the Gene's-Eye View of Evolution. *Curr. Zool.* 62, 659–665. doi:10.1093/cz/zow102

Akbari, O. S., Bellen, H. J., Bier, E., Bullock, S. L., Burt, A., Church, G. M., et al. (2015). Safeguarding Gene Drive Experiments in the Laboratory. *Science* 349, 927–929. doi:10.1126/science.aac7932

Akbari, O. S., Chen, C.-H., Marshall, J. M., Huang, H., Antoshechkin, I., and Hay, B. A. (2014). Novel Synthetic Medea Selfish Genetic Elements Drive Population Replacement in Drosophila; a Theoretical Exploration of Medea-dependent Population Suppression. *ACS Synth. Biol.* 3, 915–928. doi:10.1021/sb300079h

Asad, M., Munir, F., Xu, X., Li, M., Jiang, Y., Chu, L., et al. (2020). Functional Characterization of Thecis-regulatory Region for the Vitellogenin Gene in *Plutella xylostella*. *Insect Mol. Biol.* 29, 137–147. doi:10.1111/imb.12632

Bassett, A. R., Tibbit, C., Ponting, C. P., and Liu, J.-L. (2013). Highly Efficient Targeted Mutagenesis of *Drosophila* with the CRISPR/Cas9 System. *Cell Rep.* 4, 220–228. doi:10.1016/j.celrep.2013.06.020

Buchman, A. B., Ivy, T., Marshall, J. M., Akbari, O. S., and Hay, B. A. (2018). Engineered Reciprocal Chromosome Translocations Drive High Threshold, Reversible Population Replacement in *Drosophila*. *ACS Synth. Biol.* 7, 1359–1370. doi:10.1021/acssynbio.7b00451

Buchman, A., Gamez, S., Li, M., Antoshechkin, I., Li, H.-H., Wang, H.-W., et al. (2020). Broad Dengue Neutralization in Mosquitoes Expressing an Engineered Antibody. *PLoS Pathog.* 16, e1008103. doi:10.1371/journal.ppat.1008103

Champer, J., Chung, J., Lee, Y. L., Liu, C., Yang, E., Wen, Z., et al. (2019). Molecular Safeguarding of CRISPR Gene Drive Experiments. *eLife* 8, e41439. doi:10.7554/eLife.41439

Champer, J., Reeves, R., Oh, S. Y., Liu, C., Liu, J., Clark, A. G., et al. (2017). Novel CRISPR/Cas9 Gene Drive Constructs Reveal Insights into Mechanisms of Resistance Allele Formation and Drive Efficiency in Genetically Diverse Populations. *PLoS Genet.* 13, e1006796–1006802. doi:10.1371/journal.pgen.1006796

Champer, J., Buchman, A., and Akbari, O. S. (2016). Cheating Evolution: Engineering Gene Drives to Manipulate the Fate of Wild Populations. *Nat. Rev. Genet.* 17, 146–159. doi:10.1038/nrg.2015.34

Champer, J., Liu, J., Oh, S. Y., Reeves, R., Luthra, A., Oakes, N., et al. (2018). Reducing Resistance Allele Formation in CRISPR Gene Drive. *Proc. Natl. Acad. Sci. U.S.A.* 115, 5522–5527. doi:10.1073/pnas.1720354115

Champer, J., Zhao, J., Champer, S. E., Liu, J., and Messer, P. W. (2020). Population Dynamics of Underdominance Gene Drive Systems in Continuous Space. *ACS Synth. Biol.* 9, 779–792. doi:10.1021/acssynbio.9b00452

Chen, C.-H., Huang, H., Ward, C. M., Su, J. T., Schaeffer, L. V., Guo, M., et al. (2007). A Synthetic Maternal-Effect Selfish Genetic Element Drives Population Replacement in *Drosophila*. *Science* 316, 597–600. doi:10.1126/science.1138595

Chen, J., Luo, J., Wang, Y., Gurav, A. S., Li, M., Akbari, O. S., et al. (2021). Suppression of Female Fertility in *Aedes aegypti* with a CRISPR-Targeted Male-Sterile Mutation. *Proc. Natl. Acad. Sci. U. S. A.* 118, e2105075118. doi:10.1073/pnas.2105075118

Cong, L., Ran, F. A., Cox, D., Lin, S., Barretto, R., Habib, N., et al. (2013). Multiplex Genome Engineering Using CRISPR/Cas Systems. *Science* 339, 819–823. doi:10.1126/science.1231143

Deredec, A., Burt, A., and Godfray, H. C. J. (2008). The Population Genetics of Using Homing Endonuclease Genes in Vector and Pest Management. *Genetics* 179, 2013–2026. doi:10.1534/genetics.108.089037

Dicarlo, J. E., Chavez, A., Dietz, S. L., Esvelt, K. M., and Church, G. M. (2015). Safeguarding CRISPR-Cas9 Gene Drives in Yeast. *Nat. Biotechnol.* 33, 1250–1255. doi:10.1038/nbt.3412

Esvelt, K. M., Smidler, A. L., Catteruccia, F., and Church, G. M. (2014). Emerging Technology: Concerning RNA-Guided Gene Drives for the Alteration of Wild Populations. *eLife* 3, e03401. doi:10.7554/eLife.03401

Furlong, M. J., Wright, D. J., and Dosdall, L. M. (2013). Diamondback Moth Ecology and Management: Problems, Progress, and Prospects. *Annu. Rev. Entomol.* 58, 517–541. doi:10.1146/annurev-ento-120811-153605

Gantz, V. M., Jasinskiene, N., Tatarenkova, O., Fazekas, A., Macias, V. M., Bier, E., et al. (2015). Highly Efficient Cas9-Mediated Gene Drive for Population Modification of the Malaria Vector Mosquito *Anopheles stephensi*. *Proc. Natl. Acad. Sci. U. S. A.* 112, E6736–E6743. doi:10.1073/pnas.1521077112

Gantz, V. M., and Bier, E. (2015). The Mutagenic Chain Reaction: a Method for Converting Heterozygous to Homozygous Mutations. *Science* 348, 442–444. doi:10.1126/science.aaa5945

Gong, P., Epton, M. J., Fu, G., Scaife, S., Hiscox, A., Condon, K. C., et al. (2005). A Dominant Lethal Genetic System for Autocidal Control of the Mediterranean Fruitfly. *Nat. Biotechnol.* 23, 453–456. doi:10.1038/nbt1071

Grossman, G. L., Rafferty, C. S., Clayton, J. R., Stevens, T. K., Mukabayire, O., and Benedict, M. Q. (2001). Germline Transformation of the Malaria Vector, *Anopheles gambiae*, with the piggyBac Transposable Element. *Insect Mol. Biol.* 10, 597–604. doi:10.1046/j.0962-1075.2001.00299.x

Grunwald, H. A., Gantz, V. M., Poplawski, G., Xu, X.-R. S., Bier, E., and Cooper, K. L. (2019). Super-Mendelian Inheritance Mediated by CRISPR-Cas9 in the Female Mouse Germline. *Nature* 566, 105–109. doi:10.1038/s41586-019-0875-2

Hammond, A., Galizi, R., Kyrou, K., Simoni, A., Siniscalchi, C., Katsanos, D., et al. (2016). A CRISPR-Cas9 Gene Drive System Targeting Female Reproduction in the Malaria Mosquito Vector *Anopheles gambiae*. *Nat. Biotechnol.* 34, 78–83. doi:10.1038/nbt.3439

Huang, Y., Chen, Y., Zeng, B., Wang, Y., James, A. A., Gurr, G. M., et al. (2016). CRISPR/Cas9 Mediated Knockout of the Abdominal-A Homeotic Gene in the Global Pest, Diamondback Moth (*Plutella xylostella*). *Insect Biochem. Mol. Biol.* 75, 98–106. doi:10.1016/j.ibmb.2016.06.004

Huang, Y., Wang, Y., Zeng, B., Liu, Z., Xu, X., Meng, Q., et al. (2017). Functional Characterization of Pol III U6 Promoters for Gene Knockdown and Knockout in *Plutella xylostella*. *Insect Biochem. Mol. Biol.* 89, 71–78. doi:10.1016/j.ibmb.2017.08.009

Hwang, W. Y., Fu, Y., Reyon, D., Maeder, M. L., Tsai, S. Q., Sander, J. D., et al. (2013). Efficient Genome Editing in Zebrafish Using a CRISPR-Cas System. *Nat. Biotechnol.* 31, 227–229. doi:10.1038/nbt.2501

Jinek, M., Chylinski, K., Fonfara, I., Hauer, M., Doudna, J. A., and Charpentier, E. (2012). A Programmable Dual-RNA-Guided DNA Endonuclease in Adaptive Bacterial Immunity. *Science* 337, 816–821. doi:10.1126/science.1225829

Kandul, N. P., Liu, J., Buchman, A., Gantz, V. M., Bier, E., and Akbari, O. S. (2020). Assessment of a Split Homing Based Gene Drive for Efficient Knockout of Multiple Genes. *G3 (Bethesda)* 10, 827–837. doi:10.1534/g3.119.400985

Karaminejadranjbar, M., Eckermann, K. N., Ahmed, H. M. M., Sánchez C, H. M., Dippel, S., Marshall, J. M., et al. (2018). Consequences of Resistance Evolution in a Cas9-Based Sex Conversion-Suppression Gene Drive for Insect Pest Management. *Proc. Natl. Acad. Sci. U. S. A.* 115, 6189–6194. doi:10.1073/pnas.1713825115

Kyrou, K., Hammond, A. M., Galizi, R., Kranjc, N., Burt, A., Beaghton, A. K., et al. (2018). A CRISPR-Cas9 Gene Drive Targeting Doublesex Causes Complete Population Suppression in Caged *Anopheles gambiae* Mosquitoes. *Nat. Biotechnol.* 36, 1062–1066. doi:10.1038/nbt.4245

Li, M., Yang, T., Kandul, N. P., Bui, M., Gamez, S., Raban, R., et al. (2020). Development of a Confinable Gene Drive System in the Human Disease Vector *Aedes aegypti*. *eLife* 9, e51701. doi:10.7554/eLife.51701

Mali, P., Yang, L., Esvelt, K. M., Aach, J., Guell, M., Dicarlo, J. E., et al. (2013). RNA-guided Human Genome Engineering via Cas9. *Science* 339, 823–826. doi:10.1126/science.1232033

Marshall, J. M., and Hay, B. A. (2012). Confinement of Gene Drive Systems to Local Populations: a Comparative Analysis. *J. Theor. Biol.* 294, 153–171. doi:10.1016/j.jtbi.2011.10.032

Martins, S., Naish, N., Walker, A. S., Morrison, N. I., Scaife, S., Fu, G., et al. (2012). Germline Transformation of the Diamondback Moth, *Plutella xylostella* L., Using the piggyBac Transposable Element. *Insect Mol. Biol.* 21, 414–421. doi:10.1111/j.1365-2583.2012.01146.x

Roggenkamp, E., Giersch, R. M., Schrock, M. N., Turnquist, E., Halloran, M., and Finnigan, G. C. (2018). Tuning CRISPR-Cas9 Gene Drives in *Saccharomyces cerevisiae*. *G3 (Bethesda)* 8, 999–1018. doi:10.1534/g3.117.300557

Shapiro, R. S., Chavez, A., Porter, C. B. M., Hamblin, M., Kaas, C. S., Dicarlo, J. E., et al. (2018). A CRISPR-Cas9-Based Gene Drive Platform for Genetic Interaction Analysis in *Candida Albicans*. *Nat. Microbiol.* 3, 73–82. doi:10.1038/s41564-017-0043-0

Unckless, R. L., Clark, A. G., and Messer, P. W. (2017). Evolution of Resistance against CRISPR/Cas9 Gene Drive. *Genetics* 205, 827–841. doi:10.1534/genetics.116.197285

Unckless, R. L., Messer, P. W., Connallon, T., and Clark, A. G. (2015). Modeling the Manipulation of Natural Populations by the Mutagenic Chain Reaction. *Genetics* 201, 425–431. doi:10.1534/genetics.115.177592

Valderrama, J. A., Kulkarni, S. S., Nizet, V., and Bier, E. (2019). A Bacterial Gene-Drive System Efficiently Edits and Inactivates a High Copy Number Antibiotic Resistance Locus. *Nat. Commun.* 10, 5726–5732. doi:10.1038/s41467-019-13649-6

Wang, Y., Huang, Y., Xu, X., Liu, Z., Li, J., Zhan, X., et al. (2020). CRISPR/Cas9-based Functional Analysis of Yellow Gene in the Diamondback Moth, *Plutella xylostella*. *Insect Sci.* 27, 1–6. doi:10.1111/1744-7917.12870

Werren, J. H. (2011). Selfish Genetic Elements, Genetic Conflict, and Evolutionary Innovation. *Proc. Natl. Acad. Sci. U. S. A.* 108 (Suppl. 2), 10863–10870. doi:10.1073/pnas.1102343108

Werren, J. H., Nur, U., and Wu, C.-I. (1988). Selfish Genetic Elements. *Trends Ecol. Evol.* 3, 297–302. doi:10.1016/0169-5347(88)90105-x

Xu, J., Chen, R. M., Chen, S. Q., Chen, K., Tang, L. M., Yang, D. H., et al. (2019). Identification of a Germline-Expression Promoter for Genome Editing in *Bombyx mori*. *Insect Science* 26 (6), 991–999.

Xu, X., Harvey-Samuel, T., Siddiqui, H. A., Ang, J. X. D., Anderson, M. E., Reitmayer, C. M., et al. (2022). Toward a CRISPR-Cas9-Based Gene Drive in the Diamondback Moth *Plutella xylostella*. *CRISPR J.* 5, 224–236. doi:10.1089/crispr.2021.0129

You, M., Yue, Z., He, W., Yang, X., Yang, G., Xie, M., et al. (2013). A Heterozygous Moth Genome Provides Insights Into Herbivory and Detoxification. *Nature Genetics* 45 (2), 220–225.

Zhu, L., Mon, H., Xu, J., Lee, J. M., and Kusakabe, T. (2015). CRISPR/Cas9-mediated Knockout of Factors in Non-homologous End Joining Pathway Enhances Gene Targeting in Silkworm Cells. *Sci. Rep.* 5, 18103. doi:10.1038/srep18103

Conflict of Interest: The authors declare that the research was conducted in the absence of any commercial or financial relationships that could be construed as a potential conflict of interest.

Publisher's Note: All claims expressed in this article are solely those of the authors and do not necessarily represent those of their affiliated organizations, or those of the publisher, the editors and the reviewers. Any product that may be evaluated in this article, or claim that may be made by its manufacturer, is not guaranteed or endorsed by the publisher.

frontiers | Frontiers in Physiology

TYPE Original Research
PUBLISHED 30 August 2022
DOI 10.3389/fphys.2022.979472

OPEN ACCESS

EDITED BY
Seema Ramniwas,
Chandigarh University, India

REVIEWED BY
Divya Singh,
Chandigarh University, India
Youji Wang,
Shanghai Ocean University, China
Jia-Song Zhang,
South China Sea Fisheries Research Institute (CAFS), China
Xianyun Ren,
Yellow Sea Fisheries Research Institute (CAFS), China

*CORRESPONDENCE
Xiaobing Wang,
wangxiaobing4000@163.com
Hailong Zhou,
zhouhl@hainanu.edu.cn
Xianming Tang,
hn.tangxm@aliyun.com

†These authors share first authorship

SPECIALTY SECTION
This article was submitted to Invertebrate Physiology, a section of the journal Frontiers in Physiology

RECEIVED 27 June 2022
ACCEPTED 02 August 2022
PUBLISHED 30 August 2022

CITATION
Chang F, Li N, Shi X, Olga V, Wang X, Diao X, Zhou H and Tang X (2022), Physiological and muscle tissue responses in *Litopenaeus vannamei* under hypoxic stress *via* iTRAQ. *Front. Physiol.* 13:979472. doi: 10.3389/fphys.2022.979472

Physiological and muscle tissue responses in *Litopenaeus vannamei* under hypoxic stress *via* iTRAQ

Fengtong Chang[1,2], Na Li[1,2†], Xiang Shi[1,2], Volovych Olga[1,2], Xiaobing Wang[1,2,4*], Xiaoping Diao[1], Hailong Zhou[1,2,4*] and Xianming Tang[3*]

[1]State Key Laboratory of South China Sea Marine Resource Utilisation, Hainan University, Haikou, China, [2]School of Life Sciences, Hainan University, Haikou, China, [3]Hainan Provincial Key Laboratory of Tropical Maricultural Technology, Hainan Academy of Ocean and Fisheries Sciences, Haikou, Hainan, China, [4]One Health Institute, Hainan University, Haikou, Hainan, China

White *L. vannamei* have become the most widely cultivated shrimp species worldwide. Cultivation of *L. vannamei* is one of the predominant sectors in China's aquaculture industry. This study focused on the physiological and biochemical responses, differential protein expression, and expression characteristics of the related crucial functional protein genes under low oxygen conditions among different strains of *L. vannamei*. It was found that 6 h of hypoxic stress caused a significant reduction in the total hemocyte number in both strains, while the hypoxia-sensitive strain showed a stronger reduction. In contrast, the hemocyanin concentration showed only an overall upward trend. Proteomic analysis of *L. vannamei* muscle tissue revealed 3,417 differential proteins after 12 h of hypoxic stress. Among them, 29 differentially expressed proteins were downregulated and 244 were upregulated in the hypoxia-sensitive strain. In contrast, there were only 10 differentially expressed proteins with a downregulation pattern and 25 with an upregulation pattern in the hypoxia-tolerant strain. Five protein genes that responded significantly to hypoxic stress were selected for quantitative real-time PCR analysis, namely, hemocyanin, chitinase, heat shock protein 90 (HSP 90), programmed death protein, and glycogen phosphorylase. The results showed that the gene expression patterns were consistent with proteomic experimental data except for death protein and glycogen phosphorylase. These results can enrich the general knowledge of hypoxic stress in *L. vannamei* and the information provided differentially expressed proteins which may be used to assist breeding programs of *L. vannamei* of new strains with tolerance to hypoxia.

KEYWORDS

***Litopenaeus vannamei*, hypoxia stress, physiological responses, proteome, real-time quantitative PCR**

Introduction

Dissolved oxygen (DO) is an important factor in the aquatic environment and an indicator of water quality. The concentration of DO in water is normally approximately 6 mg/L, while lower than 2.8 mg/L is referred hypoxia (Diaz and Rosenberg 1995). Global climate change and human activities intensified hypoxic conditions in marine ecosystems especially in coastal areas around the world (Breitburg et al., 2018). The expansion of hypoxic areas in the open ocean and coastal waters are expected to continue and will have a great impact on the ecosystem and biodiversity (Keeling, Kortzinger and Gruber 2010).

Animal responses to hypoxic stress are divided into physiological, biochemical, and behavioral responses. A physiological response includes changes in heart rate, respiratory metabolism, cell proliferation, and apoptosis, hemocyanin level, immune response, antioxidant capacity, and osmotic regulation ability. Hypoxic environments may also alter the expression of certain genes that subsequently leads to a series of biochemical and physiological responses, which allow organisms to survive in such conditions.

It's been reported that hypoxia can elicit adverse effects on the behavior, growth, development, respiration, metabolism, immunity, DNA damage, and gene expression of aquatic organisms (Levin et al., 2009; Guadagnoli, Tobita and Reiber 2011; Zhou et al., 2014; Li et al., 2016). Various studies found that the rate of growth, weight gain, and feed utilization in channel catfish (*Ictalurus punctatus*), Atlantic cod (*Gadus morhua*), fish (*Leporinus elongates*), and silver catfish (*Rhamdia quelen*) were decreased under hypoxic conditions (Buentello et al., 2000; Chabot and Biology. 2005; Filho et al., 2005; Riffel et al., 2014). An extensive study of red-eared turtles under hypoxic stress revealed changes in carbohydrate metabolism and the antioxidant defense system. Along with the increase in hypoxic duration, the contents of lactic acid and blood glucose in the blood increased rapidly, while the glycogen in skeletal muscle and liver was gradually consumed (Ye et al., 2011).

According to a report by Gray, Wu and Ying (2002), the anoxic resistance of aquatic animals decreases in the following order: mollusks, annelids, echinoderms, crustaceans, and fish. Shrimp and other marine invertebrates lack adaptive immune mechanisms and rely on innate immune responses to cope with environmental stress (Tassanakajon et al., 2018). Currently, research on the effects of hypoxia on prawns and other crustaceans is mainly focused on changes in innate immune system parameters, such as total hemocyte counts (THCs) and hemocyanin concentrations (HCs), which could reveal possible adaptations to hypoxic conditions. Chen *et al.* found that the THC of scallop (*Chlamys farreri*) gradually and significantly decreased with a decline in the DO level to 2.5 mg/L (Chen et al., 2007). A similar study was performed on freshwater prawn (*Macrobrachium rosenbergii*) and revealed a reduction in THC by 36% after 12 h in a 2.75 mg/L DO concentration environment (Cheng and Chen 2000). In response to hypoxia, shrimp can increase their HC to maintain oxygen transport. In a related study, two strains of *L. vannamei* had significantly decreased THCs under hypoxic stress, while having significantly increased HCs (Wei Y et al., 2016).

The rapid development of proteomics technology in recent years has allowed its wide application in the study of aquatic crustacean pathogen infection (Chongsatja et al., 2007; Wang et al., 2007). For example, a combination of two-dimensional (2-DE) electrophoresis, mass spectrometry, and bioinformatics tools was used to discover the major allergen of freshwater prawn (*Macrobrachium rosenbergii*) (Yadzir et al., 2012). However, only a few studies have reported the hypoxic stress response in crustaceans using this approach, one of which is the investigation of hypoxia effects on oriental river prawn (*Macrobrachium nipponense*) muscle proteome using a 2D-gel-based proteomics approach coupled with mass spectrometry (MS) (Sun et al., 2016).

In marine crustaceans, changes in gene expression often underlie or reflect key physiological and biochemical acclimations to hypoxia, which has been verified by global transcriptome profiling by microarrays (Li and Brouwer, 2013). Crustaceans also respond to hypoxia by altering levels of respiratory pigments, antioxidant proteins, and enzymes involved in glycolysis, amino acid and nucleotide metabolism (Brouwer et al., 2004; Abe et al., 2007; Jiang et al., 2009). Particularly, the glycolytic enzymes hexokinase (HK), phosphofructokinase (PFK), lactate dehydrogenase (LDH) (Cota-Ruiz et al., 2015; Ulaje et al., 2019), and glyceraldehyde-3-phosphate dehydrogenase (GAPDH) (Camacho-Jim´enez et al., 2018) can be induced differentially in tissues of *L. vannamei* in response to hypoxia.

L. vannamei is one of the main species in the global shrimp aquaculture business with important economic value. However, due to the rapid economic development of coastal zones, the higher frequency of hypoxia caused an increase in expenses for rearing diets. Hypoxia has become one of the major problems that affect the normal growth and development of *L. vannamei*, and it seriously restricts the sustainable aquaculture of the species.

Additionally, the muscle tissue of *L. vannamei* takes up most of the body mass and uses a lot of oxygen, however, the responses of shrimp muscle tissues to hypoxia remain unknown. Therefore, deep investigation of the hypoxia stress response of muscle tissue, THC, HC and related genes, which can not only enrich a general understanding of the hypoxia effect and mechanisms of hypoxia tolerance, but also can provide novel insights into the assisting breeding of new shrimp strains with higher resistance to low oxygen conditions.

Materials and methods

Shrimp and hypoxia stress

The shrimp (13 ± 0.5 cm) used in the experiment were all from Hainan Guangtai Marine Culture Co., Ltd. (Wenchang City, Hainan Province, China). Only shrimp in the inter-molt stage and similar size of juvenile shrimp were used in the experiments. Before the formal experiment, they were acclimated in the aquarium for 3 days, during which the seawater salinity was 1.9% ± 0.2%, the pH value was 8.1 ± 0.2, and the temperature was 27°C ± 1°C. Food was given twice a day (no feeding during molting and hypoxic stress), and half of the seawater was changed in the bucket every day. The content of DO under hypoxic stress was 0.5 ppm, and the stress times were 0 p.m., 3 p.m., 6 h, and 12 h. The level of dissolved oxygen was maintained by filling the barrel with nitrogen.

Two different strains of *L. vannamei*, namely Zhengda and A6410 were selected for this study. The former is hypoxia-sensitive strain and the latter is hypoxia-tolerant strain. Study has shown that the HIF-1 (Hypoxia-inducible Factor 1) expression quantity of the strain Zhengda was always higher than strain A6410 in the whole phase of hypoxia, the A6410 strain did not need more HIF-1 expression to regulate target genes to deal with hypoxic stress compared to strain Zhengda at the same level of hypoxia, which indicated that strain A6410 has better hypoxia tolerance than strain Zhenda (Wei L et al., 2016).

Hemolymph collection and measuring of total hemocyte counts and hemocyanin concentrations

Three shrimps were randomly selected from each replicate, and there have three replicates at different hypoxia treatments, which used to measure the parameter of THC and HC. Pericardial blood was drawn from shrimp with a 1 ml syringe and mixed with anticoagulants (30 mM trisodium citrate, 0.34 M sodium chloride, 10 mM EDTA, and 0.115 M glucose) of the same volume on the ice. A hemolymph volume of 10 μl was absorbed by a microtransfer gun and counted under a light microscope, and the appropriate amount of hemolymph was centrifuged at 4°C and 5,000×g for 10 min. Then, 100 μl supernatant was taken and mixed with 2,900 μl of buffer solution (50 mM Tris, 10 mM $CaCl_2$, and pH = 8.0). The absorbance values of the diluted plasma were measured at 335 nm using a UV spectrophotometer (1 cm path length) (PerkinElmer Lambda 25). The hemocyanin concentration (unit: $mg.ml^{-1}$) was calculated using the following formula: $E_{335\ nm}$ ($mg.ml^{-1}$) = 2.3×$OD_{335\ nm}$ (E stands for HC; 2.3 is the extinction coefficient of hemocyanin for $mg.mL^{-1}$) (Yang and Pan 2013; Wei Y et al., 2016).

Protein extraction and digestion

The muscle of the three individuals from each treatment were mixed equally, so total nine samples for each group were subjected to protein extraction. The muscle tissues of two strains of *L. vannamei* after 0 h and 12 h hypoxia were selected respectively as proteomics experimental materials. For the convenience of bioinformatics analysis of data, the samples of hypoxia with 0 h were defined as control I and experiment I respectively. Correspondingly, samples of hypoxia with 12 h were defined as control II and experiment II respectively. The sample was ground with liquid nitrogen, transferred to precooled cracking buffer (8 M urea, 40 mM Tris-HCl or TEAB with 1 mM PMSF, 2 mM EDTA, and 10 mM DTT, pH = 8.5), and ultrasonically treated for 2 min to release proteins. After centrifugation at 25,000×g for 20 min at 4°C, the supernatant was transferred to a new test tube, reduced with 10 mM dithiothreitol (DTT) at 56°C for 1 h, and alkylated for 45 min in the dark with 55 mM iodoacetamide (IAM) at room temperature. After centrifugation (25,000×g, 4 °C, 20 min), the protein-rich supernatant was quantified by a standard Bradford protein assay. The extracted protein samples were analyzed by SDS–PAGE electrophoresis with Coomassie brilliant blue gel staining. The protein solution (100 μg) with 8 M urea was diluted 4-fold with 100 mM TEAB. Trypsin Gold (Promega, Madison, WI, United States) was used to digest the proteins at a protein: trypsin ratio of 40:1 at 37°C overnight. After trypsin digestion, peptides were desalted with a Strata X C 18 column (Phenomenex) and vacuum-dried according to the manufacturer's protocol.

Labeling and grading of polypeptides

After trypsin digestion, the peptides were dissolved by adding 30 μl of 0.5 M TEAB, and the iTRAQ labeling reagents were transferred and combined with samples at room temperature. Peptide labeling was performed using the iTRAQ reagent 8-Plex kit, according to the manufacturer's operating procedures. Labeled peptides of different reagents were desalted with a combination of Strata X C18 columns (Phenomenex) and vacuum-dried according to manufacturer specifications. The peptides were separated by the Shimadzu LC-20AB HPLC Pump system coupled with a high pH RP column. The peptides were reconstituted with buffer A [ACN:H_2O (1:19), pH = 9.8 adjusted with ammonia] to a total volume of 2 ml and loaded onto a column containing 5 μm particles (Phenomenex). The peptides were separated at a flow rate of 1 ml/min in the following sequence: 5% buffer B [H_2O:ACN (1:19), pH = 9.8 adjusted with ammonia] for 10 min, 5%–35% buffer B for 40 min, and 35%–95% buffer B for 1 min. The system was maintained in 95% buffer B for 3 min and then in 5% buffer B for 1 min before equilibration with 5% buffer B for 10 min.

Elution was monitored by measuring the absorbance at 214 nm, and its fractions were collected every minute. The eluted peptides were pooled as 20 fractions and dried by vacuum.

HPLC analysis

Each fraction was resuspended in buffer A (2% ACN and 0.1% FA in water) and centrifuged at 20,000×g for 10 min. The supernatant was loaded onto a C18 trap column at 5 μl/min for 8 min using an LC-20AD nano-HPLC instrument (Shimadzu, Kyoto, Japan) by an autosampler. The peptides were eluted with a trap column and then separated by an analytical C18 column (inner diameter 75 μm) packed in-house. The gradient was run at a rate of 300 nl/min starting with 8%–35% buffer B (2% H_2O and 0.1% FA in ACN) for 35 min and then 60% buffer B for 5 min followed by 80% buffer B for 5 min. At the final stage, 5% buffer B was used for 0.1 min and equilibrated for 10 min.

Bioinformatics analysis

High-resolution mass spectrometry data were used for further analysis. The DDA data were evaluated using MaxQuant's integrated Andromeda engine with further spectrum library generation with Spectronaut. For large-scale DIA data, Spectronaut was used constructed spectral database information to complete deconvolution extraction of data, and the mProphet algorithm was used to complete quality control of data analysis by obtaining a large number of reliable quantitative results. GO, COG, and pathway annotation analysis were also performed during this step. The cohort of differentially expressed proteins among different comparison groups was identified based on these results.

Total RNA extraction, reverse transcription, and quantitative real-time-PCR

The muscle of the three individuals from each treatment were mixed equally, so total nine samples for each group were subjected to total RNA extraction. The muscle tissues of two strains of *L. vannamei* after 0 h and 12 h hypoxia were selected respectively as the experimental materials used in RNA extraction, which were consistent with those used in proteome analysis. RNAiso Plus (TaKaRa) was used for total RNA extraction following the manufacturer's protocol. The obtained RNA samples were treated with DNase I (Promega) to remove contaminating DNA. Next, approximately 2000 μg of total RNA was reverse transcribed into cDNA using a GoScript reverse transcription system (Promega) in a 25 μL reaction mixture. The expression of the hemocyanin, chitinase, HSP90, PDCD4, and GP genes was individually determined with quantitative real-time-PCR (qRT–PCR). SYBR green Master I (Roche) was used to perform qRT–PCR using obtained cDNA samples (2 μl) in a 20 μl reaction mixture on a ROCHE LightCycler 96 Real-Time Cycler PCR Detection System (Roche Applied Science, Mannheim, Germany) using the following primers (Table 1). Ribosomal protein L8 was chosen as a reference housekeeping gene (Rojas-Hernandez et al., 2019). qRT–PCR was performed with the following cycling conditions: 94°C, 10 min; (94°C, 15 s; 60°C, 1 min) × 40 cycles. All samples were examined in triplicate on the same plate. qRT–PCR data were normalized using ribosomal protein L8 expression as a reference gene (Rojas-Hernandez et al., 2019). qRT–PCR data were analyzed using the $2^{-\triangle\triangle Ct}$ method (Livak and Schmittgen 2001) and expressed as an n-fold value against the control sample.

Results and discussion

Physiological responses of two strains under the hypoxic stress

In this study, overall, there was no significant change in THC of the two strains after 3 h of hypoxic stress compared to 0 h. However, after 6 and 12 h of hypoxic stress, the THC parameters of the two strains were significantly reduced ($p < 0.05$). Compared with 3 h of hypoxia, 6 h of hypoxia significantly decreased the THC parameter ($p < 0.05$). Compared with hypoxia for 6 h, THC decreased significantly after 12 h of hypoxia ($p < 0.05$). The THC of the hypoxic-sensitive strain was significantly lower than that of the hypoxic-tolerant strain after 12 h and 6 h of hypoxia treatment. However, there was no significant difference in THC content between the two strains at the same time of hypoxia treatment (3, 6, and 12 h) ($p > 0.05$) (Figure 1A). The HC of hypoxic and sensitive strains showed an overall upward trend, but compared with 0 h, hypoxic treatment for 3, 6, and 12 h had no significant effect on HC ($p > 0.05$) (Figure 1B).

Principal component analysis and sample correlation analysis

Principal component analysis (PCA) can reflect the variability between and within groups through the original data and present the trend of intergroup separation in the experimental model. To master the aggregation and separation of experimental Group I, experimental group II, control I, and control group II experimental groups, four histone protein expression datasets were treated as four variables and analyzed by PCA with SPSS software (Figure 2). The analysis results show good independence of the four groups of variables,

TABLE 1 Primer sequence of the selected genes.

Genes	primers (5′ to 3′)	Accession numbers
L8	F:TAGGCAATGTCATCCCCATT	DQ316258.1
	R:TCCTGAAGGAAGCTTTACACG	
Hemocyanin	F:AGTGGGCATCCTTTGTCGG	KY695246.1
	R:CTGTTGGTGAAGAGGTGCGG	
Chitinase	F:ATCGCAACCCATCAAACCTCG	AF315689.1
	R:ACAATCGTCGCAGACACGGT	
HSP 90	F:GGGTCACGTCCAACAGCAAC	QCYY01001690.1
	R:TCGCCTTCACAGACACMGAGC	
PDCD4	F:GATTAACTGTGCCAACCAGTCCAAAG	XM_027364270.1
	R:CATCCACCTCCTCCACATCATACAC	
GP	F:CCAGAATCCTCCACATAACT	MK721970.1
	R:GGAATACTGGCTCCATCAC	

so four groups of data can be used for subsequent comparative analysis. To quantitatively reflect the correlation between the four groups of proteins, the Pearson correlation coefficient of protein expression between each group was calculated by SPSS software and presented in the form of a heat map (Supplementary Figure S1). Pearson correlation coefficients of protein expression in all four groups were between 0.9 and 1.0, which indicated a strong correlation between all groups.

Statistical analysis of differential proteins

The extraction of ion peak areas was first performed by Spectronaut software, and the MSstats software package was used to calibrate and normalize the data within the system. In this study, three comparison groups were set up, namely, experimental group II vs. experiment I, control group II vs. control I, and experimental group II vs. control group II, and the differences in the expression of various comparison histones were assessed according to the set comparison group and the linear mixed effect model. When the condition of fold change ≥1.5 and corrected *p* value (adj_*p* value) < 0.05 was met, the difference was considered significant.

In this study, four groups of protein expression data were first analyzed by data-dependent acquisition (DDA) mass spectrometry and all detectable nonredundant high-quality MS/MS spectrogram information was obtained after database identification in MaxQuant software, which was used as the spectrogram database for subsequent DIA (Supplementary Figure S2). The total number of peptide and the number of protein detected in the three comparison groups were 16,603 and 3417, respectively. A total of 1,452 proteins were detected in the experimental group II vs experimental group I comparison group; among them, 1,417 proteins had no significant difference in expression level ($p > 0.05$), 10 proteins were significantly upregulated, and 25 proteins had downregulated expression levels ($p < 0.05$). In the control group II vs control group I comparison group, a total of 1,448 proteins were detected, among which 1,175 proteins had no significant difference in expression level ($p > 0.05$), 29 proteins were significantly upregulated, and 244 proteins were significantly downregulated ($p < 0.05$). In contrast, among the 1,525 proteins detected in the experimental group II vs control group II comparison group, 1,460 detected proteins had no significant difference in expression ($p > 0.05$), 49 proteins had significantly upregulated expression, while 16 proteins had significantly downregulated expression ($p < 0.05$). The volcanogram illustrates the differential protein expression in the three comparison groups in a more intuitive manner (Supplementary Figure S3).

Gene ontology classification of differential proteins

In the GO (Gene Ontology) classification diagram of experimental group II vs. experimental group I, proteins in experimental group II related to biological process, cellular component, and molecular function category, were mostly upregulated compared to experimental group I, such as genes involved in signaling, metabolic process, response to stimuli, regulation of the biological processes, and membrane systems (Figure 3A). However, all differentially expressed proteins in the category of multicellular biological processes were downregulated. In the GO classification diagram of control group II vs. group I, control group II had upregulated proteins mostly from the category belonging to biological process, cellular component, and molecular function. (Figure 3B). Among them, proteins were identified that were involved in responses to stimuli, negative and positive regulation

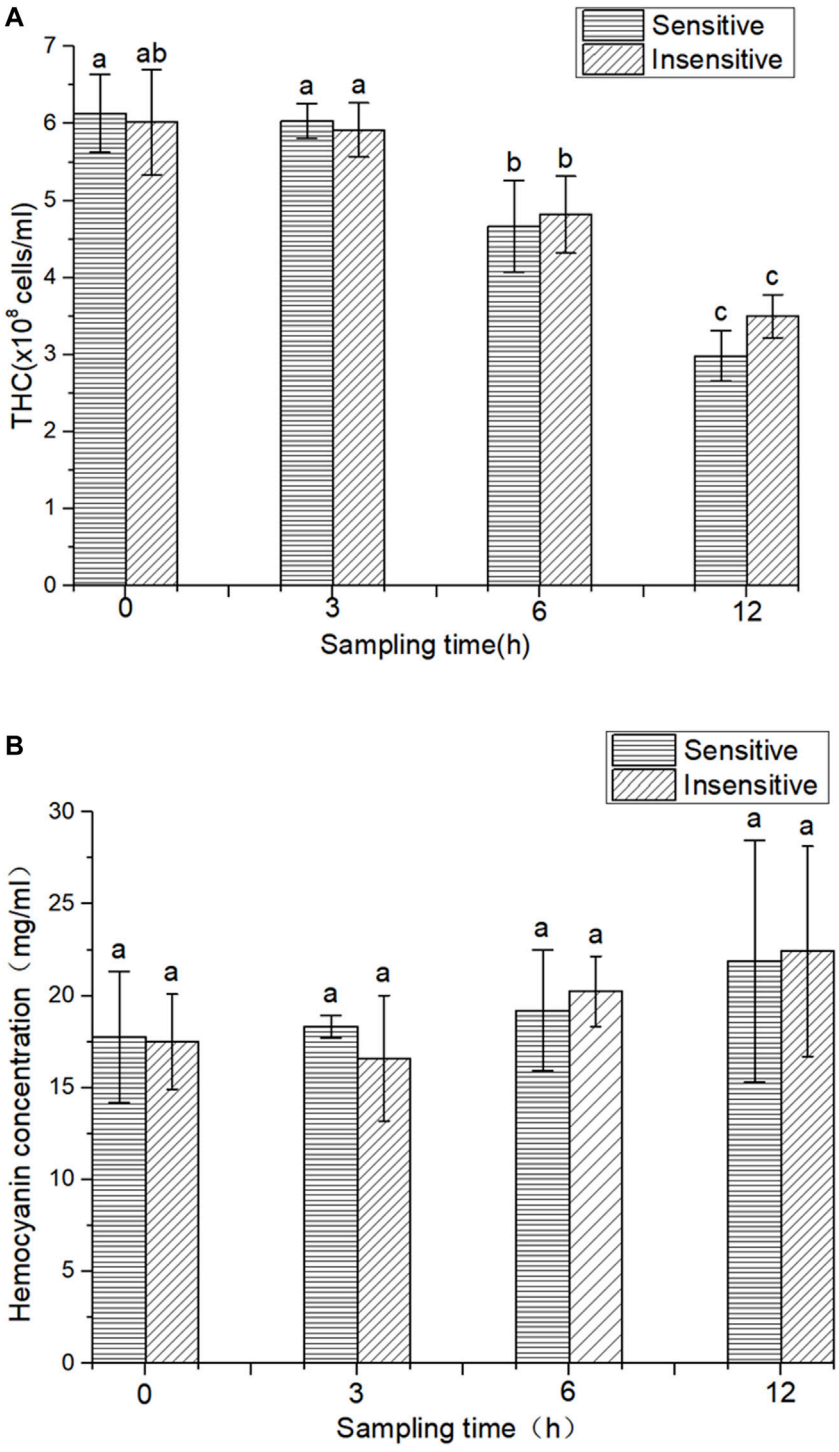

FIGURE 1
THC and HC in two strains of *L. vannamei*. **(A)** THC in two strains of *L. vannamei,* **(B)** HC in two strains of *L. vannamei*. Each bar represents the mean value of three determinations. The same letters in the data bar indicate no significant difference ($p > 0.01$), while different letters indicate significant difference ($p < 0.01$).

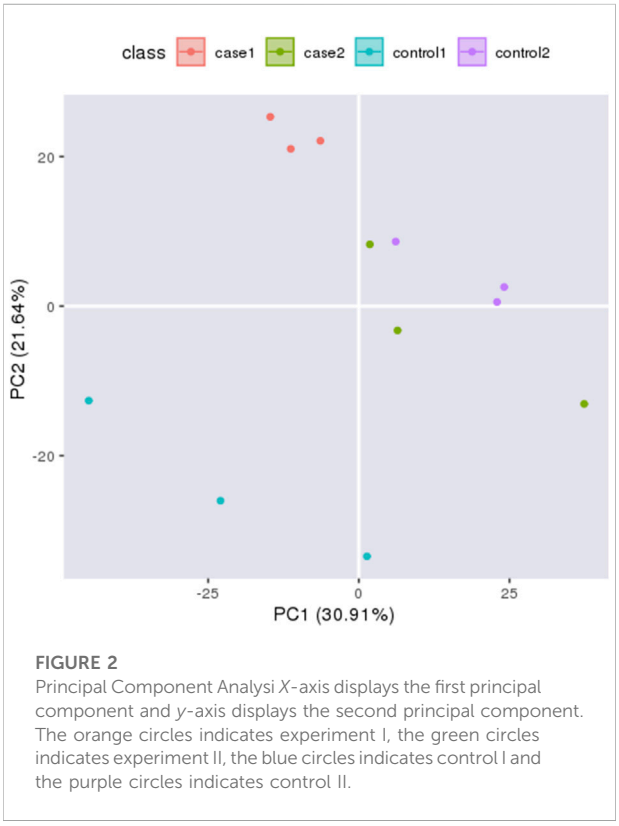

FIGURE 2
Principal Component Analysi *X*-axis displays the first principal component and *y*-axis displays the second principal component. The orange circles indicates experiment I, the green circles indicates experiment II, the blue circles indicates control I and the purple circles indicates control II.

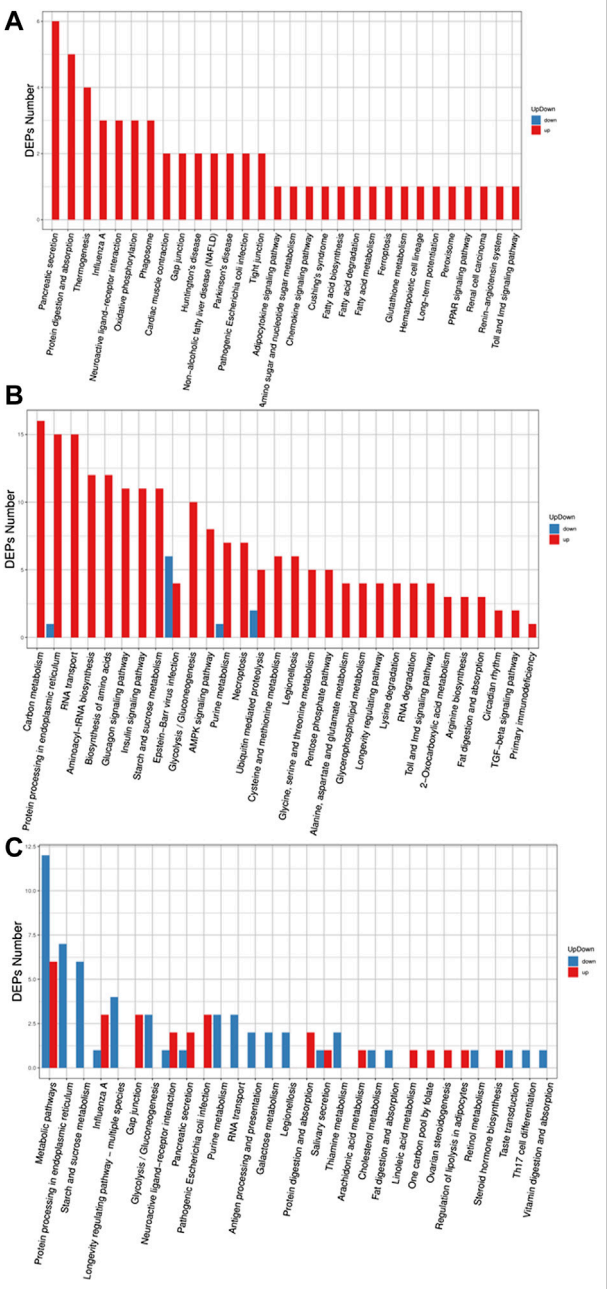

FIGURE 3
Barplot of the Gene Ontology analysis. **(A)** experiment II vs. experiment I, **(B)** control II vs. control I, **(C)** experiment II vs. control II. The bar chart shows the distribution of corresponding GO terms. Different colors represent different GO categories.

of the biological processes, signal transduction, growth, immune system processes, locomotion, pigmentation, membrane-enclosed lumen, extracellular regions, supramolecular complex, cell junction, and antioxidant activity. In the GO classification diagram of experimental group II vs control group II, some proteins were related to biological processes, cellular components, and molecular functions, while the other part was downregulated in control group II compared with experimental group II (Figure 3C). Among the upregulated proteins were those involved in cellular component organization or biogenesis, organelles, supramolecular complexes, molecular transducer activity, and structural molecule activity. However, the expression of differential proteins associated with the stress response, extracellular region part, and membrane were downregulated.

Eukaryotic orthologous groups classification of differential proteins

In this study, the identified proteins were compared with the KOG (eukaryotic orthologous groups) database to predict and classify their possible functions. In the KOG classification diagram of experimental group II vs. experimental group I, the main difference among the proteins was associated with post-translational modification function (amino acid transport and metabolism) and the cytoskeleton, as well as post-translational modification and protein turnover (chaperones) (Figure 4A). In the KOG classification diagram of control group II vs. control group I, in addition to proteins with uncertain functions, there were many differences within proteins involved in post-translational modification, protein

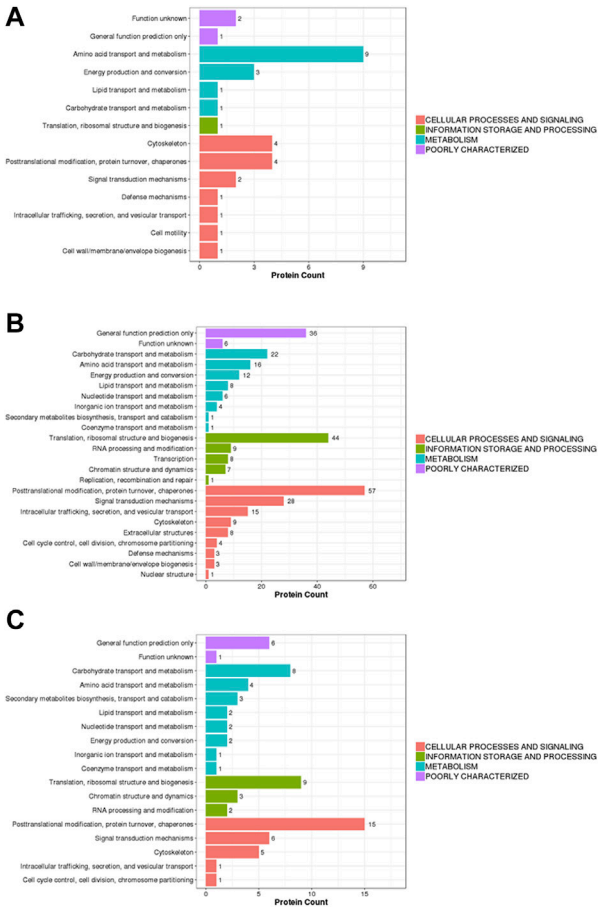

FIGURE 4
Barplot of the KOG analysis. **(A)** experiment II vs. experiment I, **(B)** control II vs. control I, **(C)** experiment II vs. control II. Eukaryotic orthologous groups (KOGs) were delineated by comparing protein sequences encoded in complete genomes, representing major phylogenetic lineages. *X*-axis displays the KOG term, *y*-axis displays the corresponding protein count illustrating the protein number of different function.

turnover, chaperones, translation, ribosome structure and biogenesis, and signal transduction mechanisms (Figure 4B). In the KOG classification diagram of experimental group II vs. the control group, most proteins were related to post-translational modification, protein turnover, chaperones, translation, ribosomal structure and biogenesis, carbohydrate transport, and metabolism (Figure 4C).

Expression analysis of important functional protein genes under the hypoxic stress in *L. Vannamei*

Hemocyanin gene, chitinase gene, heat shock protein 90 gene, programmed cell death protein gene and glycogen phosphorylase gene were selected for expression analysis (Figure 5). After 12 h of hypoxia stress, the expression levels of hemocyanin gene, programmed cell death protein gene and glycogen phosphorylase gene were significantly increased in hypoxia-sensitive and hypoxia-tolerant families ($p < 0.05$), and the expression levels of these genes were significantly different in the two families ($p < 0.05$). The expression of chitinase gene in the two families was significantly decreased ($p < 0.05$), and the expression of chitinase gene was significantly different ($p < 0.05$). The expression level of heat shock protein 90 gene in hypoxic-sensitive family was significantly increased ($p < 0.05$), while the expression level of heat shock protein 90 gene in hypoxic-resistant family was not significantly changed ($p > 0.05$).

Discussion

The dynamic changes in protein expression in the muscle tissue of *L. vannamei* under hypoxic stress were studied by the

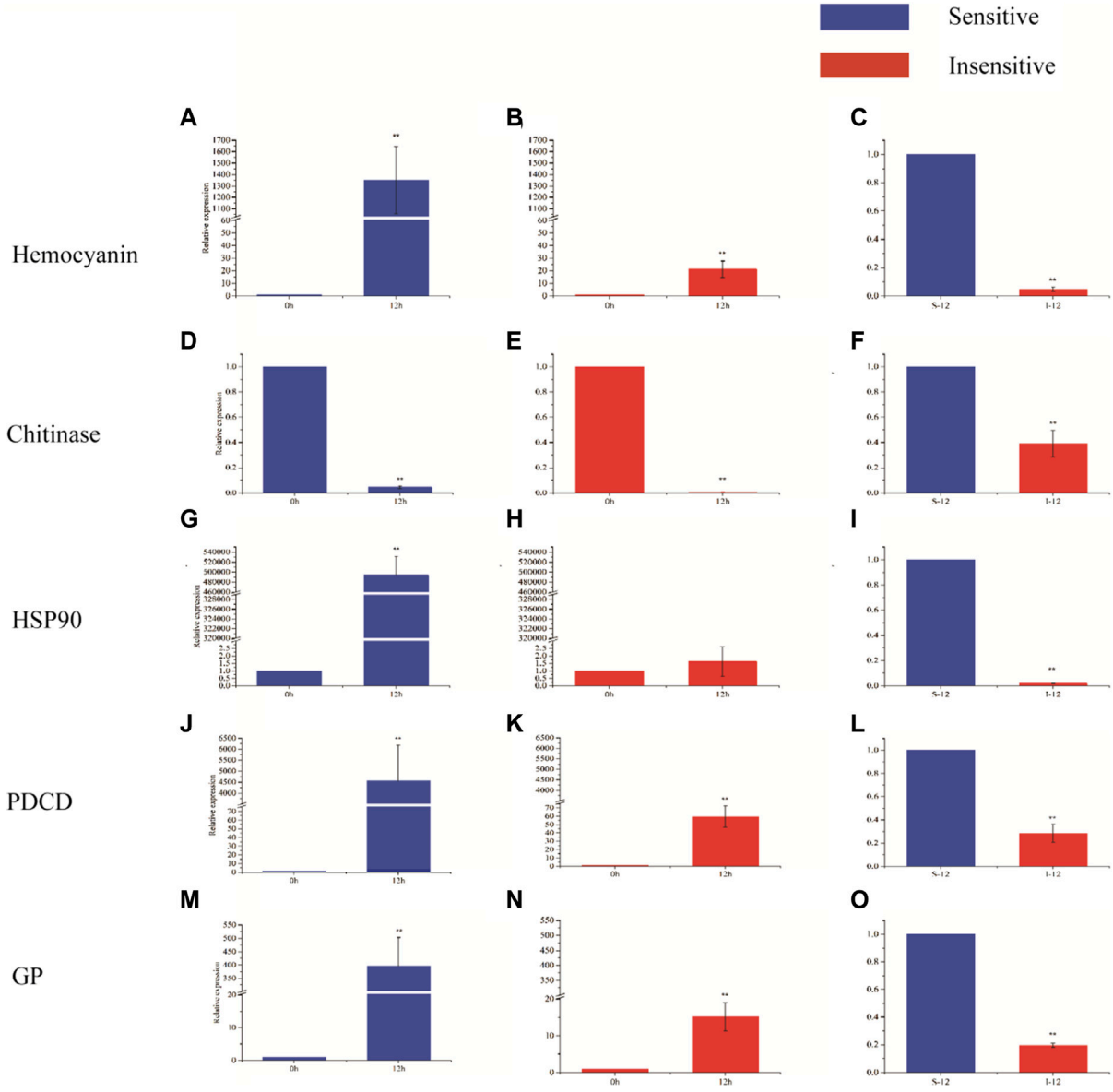

FIGURE 5
Expression of five genes in different periods of hypoxia in two strains of *L. vannamei*. *X*-axis displays the KOG term, *y*-axis displays the corresponding protein count illustrating the protein number of different function.

iTRAQ technique. A total of 3417 proteins were detected. The possible functions of all identified proteins were annotated according to GO, KEGG, and DEPS databases. By comparing the proteome of the control group and the experimental group, detailed information about the proteome response to hypoxic stress could be obtained. Low oxygen levels affect the immune function of *L. vannamei*. Crustaceans have nonspecific immunity, where hemocytes are the main effector of the immune response (Huang and Ren, 2019). Hemocytes have the ability to wrap, engulf, and degrade invading pathogens and play a crucial role in crustacean immune defense (Liu et al., 2020). A number of animal hemocytes often change in response to environmental changes or pathogenic microorganism infection (Qiu et al., 2011), so they are a marker of body health and immune capacity. Under the condition of low oxygen (1.5 PPM), THC of green-lipped mussel (*Perna viridis*) (Wang et al., 2012) and scallop (*Chlamys farreri*) (Chen et al., 2007) decreased gradually with decreasing DO value. In this experiment, the THC of the two strains of *L. vannamei* showed a downward trend at 0 h and 3 h

after hypoxia treatment, without reaching a significant difference. THC was significantly decreased at 6 and 12 h after hypoxia treatment ($p < 0.05$), which was similar to the above results.

Hemocyanin is the most important plasma protein of crustaceans and can bind and transport O_2 and CO_2 to serve as the respiratory protein of prawns. In addition to its main function as an oxygen carrier, hemocyanin has been identified as a nonspecific innate immune defense molecule of crustaceans (Coates and Nairn 2014) with antiviral and antibacterial properties (Lee, Lee and Soderhall 2003). It can be functionally converted into phenolic oxidase with agglutination abilities and hemolytic activity (Zhang et al., 2006). When oxygen levels in the environment are low, crustaceans meet their oxygen needs by increasing the concentration of hemocyanin. A previous study revealed that HC in *L. vannamei* was significantly increased ($p < 0.05$) under hypoxic conditions (Wei L et al., 2016). Another shrimp species, oriental river prawn (*Macrobrachium nipponense*), had significantly increased ($p < 0.05$) expression levels of hemocyanin in response to the hypoxic environment (Sun et al., 2016). In contrast, 10 h of hypoxic conditions negatively affected the HC rate in the southern king crab (*Lithodes santolla*) (Paschke et al., 2016).

In this study, hypoxia treatment had no significant effect on the HC of *L. vannamei* in the two strains with hypoxia tolerance and sensitivity ($p > 0.05$), and there was no significant difference in HC between the two strains at different periods of hypoxia ($p > 0.05$). However, HC showed an overall upward trend compared to the control group, consistent with previous reports. In addition, HC increased gradually with prolonged hypoxia time, which was consistent with proteomic data.

Under low DO circumstances, shrimp can adjust the use of energy substrates (carbohydrate, lipids, and proteins) to balance oxidative (Ulaje et al., 2019). In this experiment, immune-related proteins, such as hemocyanin, chitinase, and heat shock protein 90, were found among the proteins expressed at significantly different levels under hypoxic stress. Hemocyanin plays an important role in the innate immunity of *L. vannamei*, such as antibacterial, antiviral, hemolytic, anti-infective, and antitumor activities (Jiang et al., 2007; Zhang et al., 2009; Coates and Nairn 2014; Zheng et al., 2016). Chitinases are widely exist in organisms as a group of hydrolytic enzymes that hydrolyze chitin. The function of chitinases in biological processes such as the growth of fungi, the molting of arthropods, and the invasion of bacteria or parasites into chitincontaining structures of the host has been intensely studied (Arakane and Muthukrishnan, 2010; Chaudhuri et al., 2010; Pesch et al., 2016). Chitinase is a key enzyme in the innate immunity of *L. vannamei* and involved in numerous immunomodulatory responses (Zhang et al., 2016; Niu et al., 2018; Song et al., 2020), especially in preventing bacterial infection (Duo-Chuan 2006; Gao et al., 2017). Chitinase expression in *L. vannaensis* infected with white spot syndrome virus is upregulated at the translation level (Jiang et al., 2007). A previous study demonstrated that chitinase plays a role in regulation of both humoral and cellular immune responses in shrimp due to the expression of various immune related genes and other functional proteins with antibacterial and antiviral activities was widely changed in LvChi5 silencing shrimp (Niu et al., 2018).

Heat shock proteins are an important molecular chaperone in eukaryotic cells (Zininga, Ramatsui and Shonhai, 2018). They play a role in protecting cells from stress and oncogenic transformation, providing cell cycle regulation, antigen presentation, and participation in cellular stress responses, including changes in environmental conditioning stress (Kühl and Rensing 2000; Udono 2012; Wu et al., 2017; Sornchuer et al., 2018). It helps to refold the denatured protein into an appropriate conformation (Nakamoto et al., 2014).

In this study, Hsp90 was significantly upregulated in hypoxic-sensitive *L. vannamensis* after 12 h of hypoxia stress, while there was no significant change in the expression of Hsp90 in hypoxic-tolerant families. HSPs have been shown to be one of the main response proteins to hypoxic stress (Zhang, Zhang and Zhang 2016; Niu et al., 2018). Although Ulaje *et al.* showed that Hsp70 and Hsp90 gene expression in *L. vannamei* was down-regulated under hypoxia, in both the short- and the long-term (Ulaje et al.,2020), most researches in crustaceans have indicated that the up-regulation in the expression of Hsps genes is a general response to cope with hypoxia (Sun et al., 2014, 2016; Jolly et al., 2018), which was consistent with the results of this study.

The hypoxic-sensitive strain *L. vannamensis* can regulate the protein level in a timely manner in response to the hypoxic-sensitive strain, while the protein expression in the hypoxic-tolerant strain is at a normal level. In addition, after 12 h of hypoxia, the expression of neuroendocrine differentiation factor in the hypoxic sensitive family was significantly upregulated, which may be related to its role in immune regulation (Sung et al., 2016; Song et al., 2020; Junprung et al., 2017). The role of other proteins identified in this study as a part of the response to hypoxia stress in *L. vannamei* remains to be further studied.

Conclusion

Hypoxia stress has become a frequent occurrence in commercial *L. vannamei* farming, so it is important to explore the molecular mechanisms of the hypoxic response and adjustment to changing oxygen levels. This study demonstrated the changes in physiological and biochemical levels in shrimp under conditions of low oxygen stress and investigated the expression of the hypoxic stress protein regulation mechanism and its function by comparing proteomics data among two strains of *L. vannamei* with different tolerances to hypoxia. The results from proteomic analysis were confirmed with qRT–PCR to detect the gene expression level.

Studies have indicated that low oxygen levels have an effect on THC and HC parameters. The hypoxia-sensitive strain showed a decreased number of hemocytes after 3 h under hypoxic conditions, while the hypoxia-tolerant strain response

with significant changes in hemocyte number was delayed to 6 h in a hypoxic environment. Since hemocytes are involved in oxygen transportation together with the immune response, these results suggest the weakening of immune system capacity in response to low oxygen levels.

A total of 3417 proteins were detected in proteomics analysis. The hypoxia-sensitive strain showed 273 differentially expressed proteins in response to 12 h hypoxia treatment, while in the hypoxia-tolerant strain, this number was reduced to 35 proteins. The cohort of proteins that were affected in the two strains included hemocyanin, Hsp90, GP, chitinase, PD, actin, ferritin, and trypsin. These proteins were classified into immune-related proteins, energy metabolism-related proteins, cytoskeleton-related proteins, chaperones, and others.

Five protein genes with significant changes at the proteomic level in two strains of *L. vannamei* were chosen for qRT–PCR to confirm the gene expression patterns, namely, hemocyanin, chitinase, HSP90, PD, and GP. This group of proteins is probably an important component of the *L. vannamei* response to hypoxia stress and could be considered biomarkers.

Data availability statement

The raw data supporting the conclusion of this article will be made available by the authors, without undue reservation.

Author contributions

FC, resources, writing—original draft NL, investigation, validation XS, resources VO, writing—review and editing XW, conceptualization, supervision XD, project administration HZ, conceptualization, supervision, funding acquisition XT, supervision.

Funding

The research was funded by the Natural Science Foundation of Hainan Province (2019RC077, 20164159). Scientific Research General project of Hainan Provincial Department of Education (Hnky2022-10).

Acknowledgments

The authors would like to thank the editors and the reviewers for their constructive comments and suggestions for this paper.

Conflict of interest

The authors declare that the research was conducted in the absence of any commercial or financial relationships that could be construed as a potential conflict of interest.

Publisher's note

Supplementary material

The Supplementary Material for this article can be found online at: https://www.frontiersin.org/articles/10.3389/fphys.2022.979472/full#supplementary-material

SUPPLEMENTARY FIGURE S1
Sample correlation analysis heat map. The sign of correlation coefficient represents positive or negative correlation. The value represents the strength of correlation: 0.8–1.0 represents a strong correlation, 0.6–0.8 represents a strong correlation, 0.2–0.4 represents a weak correlation, 0.0–0.2 represents a very weak correlation or no correlation.

SUPPLEMENTARY FIGURE S2
Protein mass distribution. *X*-axis displays the protein mass interval (Kilodalton), *y*-axis displays the corresponding protein number.

SUPPLEMENTARY FIGURE S3
Differential protein volcano map. experiment II-vs. -Experiment I, **(B)** control II-vs.-control I, **(C)** experiment II-vs.-control II. X-axis of the volcanogram refers to the multiple protein fold change difference (log2), and the Y-axis corresponds to -log10 (P value). The green circle indicates the proteins with significantly downregulated patterns, the red circle indicates the proteins with significantly upregulated patterns, and the gray circle indicates the proteins with no significant difference.

References

Abe, H., Hirai, S., and Okada, S. (2007). Metabolic responses and arginine kinase expression under hypoxic stress of the kuruma prawn *Marsupenaeus japonicus*. *Comp. Biochem. Physiol. A Mol. Integr. Physiol.* 146, 40–46. doi:10.1016/j.cbpa.2006.08.027

Arakane, Y., and Muthukrishnan, S. (2010). Insect chitinase and chitinase-like proteins. *Cell. Mol. Life Sci.* 67, 201–216. doi:10.1007/s00018-009-0161-9

Breitburg, D., Levin, L. A., Oschlies, A., Grégoire, M., Jing, Z., Conley, D. J., et al. (2018). Declining oxygen in the global ocean and coastal waters. *Science* 359, eaam7240–12. doi:10.1126/science.aam7240

Brouwer, M., Larkin, P., Brown-Peterson, N., King, C., Manning, S., and Denslow, N. (2004). Effects of hypoxia on gene and protein expression in the blue crab, *callinectes sapidus*. *Mar. Environ. Res.* 58, 787–792. doi:10.1016/j.marenvres.2004.03.094

Buentello, J. A., Iii, D., and Neill, W. H. (2000). Effects of water temperature and dissolved oxygen on daily feed consumption, feed utilization and growth of channel catfish (*ictalurus punctatus*). *Aquaculture* 182, 339–352. doi:10.1016/s0044-8486(99)00274-4

Camacho-Jimenez, L., Peregrino-Uriarte, A. B., Martinez-Quintana, J. A., and Yepiz-Plascencia, G. (2018). The glyceraldehyde-3-phosphate dehydrogenase of the shrimp *litopenaeus vannamei* : Molecular cloning, characterization and expression during hypoxia. *Mar. Environ. Res.* 138, 65–75. doi:10.1016/j.marenvres.2018.04.003

Chabot, D., and Biology, J. ϐ . D. J. J. o. F. (2005). Reduced growth of Atlantic cod in non-lethal hypoxic conditions. *J. Fish. Biol.* 55, 472–491. doi:10.1111/j.1095-8649.1999.tb00693.x

Chaudhuri, S., Bruno, J. C., Alonzo, F., Xayarath, B., Cianciotto, N. P., and Freitag, N. E. (2010). Contribution of chitinases to listeria monocytogenes pathogenesis. *Appl. Environ. Microbiol.* 76, 7302–7305. doi:10.1128/AEM.01338-10

Chen, J., Mai, K., Ma, H., Wang, X., Deng, D., Liu, X., et al. (2007). Effects of dissolved oxygen on survival and immune responses of scallop (Chlamys farreri Jones et Preston). *Fish. Shellfish Immunol.* 22, 272–281. doi:10.1016/j.fsi.2006.06.003

Cheng, W., and Chen, J. C. (2000). Effects of pH, temperature and salinity on immune parameters of the freshwater prawn *Macrobrachium rosenbergii*. *Fish. Shellfish Immunol.* 10, 387–391. doi:10.1006/fsim.2000.0264

Chongsatja, P.-O., Bourchookarn, A., Lo, C. F., Thongboonkerd, V., and Krittanai, C. (2007). Proteomic analysis of differentially expressed proteins in *Penaeus vannamei* hemocytes upon Taura syndrome virus infection. *Proteomics* 7, 3592–3601. doi:10.1002/pmic.200700281

Coates, C. J., and Nairn, J. (2014). Diverse immune functions of hemocyanins. *Dev. Comp. Immunol.* 45, 43–55. doi:10.1016/j.dci.2014.01.021

Cota-Ruiz, K., Peregrino-Uriarte, A. B., Felix-Portillo, M., Martinez-Quintana, J. A., and Yepiz-Plascencia, G. (2015). Expression of fructose 1, 6-bisphosphatase and phosphofructokinase is induced in hepatopancreas of the white shrimp *Litopenaeus vannamei* by hypoxia. *Mar. Environ. Res.* 106, 1–9. doi:10.1016/j.marenvres.2015.02.003

Diaz, R. J., and Rosenberg, R. (1995). Marine benthic hypoxia: A review of its ecological effects and the behavioural response of benthic macrofauna. *Oceanogr. Mar. Biol.* 33, 245–303.

Duo-Chuan, L. (2006). Review of fungal chitinases. *Mycopathologia* 161, 345–360. doi:10.1007/s11046-006-0024-y

Filho, D. W., Torres, M. A., Zaniboni-Filho, E., and Pedrosa, R. C. (2005). Effect of different oxygen tensions on weight gain, feed conversion, and antioxidant status in piapara, *leporinus elongatus* (valenciennes, 1847). *Aquaculture* 244, 349–357. doi:10.1016/j.aquaculture.2004.11.024

Gao, C., Cai, X., Zhang, Y., Su, B., Song, H., Wenqi, W., et al. (2017). Characterization and expression analysis of chitinase genes (chit1, chit2 and chit3) in turbot (*scophthalmus maximus l.*) following bacterial challenge. *Fish. Shellfish Immunol.* 64, 357–366. doi:10.1016/j.fsi.2017.03.019

Gray, J., Wu, R., and Ying, Y. J. M. E. P. (2002). Effects of hypoxia and organic enrichment on the coastal marine environment. *Mar. Ecol. Prog. Ser.* 238, 249–279. doi:10.3354/meps238249

Guadagnoli, J. A., Tobita, K., and Reiber, C. L. (2011). Changes in cardiac performance during hypoxic exposure in the grass shrimp *Palaemonetes pugio*. *J. Exp. Biol.* 214, 3906–3914. doi:10.1242/jeb.060442

Huang, Y., and Ren, Q. (2019). Research progress in innate immunity of freshwater crustaceans. *Dev. Comp. Immunol.* 104, 103569. doi:10.1016/j.dci.2019.103569

Jiang, H., Li, F., Xie, Y., Huang, B., Zhang, J., Zhang, J., et al. (2009). Comparative proteomic profiles of the hepatopancreas in *Fenneropenaeus chinensis* response to hypoxic stress. *Proteomics* 9, 3353–3367. doi:10.1002/pmic.200800518

Jiang, N., Tan, N. S., Ho, B., and Ding, J. L. (2007). Respiratory protein-generated reactive oxygen species as an antimicrobial strategy. *Nat. Immunol.* 8, 1114–1122. doi:10.1038/ni1501

Jolly, E., Liang, S., Yu, X., and Wood, D. (2018). HSP70, HSP90A, and HSP90B are differentially regulated in response to thermal, osmotic and hypoxic stressors. *Osmotic Hypoxic Stressors* 1, 1–9.

Keeling, R. F., Kortzinger, A., and Gruber, N. (2010). Ocean deoxygenation in a warming world. *Ann. Rev. Mar. Sci.* 2, 199–229. doi:10.1146/annurev.marine.010908.163855

Kühl, N. M., and Rensing, L. (2000). Heat shock effects on cell cycle progression. *Cell. Mol. Life Sci.* 57, 450–463. doi:10.1007/PL00000707

Lee, S. Y., Lee, B. L., and Soderhall, K. (2003). Processing of an antibacterial peptide from hemocyanin of the freshwater crayfish *Pacifastacus leniusculus*. *J. Biol. Chem.* 278, 7927–7933. doi:10.1074/jbc.M209239200

Levin, L. A., Ekau, W., Gooday, A. J., Jorissen, F., Middelburg, J. J., Naqvi, S. W. A., et al. (2009). Effects of natural and human-induced hypoxia on coastal benthos. *Biogeosciences* 6, 2063–2098. doi:10.5194/bg-6-2063-2009

Li, T., and Brouwer, M. (2013). Gene expression profile of hepatopancreas from grass shrimp *Palaemonetes pugio* exposed to cyclic hypoxia. *Comp. Biochem. physiology. Part D, Genomics & proteomics* 8, 1–10. doi:10.1016/j.cbd.2012.10.003

Li, Y. H., Wei, L., Cao, J. R., Qiu, L. G., Jiang, X., Li, P., et al. (2016). Oxidative stress, DNA damage and antioxidant enzyme activities in the Pacific white shrimp (*Litopenaeus vannarnei*) when exposed to hypoxia and reoxygenation. *Chemosphere* 144, 234–240. doi:10.1016/j.chemosphere.2015.08.051

Liu, S., Zheng, S. C., Li, Y. L., Li, J., and Liu, H. P. (2020). Hemocyte-mediated phagocytosis in Crustaceans. *Front. Immunol.* 11, 268. doi:10.3389/fimmu.2020.00268

Livak, K. J., and Schmittgen, T. D. (2001). Analysis of relative gene expression data using real-time quantitative PCR and the 2(-Delta Delta C(T)) Method. *Methods (San Diego, Calif.)* 25, 402–408. doi:10.1006/meth.2001.1262

Nakamoto, H., Fujita, K., Ohtaki, A., Watanabe, S., Narumi, S., Maruyama, T., et al. (2014). Physical interaction between bacterial heat shock protein (Hsp) 90 and Hsp70 chaperones mediates their cooperative action to refold denatured proteins. *J. Biol. Chem.* 289, 6110–6119. doi:10.1074/jbc.M113.524801

Niu, S. W., Yang, L. W., Zuo, H. L., Zheng, H. L., Weng, J. F., Shao, P., et al. (2018). A chitinase from Pacific white shrimp *Litopenaeus vannamei* involved in immune regulation. *Dev. Comp. Immunol.* 85, 161–169. doi:10.1016/j.dci.2018.04.013

Pesch, Y. Y., Riedel, D., Patil, K. R., Loch, G., and Behr, M. (2016). Chitinases and Imaginal disc growth factors organize the extracellular matrix formation at barrier tissues in insects. *Sci. Rep.* 6, 18340. doi:10.1038/srep18340

Qiu, R. J., Cheng, Y. X., Huang, X. X., Wu, X. G., Yang, X. Z., and Tong, R. (2011). Effect of hypoxia on immunological, physiological response, and hepatopancreatic metabolism of juvenile Chinese mitten crab *Eriocheir sinensis*. *Aquac. Int.* 19, 283–299. doi:10.1007/s10499-010-9390-z

Riffel, A. P., Saccol, E. M., Finamor, I. A., Ourique, G. M., Gressler, L. T., Parodi, T. V., et al. (2014). Humic acid and moderate hypoxia alter oxidative and physiological parameters in different tissues of silver catfish (*Rhamdia quelen*). *J. Comp. Physiol. B* 184, 469–482. doi:10.1007/s00360-014-0808-1

Rojas-Hernandez, N., Véliz, D., and Vega-Retter, C. (2019). Selection of suitable reference genes for gene expression analysis in gills and liver of fish under field pollution conditions. *Sci. Rep.* 9, 3459. doi:10.1038/s41598-019-40196-3

Song, L., Lv, J., Wang, L., Sun, D., Gao, B., and Liu, P. (2020). Characterization of a chitinase-1 gene (PtCht-1) from a marine crab *Portunus trituberculatus* and its response to immune stress. *Gene*, 2020, 144523. doi:10.1016/j.gene.2020.144523

Sornchuer, P., Junprung, W., Yingsunthonwattana, W., and Tassanakajon, A. (2018). Heat shock factor 1 regulates heat shock proteins and immune-related genes in *Penaeus monodon* under thermal stress. *Dev. Comp. Immunol.* 88, 19–27. doi:10.1016/j.dci.2018.06.013

Sun, S. M., Xuan, F. J., Fu, H. T., Ge, X. P., Zhu, J., Qiao, H., et al. (2016). Comparative proteomic study of the response to hypoxia in the muscle of oriental river prawn (*Macrobrachium nipponense*). *J. Proteomics* 138, 115–123. doi:10.1016/j.jprot.2016.02.023

Sun, S., Xuan, F., Ge, X., Fu, H., Zhu, J., and Zhang, S. (2014). Identification of differentially expressed genes in hepatopancreas of oriental river prawn, *Macrobrachium nipponense* exposed to environmental hypoxia. *Gene* 534, 298–306. doi:10.1016/j.gene.2013.10.036

Tassanakajon, A., Rimphanitchayakit, V., Visetnan, S., Amparyup, P., Somboonwiwat, K., Charoensapsri, W., et al. (2018). Shrimp humoral responses against pathogens: Antimicrobial peptides and melanization. *Dev. Comp. Immunol.* 80, 81–93. doi:10.1016/j.dci.2017.05.009

Udono, H. (2012). Heat shock protein magic in antigen trafficking within dendritic cells: Implications in antigen cross-presentation in immunity. *Acta Med. Okayama* 66, 1–6. doi:10.18926/AMO/48075

Ulaje, S. A., Lluch-Cota, S. E., Sicard, M. T., Ascencio, F., Cruz-Hernández, P., Racotta, I. S., et al. (2020). *Litopenaeus vannamei* oxygen consumption and HSP gene expression at cyclic conditions of hyperthermia and hypoxia. *J. Therm. Biol.* 92, 102666. doi:10.1016/j.jtherbio.2020.102666

Ulaje, S. A., Rojo-Arreola, L., Lluch-Cota, S. E., Ascencio, F., Cruz-Hernandez, P., and Sicard, M. T. (2019). Gene expression and energetic metabolism changes in the whiteleg shrimp (*Litopenaeus vannamei*) in response to short-term hypoxia. *Aquac. Res.* 50, are.13960–1004. doi:10.1111/are.13960

Wang, H.-C., Wang, H.-C., Leu, J.-H., Kou, G.-H., Wang, A. H. J., and Lo, C.-F. (2007). Protein expression profiling of the shrimp cellular response to white spot syndrome virus infection. *Dev. Comp. Immunol.* 31, 672–686. doi:10.1016/j.dci.2006.11.001

Wang, Y. J., Hu, M. H., Cheung, S. G., Shin, P. K. S., Lu, W. Q., and Li, J. L. (2012). Immune parameter changes of hemocytes in green-lipped mussel *Perna viridis* exposure to hypoxia and hyposalinity. *Aquaculture* 356, 22–29. doi:10.1016/j.aquaculture.2012.06.001

Watanabe, T., Kono, M., Aida, K., and Nagasawa, H. (1998). Purification and molecular cloning of a chitinase expressed in the hepatopancreas of the penaeid prawn *Penaeus japonicus*. *Biochim. Biophys. Acta* 1382, 181–185. doi:10.1016/s0167-4838(97)00184-2

Wei, L., Li, Y., Qiu, L., Zhou, H., Han, Q., and Diao, X. (2016). Comparative studies of hemolymph physiology response and HIF-1 expression in different strains of *Litopenaeus vannamei* under acute hypoxia. *Chemosphere* 153, 198–204. doi:10.1016/j.chemosphere.2016.03.064

Wei, Y., Wang, J., and Xia, X. (2016). Coevolution between stop codon usage and release factors in bacterial species. *Mol. Biol. Evol.* 33, 2357–2367. doi:10.1093/molbev/msw107

Wu, J., Liu, T., Rios, Z., Mei, Q., Lin, X., and Cao, S. (2017). Heat shock proteins and cancer. *Trends Pharmacol. Sci.* 38 (3), 226–256. doi:10.1016/j.tips.2016.11.009

Yadzir, Z. H. M., Misnan, R., Abdullah, N., Bakhtiar, F., Arip, M., and Murad, S. (2012). Identification of the major allergen of *Macrobrachium rosenbergii* (giant freshwater prawn). *Asian pac. J. Trop. Biomed.* 2, 50–54. doi:10.1016/S2221-1691(11)60189-5

Yang, L. B., and Pan, L. Q. (2013). Effects of phosphatidyl serine on immune response in the shrimp *Litopenaeus vannamei*. *Open Life Sci.* 8, 1135–1144. doi:10.2478/s11535-013-0197-y

Ye, S., Huang, L. W., Cui, L., Wang, M. X., Huang, J. J., and Feng, J. (2011). Effects of acute hypoxia stress at 20°C on carbohydrate metabolism and antioxidant defense system of red-eared turtles. *J. Aquatic Biol.* 35.

Zhang, Y. L., Yan, F., Hu, Z., Zhao, X. L., Min, S. Y., Du, Z. H., et al. (2009). Hemocyanin from shrimp *Litopenaeus vannamei* shows hemolytic activity. *Fish. Shellfish Immunol.* 27, 330–335. doi:10.1016/j.fsi.2009.05.017

Zhang, Y., Wang, S., Xu, A., Chen, J., Lin, B., and Peng, X. (2006). Affinity proteomic approach for identification of an IgA-like protein in *Litopenaeus vannamei* and study on its agglutination characterization. *J. Proteome Res.* 5, 815–821. doi:10.1021/pr0503984

Zhang, Z., Zhang, P., and Zhang, Y. (2016). *Advancement on the immune function, molecular basis underlying multifunctionality and application of hemocyanin*. *Journal of Shantou University Natural Science Edition* 31 (1), 46–54.

Zheng, L. Y., Zhao, X. L., Zhang, P., Chen, C. D., Liu, S. J., Huang, R. Q., et al. (2016). Hemocyanin from shrimp *Litopenaeus vannamei* has antiproliferative effect against heLa cell *in vitro*. *Plos One* 11, e0151801. doi:10.1371/journal.pone.0151801

Zhou, H. L., Li, Y. H., Wei, L., Zhang, Z. H., Huang, H., Diao, X. P., et al. (2014). Sensitivity of larvae and adult and the immunologic characteristics of *Litopenaeus vannamei* under the acute hypoxia. *J. Chem.* 6, 1. doi:10.1155/2014/574534

Zininga, T., Ramatsui, L., and Shonhai, A. (2018). Heat shock proteins as immunomodulants. *Mol. (Basel, Switz.* 23, 2846. doi:10.3390/molecules23112846

frontiers | Frontiers in Physiology

TYPE Original Research
PUBLISHED 26 September 2022
DOI 10.3389/fphys.2022.992293

OPEN ACCESS

EDITED BY
Divya Singh,
Chandigarh University, India

REVIEWED BY
Hui Dong,
Shenyang Agricultural University, China
Kang He,
Zhejiang University, China

*CORRESPONDENCE
Kanglai He,
hekanglai@caas.cn

SPECIALTY SECTION
This article was submitted to Invertebrate Physiology, a section of the journal Frontiers in Physiology

RECEIVED 12 July 2022
ACCEPTED 02 September 2022
PUBLISHED 26 September 2022

CITATION
Quan Y, Wang Z, Wei H and He K (2022), Transcription dynamics of heat shock proteins in response to thermal acclimation in Ostrinia furnacalis. *Front. Physiol.* 13:992293. doi: 10.3389/fphys.2022.992293

Transcription dynamics of heat shock proteins in response to thermal acclimation in *Ostrinia furnacalis*

Yudong Quan[1], Zhenying Wang[1], Hongyi Wei[2] and Kanglai He[1]*

[1]State Key Laboratory for Biology of Plant Diseases and Insect Pests, Institute of Plant Protection, Chinese Academy of Agricultural Sciences, Beijing, China, [2]College of Agronomy, Jiangxi Agricultural University, Nanchang, China

Acclimation to abiotic stress plays a critical role in insect adaption and evolution, particularly during extreme climate events. Heat shock proteins (HSPs) are evolutionarily conserved molecular chaperones caused by abiotic and biotic stressors. Understanding the relationship between thermal acclimation and the expression of specific HSPs is essential for addressing the functions of HSP families. This study investigated this issue using the Asian corn borer *Ostrinia furnacalis*, one of the most important corn pests in China. The transcription of *HSP* genes was induced in larvae exposed to 33°C. Thereafter, the larvae were exposed to 43°C, for 2 h, and then allowed to recover at 27 C for 0, 0.5, 1, 2, 4, 6, and 8 h. At the recovery times 0.5–4 h, most population tolerates less around 1–3 h than without recovery (at 0 h) suffering continuous heat stress (43 C). There is no difference in the heat tolerance at 6 h recovery, with similar transcriptional levels of *HSPs* as the control. However, a significant thermal tolerance was observed after 8 h of the recovery time, with a higher level of *HSP70*. In addition, the transcription of *HSP60* and *HSC70* (heat shock cognate protein 70) genes did not show a significant effect. *HSP70* or *HSP90* significantly upregulated within 1–2 h sustained heat stress (43 C) but declined at 6 h. Our findings revealed extreme thermal stress induced quick onset of *HSP70* or *HSP90* transcription. It could be interpreted as an adaptation to the drastic and rapid temperature variation. The thermal tolerance of larvae is significantly enhanced after 6 h of recovery and possibly regulated by *HSP70*.

KEYWORDS

heat shock proteins, thermal tolerance, heat shock response, *Ostrinia furnacalis*, extreme climate events

Introduction

Ongoing global climate change has caused a substantial increase in the occurrence of extreme thermal events (Meehl and Tebaldi, 2004; Alexander et al., 2006; IPCC, 2013; Ma et al., 2021). The phenotypic plasticity of ectotherms is a nongenetic strategic response to environmental variation, including thermal extremes (Hoffmann et al., 2013; Gunderson and Stillman, 2015; van Heerwaarden et al., 2016). Insects, as ectotherms, exhibit plasticity

in a suite of traits related to thermal extremes, have fast generation times, and thus are considered good models to study plasticity (Sgrò et al., 2016; Gibert et al., 2019). Understanding plasticity has taken on increased importance in the context of rapid climate change as extreme events are more frequent and show increased variability (Fox et al., 2019). For example, insects living at higher latitudes have evolved plastic responses to survive in cold winters, but extreme events are increasingly disrupting the reliability of environmental signals (Sgrò et al., 2016; Gibert et al., 2019). Thermal extremes can lead to heat injury, as well as to a series of changes at the molecular, biochemical, and physiological levels in insects (Chown and Nicolson, 2004; Bowler, 2018; Ma et al., 2021), such as water content (Prange, 1996), cell membranes (Neven, 2000; Rensing and Ruoff, 2002), and activity of enzymes (Greenspan et al., 1980). Meanwhile, thermal acclimation of insects is a form of plasticity that enables organisms to adjust their physiology, following chronic or brief exposure to stressful stimuli (Bowler, 2005; Angilletta, 2009). The challenge is understanding how thermal extremes or stresses act on and manipulate acclimation in insects.

Heat shock proteins (HSPs) are known as stress molecular chaperones, which are essential for environmental adaptation and are associated with a wide range of physiological and biochemical processes (King and MacRae, 2015). According to their molecular size, the major families of HSPs are named HSP100, HSP90, HSP70, HSP60, and HSP40, and small proteins (sHSP). HSPs play a vital role in insects' responses to extreme temperatures (Basha et al., 2012; King and MacRae, 2015), as well as responding to cold/heat tolerances (Rutherford and Lindquist, 1998), density, starvation, poison, ultraviolet-C, and diapause (Sosalegowda et al., 2010; Tedeschiab et al., 2015; Zhang et al., 2015; Tedeschi et al., 2016). HSP70 and HSP90 are highly conserved in all eukaryotes and prokaryotes and consist of two highly conserved domains: an N-terminal ATP-binding domain and a C-terminal substrate-binding domain (Lindquist. 1986; Taipale et al., 2010). These proteins generally serve in regulating the adaptions of insects to adverse environments and serve as a predominant self-protection mechanism (Chen et al., 2015a; Guo and Feng, 2018). The heat shock protein 70 family includes stress-inducible genes (HSP70s) and constitutively expressed members or heat shock cognates (HSC70s) (Daugarrd et al., 2007). HSC70s participate in various processes in an unstressed cell, such as folding of proteins after translation or membrane translocation, and may or may not be influenced by stress (Denlinger et al., 2001; Daugarrd et al., 2007). HSP60 helps protect against protein aggregation of denaturing proteins during diapause and operates the bending and assembling of enzymes and other protein complexes related to energy metabolism (Meyer et al., 2003; Brackley and Grantham, 2009; Mayer, 2010; King and MacRae, 2015).

There is an approximate doubling in the frequency and the magnitude of regional heat wave events from 1960 to 2018 in China, with the top three regional heat wave events in the summers of 2013, 2017, and 2003 (Wang and Yan, 2021). *Ostrinia furnacalis*, Lepidoptera (Crambidae), is one of the most common pests of corn in China, which causes economic losses in summer (Zhou and He, 1995; He et al., 2018). The survey showed that it detected about 300 larvae per 100 corn plants in Jilin Province and even 100% damage in Qinhuangdao city (Hebei province) (Yuan et al., 2013). On a summer day (from July to August), the temperature often climbs to 38 or more and has been reported to significantly affect the *O. furnacalis* population (Zhou et al., 2018).

The well-known mechanism used to cope with extreme temperatures is the expression of stress-inducible HSPs (Feder and Hofmann 1999; Sørensen et al., 2003; King and MacRae, 2015; Ma et al., 2021). The transcription of genes (mRNAs) encoding inducible heat shock proteins (in the response) appears to be temperature-sensitive in insects (Lindquist, 1986; Theodorakis and Morimoto, 1987; Morimoto, 1993; Sistonen et al., 1994; Prahlad and Morimoto, 2009; Lewis et al., 2016; Jin et al., 2020; Tian et al., 2020). However, the HSP expression of thermal tolerance or acclimation of *O. furnacalis* and the molecular mechanisms in its physiology, are poorly understood. In our study, we focused on the high temperatures that induce HSPs and then investigated *O. furnacalis* thermal tolerance in progressive recovery from extremely high temperatures. We related dynamic changes of potential heat shock protein genes through reverse-transcription quantitative polymerase chain reactions (RT-qPCRs). Our study helps improve the understanding of the mechanisms of thermotolerance in *O. furnacalis* and at a molecular level, analyzes the acclimation characteristics.

Materials and methods

Insects

Asian corn borer, *O. furnacalis,* adults were collected from Luoyang city, Henan province (111.8′112.59 "E, 33.35′35.05″ N). Progenies were maintained at insectary (27 ± 1°C, 70 ± 10% RH, and L16: D8 h) with standard artificial diet and techniques (Zhou and He, 1995) in the insectary to establish a laboratory colony. The 12-day-old (4th instar) larvae, which are more resilient to stress, were used in the following experiments.

Heat shock and recovery experiments

Ten larvae were placed into a 10-ml centrifuge tube with 12 holes (0.2 cm in diameter). Three experiments for exposure to

extremely high temperatures were carried out. Two independent replicates were performed in the experiments.

Exp. 1: the extreme heat wave in August has been reported at 43 C in some parts of China (https://news.bjd.com.cn/2022/08/13/10133544.shtml). Our previous findings have shown that *O. furnacalis* eggs could not survive at 45 C (Quan et al., 2022). Larvae (ca. 400) were exposed to extremely high temperatures of 43 C with 50% ± 10% RH (usually it is ~40%–55% on 5–7 days at 35°C–40°C in the field) (Zhou et al., 1996; Chen et al., 2012) for 2 h in the chambers. Then, the larvae were transferred to 27°C, 70% ± 10% RH for recovery. After 0, 0.5, 1, 1.5, 2, 4, and 8 h, fifty larvae each were transferred to the chamber set up with a temperature of 43°C and 50% ± 10% RH. Survivors were checked by touching a larva's head with a small paintbrush, and they recorded every hour until all larvae were dead. Another fifty larvae were maintained at 27°C (70% ± 10% RH); thus, unexperienced exposure to 43 C was used as control. They were also subjected to the chamber at 43°C and 50% ± 10% RH, and survivors were checked out hourly.

Exp. 2: to generate a time series of heat shocks, 30–40 larvae were exposed to treatment temperatures of 31, 33, and 35 C for 1, 2, 4, 6, and 8 h in a chamber (VM04/100, Heraeus, Germany) with 50% ± 10% RH. Treated larvae were then frozen in liquid nitrogen and stored at −80 C before being used for mRNA extraction. Larvae were maintained at 27°C, and RH 70% ± 10% were used as a control.

Exp. 3: to investigate the effect of recovery time, 270 larvae were first exposed to 43°C and 50% ± 10% RH for 2 h. They were then transferred to 27 C for recovery. Finally, 30 larvae at a time were frozen in liquid nitrogen and stored at −80 C after 0, 0.5, 1, 1.5, 2, 4, 8, 16, and 32 h of recovery.

Exp. 4: larvae were exposed to 43 C 50% ± 10% RH for 2 h. They were then transferred to 27°C and 70% ± 10% RH for recovery. After 0, 0.5, 1, 2, 4, 6, and 8 h, the larvae were re-exposed to 43°C and 50% ± 10% RH for 0, 0.5, 1, 1.5, 2, 4, 8, and 16 h. Lastly, fifty larvae at a time were immediately frozen in liquid nitrogen and stored at −80 C before being used for mRNA extraction.

RNA isolation and cDNA synthesis

TRIzol (Invitrogen, United States) reagent was used to extract total RNA from sampled insects, following the manufacturer's instructions. In brief, frozen tissues were smashed for ~8 min (adding 15 ml liquid nitrogen per 2–3 min) by hand. Then, ~0.1 g of insect powder was homogenized with 1 ml of TRIzol reagent into a 1.5-ml centrifuge tube and incubated at room temperature for 5 min. Phase separation of RNA was performed using 200 µl chloroform, 500 µl isopropanol for precipitation, washing with 800 µl, and 70% ethanol. The reaction was stopped by washing, followed by centrifugation at 4°C, 7,500 rpm for 5 min, and the supernatant was removed. We repeated the washing several times, subsequently air-dried samples, and then re-dissolved them (the final sediment) in RNase-free water. The purity and concentration of RNA were measured by agarose gel electrophoresis using a Nanodrop 2000 spectrophotometer (ThermoScientific, United States). The samples with an A260/280 ratio of ≥1.8 were used in downstream applications. The aliquots were frozen and stored at −80 C.

The cDNA synthesis was performed using a commercial reverse transcription kit (AT341-02, TransGen Biotech, China). An aliquot of RNA (2000 ng) from each sample was mixed with the reaction including 10 µl of the sample (dissolved by RNase-free water), 1 µl of anchored Oligo (dT) $_{18}$ primer, 1 µl of the TransScript RT/RI enzyme mix, 1 µl of the gDNA remover, and 10 µl of the TS reaction mix. This solution was mixed; then, the reaction was incubated at 42 C for 30 min and 85 C for 5 s. When the reaction was stopped, the cDNA was stored at −20 C.

Quantification of *HSP* gene expression (qRT-PCR)

According to the sequences of HSP60 (accession No: XM_028317890.1), HSC70 (accession No: JF708083.1), HSP70 (accession No: XM_028322992.1), and HSP90 (accession No: GU230734.1) in Asian corn borer registered in GenBank, the specific primers were designed. Through comparison and verification, 10 primers were used to amplify selected target genes (Supplementary Table S1).

The kit used for fluorescence quantitative real-time PCR (qRT-PCR) was SYBR® Premix Ex Taq™ (TaKaRa). Ribosomal protein L8 (18sRNA) was used as a reference gene (Wang et al., 2007). The amplification program was set as follows: 1) initial denaturation 2 min at 95°C; 2) 95°C for 5 s and 60°C for 30 s; 3) step 2) was repeated for 40 cycles. Each sample was replicated three times, and we calculated the average value (Wang et al., 2007). The amplification efficiency of each heat shock protein gene was recorded, and the different heat shock protein genes related to transcription were analyzed by the $2^{-\triangle\triangle CT}$ method (Livak and Schmittgen, 2001).

Data analysis

Larval thermal tolerance data, i.e., the survival as influenced by the time in the various recovery time treatments after exposure to 43°C, were analyzed and calculated by the Kaplan–Meier function. HSP expression levels under different temperatures were analyzed using a one-way analysis of variance (one-way ANOVA). The means were compared with Fisher's protected LSD test, and statistical significance was considered at $p < 0.05$. All data analyses were processed in SPSS 17.0 software (Chicago: SPSS Inc.).

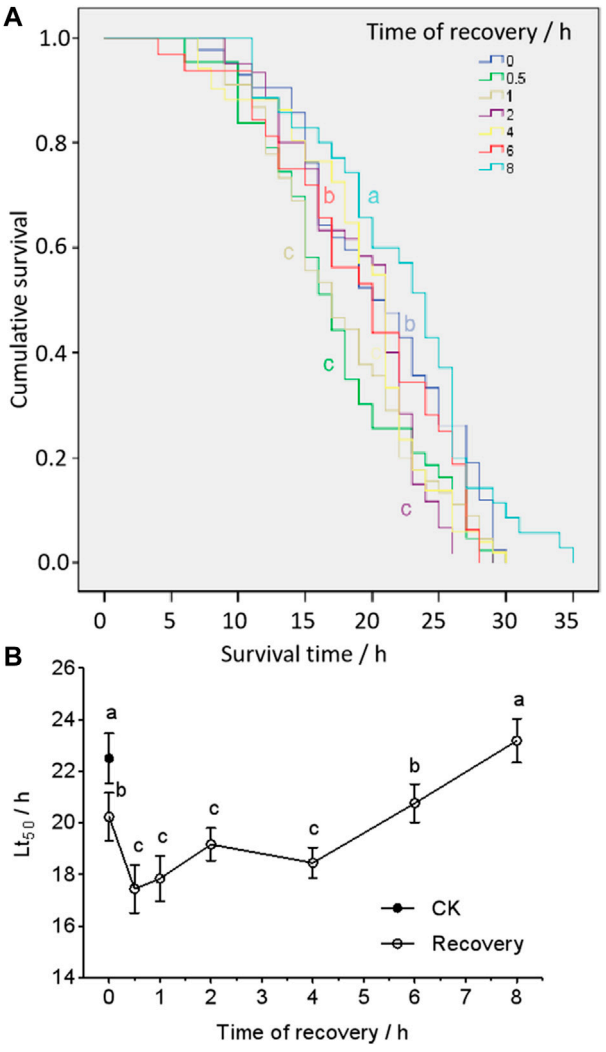

FIGURE 1
Cumulative survival curves **(A)** and medium lethal time (Lt_{50}) **(B)** of larvae post-heat shock at 43°C, 2 h treatment. The curves **(A)** were analyzed by a Kaplan–Meier analysis (chi-squared test), and Lt_{50}s **(B)** were from the Kaplan–Meier calculation. The different letters (the color of the letter stands for the same color curve) represent a significant difference ($p < 0.05$).

Results

Heat shock-induced thermal tolerance

The survival curves of different recovery time were significantly different in larvae ($df = 6$; $\chi^2 = 18.7$; $p < 0.05$) (Figure 1A). The median lethal time (Lt_{50}) (from the Kaplan–Meier function) of survival in heat-shocked larvae (43 C for 2 h) was significantly lower when they were re-exposed to 43 C within 30 min (0.5 h), but it increased as recovery time increased. This reached untreated levels after 6 h of recovery and got significantly longer hereafter (Figure 1).

Transcriptional fluctuation of *HSP* genes in larvae exposed to different temperatures

In response to the heat shock treatment, the expression levels of the *HSP* genes varied significantly ($F_{3,20} = 699$, $p < 0.001$; $F_{3,20} = 581$, $p < 0.001$) (Figures 2, 3). In comparison with the control, the transcriptional levels of *HSP*60 and *HSC*70 did not change significantly among all temperature treatments ($F_{HSP60} = 35$, $df = 3, 20$, and $p = 0.073$; $F_{HSC70} = 6$, $df = 3, 20$, and $p = 0.364$) (Figures 2, 3A,B). By contrast, transcriptional levels of *HSP70* and *HSP90* were significantly upregulated in treatments of exposure to 33 ($F_{HSP70} = 195$, $df = 8$, and $p < 0.05$; $F_{HSP90} = 163$, $df = 8$, and $p < 0.05$) and 35 C ($F_{HSP70} = 335$, $df = 8$, and $p < 0.001$; $F_{HSP90} = 584$, $df = 8$, and $p < 0.364$) for 1 h compared to the control exposed at 27°C, but there was no significant difference observed between treatment temperature of 31°C ($F_{HSP70} = 3.1$, $df = 8$, $p = 0.094$; $F_{HSP90} = 3.7$, $df = 8$, $p = 0.081$) and the control (Figures 2C,D). However, the transcriptional level declined when exposure time increased and was at the untreated level in 4 h. Moreover, *HSP70* could reach a higher peak value at the treatment of 43°C (>10-fold than the 35°C treatment) and remained high longer (16 h) (Figure 3C).

Dynamics of the transcriptional level of *HSP* genes in heat-shocked larvae

To investigate the responses of HSPs at different recovery times during the thermal tolerance, we quantified the dynamics of transcription of *HSPs* over time. The results of the qRT-PCR analysis showed that the transcriptional level of *HSP60/HSC70* was upregulated only 3- and 5-fold after heat shock compared with the control (Figure 4). It would return to the untreated level after a recovery time of 0.5 h.

By contrast, the transcriptional level of *HSP70* rapidly increased 156-fold compared with the control and reached a peak of 230-fold at a recovery time of 0.5 h. It was dropped to 30-fold at a recovery time of 2 h. It returned to the control level at 16 h (Figure 4).

The transcriptional level of *HSP90* was upregulated 50-fold in response to heat shock. It went up to 140-fold at a recovery time of 0.5 h but dropped down to 30-fold at a recovery time of 1 h. Then, it gradually decreased to the control level in 16 h.

Effects of recovery time on heat shock-induced transcriptional alteration of HSP genes

The recovery time of heat-shocked larvae significantly influenced the transcription of *HSP70* and *HSP90* genes when they were re-exposed to 43 C (Figure 5). As recovery time increased from 0.5 to 2 h, the peak of the relative transcriptional level of *HSP70* increased from 177- to 209-fold and was lower than the control (0 h recovered, 245-fold) when

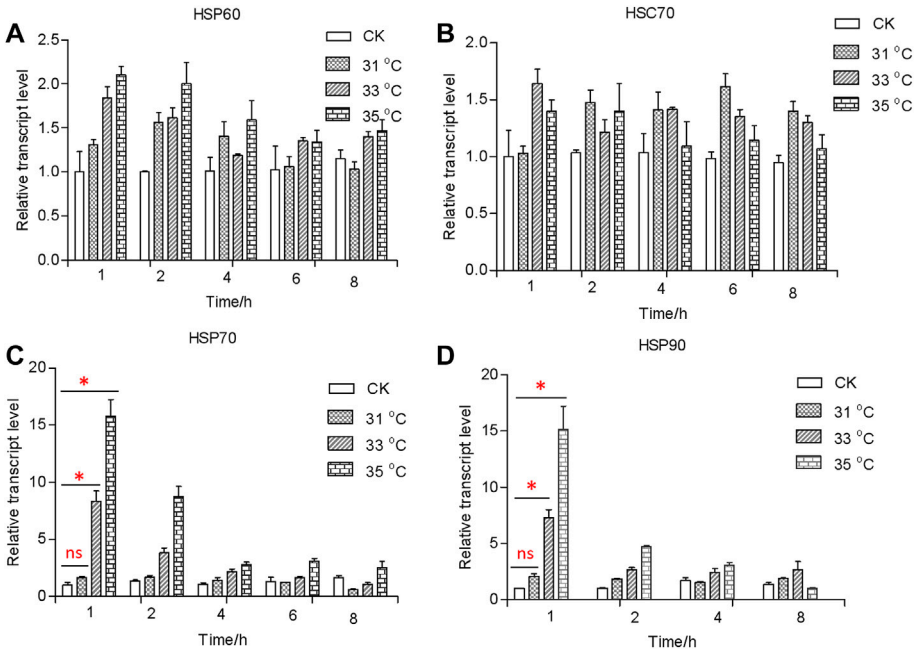

FIGURE 2
Relative transcript levels of *HSP60* **(A)**, *HSC70* **(B)**, *HSP70* **(C)**, and *HSP90* **(D)** under different temperatures. Relative mRNA levels were analyzed using the $2^{-\Delta\,\Delta CT}$ method. All values from two independent replicates are shown as the mean ± SD. The data (*HSP70* and *HSP90*) between CK (27 C) and other treatments (31/33/35 C) at 1 h were analyzed by ANOVA. "*" stands for a significant difference ($p < 0.05$) between CK (27 C) and other treatments; "ns" is not significant.

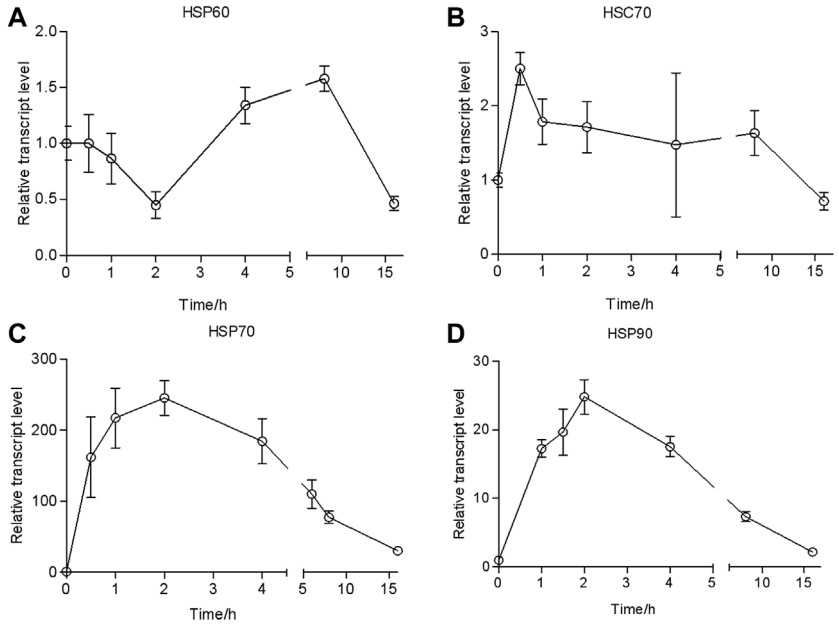

FIGURE 3
Relative transcript levels of *HSP60* **(A)**, *HSC70* **(B)**, *HSP70* **(C)**, *and HSP90* **(D)** at different times with 43°C treatment. The values from two independent replicates are shown as the mean ± SD, as analyzed by the $2^{-\Delta\Delta CT}$ method.

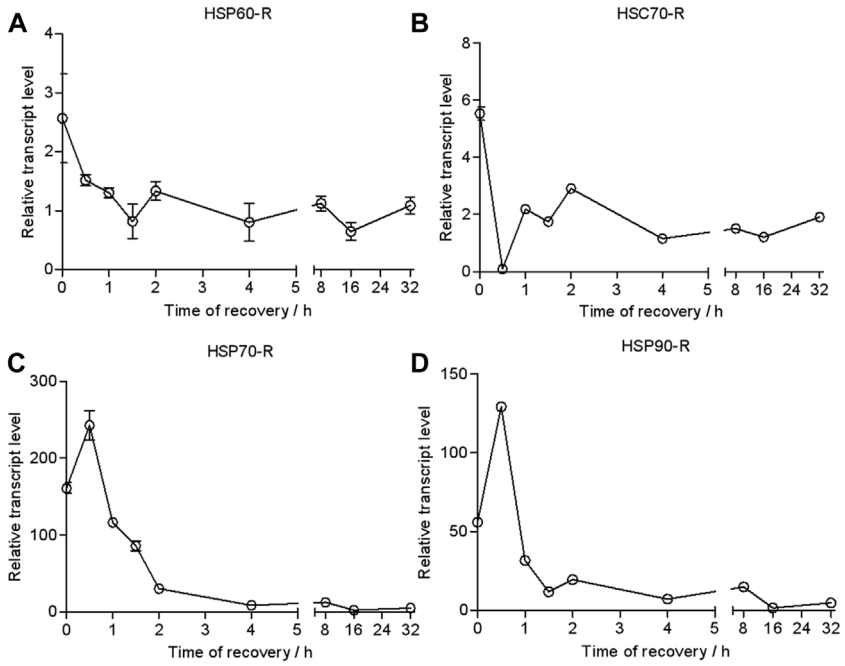

FIGURE 4
Relative transcript levels of *HSP60* **(A)**, *HSC70* **(B)**, *HSP70* **(C)**, *and HSP90* **(D)** during recovery time (43°C, 2 h treatment). Relative mRNA levels were analyzed using the $2^{-\Delta\ \Delta CT}$ method. The values from two independent replicates are shown as the mean ± SD.

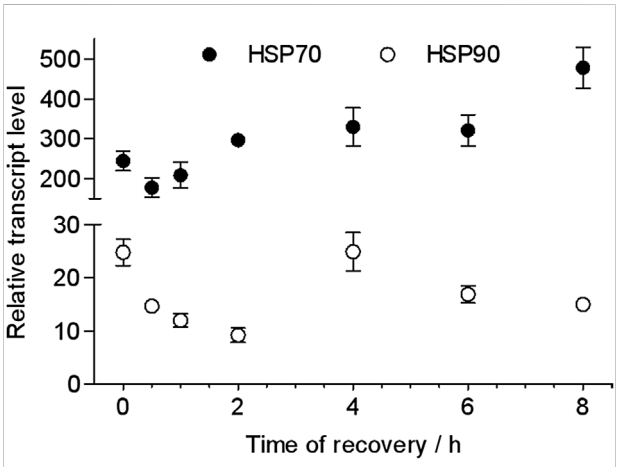

FIGURE 5
Peak relative transcript levels of *HSP70* and *HSP90* at different recovery times after heat shock at 43 C for 2 h. The values from two independent replicates are shown as the mean ± SD and analyzed by the $2^{-\Delta\Delta CT}$ method.

heat-shocked larvae were resubjected to 43 C for 2 h. However, when recovery time increased to 4–6 h, the relative transcriptional level of *HSP70* was ~300- and 478-fold (at 8 h). This was similar to *HSP70* whereas the transcription of *HSP90* was upregulated to when 0.5 h recovered larvae were re-exposed to 43 C from 0.5 to 16 h; the peak time was 1 h. However, the transcriptional level was lower than the control (0 h recovered).

Discussion

Thermal acclimation and/or heat shock can significantly alter thermotolerance in invertebrates, such as *Tribolium castaneum* (Lü and Huo, 2018), *Drosophila melanogaster* (Colinet et al., 2013), and *Nilaparvata lugens* (Piyaphongkul et al., 2014). However, thermal acclimation and/or heat shock-induced heat tolerance varies among the studies due to different exposure regimens, patterns, and hardening. (Dahlgaard et al., 1998; Ju et al., 2011; Piyaphongkul, 2013; Lu et al., 2016; Jin et al., 2019). In this study, the thermotolerance declined within 0.5–4 h after heat shock at 33°C–43°C, but it significantly increased after 6 h. This suggests that post-heat shock time is strongly related to thermotolerance.

Heat shock proteins are expressed as one of the defensive proteins in most organisms in response to various stressful conditions (Feder and Hoffmann, 1999). In most cases, heat-resistant species are characterized by a higher basal level of HSPs than more thermosensitive species. Previous studies showed that increased temperatures elicited activation of a conserved pathway involving heat shock transcription, which enhanced

the heat shock response (Rinehart and Denlinger, 2000; Kayukawa et al., 2005; Lopez-Martinez and Denlinger, 2008; Gonsalves et al., 2011; Li et al., 2012; King and MacRae, 2015). In our study, the results showed that temperatures of 31 C–33 C were the threshold triggering *HSP70* gene expression. We also detected increased transcription of *HSP70* and *HSP90* from the high-temperature (35°C–43°C) treatment. The transcription was correlated with the thermal time, but there was no significant change in the transcription of *HSP60* or *HSC70* after heat shock at 35°C–43°C. This suggests that *HSP70* and *HSP90* are responsible for heat-shocked induced defenses. This is similar to that reported for *D. melanogaster*, where expression of HSPs was affected by the heat shock treatment or response (Sørensen et al., 2007).

In addition, the upregulation of *HSP70* or *HSP90* was mostly detected after ~1–2 h of exposure to heat, then slowed in the following period, and greatly decreased after being transferred to 27 C (for recovery). These results indicated the response to extreme heat events is related to *HSP70* and *HSP90* in *O. furnacalis*. Heat shock proteins are required for survival during heat or cold but cannot maintain a high level of expression in organisms all the time (Scott et al., 1997; Krebs and Feder, 1998; Bowler, 2005). Upregulation of the *HSP70* gene in response to high temperatures was also observed in *Bemisia tabaci* (Hu et al., 2014), *Drosophila buzzatii* (Sørensen et al., 1999), *Anopheles gambiae* (Benoit et al., 2010), and *Nilaparvata lugens* (Lu et al., 2016). The temperatures >31 C upregulate the response of *HSP70* and *HSP90*, but it was not sustainable (for more than 2 h).

The extremely high temperatures can generate damage indirectly by driving an increase in water loss, disrupting the cellular ion balance (hyperkalemia), impairing neurophysiological functions, and damaging mitochondria (O'Sullivan et al., 2017; Bowler, 2018). Insects can produce and accumulate particular molecules to prevent protein denaturation or cell inactivation when they suffer from thermal stimuli (King and MacRae, 2015; Ma et al., 2021). In this study, we observed that the thermal tolerance was significantly lower at the post-heat shock time of 0.5–4 h, with no difference at 6 h, and then enhanced at 8 h. This implies that the insects had internal injuries while suffering heat shock, but it was possibly self-healing within 6 h. Immunological/defensive memory takes over "experience" from the previous injury and rebuilds the immunological/defensive system over 6 h of recovery.

A higher transcription of *HSP70* was detected in a post-heat shock time of 8 h. Correspondingly, the longest median death time was observed at this time. These findings reveal that *HSP70* and *HSP90* are related to the heat shock response and play an important role in heat shock-induced thermotolerance. It also indicates that the inducible HSP70 protects cells or tissue against thermal tolerance and delays thermal injury (Hoffmann et al., 2003; Ruell et al., 2009). Similar findings have been reported in other species. For instance, in *D. melanogaster,* the heat tolerance, metabolic rate, and gene expression significantly change after heat pretreatment (Sørensen et al., 2005; Malmendal et al., 2006). Apple maggot *Rhagoletis pomonella* expresses HSP increasingly from midday to a peak in the afternoon in summer (Lopez-Martinez and Denlinger, 2008). Locusts *Locusta migratoria* are more heat tolerant at low than at high latitudes as a result of their expression pattern of *HSP70* and *HSP90* (Chen et al., 2015b). HSPs (Feder et al., 1997; Lopez-Martinez and Denlinger, 2008) and cuticle proteins (Nguyen et al., 2009) are induced and/or accumulated to deal with extremely high temperatures in *Aphis gossypii* and sorbitol in *Bemisia argentifolii*. In this study, enhancing heat resistance could induce recovery in 6–8 h and is mostly regulated by *HSP70*.

In conclusion, our results suggested that *HSP70* and *HSP90* in *O. furnacalis* are immediately induced by heat events, but *HSP60* and *HSC70* are not. The highest upregulation of *HSP*s is achieved in 2 h and then returns to a normal level at 16 h. In addition, with a post-heat shock time of 0.5–4 h (i.e., recovery time), there is lower thermotolerance, possibly a defensive rebuilding time. Heat-induced thermotolerance achieves at a post-heat shock time of >6 h. Extreme thermal stress-induced quick dynamics of *HSP70* or *HSP90* could be interpreted as an 7adaptation to the drastic and rapid temperature variations. These findings are helpful to understand insect responses to stress.

Data availability statement

The datasets presented in this study can be found in online repositories. The names of the repository/repositories and accession number(s) can be found at: https://www.ncbi.nlm.nih.gov/nuccore/XM_028317890.1, XM_028317890.1; https://www.ncbi.nlm.nih.gov/nuccore/JF708083.1, JF708083.1; https://www.ncbi.nlm.nih.gov/nuccore/XM_028322992.1, XM_028322992.1; https://www.ncbi.nlm.nih.gov/nuccore/GU230734.1, GU230734.1.

Author contributions

KH and YQ conceptualized the research. YQ, KH, and ZW designed the experiments. YQ performed the experiment. YQ and KH contributed to data analyses. YQ wrote the manuscript, and KH revised the manuscript. All authors contributed to the manuscript and approved the submitted version.

Funding

This research was supported by the programs of the China Agriculture Research System of MOF and MARA (CARS-02) and the Agricultural Science and Technology Innovation Program (ASTIP) of CAAS.

Conflict of interest

The authors declare that the research was conducted in the absence of any commercial or financial relationships that could be construed as a potential conflict of interest.

Publisher's note

All claims expressed in this article are solely those of the authors and do not necessarily represent those of their affiliated organizations, or those of the publisher, the editors, and the reviewers. Any product that may be evaluated in this article, or claim that may be made by its manufacturer, is not guaranteed or endorsed by the publisher.

Supplementary material

The Supplementary Material for this article can be found online at: https://www.frontiersin.org/articles/10.3389/fphys.2022.992293/full#supplementary-material

References

Alexander, L. V., Zhang, X., Peterson, T. C., Caesar, J., Gleason, B. E., Klein Tank, A. M. G., et al. (2006). Global observed changes in daily climate extremes of temperature and precipitation. *J. Geophys. Res.* 111, D05109. doi:10.1029/2005JD006290

Angilletta, M. J., Jr (2009). Looking for answers to questions about heat stress: Researchers are getting warmer. *Funct. Ecol.* 23, 231–232. doi:10.1111/j.1365-2435.2009.01548.x

Basha, E., O'Neill, H., and Vierling, E. (2012). Small heat shock proteins and α-crystallins: Dynamic proteins with flexible functions. *Trends biochem. Sci.* 37, 106–117. doi:10.1016/j.tibs.2011.11.005

Benoit, J. B., Lopez-Martinez, G., Phillips, Z. P., Patrick, K. R., and Denlinger, D. L. (2010). Heat shock proteins contribute to mosquito dehydration tolerance. *J. Insect Physiol.* 56, 151–156. doi:10.1016/j.jinsphys.2009.09.012

Bowler, K. (2005). Acclimation, heat shock and hardening. *J. Therm. Biol.* 30, 125–130. doi:10.1016/j.jtherbio.2004.09.001

Bowler, K. (2018). Heat death in poikilotherms: Is there a common cause? *J. Therm. Biol.* 76, 77–79. doi:10.1016/j.jtherbio.2018.06.007

Brackley, K. I., and Grantham, J. (2009). Activities of the chaperonin containing TCP-1 (CCT): Implications for cell cycle progression and cytoskeletal organisation. *Cell Stress Chaperones* 14, 23–31. doi:10.1007/s12192-008-0057-x

Chen, B., Li, S., Ren, Q., Tong, X., Zhang, X., and Kang, L. (2015a). Paternal epigenetic effects of population density on locust phase-related characteristics associated with heat-shock protein expression. *Mol. Ecol.* 24, 851–862. doi:10.1111/mec.13072

Chen, W., Li, D., Zhang, M., Zhao, Y., Wu, W., and Zhang, G. (2015b). Cloning and differential expression of five heat shock protein genes associated with thermal stress and development in the polyphagous predatory mite *Neoseiulus cucumeris* (Acari: Phytoseiidae). *Exp. Appl. Acarol.* 67, 65–85. doi:10.1007/s10493-015-9933-0

Chen, Y., Chen, Y., Wen, Y., Zhang, X., and Chen, D. (2012). The effects of the relative humidity on the insecticidal expression level of Bt cotton during bolling period under high temperature. *Field Crops Res.* 137, 141–147. doi:10.1016/j.fcr.2012.08.015

Chown, S. L., and Nicolson, S. W. (2004). *Insect physiological ecology: Mechanisms and patterns*. Oxford, UK: Oxford Univ. Press.

Colinet, H., Overgaard, J., Com, E., and Sorensen, J. G. (2013). Proteomic profiling of thermal acclimation in *Drosophila melanogaster*. *Insect biochem. Mol. Biol.* 43, 352–365. doi:10.1016/j.ibmb.2013.01.006

Dahlgaard, J., Loeschcke, V., Michalak, P., and Justesen, J. (1998). Induced thermotolerance and associated expression of the heat-shock protein Hsp70 in adult *Drosophila melanogaster*. *Funct. Ecol.* 12, 786–793. doi:10.1046/j.1365-2435.1998.00246.x

Daugarrd, M., Rohde, M., and Jaattela, M. (2007). The heat shock protein 70 family: Highly homologous proteins with overlapping and distinct functions. *FEBS Lett.* 581, 3702–3710. doi:10.1016/j.febslet.2007.05.039

Denlinger, D. L., Rinehart, J. P., and Yocum, G. D. (2001). "Stress proteins: A role in insect diapause?," in *Insect timing: Circadian rhythmicity to seasonality*. Editors D. L. Denlinger, J. M. Giebultowicz, and D. S. Saunders (Amsterdam: Elsevier), 155–171.

Feder, M. E., Blair, N. T., and Figueras, H. (1997). Natural thermal stress and heat-shock protein expression in Drosophila larvae and pupae. *Funct. Ecol.* 11, 90–100. doi:10.1046/j.1365-2435.1997.00060.x

Feder, M. E., and Hofmann, G. E. (1999). Heat-shock proteins, molecular chaperones, and the stress response: Evolutionary and ecological physiology. *Annu. Rev. Physiol.* 61, 243–282. doi:10.1146/annurev.physiol.61.1.243

Fox, R. J., Donelson, J. M., Schunter, C., Ravasi, T., and Gaitán-Espitia, J. D. (2019). Beyond buying time: The role of plasticity in phenotypic adaptation to rapid environmental change. *Philos. Trans. R. Soc. Lond. B Biol. Sci.* 374, 20180174. doi:10.1098/rstb.2018.0174

Gibert, P., Debat, V., and Ghalambor, C. K. (2019). Phenotypic plasticity, global change, and the speed of adaptive evolution. *Curr. Opin. Insect Sci.* 35, 34–40. doi:10.1016/j.cois.2019.06.007

Gonsalves, S. E., Moses, A. M., Razak, Z., Robert, F., and Westwood, J. T. (2011). Whole-genome analysis reveals that active heat shock factor binding sites are mostly associated with non-heat shock genes in *Drosophila melanogaster*. *PLoS One* 6, e15934. doi:10.1371/journal.pone.0015934

Greenspan, R. J., Finn, J. A., Jr, and Hall, J. C. (1980). Acetylcholinesterase mutants in Drosophila and their effects on the structure and function of the central nervous system. *J. Comp. Neurol.* 189, 741–774. doi:10.1002/cne.901890409

Gunderson, A. R., and Stillman, J. H. (2015). Plasticity in thermal tolerance has limited potential to buffer ectotherms from global warming. *Proc. Biol. Sci.* 282, 20150401. doi:10.1098/rspb.2015.0401

Guo, X., and Feng, J. (2018). Comparisons of expression levels of heat shock proteins (HSP70 and HSP90) from *Anaphothrips obscurus* (Thysanoptera: Thripidae) in polymorphic adults exposed to different heat shock treatments. *J. Insect Sci.* 18, 1–10. doi:10.1093/jisesa/iey059

He, H. M., Xiao, L., Chen, Q. W., and Xue, F. S. (2018). A life-history trait of the asian corn borer, *Ostrinia furnacalis* (Lepidoptera: Pyralidae)—positive correlation between body weight and temperature. *Acta. Entomol. Sin.* 61, 340–347. doi:10.16380/j.kcxb.2018.03.009

Hoffmann, A. A., Chown, S. L., and Clusella-Trullas, S. (2013). Upper thermal limits in terrestrial ectotherms: How constrained are they? *Funct. Ecol.* 27, 934–949. doi:10.1111/j.1365-2435.2012.02036.x

Hoffmann, A. A., Sørensen, J. G., and Loeschcke, V. (2003). Adaptation of *Drosophila* to temperature extremes: Bringing together quantitative and molecular approaches. *J. Therm. Biol.* 28, 175–216. doi:10.1016/S0306-4565(02)00057-8

Hu, J., Chen, B., and Li, Z. (2014). Thermal plasticity is related to the hardening response of heat shock protein expression in two *Bactrocera* fruit flies. *J. Insect Physiol.* 67, 105–113. doi:10.1016/j.jinsphys.2014.06.009

Jin, J., Li, Y., Zhou, Z., Zhang, H., Guo, J., and Wan, F. (2020). Heat shock factor is involved in regulating the transcriptional expression of two potential Hsps (AhHsp70 and AhsHsp21) and its role in heat shock response of *Agasicles hygrophila*. *Front. Physiol.* 11, 562204. doi:10.3389/fphys.2020.562204

Jin, J., Zhao, M., Wang, Y., Zhou, Z., Wan, F., and Guo, J. (2019). Induced thermotolerance and expression of three key Hsp genes (Hsp70, Hsp21, and sHsp21) and their roles in the high temperature tolerance of *Agasicles hygrophila*. *Front. Physiol.* 10, 1593. doi:10.3389/fphys.2019.01593

Ju, R. T., Chen, G. B., Ju, R. T., Chen, G. B., Wang, F., Li, B., et al. (2011). Effects of heat shock, heat exposure pattern, and heat hardening on survival of the sycamore lace bug, *Corythucha ciliata*. *Entomol. Exp. Appl.* 141, 168–177. doi:10.1111/j.1570-7458.2011.01180.x

Kayukawa, T., Chen, B., Miyazaki, S., Itoyama, K., Shinoda, T., and Ishikawa, Y. (2005). Expression of mRNA for the t-complex polypeptide–1, a subunit of chaperonin CCT, is upregulated in association with increased cold hardiness in *Delia antiqua*. *Cell Stress Chaperones* 10, 204–210. doi:10.1379/CSC-106R.1

King, A. M., and MacRae, T. H. (2015). Insect heat shock proteins during stress and diapause. *Annu. Rev. Entomol.* 60, 59–75. doi:10.1146/annurev-ento-011613-162107

Krebs, R., and Feder, E. (1998). Hsp70 and larval thermotolerance in *Drosophila melanogaster*: How much is enough and when is more too much? *J. Insect Physiol.* 44, 1091–1101. doi:10.1016/S0022-1910(98)00059-6

Lewis, M., Götting, M., Anttila, K., Kanerva, M., Prokkola, J. M., Seppänen, E., et al. (2016). Different relationship between hsp70 mrna and hsp70 levels in the heat shock response of two salmonids with dissimilar temperature preference. *Front. Physiol.* 7, 511. doi:10.3389/fphys.2016.00511

Li, J., Moghaddam, H. H., Du, X., Zhong, B., and Chen, Y. Y. (2012). Comparative analysis on the expression of inducible HSPs in the silkworm, *Bombyx mori*. *Mol. Biol. Rep.* 39, 3915–3923. doi:10.1007/s11033-011-1170-y

Lindquist, S. (1986). The heat-shock response. *Annu. Rev. Biochem.* 55, 1151–1191. doi:10.1146/annurev.bi.55.070186.005443

Livak, K. J., and Schmittgen, T. D. (2001). Analysis of relative gene expression data using real-time quantitative PCR and the 2(-Delta C(T)) Method. *Methods* 25, 402–408. doi:10.1006/meth.2001.1262

Lopez-Martinez, G., and Denlinger, D. L. (2008). Regulation of heat shock proteins in the apple maggot *Rhagoletis pomonella* during hot summer days and overwintering diapause. *Physiol. Entomol.* 33, 346–352. doi:10.1111/j.1365-3032.2008.00639.x

Lü, J., and Huo, M. (2018). Transcriptome analysis reveals heat tolerance of *Tribolium castaneum* (Herbst) (Coleoptera: Tenebrionidae) adults. *J. Stored Prod. Res.* 78, 59–66. doi:10.1016/j.jspr.2018.06.004

Lu, K., Chen, X., Liu, W., and Zhou, Q. (2016). Characterization of heat shock cognate protein 70 gene and its differential expression in response to thermal stress between two wing morphs of *Nilaparvata lugens* (Stål). *Comp. Biochem. Physiol. A Mol. Integr. Physiol.* 199, 47–53. doi:10.1016/j.cbpa.2016.05.009

Ma, C. S., Ma, G., and Pincebourde, S. (2021). Survive a warming climate: Insect responses to extreme high temperatures. *Annu. Rev. Entomol.* 66, 163–18422. doi:10.1146/annurev-ento-041520-074454

Malmendal, A., Overgaard, J., Bundy, J. G., Sørensen, J. G., Nielsen, N. C., Loeschcke, V., et al. (2006). Metabolomic profiling of heat stress: Hardening and recovery of homeostasis in *Drosophila*. *Am. J. Physiol. Regul. Integr. Comp. Physiol.* 291, 205–212. doi:10.1152/ajpregu.00867.2005

Mayer, M. P. (2010). Gymnastics of molecular chaperones. *Mol. Cell* 39, 321–331. doi:10.1016/j.molcel.2010.07.012

Meehl, G. A., and Tebaldi, C. (2004). More intense, more frequent, and longer lasting heat waves in the 21st century. *Science* 305, 994–997. doi:10.1126/science.1098704

Meyer, A. S., Gillespie, J. R., Walther, D., Millet, I. S., Doniach, S., and Frydman, J. (2003). Closing the folding chamber of the eukaryotic chaperonin requires the transition state of ATP hydrolysis. *Cell* 113, 369–381. doi:10.1016/S0092-8674(03)00307-6

Morimoto, R. I. (1993). Cells in stress: Transcriptional activation of heat shock genes. *Science* 259, 1409–1410. doi:10.1126/science.8451637

Neven, L. G. (2000). Physiological responses of insects to heat. *Postharvest Biol. Technol.* 21, 103–111. doi:10.1016/S0925-5214(00)00169-1

Nguyen, T. T., Michaud, D., and Cloutier, C. (2009). A proteomic analysis of the aphid *Macrosiphum euphorbiae* under heat and radiation stress. *Insect biochem. Mol. Biol.* 39, 20–30. doi:10.1016/j.ibmb.2008.09.014

O'Sullivan, J., MacMillan, H. A., and Overgaard, J. (2017). Heat stress is associated with disruption of ion balance in the migratory locust, *Locusta migratoria*. *J. Therm. Biol.* 68, 177–185. doi:10.1016/j.jtherbio.2016.04.001

Piyaphongkul, J. (2013). *Effects of thermal stress on the brown planthopper Nilaparvata lugens (Stal)*. Birmingham: Diss. University of Birmingham.

Piyaphongkul, J., Pritchard, J., and Bale, J. (2014). Effects of acclimation on the thermal tolerance of the Brown planthopper *Nilaparvata lugens* (Stal). *Agric. For. Entomol.* 16, 174–183. doi:10.1111/afe.12047

Prahlad, V., and Morimoto, R. I. (2009). Integrating the stress response: Lessons for neurodegenerative diseases from *C. elegans*. *Trends Cell Biol.* 19, 52–61. doi:10.1016/j.tcb.2008.11.002

Prange, H. D. (1996). Evaporative cooling in insects. *J. Insect Physiol.* 42 (5), 493–499. doi:10.1016/0022-1910(95)00126-3

Quan, Y., Mason, C. E., He, K., Wang, Z., and Wei, H. (2022). Impact of heat waves on egg survival and biological performance across life stages in the Asian corn borer. *Entomol. Exp. Appl.* [in press].

Rensing, L., and Ruoff, P. (2002). Temperature effect on entrainment, phase shifting, and amplitude of circadian clocks and its molecular bases. *Chronobiol. Int.* 19, 807–864. doi:10.1081/CBI-120014569

Rinehart, J. P., and Denlinger, D. L. (2000). Heat-shock protein 90 is down-regulated during pupal diapause in the flesh fly, *Sarcophaga crassipalpis*, but remains responsive to thermal stress. *Insect Mol. Biol.* 9, 641–645. doi:10.1046/j.1365-2583.2000.00230.x

Ruell, P. A., Thompson, M. W., and Hoffman, K. M. (2009). Heat shock proteins as an aid in the treatment and diagnosis of heat stroke. *J. Therm. Biol.* 34, 1–7. doi:10.1016/j.jtherbio.2008.09.004

Rutherford, S. L., and Lindquist, S. (1998). Hsp90 as a capacitor for morphological evolution. *Nature* 396, 336–342. doi:10.1038/24550

Scott, M., Berrigan, D., and Hoffmann, A. A. (1997). Costs and benefits of acclimation to elevated temperature in *Trichogramma carverae*[J]. *Entomol. Exp. Appl.* 85, 211–219. doi:10.1046/j.1570-7458.1997.00251.x

Sgrò, C. M., Terblanche, J. S., and Hoffmann, A. A. (2016). What can plasticity contribute to insect responses to climate change? *Annu. Rev. Entomol.* 61, 433–451. doi:10.1146/annurev-ento-010715-023859

Sistonen, L., Sarge, K. D., and Morimoto, R. I. (1994). Human heat shock factors 1 and 2 are differentially activated and can synergistically induce hsp70 gene transcription. *Mol. Cell. Biol.* 14, 2087–2099. doi:10.1128/MCB.14.3.2087

Sørensen, J. G., Kristensen, T. N., Kristensen, K. V., and Loeschcke, V. (2007). Sex specific effects of heat induced hormesis in Hsf-deficient *Drosophila melanogaster*. *Exp. Gerontol.* 42, 1123–1129. doi:10.1016/j.exger.2007.09.001

Sørensen, J. G., Loeschcke, V., and Kristensen, T. N. (2003). The evolutionary and ecological role of heat shock proteins. *Ecol. Lett.* 6, 1025–1037. doi:10.1046/j.1461-0248.2003.00528.x

Sørensen, J. G., Michalak, P., Justesen, J., and Loeschcke, V. (1999). Expression of the Heat-shock protein HSP70 in *Drosophila buzzatii* lines selected for thermal resistance. *Hereditas* 131, 155–164. doi:10.1111/j.1601-5223.1999.00155.x

Sørensen, J. G., Nielsen, M. M., Kruhøffer, M., Justesen, J., and Loeschcke, I. (2005). Full genome expression analysis of the heat stress response in *Drosophila melanogaster*. *Cell Stress Chaperones* 10, 312–328. doi:10.1379/CSC-128R1.1

Sosalegowda, A. H., Kundapur, R. R., and Boregowda, M. H. (2010). Molecular characterization of heat shock proteins 90 (HSP83?) and 70 in tropical strains of *Bombyx mori*. *Proteomics* 10, 2734–2745. doi:10.1002/pmic.200800830

IPCC (2013). "Technical summary," in *Climate change 2013: The physical science basis. Contribution of working group I to the fifth assessment report of the intergovernmental panel on climate change*. Editors T. F. Stocker, D. Qin, G-K. Plattner, M. Tignor, S. K. Allen, J. Boschung, et al. (Cambridge, UK: Cambridge Univ. Press), 1–127.

Taipale, M., Jarosz, D. F., and Lindquist, S. (2010). HSP90 at the hub of protein homeostasis: Emerging mechanistic insights. *Nat. Rev. Mol. Cell Biol.* 11, 515–528. doi:10.1038/nrm2918

Tedeschi, J. N., Kennington, W. J., Tomkins, J. L., Berry, O., Whiting, S., Meekan, M. G., et al. (2016). Heritable variation in heat shock gene expression: A potential mechanism for adaptation to thermal stress in embryos of sea turtles. *Proc. Biol. Sci.* 283, 20152320–20152327. doi:10.1098/rspb.2015.2320

Tedeschiab, J. N., Kenningtona, W. J., Berryc, O., Whitingd, S., Meekanbe, M., and Mitchellab, N. J. (2015). Increased expression of Hsp70 and Hsp90 mRNA as biomarkers of thermal stress in loggerhead turtle embryos (*Caretta Caretta*). *J. Therm. Biol.* 47, 42–50. doi:10.1016/j.jtherbio.2014.11.006

Theodorakis, N. G., and Morimoto, R. I. (1987). Posttranscriptional regulation of hsp70 expression in human cells: Effects of heat shock, inhibition of protein synthesis, and adenovirus infection on translation and mRNA stability. *Mol. Cell. Biol.* 7, 4357–4368. doi:10.1128/MCB.7.12.4357

Tian, C. B., Li, Y. Y., Huang, J., Chu, W. Q., Wang, Z. Y., and Liu, H. (2020). Comparative transcriptome and proteome analysis of heat acclimation in predatory mite *Neoseiulus barkeri*. *Front. Physiol.* 11, 426. doi:10.3389/fphys.2020.00426

van Heerwaarden, B., Kellermann, V., and Sgro, C. M. (2016). Limited scope for plasticity to increase upper thermal limits. *Funct. Ecol.* 30, 1947–1956. 56. doi:10.1111/1365-2435.12687

Wang, H. S., Wang, X. H., Zhou, C. S., Huang, L. H., Zhang, W., Guo, W., et al. (2007). cDNA cloning of heat shock proteins and their expression in the two phases of the migratory locust. *Insect Mol. Biol.* 16, 207–219. doi:10.1111/j.1365-2583.2006.00715.x

Wang, J., and Yan, Z. (2021). Rapid rises in the magnitude and risk of extreme regional heat wave events in China. *Weather Clim. Extrem.* 34, 100379. doi:10.1016/j.wace.2021.100379

Yuan, Z., Guo, J., Wang, Z., He, K., and Bai, S. (2013). Feeding preference of the Asia corn borer larvae for different host plants. *Acta phytophy. Sin.* 40, 205–210.

Zhang, Y., Liu, Y., Zhang, J., Guo, Y., and Ma, E. (2015). Molecular cloning and mRNA expression of heat shock protein genes and their response to cadmium stress in the grasshopper *Oxya chinensis*. *PLOS One* 7, e0131244–16. doi:10.1371/journal.pone.0131244

Zhou, D. R., and He, K. L. (1995). *The integrated control technology of corn borer*. Beijing, China: Golden Shield Press.

Zhou, G. Y., Yang, F. X., Fu, X. Q., and Wang, X. L. (1996). The inflfluence of climatic differences in the Yangtze River Valley on cotton yield and fibre quality. *China Cott.* 10, 15–18.

Zhou, J. C., Liu, Q. Q., Han, Y. X., and Dong, H. (2018). High temperature tolerance and thermal-adaptability plasticity of Asian corn borer (*Ostrinia furnacalis* guenée) after a single extreme heat wave at the egg stage - sciencedirect. *J. Asia. Pac. Entomol.* 21 (3), 1040–1047. doi:10.1016/j.aspen.2018.07.024

frontiers | Frontiers in Physiology

TYPE Original Research
PUBLISHED 29 September 2022
DOI 10.3389/fphys.2022.992306

OPEN ACCESS

EDITED BY
Dr. Divya Singh,
Chandigarh University, India

REVIEWED BY
Nader R. Abdelsalam,
Alexandria University, Egypt
Dr. Sachin Kumar,
Chaudhary Sarwan Kumar Himachal Pradesh Krishi Vishvavidyalaya, India
Balasubramani Ravindran,
Kyonggi University, South Korea

*CORRESPONDENCE
Guohua Zhong,
guohuazhong@scau.edu.cn

SPECIALTY SECTION
This article was submitted to Invertebrate Physiology, a section of the journal Frontiers in Physiology

RECEIVED 12 July 2022
ACCEPTED 12 August 2022
PUBLISHED 29 September 2022

CITATION
Khalid MZ, Sun Z, Zhang J, Zhang S and Zhong G (2022), Cyromazine affects the ovarian germ cells of Drosophila via the ecdysone signaling pathway. *Front. Physiol.* 13:992306. doi: 10.3389/fphys.2022.992306

Cyromazine affects the ovarian germ cells of *Drosophila via* the ecdysone signaling pathway

Muhammad Zaryab Khalid, Zhipeng Sun, Jing Zhang, Shijie Zhang and Guohua Zhong*

Key Laboratory of Natural Pesticide and Chemical Biology, Ministry of Education, South China Agricultural University, Guangzhou, China

Cyromazine, an insect growth regulator, has been extensively used against the insect pests of livestock and households. Previously, it was observed that the continuous selection of cyromazine from the larval to the adult stage decreased the number of germline stem cells (GSCs) and cystoblasts (CBs) in the adult ovary. In addition, in this study, we observed that the number of primordial germ cells (PGCs) was also decreased in the larval ovary after treatment with cyromazine. However, the mechanism by which it affects the germ cells is yet to be explored. Consequently, to deeply investigate the effects of cyromazine on the germ cells, we performed tissue-specific RNA sequencing. Bioinformatics analysis revealed that the ecdysone signaling pathway was significantly influenced under cyromazine stress. Based on that, we screened and selected 14 ecdysone signaling responsive genes and silenced their expression in the germ cells only. Results of that showed a considerable reduction in the number of germ cells. Furthermore, we mixed exogenous 20E with the cyromazine-containing diet to rescue the ecdysone signaling. Our results supported that the application of exogenous 20E significantly rescued the germ cells in the transgenic lines. Therefore, this implies that the cyromazine decreased the number of germ cells by affecting the ecdysone signaling pathway.

KEYWORDS

germline stem cells, primordial stem cells, RNA sequencing, RNA interference, ecdysone signaling, apoptosis

1 Introduction

Reproduction is an inherent ability of organisms by which they multiply. *Drosophila melanogaster*'s ovary is an excellent model system for studying the germ cell's proliferation and differentiation (Ting, 2013). The primordial germ cells (PGCs) continue to increase during the larval ovary development (Gilboa and Lehmann, 2006), while the terminal filament (TF) cells are completely formed at the early pupal stage. However, very few cap cells had formed at this early pupal stage (Zhu and Xie, 2003). It is worth mentioning that both TF and cap cells play a crucial role in the maintenance of PGCs by producing Decapentaplegic (Dpp) and Hedgehog (Hh) signaling

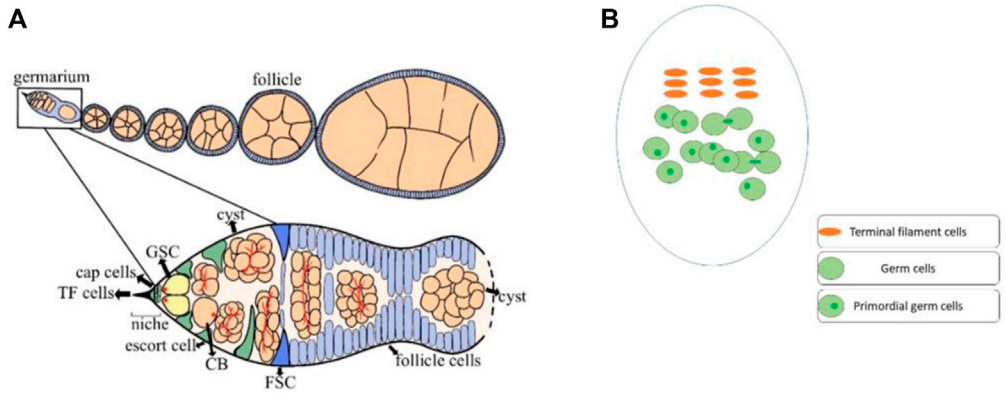

FIGURE 1
Ovaries of *Drosophila* house different types of cells. **(A)** The adult ovary of *Drosophila* consists of 16–20 ovarioles, and the germarium of each ovariole has different types of cells. The germline stem cells (GSCs) strictly maintain and differentiate under the regulation of signals from the somatic cells. At every stage of early cell division, the GSCs are surrounded by somatic cells for their proper regulation. GSCs divide into cystoblasts (CBs), which later undergo four rounds of mitotic division to generate a 16-cells cyst. In the end, only one cell among these 16-cell cysts differentiates as an oocyte. **(B)** The third instar larval ovary of *Drosophila*, also consists of somatic cells and germ cells. Before pupation, most of the terminal filaments (TF) cells has formed. While the TF cells completely formed at the early pupal stage. The germ cells can be identified with a germ cell-specific marker (anti-vasa). However, only the germ cells with single dot-shaped spectrosome were considered as PGCs.

(member of bone morphogenetic protein) (Sato et al., 2010). In adults of *Drosophila*, the ovary consists of 16–20 ovarioles and 2–3 germline stem cells (GSCs) are found in the germarium. These germ cells are regulated by a number of GSCs specific intrinsic factors, and extrinsic niche signals (Ji et al., 2017; Weaver and Drummond-Barbosa, 2018; Gao et al., 2019; Yoshinari et al., 2020). Furthermore, the GSC niche is formed of different types of somatic cells, including TF, cap cells, and escort cells (ECs) (Eliazer and Buszczak, 2011; Ben-Zvi and Volk, 2019; Drummond-Barbosa, 2019). These niche cells also produce Dpp and Hh signaling, which is necessary for the maintenance and differentiation of GSCs (Liu et al., 2015). In the germarium, GSCs are connected with cap cells through E-cadherin, the loss of which results in a sharp decline in the GSC number (Jin et al., 2008). Each niche signaling molecule is crucial for the maintenance and differentiation of GSCs (Huang et al., 2017; Panchal et al., 2017; Mao et al., 2019). For example, loss of *Traffic jam* (*Tj*), a Maf transcriptional factor, from cap cells not only results in the loss of cap cells but also causes a reduction in GSCs. However, *Tj* loss from escort cells arrests cystoblast (CB) differentiation (Li et al., 2019). Thus, under the strict regulation of these signaling factors, the GSCs divide asymmetrically into CBs, which later complete four rounds of mitotic divisions to produce 16-cell cysts (Hinnant et al., 2020). While the early dividing gem cells are accompanied by escort cells, the newly developed 16-cell cyst, on the other hand, is enveloped by follicle cells (Figure 1) (Morris and Spradling, 2012; Eliazer et al., 2014).

Cyromazine is an insect growth regulator, which is among the most widely used biorational insecticides (Khan and Akram, 2017). It is used to control the important pests of livestock, including *Stomoxys calcitrans* and *Lucilia cuprina*, and also to control *Musca domestica*, by affecting the immature stage of the fly (Taylor et al., 2012). The treatment of *D. melanogaster*'s larvae with cyromazine resulted in the early emergence of adults. Furthermore, the mode of action of cyromazine is thought to be related to 20-hydroxyecdysone (20E), as the exogenous application of 20E decreased larval mortality (Van De Wouw et al., 2006). Furthermore, the number of GSCs was significantly reduced in the *EcR* mutant females, indicating that the ecdysone signaling directly controls the GSC maintenance and proliferation (Ables and Drummond-Barbosa, 2010).

Our previous study showed that the continuous selection of *D. melanogaster* from the larval to the adult stage affected the GSCs and CBs in the adult ovary. Furthermore, we observed that the expression of selected ecdysone signaling-related genes and ecdysone titer significantly decreased in the treated ovaries (Khalid et al., 2022). Therefore, to deeply investigate how this chemical affected the germ cells in the adult ovaries, we first counted the number of PGCs in the larval ovaries. Our results indicated a significant decrease in the number of PGCs compared to the control group. Thus, we concluded that the continuous selection of cyromazine resulted in a significant decrease in the number of germ cells from the larval to the adult stage. Later, we performed tissue-specific next-generation RNA sequencing of both larval and adult ovaries, to screen genes involved in the ecdysone signaling pathway under cyromazine stress. Furthermore, based on our RNA-Seq result, we selected 14 ecdysone signaling responsive genes and performed germ cell-specific RNA interference (RNAi) of selected genes to

functionally study the effect of cyromazine on the germ cells of *D. melanogaster*. In addition, the exogenous application of 20E significantly rescued the germ cells in both larval and adult ovaries, which further confirmed that the effect of cyromazine, on the germ cells of *Drosophila*, is through the ecdysone signaling pathway. We further performed the TUNEL assay to find out if the decrease in the number of germ cells is due to cell death. However, no positive apoptotic signal was observed as compared to the control group, indicating that the decrease in the number of germ cells is not due to cell death.

2 Materials and methods

2.1 *Drosophila* strains and breeding conditions

Standard cornmeal agar medium was used to rear the flies at a constant temperature of 25°C and humidity of 75% with a 12: 12 h light/dark cycle. The details of the transgenic lines used in the study are provided (Supplementary Table S1).

2.2 Insecticide treatment and next-generation RNA sequencing

Technical-grade cyromazine was purchased from Guangzhou Qixiang Biotechnology Co., Ltd. (Guangzhou). The stock solution of 1 mg/ml cyromazine dissolved in distilled water was used for serial dilutions. The required volume of cyromazine was mixed with a freshly prepared diet before solidification. The larvae of *D. melanogaster* were allowed to feed on 0.3 PPM of cyromazine for 12 h, while after the adult emergence, the adults were fed on a diet containing 50 PPM.

At the late third instar larvae, we carefully dissected ovaries from the control and insecticide-treated groups. The adult ovaries were dissected after 7 days of adult emergence. All the ovaries were dissected in phosphate buffer saline (PBS) with a sterilized dissection kit and immediately frozen in liquid nitrogen. The Trizol Reagent Kit (Invitrogen, Carlsbad, CA, United States) was used to extract total RNA following the manufacturer's protocol. The integrity of RNA was measured on Agilent 2100 Bioanalyzer (Agilent, Palo Alto, CA, United States). mRNA was enriched by magnetic beads with Oligo (dT). Later, mRNA was fragmented and reverse-transcribed into cDNA by fragmentation buffer and random primers, respectively. While for synthesizing the second-strand cDNA, RNase H, dNTP, DNA polymerase I, and buffer were used. The QiaQuick PCR Extraction Kit (Qiagen, Venlo, Netherlands) was used to purify the cDNA fragments, end-repaired, poly (A) added, and ligated to Illumina sequencing adapters. Agarose gel electrophoresis was used to recover the target fragment, PCR amplified, and sequenced using Illumina HiSeq 2500 by gene Denovo Biotechnology Co. (Guangzhou, China).

2.3 Bioinformatics analysis

High-quality clean reads were acquired through removing adapters above 10% of unknown nucleotides (N) and low-quality reads with more than 50% of low-quality (Q-value ≤ 20) bases using fastp (version 0.18.0). Later, Bowtie2 (version 2.2.8) was used, and reads were mapped to the ribosome RNA (rRNA) database. Mapped reads were then removed, and clean reads were mapped to *D. melanogaster*'s reference genome (GCF_000001215.4) using HISAT2 (Kim et al., 2015). DESeq2 software was used for differential expression analysis, while a false discovery rate (FDR) below 0.05 and absolute fold change ≥2 were used to identify differentially expressed gene/transcripts. Furthermore, for functional annotation, both Gene Ontology (GO) enrichment analysis and Kyoto Encyclopedia of Gene and Genomes (KEGG) pathway enrichment analysis of all predicted genes were performed. However, FDR correction was followed for the *p*-value, where FDR ≤ 0.05 was taken as a threshold. However, GO terms and KEGG pathways with corrected *p*-value < 0.05 were considered as significantly enriched among differentially expressed genes (DEGs) (Cao and Jiang, 2017).

2.4 Validation through RT-qPCR

For validating the RNA-Seq results, real-time quantitative PCR (RT-qPCR) was performed on 14 DEGs that were differentially expressed in larval and adult ovaries. Total RNA was extracted from both larval and adult ovaries, and cDNA was synthesized by using the PrimeScript RT reagent Kit containing gDNA eraser (Takara, China). Later, RT-qPCR was performed by using SsoFast EvaGreen Supermix (Bio-Rad, Hercules, CA, United States). The following working program was set as 2 min at 95°C, 40 cycles of 5 s at 95°C, 10 s at 60°C, and a melting curve from 65 to 95°C (Zafar et al., 2021). For internal control, several housekeeping genes were investigated for normalization according to the $2^{-\Delta\Delta}$CT method, and finally, *rp49* was selected. Primers were constructed by Primer Premier 5 (software) and are provided (Supplementary Table S2).

2.5 Germ cell-specific RNAi-mediated gene silencing

From our RNA-sequencing results and based on the previously published articles, we selected 14 ecdysone-responsive genes for RNAi-mediated gene silencing experiments. Furthermore, we divided these lines into three categories (primary genes, Halloween genes, and ecdysone-responsive genes). Later, the virgin females of nos-Gal4 were crossed with the males of *UAS-RNAi* transgenic flies to drive the RNAi-mediated gene silencing in the germ cells. While for

control, the virgin females of nos-Gal4 were crossed with the males of yw. In total, 10 males together with 10 females were kept in each vial, and all the vials were maintained at 25°C. Both the larvae and adults were allowed to feed on the cyromazine mixed diet. The late 3rd instar larvae were used to dissect larval ovaries, while adult ovaries were dissected after 7 days of eclosion.

2.6 Immunohistochemistry and microscopy

Antibody staining was performed as previously described (Liu et al., 2015). In brief, the ovaries were first fixed in 4% paraformaldehyde (PFA), washed three times with PBST (0.1% Triton X-100 in PBS), blocked in 5% normal goat serum (NGS), and incubated with primary antibodies at 4°C overnight. The next day, ovaries were washed with PBST three times, blocked in 5% NGS, incubated with secondary antibodies for 2 h, and washed with PBST three times. In addition, Hoechst (1:5,000; Cell Signaling Technology, Danvers, MA, United States) was used to stain the DNA. The samples were then mounted in 90% glycerol (Sigma).

Following primary antibodies were used: rabbit anti-pMad (1:400; cell signaling), mouse anti-α-Spectrin [3A9, 1:100; Developmental Studies Hybridoma Band (DSHB)], and rabbit anti-vasa (1:3,000). Secondary antibodies used were rabbit cy3 (1:1,000) and mouse 488 (1:1,000). Nikon A1 plus confocal microscope was used to take images (Nikon, Tokyo, Japan).

2.7 Counting the number of germ cells

At the larval stage, the germ cells are known as PGCs, which are identified on the base of germ cell exclusive proteins such as vasa (Yatsenko and Shcherbata, 2021). Therefore, for counting the PGCs, we stained the larval ovaries with both anti-vasa and anti-α-Spectrin (3A9). The germ cells having a single dot-shaped spectrosome were counted as PGCs. While for counting the number of GSCs in the adults, we used anti-pMad. The expression of pMad is used as a marker for GSCs (Liu et al., 2015). So, we stained the adult ovaries with both anti-pMad and anti-α-Spectrin (3A9). Only the GSCs and CBs express a single round spectrosome. So, the CBs were identified from the dividing cells based on the presence of a single dot containing spectrosome.

2.8 Rescue experiment by feeding exogenous 20E

20E was purchased as a stock solution of 10 mM/ml (CAS 5289-74-7, Shanghai Taoshu Biotechnology Co., Ltd.). For the rescue experiment, to further validate the effect of cyromazine on the germ cells, exogenous 20E was mixed with the food containing cyromazine at a final concentration of 500 μM. The 20E was uniformly mixed with the food by continuously blending it for 3 min. The number of germ cells was then counted from both the larval and adult ovaries.

2.9 TUNEL assay to detect cell death

To detect whether the feeding of cyromazine caused the cell death of the germ cells, we used the *in situ* cell death detection kit (Roche, Mannheim, Germany, 11684795910). Concisely, the ovaries were fixed in 4% paraformaldehyde for 20 min, followed by washing for 30 min and incubation with TUNEL reaction mixture (containing label solution and enzyme solution) for 60 min at 37°C. Later, blocking was performed in NGS and immunofluorescence staining was followed as described in Section 2.6.

2.10 Statistical analysis

Excel (Microsoft) and Prism 9.0 (GraphPad) were used to record the statistical data. Student's *t*-test was used to determine *p*-values, and *p*-values are provided in comparison with the control except for the rescue experiment. For the *t*-test, $^{*}p < 0.05$; $^{**}p < 0.01$; $^{***}p < 0.001$.

3 Results

3.1 RNA-sequencing analysis

We used next-generation Illumina RNA sequencing for 12 libraries, including insecticide-treated and control groups, which generated 164,933,474 (CK-L), 172,672,572 (T-L), 140,249,820 (CK-A), and 166,956,380 (T-A) raw quality reads. Later, 164,335,506 (CK-L), 172,167,904 (T-L), 139,912,686 (CK-A), and 166,568,432 (T-A) of high-quality clean reads were obtained by data filtering through fastp. The percentage clean reads ratio of all libraries was higher than 99%, with an average of 99.71%. The Q20 value of clean base pairs of all 12 libraries was higher than 97.30%, displaying good quality clean reads. The Q30 value and GC content of each replication are also shared (Supplementary Table S3). Clean reads were then mapped to the *D. melanogaster* genome (GCF_000001215.4), and the percentage of mapped reads ranged from 95.49% to 97.01%.

3.2 Identification of differentially expressed genes

The FPKM value was used to identify DEGs between the control and the insecticide-treated groups. A total of 863 genes were considered as DEGs between the control and insecticide-

treated adult ovaries, among which 85 genes were upregulated and 778 genes were downregulated (Supplementary Table S4). However, a total of 26 genes were considered as DEGs among control and treated larval ovaries, where 24 genes were upregulated and only two genes were downregulated (Supplementary Table S5). In addition, we used the GO enrichment analysis to understand the functions of our target genes in cellular components, biological processes, and molecular functions (Supplementary Figures S1, S2), while the KEGG pathway enrichment analysis was used to cluster genes into different pathways (Supplementary Figures S3, S4). The grouped genes of the same pathway normally participate in the same biological process.

The ecdysone signaling controls the germ cell maintenance and differentiation (Ables and Drummond-Barbosa, 2010). Therefore, in this study, we selected 14 key genes from the ecdysone signaling pathway to validate the effect of cyromazine on the germ cells of *Drosophila*'s ovary.

3.3 RT-qPCR validation of RNA-seq

We randomly selected DEGs from both larval and adult transcriptomic data to validate RNA-Seq results by RT-qPCR. From larval transcriptomic data, we selected *Lcp4*, *TotC*, *onecut*, *lectin-37Da*, *LysS*, *Hsp70Aa*, and *Lcp65Ab1*, while from adult transcriptomic data, we randomly selected *Iva*, *blw*, *mus312*, *NLK*, *Act88F*, *Diedel*, and *DptA*. The mRNA expression level is presented in Supplementary Figure S5. Overall, the results showed reliability between the RNA-Seq and RT-qPCR.

3.4 Cyromazine affects the germ cells in the larval ovary

During larval development, female PGCs progress to proliferate instead of differentiating (Sato et al., 2010). An important differentiation factor, *Bag of Marbles (Bam)*, is not expressed before the early pupal stage (Gilboa and Lehmann, 2004). To identify the PGCs, we stained germ cells with mouse anti-α-Spectrin (3A9) and rabbit anti-vasa antibodies (Gilboa and Lehmann, 2006; Sato et al., 2010; Gancz et al., 2011). Later, we carefully counted the number of PGCs. However, germ cells with a single dot containing spectrosome were counted as PGCs (Yatsenko and Shcherbata, 2021).

First, we observed that the treatment with cyromazine significantly decreased the number of PGCs in the insecticide-treated ovaries (79 ± 5) of nos-Gal4 * yw, as compared to the control (113 ± 9). Later, to further investigate if cyromazine affects the germ cells of *D. melanogaster* by the ecdysone signaling pathway, we performed germ cell-specific RNAi of selected ecdysone signaling responsive genes by using germ cell-specific driver. Results indicated that knockdown of selected genes significantly decreased the number of PGCs in the cyromazine-treated ovaries as compared to the control group (Figure 2).

Overall, knockdown of these ecdysone-responsive genes further decreased the number of PGCs as compared to the nos-Gal4 * yw in the cyromazine-treated group, implying that the effect of cyromazine on the PGCs is through the ecdysone signaling pathway. Furthermore, the maximum numbers of PGCs were decreased against *EcR* mutant flies (Figure 2A) followed by *sad* and *dib* mutant flies (Figure 2B), while the least numbers of PGCs were decreased against *shd* mutant flies (Figure 2B).

3.5 Cyromazine affects the germline stem cells and cystoblasts in the adult ovary

pMad expression is highly specific for the GSCs. Therefore, we stained the GSCs with anti-pMad and anti-α-Spectrin (3A9). The CBs were identified based on the presence of a single spherical spectrosome (Figure 3D). We observed that cyromazine significantly reduced both the GSCs and CBs in the female adult ovary of nos-Gal4 * yw, as compared to the control (Figures 3, 4).

In addition, RNAi results showed that knockdown of the selected genes significantly reduced the numbers of both GSCs and CBs in the cyromazine-treated group, as compared to the control group. While knockdown of ecdysone-responsive genes among the cyromazine-treated group further decreased the number of both GSCs and CBs as compared to the nos-Gal4 * yw, implying that the effect of cyromazine on the germ cells is through the ecdysone signaling pathway. Maximum number of GSCs were decreased against *EcR* mutant flies (Figure 3A) followed by *E78* and *sad* mutant flies (Figures 3A,B), among the cyromazine-treated group, while least numbers of GSCs decreased in *phm* mutant flies (Figure 3B). Furthermore, cyromazine significantly decreased the number of GSCs against the ecdysone-responsive genes (Figure 3C). Many germerium contain only one GSC (Figure 3E), while few germarium lack any germ cell (Figure 3F).

Likewise, *EcR* mutant flies (Figure 4A) displayed the highest decrease in the number of CBs followed by *ftz-f1* and *Br* mutant flies (Figures 4A,C), while *phm* mutant flies displayed the minimum decrease in the number of CBs, among the cyromazine-treated group (Figure 4B).

3.6 Rescue experiment

To further support our experiment that the cyromazine decreased the germ cells in both the larval and adult ovaries by affecting the ecdysone signaling pathway, we performed rescue experiments by mixing exogenous 20E with a

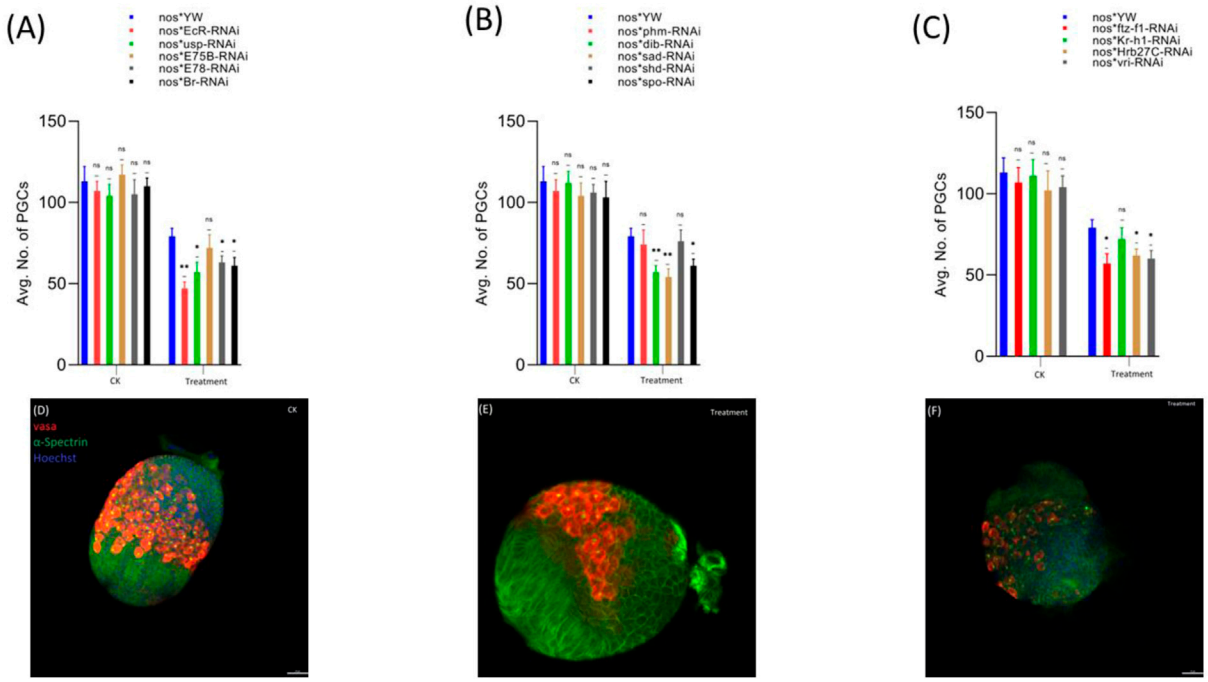

FIGURE 2
Effect of cyromazine on the germ cells of larval ovaries. **(A)** RNAi of ecdysone-responsive primary genes and the effect of cyromazine on the PGCs. **(B)** RNAi of Halloween genes and the effect of cyromazine on the PGCs. **(C)** RNAi of ecdysone-responsive genes and the effect of cyromazine on the PGCs. CK means that the flies were fed on a normal diet, while treatment means the flies were fed insecticide containing diet. **(D)** Larval ovary from the CK group. **(E,F)** Larval ovaries from the cyromazine-treated group (scale bar, 25 μm). For the *t*-test: $*p < 0.05$; $**p < 0.01$; $***p < 0.001$; ns indicates not significant ($p > 0.05$).

cyromazine-containing diet. We observed that the addition of 20E remarkably decreased the effect of cyromazine on the germ cells of larvae and adult ovaries (Figures 5–7).

We observed that the number of PGCs, against nos-Gal4* yw, increased from 79 ± 5 to 101 ± 7 after mixing 20E in the cyromazine-containing diet (Figure 5A). However, among treated transgenic lines, maximum numbers of PGCs were rescued against *Br* mutant flies (54.1%) (Figure 5A) followed by *sad* (51.8%) (Figure 5B) and *EcR* (51%) mutant flies (Figure 5A).

Furthermore, the maximum numbers of GSCs were rescued against *EcR* mutant flies (23%), followed by *Br* (20.5%) (Figure 6A) and *sad* (17.7%) (Figure 6B). The maximum numbers of CBs were also rescued against *EcR* (39.3%) (Figure 7A), followed by *ftz-f1* (27.4%) (Figure 7C) and *Br* (26.2%) (Figure 7A), after the addition of 20E.

These results indicated that the cyromazine significantly reduced the germ cell number in the larval and adult ovaries through interference in the ecdysone signaling pathway, as the addition of 20E notably rescued the germ cells. However, the addition of exogenous 20E in the control group showed no significant effect on the germ cells of *D. melanogaster* (results not shown).

3.7 TUNEL assay to detect apoptosis

We further performed the TUNEL assay to see if the reduction in germ cell number was associated with apoptosis. However, no positive apoptotic signal was observed in the ovaries of *D. melanogaster* treated with cyromazine, indicating that the decrease in the number of germ cells is not due to cell death (results not shown).

4 Discussion

Ecdysone signaling is crucial for insect reproduction (Kannangara et al., 2021). In *Drosophila*, both ecdysone receptor (*EcR*) and ultraspiracle (*usp*) control early response genes' expression. These early genes later activate transcription factors which regulate the late-response genes to produce a tissue-specific response (Gauhar et al., 2009; Mazina et al., 2017). The ovary is the crucial source of ecdysone production in female adults (Lenaerts et al., 2019). Furthermore, ecdysone signaling is necessary for not only the proper ovary development but also for the maintenance and proliferation of GSCs (Ables and Drummond-Barbosa, 2010; Khalid et al., 2021). The present

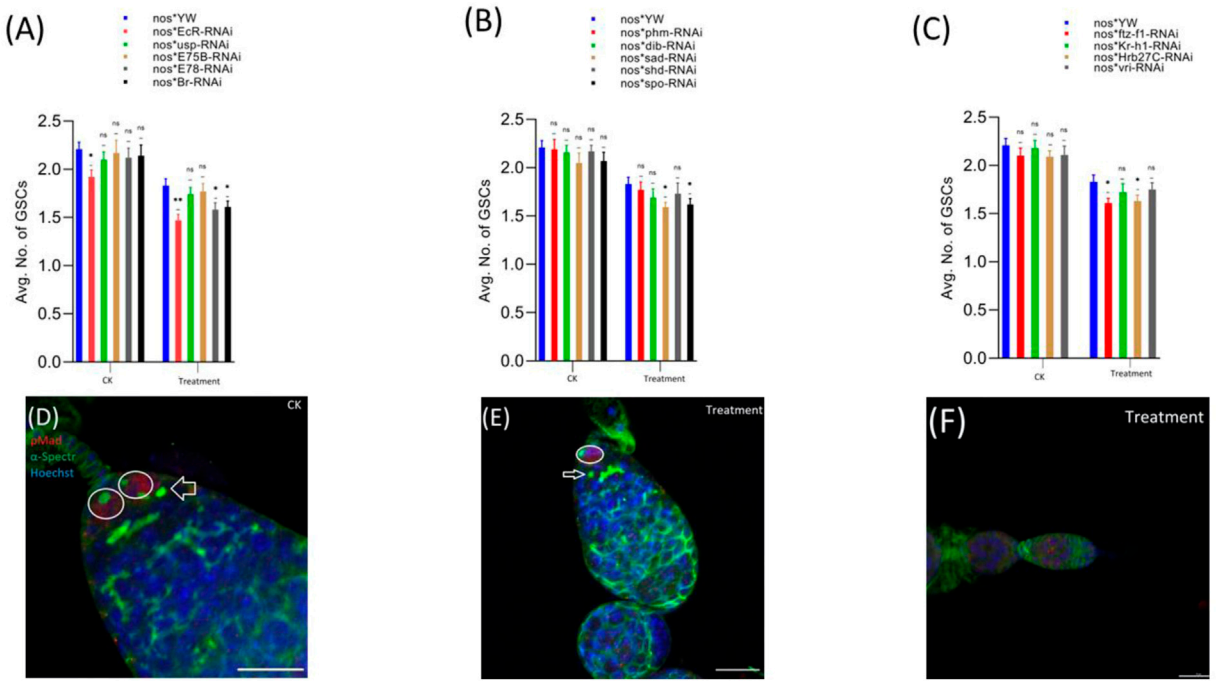

FIGURE 3
Effect of cyromazine on the GSCs of adult ovaries. **(A)** RNAi of ecdysone-responsive primary genes and the effect of cyromazine on the GSCs. **(B)** RNAi of Halloween genes and the effect of cyromazine on the GSCs. **(C)** RNAi of ecdysone-responsive genes and the effect of cyromazine on the GSCs. CK means that the flies were fed on a normal diet, while treatment means the flies were fed insecticide containing diet. **(D)** The adult ovariole from the CK group. White circle indicates GSCs, while white arrow represents CBs. **(E)** Only one GSCs and one CB is present in the cyromazine-treated ovariole. **(F)** The ovariole lacking any GSC in the germarium (scale bar, 10 μm **(D,E)**, 25 μm **(F)**). For the *t*-test: $*p < 0.05$; $**p < 0.01$; $***p < 0.001$; ns indicates not significant ($p > 0.05$).

study also supported that ecdysone signaling is required to properly maintain germ cells in the *D. melanogaster*'s ovary. Mutations in *EcR*, *usp*, *E75B*, *E78*, and *Br* affected the GSCs' maintenance and interfered with the germ cell differentiation and cyst development (König and Shcherbata, 2015; Ables et al., 2016). In addition, *E78* has been known to interact with *EcR*. The germ cell-specific knockdown of *E78* significantly reduced female fertility and also decreased the number of GSCs (Ables et al., 2015). Thus, the proper regulation of ecdysone signaling is essential for proper germ cell maintenance and proliferation.

In insects, cyromazine effects both metamorphosis and reproduction (Zhou et al., 2016). The mode of action of cyromazine has been reported to be related to the ecdysone signaling pathway. As in *Drosophila*'s larvae, the exogenous application of 20E significantly reduced the determinantal effect of cyromazine and also caused the early emergence of the adults (Van De Wouw et al., 2006). Previously, we observed that the continuous selection of cyromazine affected the reproduction of *Drosophila* by decreasing the number of GSCs and CBs in the ovary of a 3-day-old female. In the present study, we observed that the cyromazine also decreased the number of PGCs in the larvae ovaries, implying that the cyromazine affected the number of germ cells in the adult ovary by decreasing the numbers of PGCs in the larvae ovaries. In addition, RNA-Seq has been extensively utilized to detect changes in gene expression under various conditions, including insects treated with insecticides (Wei et al., 2019; Shu et al., 2021). Furthermore, no ovary-specific transcriptome study after treatment with cyromazine has been performed before. Therefore, to deeply understand how this insect growth regulator affected the germ cells of *D. melanogaster*, we performed tissue-specific next-generation RNA-Seq. Comparative transcriptomic analyses, between control and cyromazine-treated larval and adult ovaries of *D. melanogaster*, indicated a total of 26 and 863 DEGs, respectively. Furthermore, we observed that the ecdysone signaling related genes were differentially expressed after treatment with the cyromazine, indicating that the cyromazine significantly affected the ecdysone signaling pathway.

Later, we selected 14 key ecdysone-responsive genes and performed germ cell-specific RNA interference of selected genes to further validate our experiment. The results indicated a remarkable reduction in the number of germ cells among the cyromazine-treated transgenic lines as compared to nos-Gal4 * yw. We divided these selected genes into three categories: primary genes, Halloween genes, and ecdysone-responsive genes. Among the primary genes, significant numbers of

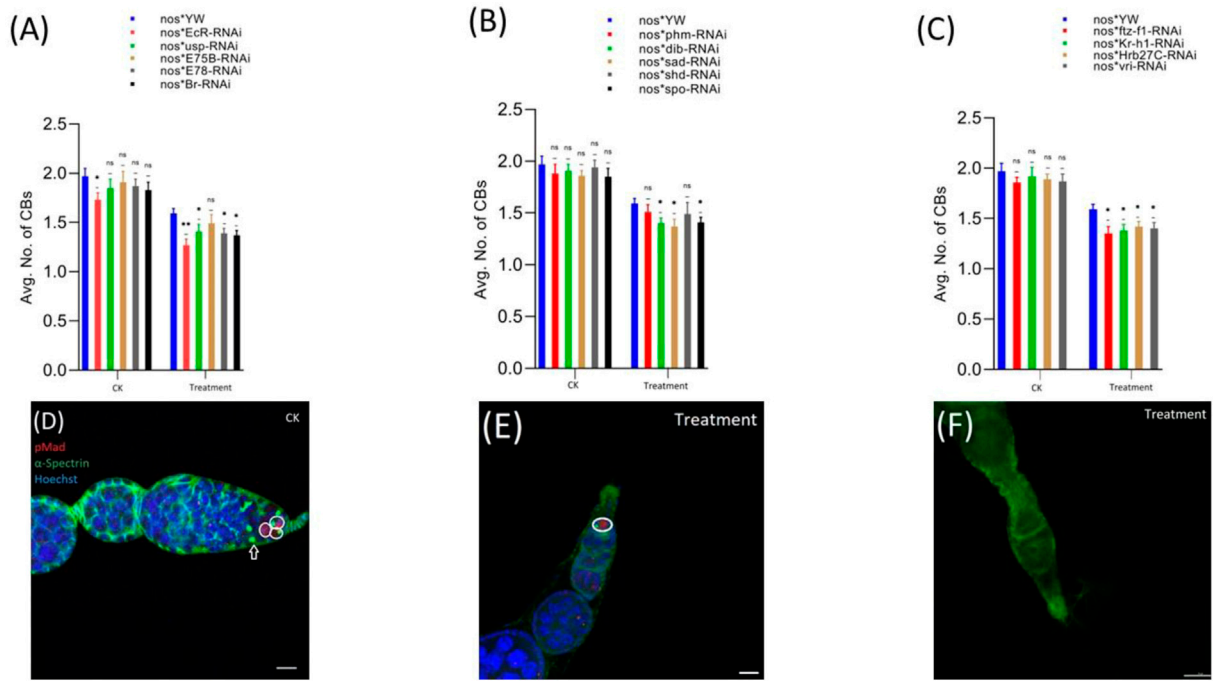

FIGURE 4
Effect of cyromazine on the CBs of adult ovaries. **(A)** RNAi of ecdysone-responsive primary genes and the effect of cyromazine on the CBs. **(B)** RNAi of Halloween genes and the effect of cyromazine on the CBs. **(C)** RNAi of ecdysone-responsive genes and the effect of cyromazine on the CBs. CK means that the flies were fed on a normal diet, while treatment means the flies were fed insecticide containing diet. **(D)** The adult ovariole from the CK group. White circle indicates GSCs, while white arrow represents CBs. **(E)** Only one GSCs and no CB can be seen against the cyromazine-treated ovariole. **(F)** The ovariole lacking any germ cell in the germarium (scale bar, 10 μm **(D,E)**, 25 μm **(F)**). For the *t*-test: $*p < 0.05$; $**p < 0.01$; $***p < 0.001$; ns indicates not significant ($p > 0.05$).

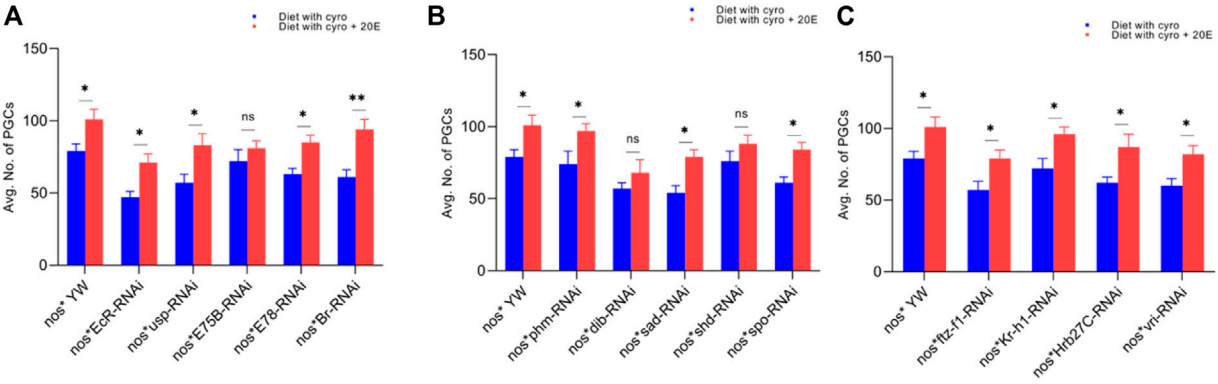

FIGURE 5
Rescue experiment of PGCs. **(A)** The number of PGCs against ecdysone-responsive primary genes. **(B)** The number of PGCs against Halloween genes. **(C)** The numbers PGCs against ecdysone-responsive genes. The blue bars indicate the numbers of PGCs against the cyromazine treatment, while the red bars indicate the numbers of PGCs from the flies fed on a diet containing 20E with the cyromazine. For the *t*-test: $*p < 0.05$; $**p < 0.01$; $***p < 0.001$; ns indicates not significant ($p > 0.05$).

PGCs, GSCs, and CBs were decreased against the cyromazine-treated *EcR* and E78 mutant flies (40.5%, 19.6%, and 20.1%, respectively), as compared to the nos-Gal4 * yw. However, no significant decrease in the numbers of PGCs, GSCs, and CBs was observed against *E75B* mutant flies compared to the nos-Gal4 * yw. Previous studies have reported that germ cells directly receive ecdysone signaling and inhibition of which significantly affect their maintenance. In addition, *E78* is required for the

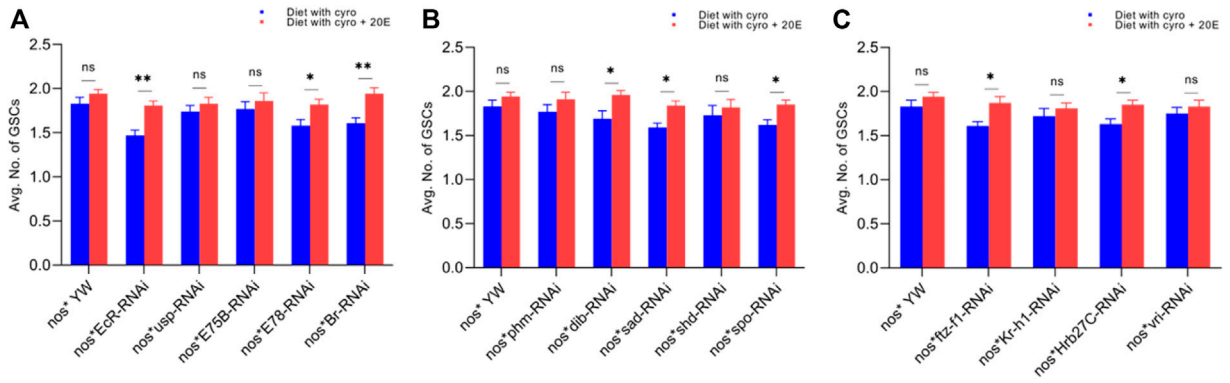

FIGURE 6
Rescue experiment of GSCs. **(A)** The number of GSCs against ecdysone-responsive primary genes. **(B)** The number of GSCs against Halloween genes. **(C)** The number of GSCs against ecdysone-responsive genes. The blue bars indicate the numbers of GSCs against the cyromazine treatment, while red bars indicate the numbers of GSCs from the flies fed on a diet containing 20E with the cyromazine. For the *t*-test: $*p < 0.05$; $**p < 0.01$; $***p < 0.001$; ns indicates not significant ($p > 0.05$).

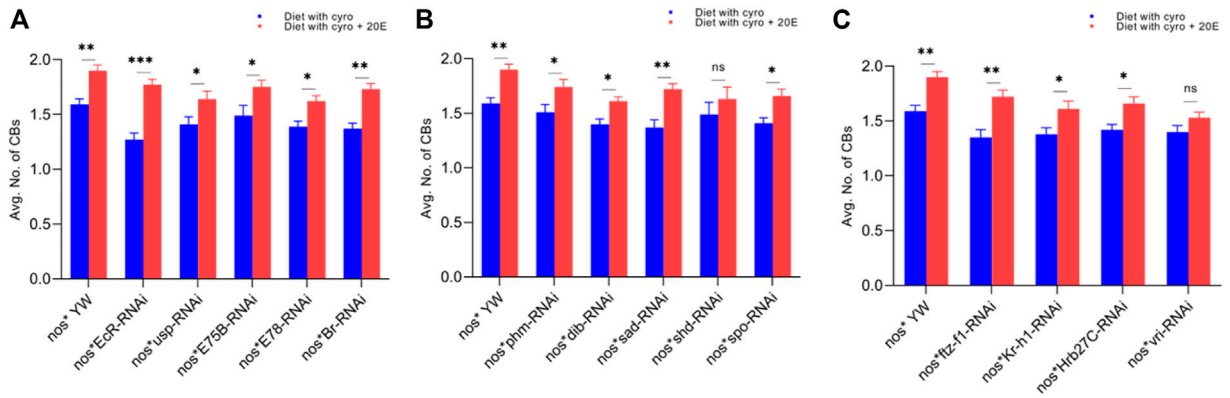

FIGURE 7
Rescue experiment of CBs. **(A)** The number of CBs against ecdysone-responsive primary genes. **(B)** The number of CBs against Halloween genes. **(C)** The number of CBs against ecdysone-responsive genes. The blue bars indicate the number of CBs against the cyromazine treatment, while the red bars indicate the number of CBs from the flies fed on a diet containing 20E with the cyromazine. For the *t*-test: $*p < 0.05$; $**p < 0.01$; $***p < 0.001$; ns indicates not significant ($p > 0.05$).

establishment of required numbers of GSCs (Ables et al., 2015). However, the mutation in *E75B* produced little effect on the maintenance of germ cells, indicating that *E75B* is not required in germ cells for their proper maintenance (Ables and Drummond-Barbosa, 2010). While among Halloween genes, the maximum number of PGCs, GSCs, and CBs were decreased against cyromazine-treated *sad* mutant flies, as compared to the nos-Gal4 * yw. However, no significant decrease in the number of PGCs, GSCs, and CBs was observed against *phm* and *shd* mutant flies. Such results can be supported by previous findings where the germ cells received the required amount of ecdysone signaling even in the absence of *phm* and *shd* (Domanitskaya et al., 2014). Furthermore, significant number of PGCs, GSCs, and CBs were reduced against *ftz-f1* and *Hrb27C* mutant flies. The mRNA expression of *Hrb27C* in the *EcR* mutant flies indicated that it is ecdysone-responsive. In addition, more than 60% loss in the GSCs was observed in *Hrb27C* mutant flies (Ables et al., 2016). Likewise, *ftz-f1* has also been reported to be ecdysone-responsive, the loss of which affects the number of germ cells (Sanders, 2022), while no significant decrease in the numbers of PGCs and GSCs was observed against *Kr-h1* mutant flies, which further supported that the decrease in the numbers of germ cells is due to the ecdysone signaling pathway. *Kr-h1* is a juvenile hormone (JH) response transcriptional factor which inhibits *Br* expression to decrease ecdysone signaling (Jiang et al., 2017; He et al., 2020).

In *D. melanogaster*, ecdysone signaling is necessary to suppress the PGC differentiation (Gancz et al., 2011). In addition, the

mutations in primary response genes also decreased oogenesis (Belles and Piulachs, 2015). Furthermore, RNAi-mediated mutations in the other ecdysone-responsive genes such as *Hrb27C*, *vkg*, *Acer*, *Trn-SR*, *CG12050*, *MESR3*, and *CycE* resulted in more than 50% loss in the GSC numbers, as compared to the control (Ables et al., 2016). Furthermore, it has been reported that the maintenance of CBs, formation, and encapsulation of cysts are also controlled by ecdysone (König et al., 2011; Morris and Spradling, 2012; Xuan et al., 2013; Ables et al., 2015; König and Shcherbata, 2015). Likewise, further decrease in the number of germ cells against the cyromazine-treated transgenic lines further supported that the effect of the cyromazine on the germ cells is through the ecdysone signaling pathway.

The ecdysone hormone is known to control the stem cell fate (intestinal stem cells) in the *Drosophila*'s ovary (Zipper et al., 2020). In addition, we observed that the feeding of exogenous 20E significantly reduced the chemical's effect on the germ cells of both the larval and adult ovaries (Figures 5–7). Among the primary response genes, number of GSCs were significantly rescued against the *EcR*, *E78*, and *Br* mutant flies fed on a diet containing 20E, as compared to flies fed on a diet containing cyromazine alone, similarly significant numbers of PGCs and CBs were rescued against nos-Gal4 * yw and *usp* mutant flies. However, no significant difference in the numbers of GSCs was observed against nos-Gal4 * yw and *usp* mutant flies fed on a diet containing exogenous 20E (Figure 4A). A significant number of PGCs, GSCs, and CBs were rescued against *sad* and *spo* mutant flies fed on a diet containing 20E, as compared to flies fed on a diet containing cyromazine alone. No significant increase in the number of PGCs and GSCs was observed against the *shd* mutant flies (Figures 5A,B). However, a significant number of PGCs were rescued against all selected primary genes of ecdysone signaling (Figure 4). Likewise, a significant number of CBs were rescued against selected ecdysone-responsive genes except for *vri* mutant flies (Figure 7C). However, a significant increase in the number of GSCs was only observed against the *ftz-f1* and *Hrb27C* mutant flies fed on a diet containing 20E (Figure 6C). Such results were observed previously, where the exogenous application of 20E rescued the GSCs due to mutation in *Hrb27C* (Ables et al., 2016).

The exogenous application of 20E not only decreased the larval mortality but also caused early eclosion of adult flies (Van De Wouw et al., 2006). Thus, our results supported that the effect of cyromazine, on the germ cells of *D. melanogaster*, is through the ecdysone signaling pathway.

5 Conclusion

In this study, the ovarian transcriptome of *D. melanogaster* was systematically analyzed at both larval and adult stages, after treatment with cyromazine. Data analysis showed that the ecdysone signaling pathway was significantly affected due to cyromazine stress. Subsequently, we selected 14 genes that were receptive to ecdysone signaling, and solely inhibited their expression in the germ cells. Results revealed a significant decrease in the number of germ cells against the cyromazine fed transgenic lines, as compared to the cyromazine fed nos-Gal4 * yw. To restore ecdysone signaling, we mixed exogenous 20E with the cyromazine-containing diet. Our findings confirmed that the administration of exogenous 20E significantly rescued the germ cells, thereby suggesting that the cyromazine affected the germ cells by the ecdysone signaling pathway.

Data availability statement

The data presented in the study are deposited in the NCBI repository, accession number PRJNA865070.

Author contributions

Conceptualization, MZK and GZ; methodology, MZK and ZS; validation, MZK, ZS, and GZ; formal analysis, MZK and JZ; investigation, MZK, JZ, and SZ; resources, GZ; data curation, MZK and JZ; writing—original draft preparation, MZK; writing—review and editing, MZK; visualization, SZ and JZ; supervision, GZ; project administration, GZ; funding acquisition, GZ. All authors have read and agreed to the published version of the manuscript.

Funding

This work was financially supported by the National Natural Science Foundation of China (Grant No. 31572335).

Acknowledgments

We thank Yang liying for drawing Figure 1 and Junaid Zafar for his useful comments on the manuscript.

Conflict of interest

The authors declare that the research was conducted in the absence of any commercial or financial relationships that could be construed as a potential conflict of interest.

Publisher's note

All claims expressed in this article are solely those of the authors and do not necessarily represent those of their

affiliated organizations, or those of the publisher, the editors, and the reviewers. Any product that may be evaluated in this article, or claim that may be made by its manufacturer, is not guaranteed or endorsed by the publisher.

Supplementary material

The Supplementary Material for this article can be found online at: https://www.frontiersin.org/articles/10.3389/fphys.2022.992306/full#supplementary-material

References

Ables, E. T., Bois, K. E., Garcia, C. A., and Drummond-Barbosa, D. J. D. B. (2015). Ecdysone response gene *E78* controls ovarian germline stem cell niche formation and follicle survival in *Drosophila*. *Dev. Biol.* 400, 33–42. doi:10.1016/j.ydbio.2015.01.013

Ables, E. T., and Drummond-Barbosa, D. J. C. S. C. (2010). The steroid hormone ecdysone functions with intrinsic chromatin remodeling factors to control female germline stem cells in *Drosophila*. *Cell stem Cell* 7, 581–592. doi:10.1016/j.stem.2010.10.001

Ables, E. T., Hwang, G. H., Finger, D. S., Hinnant, T. D., and Drummond-Barbosa, D. J. G. G. (2016). A genetic mosaic screen reveals ecdysone-responsive genes regulating *Drosophila* oogenesis. *G3* 6, 2629–2642. doi:10.1534/g3.116.028951

Belles, X., and Piulachs, M. D. J. B. E. B. a.-G. R. M. (2015). Ecdysone signalling and ovarian development in insects: from stem cells to ovarian follicle formation. *Biochim. Biophys. Acta* 1849, 181–186. doi:10.1016/j.bbagrm.2014.05.025

Ben-Zvi, D. S., and Volk, T. J. B. O. (2019). Escort cell encapsulation of *Drosophila* germline cells is maintained by irre cell recognition module proteins. *Biol. Open* 8, bio039842. doi:10.1242/bio.039842

Cao, X., and Jiang, H. J. B. G. (2017). An analysis of 67 RNA-seq datasets from various tissues at different stages of a model insect, *Manduca sexta*. *BMC Genomics* 18, 796–814. doi:10.1186/s12864-017-4147-y

Domanitskaya, E., Anllo, L., and Schüpbach, T. (2014). Phantom, a cytochrome P450 enzyme essential for ecdysone biosynthesis, plays a critical role in the control of border cell migration in *Drosophila*. *Dev. Biol.* 386 (2), 408–418. doi:10.1016/j.ydbio.2013.12.013

Drummond-Barbosa, D. J. G. (2019). Local and physiological control of germline stem cell lineages in *Drosophila melanogaster*. *Genetics* 213, 9–26. doi:10.1534/genetics.119.300234

Eliazer, S., and Buszczak, M. (2011). Finding a niche: studies from the *Drosophila* ovary. *Stem Cell Res. Ther.* 2, 45–48. doi:10.1186/scrt86

Eliazer, S., Palacios, V., Wang, Z., Kollipara, R. K., Kittler, R., and Buszczak, M. J. P. G. (2014). *Lsd1* restricts the number of germline stem cells by regulating multiple targets in escort cells. *PLoS Genet.* 10, e1004200. doi:10.1371/journal.pgen.1004200

Gancz, D., Lengil, T., and Gilboa, L. J. P. B. (2011). Coordinated regulation of niche and stem cell precursors by hormonal signaling. *PLoS Biol.* 9, e1001202. doi:10.1371/journal.pbio.1001202

Gao, Y., Mao, Y., Xu, R. G., Zhu, R., Zhang, M., Sun, J., et al. (2019). Defining gene networks controlling the maintenance and function of the differentiation niche by an *in vivo* systematic RNAi screen. *J. Genet. Genomics.* 46, 19–30. doi:10.1016/j.jgg.2018.10.008

Gauhar, Z., Sun, L. V., Hua, S., Mason, C. E., Fuchs, F., Li, T.-R., et al. (2009). Genomic mapping of binding regions for the Ecdysone receptor protein complex. *Genome Res.* 19, 1006–1013. doi:10.1101/gr.081349.108

Gilboa, L., and Lehmann, R. J. C. B. (2004). Repression of primordial germ cell differentiation parallels germ line stem cell maintenance. *Curr. Biol.* 14, 981–986. doi:10.1016/j.cub.2004.05.049

Gilboa, L., and Lehmann, R. J. N. (2006). Soma–germline interactions coordinate homeostasis and growth in the *Drosophila* gonad. *Nature* 443, 97–100. doi:10.1038/nature05068

He, Q., Zhang, Y., and Dong, W. (2020). MicroRNA miR-927 targets the juvenile hormone primary response gene Krüppel homolog1 to control *Drosophila* developmental growth. *Insect Mol. Biol.* 29, 545–554. doi:10.1111/imb.12662

Hinnant, T. D., Merkle, J. A., Ables, E. T. J. F. I. C., and Biology, D. (2020). Coordinating proliferation, polarity, and cell fate in the *drosophila* female germline. *Front. Cell Dev. Biol.* 8, 19. doi:10.3389/fcell.2020.00019

Huang, J., Reilein, A., and Kalderon, D. J. D. (2017). Yorkie and Hedgehog independently restrict BMP production in escort cells to permit germline differentiation in the *Drosophila* ovary. *Development* 144, 2584–2594. doi:10.1242/dev.147702

Ji, S., Li, C., Hu, L., Liu, K., Mei, J., Luo, Y., et al. (2017). Bam-dependent deubiquitinase complex can disrupt germ-line stem cell maintenance by targeting cyclin A. *Proc. Natl. Acad. Sci. U. S. A.* 114, 6316–6321. doi:10.1073/pnas.1619188114

Jiang, J., Xu, Y., and Lin, X. (2017). Role of Broad-Complex (Br) and Krüppel homolog 1 (Kr-h1) in the ovary development of Nilaparvata lugens. *Front. Physiol.* 8, 1013. doi:10.3389/fphys.2017.01013

Jin, Z., Kirilly, D., Weng, C., Kawase, E., Song, X., Smith, S., et al. (2008). Differentiation-defective stem cells outcompete normal stem cells for niche occupancy in the *Drosophila* ovary. *Cell Stem Cell* 2, 39–49. doi:10.1016/j.stem.2007.10.021

Kannangara, J. R., Mirth, C. K., and Warr, C. G. J. O. B. (2021). Regulation of ecdysone production in *Drosophila* by neuropeptides and peptide hormones. *Open Biol.* 11, 200373. doi:10.1098/rsob.200373

Khalid, M. Z., Ahmad, S., Ngegba, P. M., and Zhong, G. J. B. (2021). Role of endocrine system in the regulation of female insect reproduction. *Biology* 10, 614. doi:10.3390/biology10070614

Khalid, M. Z., Sun, Z., Chen, Y., Zhang, J., and Zhong, G. (2022). Cyromazine effects the reproduction of *Drosophila* by decreasing the number of germ cells in the female adult ovary. *Insects* 13 (5), 414. doi:10.3390/insects13050414

Khan, H. a. A., and Akram, W. J. C. (2017). Cyromazine resistance in a field strain of house flies, *Musca domestica L.*: Resistance risk assessment and bio-chemical mechanism. *Chemosphere* 67, 308–313. doi:10.1016/j.chemosphere.2016.10.018

Kim, D., Langmead, B., and Salzberg, S. L. J. N. M. (2015). HISAT: a fast spliced aligner with low memory requirements. *Nat. Methods* 12, 357–360. doi:10.1038/nmeth.3317

König, A., and Shcherbata, H. R. J. B. O. (2015). Soma influences GSC progeny differentiation via the cell adhesion-mediated steroid-let-7-Wingless signaling cascade that regulates chromatin dynamics. *Biol. Open* 4, 285–300. doi:10.1242/bio.201410553

König, A., Yatsenko, A. S., Weiss, M., and Shcherbata, H. R. J. T. E. J. (2011). Ecdysteroids affect *Drosophila* ovarian stem cell niche formation and early germline differentiation. *EMBO J.* 30, 1549–1562. doi:10.1038/emboj.2011.73

Lenaerts, C., Marchal, E., Peeters, P., and Broeck, J. V. J. S. R. (2019). The ecdysone receptor complex is essential for the reproductive success in the female desert locust, *Schistocerca gregaria*. *Sci. Rep.* 9, 15–12. doi:10.1038/s41598-018-36763-9

Li, M., Hu, X., Zhang, S., Ho, M. S., Wu, G., and Zhang, L. J. S. R. (2019). Traffic jam regulates the function of the ovarian germline stem cell progeny differentiation niche during pre-adult stage in Drosophila. *Sci. Rep.* 9, 10124–10216. doi:10.1038/s41598-019-45317-6

Liu, Z., Zhong, G., Chai, P. C., Luo, L., Liu, S., Yang, Y., et al. (2015). Coordinated niche-associated signals promote germline homeostasis in the *Drosophila* ovary. *J. Cell Biol.* 211, 469–484. doi:10.1083/jcb.201503033

Mao, Y., Tu, R., Huang, Y., Mao, D., Yang, Z., Lau, P. K., et al. (2019). The exocyst functions in niche cells to promote germline stem cell differentiation by directly controlling EGFR membrane trafficking. *Development* 146, dev174615. doi:10.1242/dev.174615

Mazina, M. Y., Kocheryzhkina, E., Nikolenko, J., Krasnov, A., Georgieva, S., and Vorobyeva, N. (2017). Nuclear receptors *EcR, Usp, E75, DHR3*, and *ERR* regulate transcription of ecdysone cascade genes. *Dokl. Biochem. Biophys.* 473, 145–147. doi:10.1134/S1607672917020144

Morris, L. X., and Spradling, A. C. (2012). Steroid signaling within *Drosophila* ovarian epithelial cells sex-specifically modulates early germ cell development and meiotic entry. *PLoS ONE* 7, e46109. doi:10.1371/journal.pone.0046109

Panchal, T., Chen, X., Alchits, E., Oh, Y., Poon, J., Kouptsova, J., et al. (2017). Specification and spatial arrangement of cells in the germline stem cell niche of the *Drosophila* ovary depend on the Maf transcription factor Traffic jam. *PLoS Genet.* 13, e1006790. doi:10.1371/journal.pgen.1006790

Sanders, S. O. (2022). "The role of Drosophila nuclear receptor ftz-f1 in somatic cells is neccessary for germline stem cell maintenance," [Master's Thesis]. (Greenville (NC): East Carolina University).

Sato, T., Ogata, J., and Niki, Y. J. Z. S. (2010). BMP and Hh signaling affects primordial germ cell division in *Drosophila*. *Zool. Sci.* 27, 804–810. doi:10.2108/zsj.27.804

Shu, B., Yu, H., Li, Y., Zhong, H., Li, X., Cao, L., et al. (2021). Identification of azadirachtin responsive genes in Spodoptera frugiperda larvae based on RNA-seq. *Pestic. Biochem. Physiol.* 172, 104745. doi:10.1016/j.pestbp.2020.104745

Taylor, D. B., Friesen, K., Zhu, J. J., and Sievert, K. J. J. O. E. E. (2012). Efficacy of cyromazine to control immature stable flies (Diptera: Muscidae) developing in winter hay feeding sites. *J. Econ. Entomol.* 105, 726–731. doi:10.1603/ec11317

Ting, X. J. W. I. R. D. B. (2013). Control of germline stem cell self-renewal and differentiation in the *Drosophila* ovary: concerted actions of niche signals and intrinsic factors. *Wiley Interdiscip. Rev. Dev. Biol.* 2, 261–273. doi:10.1002/wdev.60

Van De Wouw, A. P., Batterham, P., and Daborn, P. (2006). The insect growth regulator insecticide cyromazine causes earlier emergence in *Drosophila melanogaster*. *Arch. Insect Biochem. Physiol.* 63, 101–109. doi:10.1002/arch.20146

Weaver, L. N., and Drummond-Barbosa, D. J. G. (2018). Maintenance of proper germline stem cell number requires adipocyte collagen in adult *Drosophila* females. *Genetics* 209, 1155–1166. doi:10.1534/genetics.118.301137

Wei, N., Zhong, Y., Lin, L., Xie, M., Zhang, G., Su, W., et al. (2019). Transcriptome analysis and identification of insecticide tolerance-related genes after exposure to insecticide in *Sitobion avenae*. *Genes* 10 (12), 951. doi:10.3390/genes10120951

Xuan, T., Xin, T., He, J., Tan, J., Gao, Y., Feng, S., et al. (2013). dBre1/dSet1-dependent pathway for histone H3K4 trimethylation has essential roles in controlling germline stem cell maintenance and germ cell differentiation in the *Drosophila* ovary. *Dev. Biol.* 379, 167–181. doi:10.1016/j.ydbio.2013.04.015

Yatsenko, A. S., and Shcherbata, H. R. J. P. G. (2021). Distant activation of Notch signaling induces stem cell niche assembly. *PLoS Genet.* 17, e1009489. doi:10.1371/journal.pgen.1009489

Yoshinari, Y., Ameku, T., Kondo, S., Tanimoto, H., Kuraishi, T., Shimada-Niwa, Y., et al. (2020). Neuronal octopamine signaling regulates mating-induced germline stem cell increase in female *Drosophila melanogaster*. *Elife* 9, e57101. doi:10.7554/eLife.57101

Zafar, J., Zhang, Y., Huang, J., Freed, S., Shoukat, R. F., Xu, X., et al. (2021). Spatio-temporal profiling of *Metarhizium anisopliae*—responsive microRNAs involved in modulation of plutella xylostella immunity and development. *J. Fungi* 7, 942. doi:10.3390/jof7110942

Zhou, F., Zhu, G., Zhao, H., Wang, Z., Xue, M., Li, X., et al. (2016). Sterilization effects of adult-targeted baits containing insect growth regulators on *Delia antiqua*. *Sci. Rep.* 6, 32855–32859. doi:10.1038/srep32855

Zhu, C.-H., and Xie, T. (2003). Clonal expansion of ovarian germline stem cells during niche formation in Drosophila. *Development* 130 (12), 2579–2588. doi:10.1242/dev.00499

Zipper, L., Jassmann, D., Burgmer, S., Görlich, B., and Reiff, T. J. E. (2020). Ecdysone steroid hormone remote controls intestinal stem cell fate decisions via the PPARγ-homolog Eip75B in *Drosophila*. *Elife* 9, e55795. doi:10.7554/eLife.55795

frontiers | Frontiers in Physiology

TYPE Original Research
PUBLISHED 05 October 2022
DOI 10.3389/fphys.2022.990390

OPEN ACCESS

EDITED BY
Seema Ramniwas,
Chandigarh University, India

REVIEWED BY
Fouzia Haider,
Carleton University, Canada
Robin Lewis Cooper,
University of Kentucky, United States

*CORRESPONDENCE
Emily E. King,
emily_king@berkeley.edu

SPECIALTY SECTION
This article was submitted to Invertebrate Physiology, a section of the journal Frontiers in Physiology

RECEIVED 09 July 2022
ACCEPTED 24 August 2022
PUBLISHED 05 October 2022

CITATION
King EE and Stillman JH (2022), Mild temperatures differentiate while extreme temperatures unify gene expression profiles among populations of *Dicosmoecus gilvipes* in California. *Front. Physiol.* 13:990390. doi: 10.3389/fphys.2022.990390

Mild temperatures differentiate while extreme temperatures unify gene expression profiles among populations of *Dicosmoecus gilvipes* in California

Emily E. King[1]* and Jonathon H. Stillman[1,2]

[1]Department of Integrative Biology, University of California, Berkeley, Berkeley, CA, United States, [2]Department of Biology, San Francisco State University, San Francisco, CA, United States

Accurately predicting the effects of future warming on aquatic ectotherms requires an understanding how thermal history, including average temperature and variation, affects populations of the same species. However, many laboratory studies simplify the thermal environment to focus on specific organismal responses and sacrifice environmental realism. Here, we paired laboratory-based transcriptomic RNA-seq analysis to identify thermally responsive genes with NanoString analysis of a subset of those genes to characterize natural field-based variation in thermal physiology among populations. We tested gene expression responses of three populations of field-acclimatized larval caddisflies (*Dicosmoecus gilvipes*) from streams in different eco-regions (mountain, valley, and coast) following exposure to current and future summertime temperatures. We hypothesized that distinct thermal histories across eco-regions could differentiate populations at baseline "control" levels of gene expression, as well as gene expression changes in response to daily warming and heat shock. Population-specific patterns of gene expression were apparent under the control and daily warming conditions suggesting that local acclimatization or local adaptation may differentiate populations, while responses to extreme temperatures were similar across populations, indicating that response to thermal stress is canalized. Underlying gene co-expression patterns in the daily warming and heat shock treatments were different, demonstrating the distinct physiological mechanisms involved with thermal acclimatization and response to thermal stress. These results highlight the importance and limitations of studies of the thermal biology of wild-caught organisms in their natural environment, and provide an important resource for researchers of caddisflies and aquatic insects in general.

KEYWORDS

gene expression, caddisfly, thermal, ectotherm, warming, local adaptation, acclimation, acclimatization

Introduction

Predicting the responses of aquatic ectothermic animals to changing temperature regimes is critical for managing biodiversity in the future. Temperature influences many vital aspects of physiology, development, and life history, and ultimately shapes biogeography (Sweeny et al., 1992; Gillooly et al., 2001; Seebacher et al., 2015). Animals can deal with changes in temperature at different time and biological scales. At the organismal level, animals can acclimate or adjust their physiology after long-term exposure to a thermal stimulus (days to weeks) (Bowler, 2005; Angilletta, 2009; Shah et al., 2017). Organisms from more variable environments are expected to have a greater capacity for acclimation than organisms in stable environments (Shah et al., 2017). Warm acclimated individuals are expected to have higher thermal tolerances than cold-acclimated individuals. In freshwater organisms specifically, this results in decreased thermal sensitivity of organismal traits to further warming for already warm acclimated populations (Seebacher et al., 2015). At the biochemical level, organisms can change the regulation of gene expression in response to thermal exposures. Specifically, expression of heat shock proteins and other molecular chaperones, macromolecules that quickly protect damaged or denaturing proteins, is a reliable indicator of rapid temperature changes (over hours) (Feder and Hoffman, 1999; Dahlhoff, 2004; Somero, 2005; Somero, 2010).

Thermal history is made up of both average temperatures and thermal variation and can lead to sustained differences in physiological responses between environments or populations. Protein expression of aquatic stonefly species in Japan differs along stream temperature gradients that covary with latitude and elevation. Protein expression was more similar between species with shared thermal history than within a species across regions (Gamboa et al., 2017). Acclimation to different thermal histories can also cause warm-acclimated populations to induce heat shock protein expression at higher temperatures than cold-acclimated populations (Bowler, 2005). What may appear as a muted response to a temperature change in one population may indicate a warmer thermal history. Thermal history plays a critical role in our ability to forecast future responses to temperature change in wild populations.

Physiologists often acclimate animals to constant temperatures before an experiment and use "average" conditions as the experimental treatments (e.g., average summer temperature vs. average winter temperature) (Morash et al., 2018). In these highly controlled lab studies, we can focus on responses to a particular stimulus without certain complexity (e.g., individual variation, temperature variation), but this simplicity comes at the cost of biological realism. Stable laboratory conditions mask thermal history and rarely elicit responses similar to those measured under fluctuating conditions (Denny, 2017; Morash et al., 2018; Marshall et al., 2021). One solution is to study animals in their natural, variable environments to understand how thermal history affects the response of different populations. To make the best conclusions about future changes in biogeography and population dynamics under future warming conditions, we need to make population-level inferences under realistic conditions (Pörtner and Knust, 2007; Dong et al., 2015; Morash et al., 2018).

Caddisfly larvae are an integral element of California river ecosystems. *Dicosmoecus gilvipes* occur in various eco-regions of California, including mountain, valley, and coastal populations experiencing different thermal means and variabilities. Mountain streams freeze over then warm dramatically through the summer, while coastal streams stay within a much warmer, narrower temperature range. Future warming is likely to raise the maximum water temperatures in all eco-regions (Null et al., 2013). Temperature has clear effects on the physiology and life history of *D. gilvipes*. Larvae develop faster in stream regions with a higher number of degree days until they disappear in the most downstream regions (Hannaford, 1998; Resh et al., 2011). There is low gene flow between populations due to a short-lived adult stage (~2 weeks) and short-range mating cues (Resh and Wood, 1985; Peterson et al., 2017), thus separating populations genetically and by thermal environment. Therefore, *D. gilvipes* is a good model for understanding how temperature warming will impact wild, free-living aquatic animals with different thermal histories.

This study tests the hypotheses that wild populations of larval *D. gilvipes* will differ in baseline gene expression and responses to current and future warming scenarios due to differences in thermal history. Specifically, we expect that 1) populations from warm locations will have less thermally sensitive gene expression responses, 2) that the more extreme warming scenario will generate more extreme transcriptional responses, 3) that long and short summer acclimatization will generate different transcriptional responses, and that 4) gene co-expression will be similar between warming scenarios. To test these hypotheses, we assayed the expression of thermally sensitive mRNA transcripts in three populations of field acclimated *D. gilvipes* from three eco-regions at two dates through the summer.

Materials and methods

Animal collection and thermal exposure

We collected larval *Dicosmoecus gilvipes* (Hagen, 1875) from three distinct populations at stream sites within the University of California Natural Reserve System. Larvae in the fifth (terminal) instar stage were collected by hand in the morning on the day of each experiment from Angelo Coast Range Reserve (39.7186°, −123.6528°), Sagehen Creek Reserve (39.4333°, −120.2407°), and Landels-Hill Big Creek Reserve

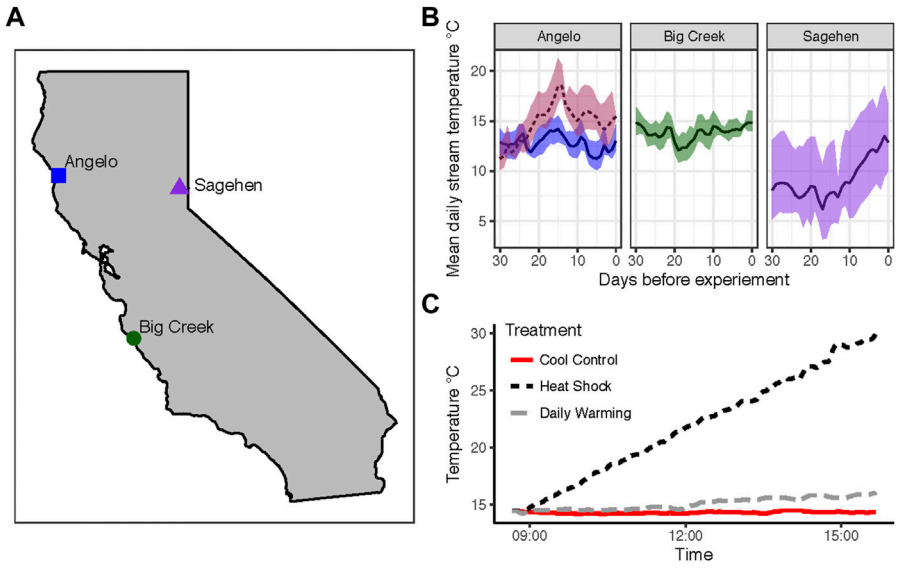

FIGURE 1
Thermal histories and experimental exposures of larval *Dicosmoecus gilvipes* caddisflies **(A)** Three California populations used in this study and **(B)** stream temperatures at each of these sites in the 30 days before the experiment. The data represent the following dates from each site: Angelo (4/29/13–5/29/13 and 5/24/13–6/22/13) in blue and pink, respectively, Big Creek (5/10/13-6/9/13) in green, and Sagehen (5/12/13–6/11/13) in violet. The solid line represents the mean daily stream temperature. The shaded area around the line indicates the daily temperature range **(C)** Example of experimental temperature treatments from Big Creek (6/9/13). Colors and line types represent the warming treatment.

TABLE 1 Stream temperatures in the field for 30 days before collection (°C).

Site	Avg. Daily Temp	Avg. Daily Max	Avg. Daily Min	Avg. Daily range	Absolute Max	Absolute Min	Source	Date range
Angelo	12.8	14.0	11.7	2.4	15.6	10.1	Berkeley Sensor Database[a]	4/29–5/29/2013
Big Creek	13.8	15.0	12.8	2.2	16.4	10.9	NOAA Fisheries, Santa Cruz[b]	5/10-6/9/2013
Sagehen	9.19	13.9	6.1	7.9	18.5	3.2	USGS NWIC[c]	5/12–6/11/2013
Angelo	14.9	17.0	13.6	3.4	21.2	10.1	Berkeley Sensor Database[a]	5/24–6/22/2013

[a]http://sensor.berkeley.edu/cgi/sensor_query2?view=check_password&Access=4&username=Guest+User&MC_Name=Angelo+Reserve&VariableCode=Water+Temp+C&ONEVAR=1.
[b]Personal communication with Dave Rundio.
[c]https://waterdata.usgs.gov/ca/nwis/uv/?site_no=10343500&PARAmeter_cd=00065,00060.

(36.071298°, −121.599153°) (Figure 1A). Larval stage was determined by case-building materials (Resh et al., 2011; Holomuzki et al., 2013). Thermal stress experiments were performed streamside May-June of 2013 (Table 2). The experiment was run twice at the Angelo site (i.e., "Angelo early," "Angelo late") just under 1 month apart to measure the effects of seasonal acclimatization on the same population. Stream temperatures for the 30 days preceding each experiment were obtained from stream sensor data collected by other researchers (Table 1; Figure 1B). These sites represent three temperature regions in California: mountain (Sagehen, elevation 1972m), valley (Angelo), and coastal (Big Creek).

Three to four individual caddisflies were held in continuously aerated 1 L glass jars inside one of three insulated water coolers to maintain specific temperatures (Table 2). We collected a small number of individuals for each treatment due to the availability of appropriate larval stage on the experimental dates. Cooler temperatures were manipulated to represent three temperature

TABLE 2 Experimental temperatures treatments (°C) and number of individuals analyzed in parentheses.

Site	Experiment date	Control	Daily warming	Heat shock
Angelo early	29 May 2013	12°(3)	12°–15°(3)	12°–30°(4)
Sagehen	9 June 2013	13°(4)	13°–17°(4)	13°–30°(3)
Big Creek	11 June 2013	14°(4)	14°–16°(4)	14°–30°(3)
Angelo late	22 June 2013	14°(4)	14°–17°(4)	14°–30°(2)

treatments: a cool control, gradual warming mimicking the daily increase in stream temperature, or a heat shock to 30°C. We will refer to the treatments as "cool control," "daily warming," and "heat shock." The cool control treatment was held at the temperature of the stream at the time the caddisflies were collected in the morning (Table 2; Figure 1C) for the duration of the experiment, approximately 9 h. The daily warming treatment matched the warming stream through the day by measuring the temperature of the stream every 2 minutes with an Omega HH603A handheld thermometer. The temperature of the treatment water was manipulated manually by adding hot water or bags of ice into the outer chamber of the cooler to achieve a temperature matching the stream. Each site had a slightly different natural warming profile, but endpoint temperatures were between 15° and 17°C (Table 2). The heat shock treatment water was warmed from the control temperature to 30°C at a rate of approximately 3 C/h. The maximum temperature, 30°C, reflects the annual maximum temperature observed at the Angelo Coast Reserve plus a 4°C warming based on end-century climate change predictions (Hannaford, 1998; IPCC, 2019). After a 1-h exposure to the maximum temperature of the respective treatment, individuals were removed from their case, blotted dry, flash-frozen in liquid nitrogen, and stored at −80°C prior to RNA extraction. There were no mortalities in any treatment at any site.

Selection of biomarkers

Target genes were chosen for NanoString analysis from among the most differentially expressed genes in a laboratory temperature exposure RNA-Seq experiment (Supplementary Material; Supplementary Figures S1, S2; Supplementary Table S1) ([*D. gilvipes* transcriptomic response] Stillman, 2022). Reference candidate genes were selected based on the lowest coefficient of variation in FPKM (fragments per kilobase of exon per million fragments mapped) values from the same RNA-Seq experiment with a range of expression levels and reasonable biological function (i.e., transcription apparatus, cytoskeleton). Thirty-one NanoString targets were selected, representing both those that increased and decreased with warming, to be normalized to the three reference genes described above (Supplementary Table S2).

RNA preparation

Head and thorax tissues were homogenized with stainless steel ball bearings (3 mm, McMaster Carr) in Tri Reagent (Molecular Research Center, United States) using a TissueLyser II (Qiagen). RNA was isolated according to the manufacturer's recommended protocol, using bromochloropropane (BCP, Molecular Research Center, United States) for phase separation and isopropanol for RNA precipitation (Chomczyński and Sacchi, 1987). RNA quality and quantity were measured with a Bioanalyzer (Agilent). Only samples with little to no degradation and adequate concentration were used in downstream steps.

DNA-free RNA was prepared by mixing 5 µg of RNA, 5 µl of 10x reaction buffer (Thermo Scientific, 100 mM Tris-HCl, 25 mM $MgCl_2$, 1 mM $CaCl_2$) and 5 U of DNase I enzyme (Thermo Scientific). RNase-free water was added to a final volume of 55 µl. The DNase reaction proceeded at 37°C for 30 min and was stopped by adding 5 µl of 50 mM EDTA with heating at 65°C for 10 min. The DNA-free RNA was stored at −80°C.

NanoString expression and data quality control

Gene expression was measured using the nCounter System (NanoString Technologies) (Geiss et al., 2008). Some of the RNA extracted from each caddisfly sample was diluted with RNase-free water to a concentration of 20 ng/µl in a final volume of 20 µl. Samples were then sent to NanoString Technologies in Seattle, WA, USA for processing and gene expression quantification. This method allows for many genes to be analyzed at once without cDNA reverse transcription or amplification to reduce bias in counts of rare or abundant transcripts. The resulting expression data were background corrected by subtracting the mean plus two standard deviations of the negative controls. Transcripts with post-background correction expression values in the negative range were excluded. Expression levels of the remaining transcripts were normalized to the geometric mean of the three reference genes for that individual and log-transformed.

Data analysis

All analysis was completed in the R Computing Environment (R Core Team 2018). Principal components analysis using the "pcaMethods" package in R (v1.72.0, Stacklies et al., 2007) was used to identify potential population-level differences in the entire suite of genes. The data were mean-centered and scaled using the Pareto scaling method prior to running the principal components analysis. The Pareto method scales the data with the square root of the standard deviation (Eriksson et al., 1999). We tested for statistical differences in PC scores between groups using a MANOVA with the Wilks λ test statistic. One analysis compared the first sampling date at all sites and the second analysis compared the two sampling dates from Angelo (early and late). The model structures were: PC1+PC2~Population*Treatment and PC1+PC2~Date*Treatment. We ran univariate ANOVAs on the significant components of the MANOVA to do Tukey's multiple pairwise comparisons (Supplementary Table S2). We excluded one individual (from Sagehen control) from the PCA analysis because inspection of residuals suggested that it was a multivariate outlier and thus violated the assumptions of MANOVA (Supplementary Figures S3, S4). The overall conclusions did not change when this outlier was excluded, and normality of residuals was improved (Supplementary Figure S4).

To focus on the responses to the two warming scenarios, we analyzed the change in expression between the cool control and each of the warming treatments. For each transcript, the average expression level for that population under control conditions was subtracted from each individuals' warming response to give Δ expression, separately for daily warming and heat shock. The resulting positive values indicate increased expression under a warming treatment, while negative values indicate decreased expression relative to the control. This procedure was performed for the daily warming treatment and the heat shock treatment. Comparisons between sites within one warming treatment and between warming treatments were made using Kruskal-Wallis tests and Nemenyi post-hoc tests to handle non-parametric datasets.

Heatmaps were created with "heatmap3" (v1.1.9, Zhao et al., 2021). Dendrograms clustered rows of genes by similarity of Δ expression from the treatment control. The colors of the heat map cells represent the magnitude and direction of the change in expression, scaled and centered by row.

Gene co-expression matrices were created for each warming treatment using "corrplot" (v0.84, Wei and Simko 2016). Matrix data were Pearson's correlations of gene expression in each treatment and were ordered by gene function. The threshold for a significant correlation was $\alpha = 0.05$. Populations were combined to provide a sufficient sample size for correlation analysis. Clusters of important genes were identified by visual inspection.

Results

Thermal history

In the month preceding the first round of sampling, the stream temperature was very similar at Angelo (valley) and Big Creek (coastal) (Table 1; Figure 1B). Stream temperature at Sagehen, a montane site, is characterized by much lower minimum temperatures and a much larger daily temperature range. At Sagehen, there was also a sustained warming trend in the 10 days before the experiment (Figure 1B). A few days before the experiment, maximum daily water temperatures exceeded the temperature of the daily warming treatment for that population (Tables 1, 2). The mean temperature preceding the Angelo "late" sampling was 2°C warmer with a wider range and higher maximum temperature relative to the Angelo "early" sampling. Fifteen days before the Angelo "late" sampling time, maximum temperatures were higher than any daily warming treatment and were only exceeded by the heat shock treatments (Table 1).

Gene expression differentiates populations and treatments

Population, treatment, and their interaction had significant effects on PCs 1 and 2 for the first sampling time from all populations (Figure 2A; Tables 3A,B). PC1 represented 28% of the variation in expression, while PC 2 represented 15% of the variation. Differences along PC1 were significantly positively correlated with 4 of 5 heat shock proteins in our study (Supplementary Figure S5). PC1 was negatively correlated with *apoptosis inhibitor* and *circadian clock protein*. PC 2 was positively correlated with a suite of genes containing metabolic genes and molecular transporters, among genes of other functions. Broadly, all treatments in the same populations grouped together (Figure 2A). Angelo typically had low PC1 scores and high PC2 scores. Big Creek had significantly lower PC2 scores than the other populations (Supplementary Table S3B). Sagehen had medium to high PC1 scores significantly different from the other populations (Supplementary Table S3A). When the treatments are compared separately, they group by population in the control and daily warming treatments, but not in the heat shock treatment (Figures 2B–D).

We compared the early and late sampling times from Angelo to understand if gene expression responses to warming change with seasonal acclimatization during summer warming. The two sampling dates and the treatments significantly differed along PC1, but there was no differentiation on PC2 (date: $p < 0.001$, treatment: $p < 0.01$) (Table 3B). The Angelo "late" samples generally had lower scores on PC1 compared to the Angelo "early" samples. The daily warming treatment did not differ from

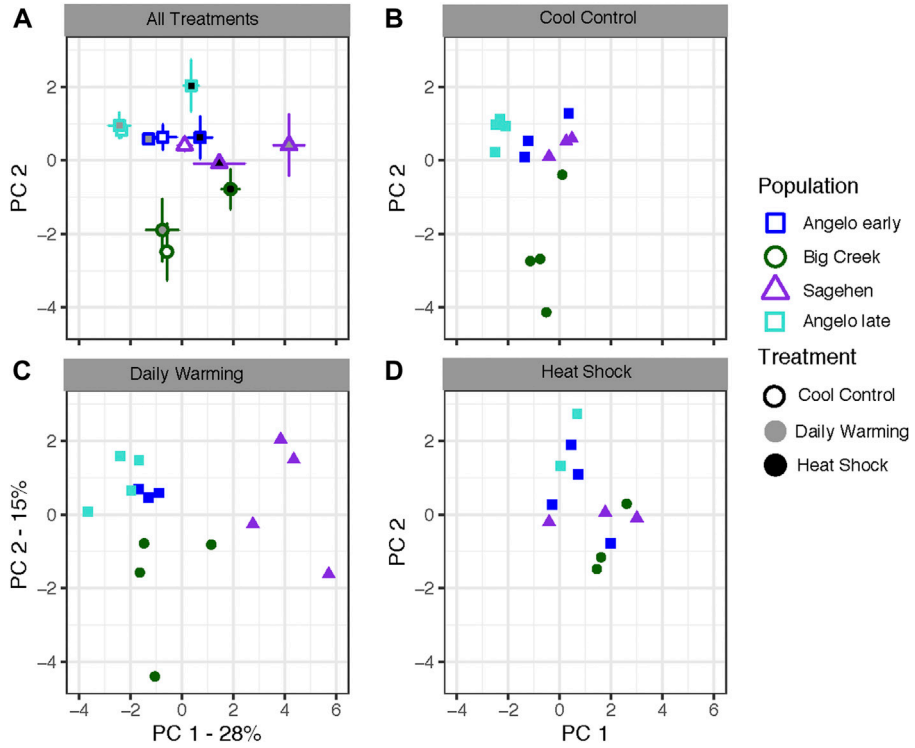

FIGURE 2
Gene expression analysis of *Dicosmoecus gilvipes* caddisflies exposed to three different temperature treatments. PC 1 represents 28% of the variation, while PC 2 represents 15% of the variation. **(A)** Mean PC scores for all population and treatment combinations. Points represent means with standard error bars along both axes. Point outlines represent population of origin, fill color represents the treatment **(B–D)** Individuals plotted by their scores on PC1 and PC2 in the **(B)** cool control treatment, **(C)** daily stream warming treatment, and **(D)** heat shock treatment. This analysis removed one outlier point from Sagehen control.

TABLE 3A Effect of population and date on principal component scores of temperature-sensitive transcripts in *Dicosmoecus gilvipes*. Results of MANOVA tests to determine the effects of population on the early experiments.

	df	Wilks λ	F	Num df	Den df	*p*
Population	2	0.18238	14.0869	4	42	**2.27e-07**
Treatment	2	0.57752	3.3168	4	42	**0.019**
Population*Treatment	4	0.33791	3.7815	8	42	**0.002**
Residuals	22					

Significant results are bolded.

the control treatment, but all other treatments were distinct from each other (Supplementary Table S3).

Response to warming is site and treatment specific

The magnitude of changes in gene expression relative to the control treatment was larger in the heat shock treatment than the daily warming treatment (Figure 3A) (Kruskal-Wallis test, $\chi^2 = 6.3835$, $p < 0.05$). At Sagehen, Δ expression in the daily warming treatment is more than two times higher than at Angelo (Kruskal-Wallis test, $p < 0.05$, Table 4A). Δ expression in the heat shock treatment did not differ across populations (Kruskal-Wallis test, $p > 0.05$).

Five genes were clustered together with the most similar Δ expression profiles (Figure 3B). Three genes in that cluster are molecular chaperones (hsp10, hsp23, hsp90 activator), and the

TABLE 3B Effect of population and date on principal component scores of temperature-sensitive transcripts in *Dicosmoecus gilvipes*. Results of MANOVA tests to determine the the effect of the additional warming between the two Angelo dates.

	df	Wilks λ	F	Num df	Den df	*p*
Date	1	0.34354	12.4207	2	13	**0.001**
Treatment	2	0.28410	5.6949	4	26	**0.002**
Date*Treatment	2	0.77925	0.8634	4	26	0.499
Residuals	14					

Significant results are bolded.

others are related to metabolism (ATPase inhibitor, carbonic anhydrase). There are significant differences in Δ expression with the main effects of population, treatment, and their interaction (MANOVA, Table 4B). Within that cluster, gene expression was generally up-regulated to a greater degree in response to heat shock than daily warming at Angelo and Big Creek, with little or no up-regulation of gene expression in response to daily warming (Figure 4). In contrast, Sagehen individuals up-regulated expression of these genes to similar levels in both warming treatments (Figure 4).

Gene co-expression differs between warming treatments

We constructed co-expression matrices to explore patterns of co-regulation among genes. There were a greater number of significant correlations in the daily warming treatment than the heat shock treatment, 295 and 244, respectively (Figure 5; Table 5). Positive correlations in expression levels among genes were more prevalent under daily warming conditions than heat shock, while the number of negative correlations in expression levels was similar between treatments (Table 5). Correlations in the daily warming treatment were stronger on average than correlations in the heat shock treatment, both more positive and more negative (Table 5). In the daily warming treatment, there were three major clusters of strong positive correlations: 1) between molecular chaperones, 2) molecular chaperones and a mixed group of metabolic genes, transporters, and transcription/translation regulators, and 3) the group of metabolic genes, transporters and transcription/translation regulators with themselves. In the heat shock treatment, cluster 1was maintained (between molecular chaperones) while cluster 2 was reduced. In the daily warming treatment, there were 3 genes with strong negative correlations with many other genes: *protein henna, apoptosis inhibitor,* and *GST*. However, the sign of the correlations between protein henna and the molecular chaperones changed under heat shock conditions. *Protein henna* was positively correlated with molecular chaperones under heat shock conditions but negatively correlated with the same genes under daily warming.

Discussion

Accurately predicting the future of ectotherms to warming requires studies that include populations with distinct thermal histories to understand variations in the physiological response to warming. In the current study, we tested the molecular physiology responses of three populations of *D. gilvipes* from different eco-regions (mountain, valley, and coast) to different heat exposures. We found population-specific responses under the control and daily warming conditions, while responses to heat shock were similar across populations. In addition, underlying gene expression patterns in the daily warming and heat shock treatments were different.

Mild temperatures differentiate populations, but extremes connect them

Under control conditions, the three populations had distinct expression profiles. As temperature-sensitive biomarkers, heat shock proteins can signal current stress or the effects of thermal history (Feder and Hoffman, 1999; Dahlhoff, 2004; King and Macrae, 2015). Given that these animals were not exposed to temperatures we expected to induce stress, differences in constitutive expression of thermally sensitive transcripts support our hypothesis that the populations experienced distinct thermal histories (Bowler 2005; King and Macrae 2015).

Thermal history likely also contributed to and magnified the gene expression responses in the daily warming treatment. There was a 5°C warming trend at the Sagehen site beginning 12 days before the experiment was performed, while the other sites stayed within 2.5°C. This rapid warming may have already induced a warming response that was magnified during an otherwise mild temperature increase that resulted in molecular chaperone expression under daily warming conditions that was greater than or equal to the expression of those genes under heat shock (Figures 3, 4). This difference between the response to daily warming at Sagehen and the other sites may also be related to differences in the thermal sensitivity of gene expression. The average Δ expression at Sagehen was two times that of other populations after a similar increase in temperature. Big Creek and Angelo are generally warmer than Sagehen throughout the year. This supports our hypothesis that warm-adapted populations would be less thermally sensitive and exhibit a more muted expression response to warming. Similarly, the common killifish, *Fundulus heteroclitus*, from warm-acclimated populations showed a muted response in the expression of several hsp70 isoforms in response to high

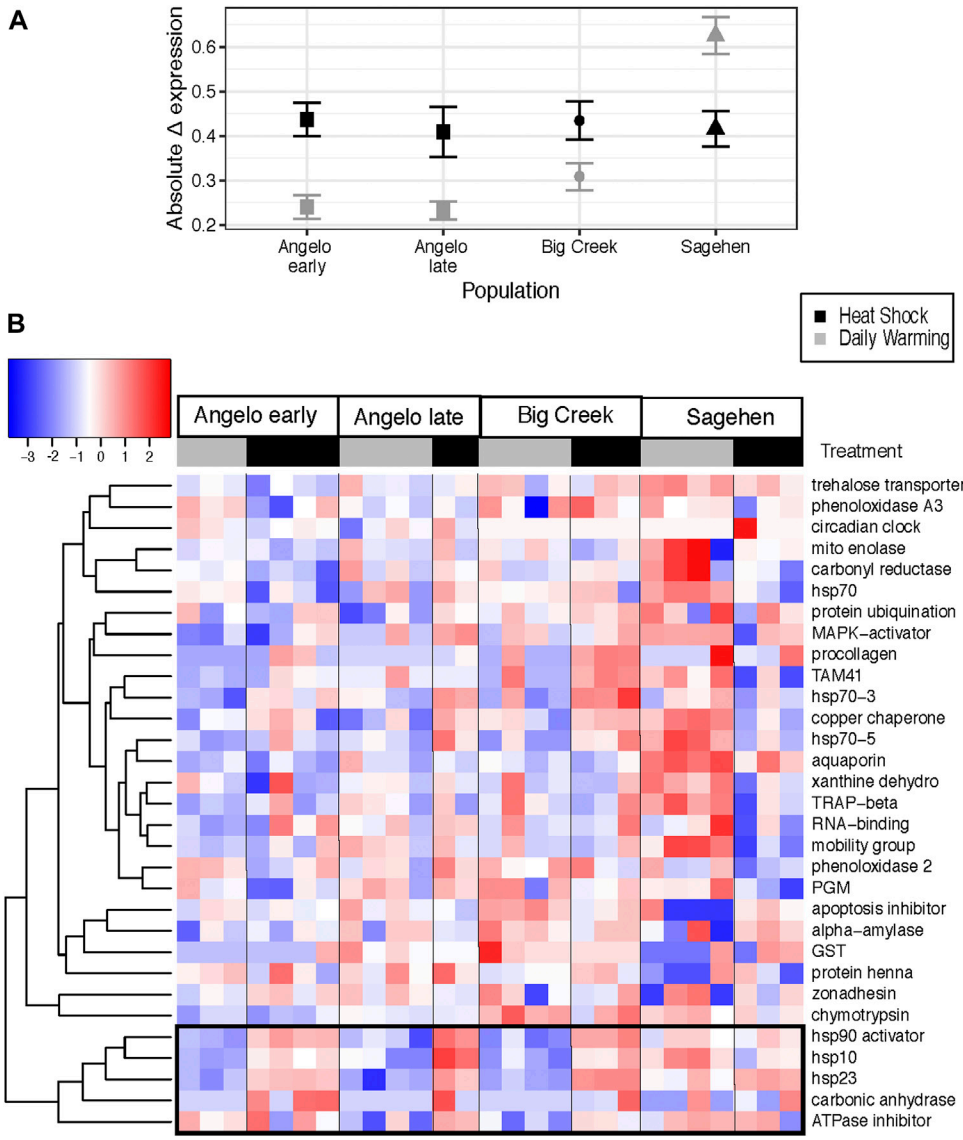

FIGURE 3
Change in expression between cool control and warming treatments for *Dicosmoecus gilvipes* from three California streams **(A)** Mean ± standard error of the absolute change in expression (Δ expression) from the control at each site and treatment. Gray points represent the daily stream warming treatment, and black points represent the heat shock treatment. **(B)** Heatmap of difference in gene transcript abundance relative to the cool control treatment. Genes are arranged in rows and grouped by similarity of induction value (dendrogram). Each column is an individual caddisfly, labeled by its warming treatment. Black and grey bars correspond to the daily warming treatment and heat shock, respectively. The colors of the heat map cells represent the magnitude and direction of the change in expression, scaled and centered by row. The black box highlights a cluster of genes with similar expression patterns (See Figure 4).

temperatures when compared with cold-adapted populations (Fangue et al., 2006). Muted responses in other physiological traits have also been measured in response to warmer thermal histories (Seebacher et al., 2015; Tanner et al., 2019).

Under heat shock conditions, there were no differences between the populations. Potentially, 30°C is approaching a sub-lethal thermal limit and the response to such temperatures is canalized evolutionarily. The CTmax for several North American aquatic insects, including caddisflies, is near 30°C (Houghton et al., 2014; Houghton and Shoup, 2014; Hotaling et al., 2020). Hotaling et al. (2020) also found no transcriptomic grouping by population in high altitude stoneflies exposed to their CTmax. This evidence does not support our hypothesis that we would see a muted thermal response in populations that are already warmer since all populations responded similarly. This contrasts

TABLE 4A Effect of population and treatment on gene expression responses to warming results of Kruskal-Wallis test to determine population differences for absolute Δ expression of genes in the daily warming treatment and the Nemenyi post-hoc test.

Kruskal-Wallis test

	$\chi^2 = 60.317$	df: 3	**p < 0.001**
Post-hoc comparisons using Nemenyi test			
	Angelo early	Angelo late	Big Creek
Angelo late	0.9988	—	—
Big Creek	0.0727	**0.0330**	—
Sagehen	**3.8e-07**	**4.0e-10**	**0.0064**

Significant results are bolded.

TABLE 4B Effect of population and treatment on gene expression responses to warming results of MANOVA to determine the effects of population and treatment on the expression of genes grouped together in Figures 3, 4.

	df	Wilks λ	F	Num df	Den df	*p*
Population	3	0.15806	2.6503	15	41.81	**0.007**
Treatment	1	0.09988	27.0362	5	15	**<0.001**
Population*Treatment	3	0.15948	2.6327	15	41.81	**0.007**
Residuals	19					

Significant results are bolded.

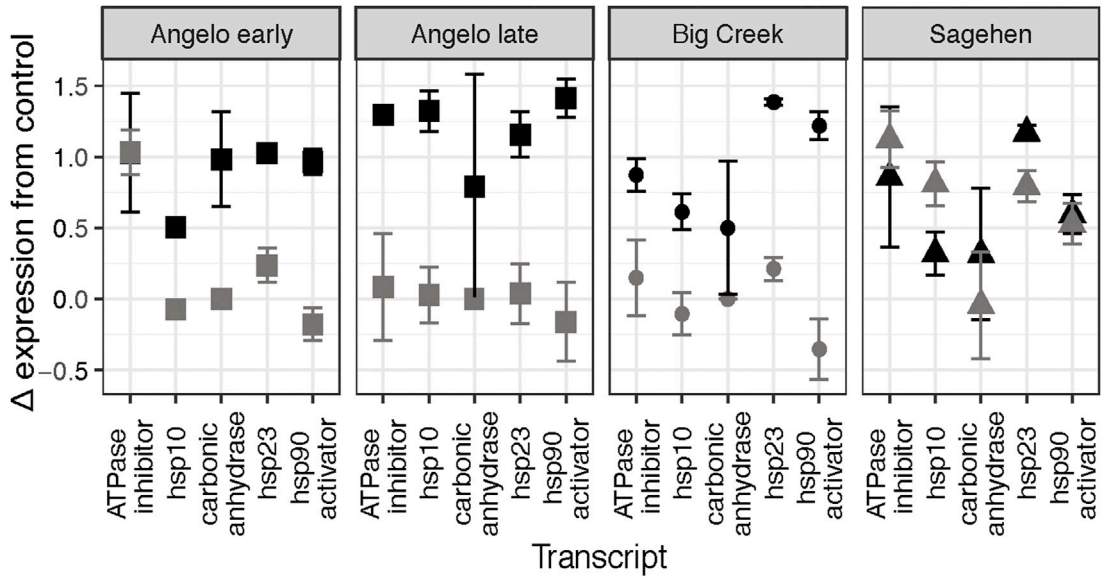

FIGURE 4
Change in expression relative to the control treatment for the five genes clustered in the box in Figure 3B for each site. The daily warming treatment is represented in gray, and the heat shock treatment is represented in black.

with the differences in thermal sensitivity we saw in the daily stream warming treatment. Extreme warming (rate and maximum temperature achieved) may trigger a consistent species-level response that supersedes differences in thermal history.

Population-specific responses may mask the effects of seasonal acclimatization

We repeated our experiment at Angelo 1 month later in the summer to assess the effect of a warmer thermal history on the

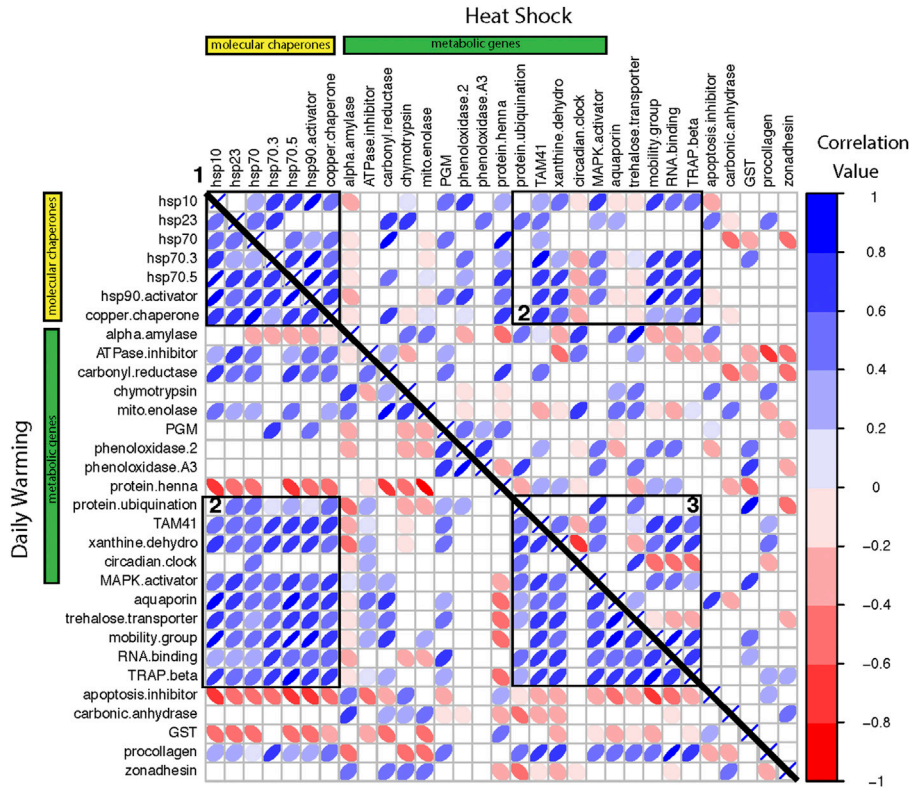

FIGURE 5
Correlation matrices of gene expression change ordered by functional category for the daily warming treatment on the lower triangle and the heat shock treatment on the upper triangle. The yellow bar indicates molecular chaperones. The green bar indicates metabolic genes. The remaining genes have various functions (see Supplementary Table S2). Each row/column is one gene-by-gene comparison. The color and width of the ellipse indicate the correlation strength and direction. Blank cells represent non-significant correlations. Numbered boxes denote clusters of strong positive correlations described in the text.

TABLE 5 Significant gene correlations in each warming treatment.

Treatment	Mean positive	SE positive	N positive	Mean negative	SE negative	N negative	Total significant
Daily Warming	0.552	0.013	198	−0.349	0.018	97	295
Heat Shock	0.390	0.020	152	−0.254	0.020	92	244

same population's gene expression response. The late samples had lower expression of molecular chaperones than the early samples, especially in the control and daily warming treatments (Figure 2, Supplementary Figure S4). This may be evidence of the effect of thermal history on thermal sensitivity, an effect of developmental stage of the individual caddisflies, or some combination of the two. Several individuals observed in the creek on the experiment day were older but were not included in the experiment. The month between the two trials at Angelo represented a large number of the degree-heating days for emergence. By late June, most caddisflies near our study site on the Eel River will have entered prepupal diapause (Hannaford, 1998; Resh et al., 2011). Similar gene expression effects have been measured in walleye maintained in warming regions of Lake Manitoba for a short or long portion of the summer (Jeffrey et al., 2020). Fish held in the lake until later in the summer had increased expression of molecular chaperones. Though the directionality was reversed in our experiment, it is clear that seasonal acclimation can change gene expression patterns.

The main difference between the early and late experiments is that the later time point had lower values on PC1, which were driven by expression of *apoptosis inhibitor* and *circadian clock*

protein (Figure 2, Supplementary Figure S4). This circadian-clock protein, named *daywake* in *Drosophila melanogaster*, was primarily expressed in individuals from Angelo. Only one individual from elsewhere, Sagehen, expressed this gene. In *D. melanogaster*, *daywake* acts as a behavioral thermometer that promotes daytime sleep under warm conditions to avoid heat damage (Yang and Edery, 2019). Higher expression of *daywake* in the later Angelo samples would indicate warmer days, which matches the actual thermal history at the site. However, we would expect to see this gene expressed more widely at Sagehen after the warming trend. Surprisingly, the late Angelo samples were more similar to the earlier Angelo samples and even further differentiated than the other groups from the Sagehen samples in every treatment (Figure 2). This indicates some combination of population-specific and temperature-specific responses occurring under natural conditions.

Differences between mild and extreme warming are greatest in a subset of genes

The differences we expected to see between the daily warming treatment and the heat shock treatment were only apparent relative to control expression (Figures 3, 4). Even then, the differences were gene- and population-specific. Consistently, the heat shock proteins were more strongly induced in the heat shock treatment at all sites except Sagehen. A large body of research supports our findings that heat shock protein expression increases with higher temperature exposure (Feder and Hoffman, 1999; King and Macrae, 2015; Somero, 2020).

Co-expression patterns between genes also changed between warming treatments suggesting that it is important to focus on the relationships between genes in addition to individual genes. Under daily warming conditions, protein henna, an amino acid metabolism gene, was negatively correlated with molecular chaperones, suggesting that the importance of protein protection superseded energy production. However, the correlation changed sign under the heat shock conditions. This may indicate that our heat shock treatment was so stressful that energy production and protein homeostasis both needed to increase simultaneously. Similarly, Dong and Zhang (2016) also found that molecular chaperones, specifically *hsp70*, were only positively correlated with metabolic genes under extreme heat conditions. Some other changes in co-expression between treatments signaled that some macromolecules were not further protected under extreme heat. Under daily warming conditions, *trehalose transporter* was positively correlated with many genes but negatively correlated with them under heat shock. Trehalose has multiple protective roles during heat stress, such as stabilizing membranes and preventing further unfolding of proteins (Ebner et al., 2019; Somero, 2020). Its decrease in relation to other molecular chaperones at very high temperatures may highlight a change in exactly which molecules are being protected (Ebner et al., 2019).

Importance of individual and environmental variation

We studied wild-caught and naturally acclimatized individuals, thus incorporating ecologically relevant impacts of thermal history. In addition, we used a warming treatment that mirrored natural increases in water temperature throughout the day. Maintenance of population-specific thermal history allowed us to measure the baseline expression levels of each population more accurately than a laboratory study could. For example, we can contrast the effects of the warming trend that occurred before sampling at Sagehen with stable temperatures before early sampling at Angelo and Big Creek.

However, ecological realism comes at the cost of control and standardization; and in our study, undetected differences in developmental stage, body condition, or sex may have influenced gene expression patterns. We collected individuals in the final larval instar, indicated by case-building materials in this species (Hannaford, 1998; Holomuzki et al., 2013), but we do not know the individual's age or proximity to pupation. Warming is known to increase developmental rate and has even been seen to drive pupation and emergence during thermal stress experiments in stoneflies (Hannaford, 1998; Hotaling et al., 2020). Though the differences in developmental state were likely products of degree heating days at each site, we must consider that the warming treatment itself may have had an effect.

Studies of ecologically relevant stress must also consider the timing, intensity, duration, and frequency of the stress. Our study matches the ecological timing of stress to the later larval period and used a relevant duration and two relevant warming intensities (current and future), but for only one cycle. In nature, both warming and cooling on a diel cycle contribute to population acclimatization. Under future warming scenarios, caddisflies may experience warming to 30°C repeatedly with carryover effects each day that influence gene expression and phenotypes that may take longer to appear. These carryover effects may be detrimental such as reduced growth and faster development, resulting in small individuals that are phenologically mismatched, or positive effects such as rapid heat hardening that prepare and protect them from the effects of future thermal stress (Bowler, 2005; Bergmann et al., 2010; Verberk and Calosi, 2012; King and Macrae, 2015; Bernhardt et al., 2020; Hotaling et al., 2020). Field-acclimatized gene expression in response to warming over 1 day is a critical snapshot of the processes that underlie the whole organism response. Still, it is only part of the story that will help us understand the future of the species. Aquatic invertebrates in California face a warmer future due to climate change induced droughts and surface water warming (Null et al., 2013; Swain et al., 2014; Diffenbaugh et al., 2015). Using physiology to understand the effects of warming may help us understand which populations are likely to persist or not.

The present study investigated the field-acclimatized transcriptional response to two warming regimes in the three populations of the larval caddisfly *Dicosmoecus gilvipes* from three eco-regions. We found that gene expression of populations from different eco-regions differ in cool control and mild warming scenarios, but not under extreme warming. Populations from warmer eco-regions showed evidence of decreased thermal sensitivity under mild warming conditions. Co-expression between genes should be considered to understand the interactions between molecular processes affected by warming. Our results highlight the importance and limitations of measuring the stress response of wild-caught organisms in their natural environment.

Data availability statement

The datasets presented in this study can be found in online repositories. The names of the repository/repositories and accession number(s) can be found below: The RNA-Seq shotgun assembly can be accessed at: https://www.ncbi.nlm.nih.gov/nuccore/GJZL00000000.1/; The unmodified eXpress output data (library) can be accessed at: https://www.ncbi.nlm.nih.gov/geo/query/acc.cgi?acc=GSE206349; The data generated specifically for this manuscript and from which the conclusions are drawn have been submitted to Dryad : https://doi.org/10.6078/D1T41G.

Author contributions

JS designed the experiment, oversaw data collection and analysis and contributed to writing and revising the manuscript. EK analyzed the data and wrote the manuscript.

Funding

This work was supported by the Gordon and Betty Moore Foundation through the Berkeley Initiative for Global Change Biology, and the University to JS. Publication made possible in part by support from the Berkeley Research Impact Initiative (BRII) sponsored by the UC Berkeley Library, and through funds from the UC Berkeley Department of Integrative Biology.

Acknowledgments

Carl Hendrickson and Joseph Gapuz performed the field-based experiments. Scott Fay (SF) performed the laboratory experiments. SF and Cecilia Tran prepared RNA samples for RNA-seq and NanoString, and SF developed the bioinformatics pipeline used in the RNA-seq study. Special thanks to Dave Rundio (NOAA Fisheries, Santa Cruz) for Big Creek stream temperature data. This work was supported by the Gordon and Betty Moore Foundation through the Berkeley Initiative for Global Change Biology. This work appeared in a modified form in EK's doctoral dissertation at the University of California, Berkeley.

Conflict of interest

The authors declare that the research was conducted in the absence of any commercial or financial relationships that could be construed as a potential conflict of interest.

Publisher's note

All claims expressed in this article are solely those of the authors and do not necessarily represent those of their affiliated organizations, or those of the publisher, the editors and the reviewers. Any product that may be evaluated in this article, or claim that may be made by its manufacturer, is not guaranteed or endorsed by the publisher.

Supplementary material

The Supplementary Material for this article can be found online at: https://www.frontiersin.org/articles/10.3389/fphys.2022.990390/full#supplementary-material

References

Angilletta, M. J. (2009). *Thermal adaptation: A theoretical and empirical synthesis*. New York: Oxford University Press. doi:10.1093/acprof:oso/9780198570875.001.1

Bergmann, N., Winters, G., Rauch, G., Eizaguirre, C., Gu, J., Nelle, P., et al. (2010). Population-specificity of heat stress gene induction in northern and southern eelgrass *Zostera marina* populations under simulated global warming. *Mol. Ecol.* 19, 2870–2883. doi:10.1111/j.1365-294X.2010.04731.x

Bernhardt, J., O'Connor, M., Sunday, J., and Gonzalez, A. (2020). Life in fluctuating environments. *Phil. Trans. R. Soc. B* 375, 20190454. doi:10.1098/rstb.2019.0454

Bowler, K. (2005). Acclimation, heat shock and hardening. *J. Therm. Biol.* 30, 125–130. doi:10.1016/j.jtherbio.2004.09.001

Chomczyński, P., and Sacchi, N. (1987). Single-step method of RNA isolation by acid guanidinium thiocyanate-phenol-chloroform extraction. *Anal. Biochem.* 162, 156–159. doi:10.1006/abio.1987.9999

Dahlhoff, E. P. (2004). Biochemical indicators of stress and metabolism: Applications for marine ecological studies. *Annu. Rev. Physiol.* 66, 183–207. doi:10.1146/annurev.physiol.66.032102.114509

Denny, M. (2017). The fallacy of the average: On the ubiquity, utility and continuing novelty of jensen's inequality. *J. Exp. Biol.* 220, 139–146. doi:10.1242/jeb.140368

[*D. gilvipes* transcriptomic response] Stillman, J. H. (2022). *Transcriptomic responses of caddisfly Dicosmoecus gilvipes to temperature*. NCBI GEO. Avaliable at: https://www.ncbi.nlm.nih.gov/geo/query/acc.cgi?acc=GSE206349.

Diffenbaugh, N. S., Swain, D. L., and Touma, D. (2015). Anthropogenic warming has increased drought risk in California. *Proc. Natl. Acad. Sci. U. S. A.* 112, 3931–3936. doi:10.1073/pnas.1422385112

Dong, Y. W., and Zhang, S. (2016). Ecological relevance of energy metabolism: Transcriptional responses in energy sensing and expenditure to thermal and osmotic stresses in an intertidal limpet. *Funct. Ecol.* 30, 1539–1548. doi:10.1111/1365-2435.12625

Dong, Y. W., Han, G. D., Ganmanee, M., and Wang, J. (2015). Latitudinal variability of physiological responses to heat stress of the intertidal limpet *Cellana toreuma* along the Asian coast. *Mar. Ecol. Prog. Ser.* 529, 107–119. doi:10.3354/meps11303

Ebner, J. N., Ritz, D., and von Fumetti, S. (2019). Comparative proteomics of stenotopic caddisfly *Crunoecia irrorata* identifies acclimation strategies to warming. *Mol. Ecol.* 28, 4453–4469. doi:10.1111/mec.15225

Eriksson, L., Johansson, E., and Kettaneh-Wold, N. W. S. (1999). *Introduction to multi- and megavariate data analysis using projection methods (PCA & PLS)*. Umeå, Sweden: Umetrics AB. Available at: https://www.worldcat.org/title/introduction-to-multi-and-megavariate-data-analysis-using-projection-methods-pca-pls/oclc/473695569

Fangue, N. A., Hofmeister, M., and Schulte, P. M. (2006). Intraspecific variation in thermal tolerance and heat shock protein gene expression in common killifish, *Fundulus heteroclitus*. *J. Exp. Biol.* 209, 2859–2872. doi:10.1242/jeb.02260

Feder, M. E., and Hoffman, G. E. (1999). Heat-shock proteins, molecular chaperones, and the stress response: Evolutionary and ecological physiology. *Annu. Rev. Physiol.* 61, 243–282. doi:10.1146/annurev.physiol.61.1.243

Gamboa, M., Tsuchiya, M. C., Matsumoto, S., Iwata, H., and Watanabe, K. (2017). Differences in protein expression among five species of stream stonefly (Plecoptera) along a latitudinal gradient in Japan. *Arch. Insect Biochem. Physiol.* 96, e21422–16. doi:10.1002/arch.21422

Geiss, G. K., Bumgarner, R. E., Birditt, B., Dahl, T., Dowidar, N., Dunaway, D. L., et al. (2008). Direct multiplexed measurement of gene expression with color-coded probe pairs. *Nat. Biotechnol.* 26, 317–325. doi:10.1038/nbt1385

Gillooly, J. F., Brown, J. H., West, G. B., Savage, V. M., and Charnov, E. L. (2001). Effects of size and temperature on metabolic rate. *Science* 293 (80), 2248–2251. doi:10.1126/science.1061967

Hannaford, M. (1998). *Development and comparison of biological indicators of habitat disturbance for streams and wetlands*. Berkeley: Univ California. doi:10.16953/deusbed.74839

Holomuzki, J. R., Furey, P. C., Lowe, R. L., and Power, M. E. (2013). Microdistributional variability of larval caddisflies in Mediterranean-climate streams in Northern California. *West. N. Am. Nat.* 73, 261–269. doi:10.3398/064.073.0304

Hotaling, S., Shah, A. A., McGowan, K. L., Tronstad, L. M., Giersch, J. J., Finn, D. S., et al. (2020). Mountain stoneflies may tolerate warming streams: Evidence from organismal physiology and gene expression. *Glob. Chang. Biol.* 26, 5524–5538. doi:10.1111/gcb.15294

Houghton, D. C., Logan, A. C., and Pytel, A. J. (2014). Validation of CTmax protocols using cased and uncased *Pycnopsyche guttifer* (Trichoptera: Limnephilidae) larvae. *Gt. Lakes Entomol.* 47, 1–8.

Houghton, D. C., and Shoup, L. (2014). Seasonal changes in the critical thermal maxima of four species of aquatic insects (Ephemeroptera, Trichoptera). *Environ. Entomol.* 43, 1059–1066. doi:10.1603/EN13344

IPCC (2019). Climate change and land: An IPCC special report on climate change, desertification, land degradation, sustainable land management, food security, and greenhouse gas fluxes in terrestrial ecosystems. Report.

Jeffrey, J. D., Carlson, H., Wrubleski, D., Enders, E. C., Treberg, J. R., and Jeffries, K. M. (2020). Applying a gene-suite approach to examine the physiological status of wild-caught walleye (*Sander vitreus*). *Conserv. Physiol.* 8, coaa099–12. doi:10.1093/conphys/coaa099

King, A. M., and Macrae, T. H. (2015). Insect heat shock proteins during stress and diapause. *Annu. Rev. Entomol.* 60, 59–75. doi:10.1146/annurev-ento-011613-162107

Marshall, K. E., Anderson, K. M., Brown, N. E. M., Dytnerski, J. K., Flynn, K. L., Bernhardt, J. R., et al. (2021). Whole-organism responses to constant temperatures do not predict responses to variable temperatures in the ecosystem engineer *Mytilus trossulus*. *Proc. R. Soc. B* 288, 2968. doi:10.1098/rspb.2020.2968

Morash, A. J., Neufeld, C., MacCormack, T. J., and Currie, S. (2018). The importance of incorporating natural thermal variation when evaluating physiological performance in wild species. *J. Exp. Biol.* 221, jeb164673. doi:10.1242/jeb.164673

Null, S. E., Viers, J. H., Deas, M. L., Tanaka, S. K., and Mount, J. F. (2013). Stream temperature sensitivity to climate warming in California's Sierra Nevada: Impacts to coldwater habitat. *Clim. Change* 116, 149–170. doi:10.1007/s10584-012-0459-8

Peterson, M. G., O'Grady, P. M., and Resh, V. H. (2017). Phylogeographic comparison of five large-bodied aquatic insect species across the Western USA. *Freshw. Sci.* 36, 823–837. doi:10.1086/694466

Pörtner, H. O., and Knust, R. (2007). Climate change affects marine fishes through the oxygen limitation of thermal tolerance. *Science* 80315, 95–97. doi:10.1126/science.1135471

R Core Team (2018). R: A language and environment for statistical computing. Avaliable at: https://www.R-project.org/.

Resh, V. H., Hannaford, M., Jackson, J. K., Lamberti, G. a., and Mendez, P. K. (2011). The biology of the limnephilid caddisfly *Dicosmoecus gilvipes* (Hagen) in Northern California and Oregon (USA) streams. *Zoosymposia* 5, 413–419. doi:10.11646/zoosymposia.5.1.34

Resh, V. H., and Wood, J. R. (1985). Site of sex pheromone production in three species of Trichoptera. *Aquat. Insects* 7, 65–71. doi:10.1080/01650428509361202

Seebacher, F., White, C. R., and Franklin, C. E. (2015). Physiological plasticity increases resilience of ectothermic animals to climate change. *Nat. Clim. Chang.* 5, 61–66. doi:10.1038/nclimate2457

Shah, A. A., Chris Funk, W., and Ghalambor, C. K. (2017). Thermal acclimation ability varies in temperate and tropical aquatic insects from different elevations. *Integr. Comp. Biol.* 57, 977–987. doi:10.1093/icb/icx101

Somero, G. N. (2005). Linking biogeography to physiology: Evolutionary and acclimatory adjustments of thermal limits. *Front. Zool.* 2, 1. doi:10.1186/1742-9994-2-1

Somero, G. N. (2020). The cellular stress response and temperature: Function, regulation, and evolution. *J. Exp. Zool. A Ecol. Integr. Physiol.* 333, 379–397. doi:10.1002/jez.2344

Somero, G. N. (2010). The physiology of climate change: How potentials for acclimatization and genetic adaptation will determine "winners" and "losers. *J. Exp. Biol.* 213, 912–920. doi:10.1242/jeb.037473

Stacklies, W., Redestig, H., Scholz, M., Walther, D., and Selbig, J. (2007). pcaMethods - a bioconductor package providing PCA methods for incomplete data. *Bioinformatics* 23, 1164–1167. doi:10.1093/bioinformatics/btm069

Swain, D. L., Tsiang, M., Haugen, M., Singh, D., Charland, A., Rajaratnam, B., et al. (2014). The extraordinary California drought of 2013/2014: Character, context, and the role of climate change. *Bull. Amer Meteor Soc.* 95, S3–S7.

Sweeny, B. W., Jackson, J. K., Newbold, J. D., and Fun, D. H. (1992). "Climate change and the life histories and biogeography of aquatic insects in eastern North America," in *Global climate change and freshwater ecosystems*. Editors P. Firth and S. G. Fisher (New York: Springer-Verlag), 143–176.

Tanner, R. L., Faye, L. E., and Stillman, J. H. (2019). Temperature and salinity sensitivity of respiration, grazing, and defecation rates in the estuarine eelgrass sea hare, *Phyllaplysia taylori*. *Mar. Biol.* 166, 109–112. doi:10.1007/s00227-019-3559-4

Verberk, W. C. E. P., and Calosi, P. (2012). Oxygen limits heat tolerance and drives heat hardening in the aquatic nymphs of the gill breathing damselfly *Calopteryx virgo* (Linnaeus, 1758). *J. Therm. Biol.* 37, 224–229. doi:10.1016/j.jtherbio.2012.01.004

Wei, T., and Simko, V. (2016). The corrplot package R Core Team. Available at: http://www.sthda.com/french/wiki/matrice-de-correlation-la-fonction-r-qui-fait-tout.

Yang, Y., and Edery, I. (2019). Daywake, an anti-siesta gene linked to a splicing-based thermostat from an adjoining clock gene. *Curr. Biol.* 29, 1728–1734. e4. doi:10.1016/j.cub.2019.04.039

Zhao, S., Yin, L., Guo, Y., Sheng, Q., and Shyr, Y. (2021). Advanced heat map and clustering analysis using heatmap3. *Heatmap* 3, 986048. doi:10.1155/2014/986048

frontiers | Frontiers in Physiology

TYPE Original Research
PUBLISHED 11 October 2022
DOI 10.3389/fphys.2022.991923

OPEN ACCESS

EDITED BY
Divya Singh,
Chandigarh University, India

REVIEWED BY
Dori Edson Nava,
Embrapa Clima Temperado, Brazil
Flávio Garcia,
Federal University of Pelotas, Brazil

*CORRESPONDENCE
Larissa Guillén,
larissa.guillen@inecol.mx
Martín Aluja,
martin.aluja@inecol.mx

SPECIALTY SECTION
This article was submitted to Invertebrate Physiology, a section of the journal Frontiers in Physiology

RECEIVED 12 July 2022
ACCEPTED 20 September 2022
PUBLISHED 11 October 2022

CITATION
Guillén L, Pascacio-Villafán C, Osorio-Paz I, Ortega-Casas R, Enciso-Ortíz E, Altúzar-Molina A, Velázquez O and Aluja M (2022), Coping with global warming: Adult thermal thresholds in four pestiferous *Anastrepha* species determined under experimental laboratory conditions and development/survival times of immatures and adults under natural field conditions.
Front. Physiol. 13:991923.
doi: 10.3389/fphys.2022.991923

Coping with global warming: Adult thermal thresholds in four pestiferous *Anastrepha* species determined under experimental laboratory conditions and development/survival times of immatures and adults under natural field conditions

Larissa Guillén*, Carlos Pascacio-Villafán, Ixchel Osorio-Paz, Rafael Ortega-Casas, Erick Enciso-Ortíz, Alma Altúzar-Molina, Olinda Velázquez and Martín Aluja*

Red de Manejo Biorracional de Plagas y Vectores, Clúster Científico y Tecnológico BioMimic®, Instituto de Ecología, A. C. —INECOL, Xalapa, Veracruz, Mexico

Climate change, particularly global warming, is disturbing biological processes in unexpected ways and forcing us to re-study/reanalyze the effects of varying temperatures, among them extreme ones, on insect functional traits such as lifespan and fecundity/fertility. Here we experimentally tested, under both laboratory and field conditions, the effects of an extreme range of temperatures (5, 10, 15, 20, 30, 40, and 45 °C, and the naturally varying conditions experienced in the field), on survivorship/lifespan, fecundity, and fertility of four pestiferous fruit fly species exhibiting contrasting life histories and belonging to two phylogenetic groups within the genus *Anastrepha*: *A. ludens, A. obliqua, A. striata*, and *A. serpentina*. In the field, we also measured the length of the entire life cycle (egg to adult), and in one species (*A. ludens*), the effect on the latter of the host plant (mango and grapefruit). Under laboratory conditions, none of the adults, independent of species, could survive a single day when exposed to a constant temperature of 45 °C, but *A. striata* and *A. serpentina* females/males survived at the highly contrasting temperatures of 5 and 40 °C at least 7 days. Maximum longevity was achieved in all species at 15 °C (375, 225, 175 and 160 days in *A. ludens, A. serpentina, A. striata* and *A. obliqua* females, respectively). *Anastrepha ludens* layed many eggs until late in life (368 days) at 15 °C, but none eclosed. Eclosion was only observed in all species at 20 and 30 °C. Under natural conditions, flies lived ca. 100 days less than in the laboratory at 15 °C, likely due to the physiological cost of dealing with the highly varying environmental patterns over 24 h (minimum and maximum temperatures and relative humidity of ca. 10–40 °C, and 22–100%, respectively). In the case of *A. ludens*, the immature's developmental time was shorter in mango, but adult survival was longer than in grapefruit. We

discuss our results considering the physiological processes regulating the traits measured and tie them to the increasing problem of global warming and its hidden effects on the physiology of insects, as well as the ecological and pest management implications.

KEYWORDS

global warming, thermal thresholds, life-history traits, physiology, *Anastrepha*, Diptera: Tephritidae

Introduction

The effects of climate change such as global warming and environmental moisture changes are disturbing biological cycles in unexpected ways and forcing us to re-study/reanalyze processes that were well understood in the past (Wang and Schimel, 2003; Parmesan, 2006; Jaworski and Hilszczański, 2013). As temperature and humidity lie at the heart of basically all biological processes, it comes as no surprise that global warming is reaping havoc in both natural and anthropic environments, among them agroecosystems, modifying for example rainfall patterns and relative humidity (Trenberth, 2011; Jiang et al., 2015; Byrne and O'Gorman, 2016) or temperature cycles in such a way that cold/warm spells can be experienced in the middle of summer or winter (Yan et al., 2002; Ratajczak, 2020; Yu et al., 2022). This in turn influences tree flowering/fruit ripening patterns and can modify relationships with pests, which also suffer alterations in their biological cycles or biological attributes such as fecundity, egg survival, longevity, and duration of immature cycles (Jaworski and Hilszczański, 2013; Carnicer et al., 2018; Huang et al., 2020). The effects can be apparent (e.g., decrease in body size (Carnicer et al., 2018), increase in the number of generations per year (Lisbôa et al., 2020; Rashmi et al., 2020)) or subtle/hidden (e.g., slight modifications in hydrocarbon structures in the *epidermis* altering recognition between mating partners (Chung and Carroll, 2015; Sentis et al., 2015; Boullis et al., 2016; Menzel et al., 2018) or alterations in the interactions of odorant/pheromone binding proteins (Weng et al., 2015; Boullis et al., 2016).

Insects are adapted to live in wide temperature ranges, all the way from subzero to extremely hot temperatures, although each species has an optimal range of temperatures where their fitness is maximized (Chapman, 1998). Thermal and humidity stress are two of the most important barriers to the development and survival of insects (Chang et al., 2008; Richter et al., 2010). Since temperature gradients in the field can affect the physiology, reproduction, and distributions of insects, many of them with significant agroecological importance, research on their thermal thresholds remains a relevant scientific endeavor.

Among the most notorious pests worldwide, fruit flies (Diptera: Tephritidae) stand out because of their direct damage to fruit (larvae feed in the pulp rendering the fruit unmarketable) and the quarantine restrictions their presence trigger (Aluja and Mangan, 2008; Qin et al., 2015). Given their economic impact, studies on thermal thresholds and direct effect of temperature on fruit fly biology and behavior have been numerous and started at the beginning of last century. The pioneering studies by Darby and Kapp (1933), McPhail and Bliss (1933), Meats (1976), Meats (1984), Meats (1989), among others stand out in this respect. Other studies on temperature relationships on various biological attributes have been performed with the Mediterranean fruit fly, *Ceratitis capitata* Wiedemann (Duyck and Quilici, 2002; Nyamukondiwa and Terblanche, 2009), the Olive fly, *Bactrocera oleae* Gmelin (Genç and Nation, 2008; Wang et al., 2012), the Oriental fruit fly, *Bactrocera dorsalis* (Hendel) (Samayoa et al., 2018; Motswagole et al., 2019; Rashmi et al., 2020), the Apple Maggot fly, *Rhagoletis pomonella* (Walsh) (Reissig et al., 1979; Kasana and AliNiazee, 1994; Drummond and Collins, 2019) and various other species (Liu and Ye, 2009; Adly, 2016; Rull et al., 2016; Bayoumy et al., 2021). Broadly speaking, temperature affects the reproduction and development of tephritid flies (Telles-Romero et al., 2011; Bolzan et al., 2017; Fiaboe et al., 2021), mainly by influencing the metabolic processes that are linked to their development (Moloń et al., 2020).

In the case of flies within the genus *Anastrepha*, most work on temperature relationships stems from the United States, Mexico, and Brazil. Variation of developmental time at different temperature conditions have been studied in the Mexican fruit fly *Anastrepha ludens* (Loew) (Darby and Kapp, 1933; McPhail and Bliss, 1933; Flitters and Messenger, 1965; Leyva-Vazquez, 1988; Thomas, 1997; Hallman et al., 2005; Aluja et al., 2010) and the Sapote fruit fly, *Anastrepha serpentina* Wiedemann (Shaw and Starr, 1946). Thomas (1997) determined that larvae of *A. ludens* survive inside fruit when temperatures drop below zero. Other studies have been performed on *Anastrepha suspensa* (Loew) (Sivinski et al., 2007) and *Anastrepha grandis* (Macquart) (Bolzan et al., 2017; Silva et al., 2019; Lisbôa et al., 2020; Teixeira et al., 2021; Teixeira et al., 2022).

Based on the need to retake this topic because of the phenomenon of Global Warming and its possible effect on the management of pestiferous species within *Anastrepha*, here we report the results of a broad study aimed at determining the effect of temperature on basic biological parameters such as duration of the life cycle, egg and adult survival, female fecundity/egg fertility and adult longevity of wild

A. ludens, *Anastrepha obliqua* (Macquart), *A. serpentina* and *Anastrepha striata* (Schiner). The four species are distributed in the tropical zones of Mexico where temperatures tend to be warm, but in the case of *A. ludens* it has been recently expanding its distribution range invading high altitude, temperate areas where apples (*Malus* × *domestica* Borkh.) and pears (*Pyrus communis* L.) are grown (M. Aluja personal observations; Ruiz-Montoya et al., 2020). We note that these species belong to two different species groups which render our study more robust and interesting. *Anastrepha ludens* and *A. obliqua* belong to the *fraterculus* group (Smith-Caldas et al., 2001; Mengual et al., 2017), while *A. serpentina* and *A. striata* to the *serpentina* group (Norrbom, 2002), although Mengual et al. (2017) placed them again in separate groups. Studies were conducted under natural conditions (under a tree in an orchard) and in bioclimatic chambers. As we wanted to test extreme as well as "typical" temperatures to determine the adaptation potential of these flies to the anomalous worldwide temperature patterns, we experimented with the following temperature regimes: 5, 10, 15, 20, 30, 40, and 45°C. Based on what has been published on temperature effects on fruit flies (reviewed above), we predicted that within the *fraterculus* species group, adults of *A. obliqua*, a species commonly found in very hot, drier tropical areas (temperatures can easily reach 40°C or over at midday), would tolerate high temperatures better than species such as *A. ludens*. We also predicted that within the *serpentina* species group, *A. serpentina* would better tolerate extremely high temperatures. We further predicted that flies exposed to the highly variable field conditions, would exhibit shorter lifespans than flies exposed to similarly averaged temperatures but devoid of variance. Finally, we predicted that *A. ludens* would suffer the most under extremely hot temperatures, with the end results that the distribution of this species would shift towards higher altitude biomes. Our findings are discussed in the light of the physiological processes likely modulating the responses observed.

Materials and methods

Insect collection and maintenance

In the case of both laboratory and field studies (details follow), the four fly species used in the experiments, *A. ludens*, *A. obliqua*, *A. striata,* and *A. serpentina*, stemmed from a semi-wild colony kept under laboratory conditions. By semi-wild we mean first-fourth generation adults that originated from wild individuals that were reared in their natural hosts (grapefruit [*Citrus* x *paradisi* Macfad], mango [*Mangifera indica* L.], guava [*Psidium guajava* L.], and sapodilla [*Manilkara sapota* (L.) P. Royen], respectively, for *A. ludens*, *A. obliqua*, *A. striata* and *A. serpentina*), at laboratory environmental conditions (26 ± 1°C, 60 ± 5% RH and 12:12 h L: D photoperiod). Fruit was placed over plastic baskets with many openings over 27 × 13 × 39 (length, width, depth) cm plastic washbowls with vermiculite as a rearing medium on the floor. Third-stage larvae jumped out of the rotten fruit to pupate. Subsequently, the pupae were collected and placed in 100 ml plastic containers with vermiculite, which was sprinkled with a 0.2% sodium benzoate solution every third day until emergence to prevent the development of pathogens, particularly bacteria and fungi. Once the first flies started to emerge, the container with pupae was transferred to 30 × 30 × 30 cm Plexiglas cages with ample aeration (walls and roof were covered with fiberglass mesh) kept at ambient conditions (27 ± 1°C, 65 ± 5% RH, and light: dark 12:12 h). Inside cages, newly emerged flies were provided with *ad libitum* food (a mixture of sugar: hydrolyzed yeast protein 3:1) and water until they were transferred to the experimental units for field or laboratory experiments (details follow).

Experiment 1—Laboratory conditions

Adults of the four species were exposed to seven temperature treatments (5, 10, 15, 20, 30, 40, and 45°C). For each fly species (i.e., *A. ludens*, *A. obliqua*, *A. striata* and *A. serpentina*), temperature treatments were tested in two parts. First, four Lumistell growth chambers (Model ICP-20) were programmed with temperatures of 5, 10, 15, and 20°C. Each chamber housed five 20 × 20 × 20 cm Plexiglas cages with plastic mesh walls and 20 newly emerged flies (10 females and 10 males) of one species. The cage with flies was considered as the replication unit. When all the flies in all five cages died, chambers were cleaned and scheduled for the remaining temperature treatments (30, 40, and 45°C). As the presence of the different fly species is tied to the availability of their host plants along the year, we ran the tests in blocks of species. That is, at any given moment, only one species was studied, then the next and so on, until all species were covered. But given that we worked with tightly controlled temperature and relative humidity conditions, this did not preclude us from comparing the results among species. The varying temperatures were kept constant throughout the experiment (day one until the last fly died). For all treatments, photoperiod and relative humidity inside chambers were, respectively, 12:12 h (L: D) and 65 ± 5%. Inside cages, we hung daily one colored, 3 cm diam agar sphere wrapped in Parafilm as oviposition substrates to measure female's fecundity. The color of the spheres was green (910 µL of foliage-green, food grade dye Colorchef in 900 mL of water and 29.4 g of agar) in the case of *A. ludens*, *A. obliqua* and *A. striata*, and light brown (150 µL of yellow dye [yellow 370L, Deimp], 50 µL of red dye [red 370L, Deimp] and 25 µL of black dye [black 370L, Deimp] in 900 ml of water and 29.4 g of agar) for *A. serpentina* (as their common hosts such as *M. sapota* or *Pouteria sapota* (Jacq.) Moore & Stearn have a light brown skin). Five replicates (i.e., one cage per replicate) were run for each temperature and fly species. Every day, adult survival,

FIGURE 1
White organza fabric cage with mango fruit cv 'Manila' exposed to gravid females (three females per fruit) during 24 h in the field experiment to generate fruit infestation.

fecundity, and egg fertility were measured. Eggs were dissected daily from the agar spheres and placed over a moist blue polysilk cloth in turn placed inside a 9 cm covered Petri dish to measure fecundity (number of eggs) and fertility (proportion of egg hatched). The explanatory variables of the experimental design were: i) the temperature measured in a continuous scale from 5 to 45°C, and ii) the fly species as a categorical variable with four levels: *A. ludens*, *A. obliqua*, *A. striata*, and *A. serpentina*. The response variables were: i) the life expectancy of adult females and males (mean time in days from adult emergence until death), ii) the estimated daily egg production per female, iii) egg hatch (proportion) and iv) egg development time (in days).

Experiment 2—Natural field conditions

As conditions in the field are not stable and considerable fluctuations occur along the 24 h of a day (particularly between mid-day and early morning hours), we also determined the length of the life cycle and adult life span, under natural field conditions, and measured every 15 min temperature and relative humidity throughout the experiment in the studies sites using a Datta logger Hobo Pro v2. As was the case with the laboratory studies, fly availability depended on host fruiting phenology and that is the reason why the observations per species could not be carried out simultaneously. We started by allowing sexually mature females to lay eggs into their respective hosts in fruit naturally attached to bagged tree branches. We worked in the following localities in Veracruz, Mexico (I) Apazapan (19°19′18″N, 96°43′02″W) with *A. ludens* infesting 'Manila' mango from May 2014 to March 2015, *A. striata* infesting guava from November 2017 to August 2018, and *A. serpentina* sapodilla from May 2017 to November 2017; (II) Tolome Paso de Ovejas (19°16′00″N, 96°22′54″W) with *A. ludens* infesting 'Marsh' grapefruit from December 2014 to September 2015 and (III) Ídolos, Actopan (19°24′44″N, 96°31′15″W) with *A. obliqua* infesting 'Manila' mango from June 2015 to February 2016. For all types of fruit and locations, we used the following procedure: in ten trees, we randomly selected branches containing five healthy fruits. Five weeks before running tests, the branches were covered with gauze bags to protect the fruit from the oviposition activity of wild flies or the attack by other insects (e.g., beetles, wasps, caterpillars). When the fruit were close to reaching maturity, the protective bag was removed from each branch and replaced with a white organza fabric cage (Figure 1). Fifteen, 15-d old, sexually mature, mated female flies of each species, respectively, were released into each cage and provided with food and water *ad libitum* (same food as described above). Flies were allowed to lay eggs over a 24-h period, after which time they were removed. All bagged fruit were left until the first fruit was naturally abscised from the branch at which moment, the rest of the fruits were harvested and removed from the cage and, depending on their size, placed in individual plastic 500- or 1000-ml containers with aerated lids and vermiculite in the bottom to allow for larval pupation. We kept one fruit per container. The containers with fruits were arranged on shelves inside a field cage placed under the canopy of one of the trees from which the infested fruit stemmed to expose them to natural ambient environmental conditions throughout the study period. The date on which the third-stage larvae naturally abandoned the fruit, the pupation day, adult emergence dates and sex were recorded daily. The day of emergence, three male and three female flies were isolated in new plastic cages with artificial diet and water *ad libitum* to evaluate lifespan, fertility, fecundity, and length of the complete life cycle, also under completely natural conditions (4–7 replicates per treatment).

The following parameters were measured in both experiments:

Length of life cycle: Time elapsed between egg deposition and adult emergence and new egg deposition (sexual maturity of adults).

Lifespan. To determine median and maximal survival, the number of dead flies was scored daily in each cage since the first day of life.

Fecundity and Fertility. To estimate fecundity and fertility, starting at day eight (when the first eggs were recorded on cage

walls), flies inside cages were offered an agar sphere into which they could oviposit. The spheres were dissected daily to retrieve the eggs, which were incubated in Petri dishes containing a blue polysilk cloth on top of cotton moistened with 0.2% sodium benzoate. In Experiment 1, the Petri dishes were placed inside the bioclimatic chambers and exposed to the same temperature regimes the mothers and fathers were exposed to. In the case of Experiment 2 (field), the eggs were kept at ambient conditions. The number of eggs laid per female (fecundity) and egg hatch (fertility) were recorded daily. We note that due to the complexities experienced in the field, among them personnel safety, we only recorded fecundity and egg hatch for a period of 10 continuous days under field conditions. Under laboratory conditions, measurements were made daily until the last egg was oviposited into the agar spheres.

Length of complete life cycle. To assess the effect temperature (environmental conditions) on the length of the life cycle, eggs from the first 10 Petri dishes were transferred to a standard artificial larval diet (details in Pascacio-Villafán et al., 2016), and the number of larvae developing as well as the time it took them to pupate were recorded. The pupae obtained were isolated in new containers with moistened vermiculite. In Experiment 1, they were placed in the bioclimatic chambers with the temperature from which the larvae and parents came from. In Experiment 2 (field) the pupae were maintained at ambient conditions. The date of emergence of each individual and the sex were recorded and after this, they were monitored daily until death.

Statistical analyses

Data on flies' survival (proportion) from laboratory experiments were first analyzed with "Kaplan-Meier" survival curves using the software Graph Pad Prism 6 (CA, United States). Curves were constructed to examine the time at which 50% of the fly populations perished. First, curves were constructed to analyze differences in the survival of the different fly species at each of the temperatures tested and differences between females and males by fly species at each temperature. Then, the comparison focused on differences in temperatures for each fly species. The differences among the means of the median lifespans of flies were analyzed with Kruskal–Wallis and U-Mann-Whitney post hoc tests (Brooks et al., 1994). The differences between the survival means between females and males per species and temperature were analyzed with a *t*-Test for Dependent Samples (i.e., females and males were not independent from one another as they were grouped together in each replicated cage) with Statistica 10® software (Stat Soft, Inc., 2011).

Data on mean female and male life expectancy (days), daily egg production per female (no. of eggs), egg hatch (proportion) and egg development time (days) of flies from the laboratory trials were analyzed using response surface methods (Anderson and Whitcomb, 2005). The goal was to model the response variables as a function of main and interaction effects of the explanatory variables (temperature in a continuous scale and fly species as a categorical variable). Polynomial models were fitted to the values of each response variable and analyzed by analysis of variance (ANOVA). Analyses were performed following the procedure of the Design-Expert® 10 software (Anderson and Whitcomb, 2005). To improve the normal distribution and constant variance of the residuals of models, data on female and male life expectancy were natural log-transformed, data on the estimated number of eggs per female per day were natural log-transformed after adding a constant value of 0.051 to the data, and data on egg hatch were logit transformed. Transformations were based on Box-Cox analyses and the graphical examination of the model residuals (Anderson and Whitcomb, 2005).

We used descriptive statistics to show the variability of temperatures and relative humidity during the field experiments at each site. Kaplan-Meier survival curves were also constructed to examine the survival of flies in the field. To compare the means of median survival between species (considering females and males together), we used the same method described before for the laboratory experiments (i.e., the Kruskal–Wallis and U-Mann-Whitney post hoc tests). To determine if the survival of *A. ludens* was affected by the type of host fruit as well as male and female differences in all species, survival curves were analyzed using Log-rank (Mantel-Cox) tests run with the Graph Pad Prism 6 (CA, United States). Mean fly survival in the field for all species was analyzed by means of one-way ANOVAs.

Data on the development time of the immature stages of the different fly species under field conditions were analyzed with a non-parametric Kruskal–Wallis test, as the residuals of linear models fitted to the data did not comply with the assumptions of normality and homoscedasticity. Finally, for each immature stage, we performed multiple pairwise comparisons of the median values of fly species with the Dwas-Steel-Critchlow-Fligner test (Hollander and Wolfe, 1999). Analyses were performed with XLSTAT.

Hypothetical scenario of *A. ludens* invasion to two places in Europe. After models were fitted to experimental data, a prediction analysis (Anderson and Whitcomb, 2005) was used to formulate scenarios of the potential invasion and establishment of *A. ludens* in temperate areas under global warming conditions (Birke et al., 2013; Aluja et al., 2014). We focused on Switzerland as a scenario because it is one of the European countries that has suffered the most from the ravages of climate change and associated insect pest problems (Schneider et al., 2021), including the recent invasion of the American tephritid fruit fly *Rhagoletis completa* Cresson (Aluja et al., 2011). We retrieved the 2021 monthly average temperature data in Basel (Latitude: 47.5584°N, Longitude: 7.5733°E) and Geneva (Latitude:

TABLE 1 Female and male survivorship (mean ± SE, minimum and maximum values of days) of four *Anastrepha* species exposed to different temperatures in bioclimatic chambers. Results of the *t*-Test for Dependent Samples analysis to compare female and male survivorship of each species (t and *p*-values), mean ± SE of median survivorship of each species (females and males together) and Kruskal–Wallis test results (H and *p*-value) to compare mean of medians by temperature. *p*-values in bold denotes statistically clear differences.

	Species	Sex	5°C	10°C	15°C	20°C	30°C	40°C
Mean ± SE	*A. ludens*	F	18.2 ± 3.7	100.2 ± 8.8	212.6 ± 19.7	89.2 ± 11.8	43.1 ± 5.7	1.8 ± 0.4
		M	15.9 ± 3.6	86.9 ± 7.9	148.0 ± 10.0	95.7 ± 7.0	55.8 ± 6.1	1.8 ± 0.4
	t/*p*-values		2.28/0.083	1.32/0.255	3.22/**0.032**	-0.44/0.681	-3.75/**0.019**	0.11/0.913
	X̄ Median	F + M	17.5 ± 4.9	105.9 ± 4.9	177.1 ± 22.7	101.4 ± 11.4	50.5 ± 5.98	1.8 ± 0.6
	A. obliqua	F	13.1 ± 2.0	32.2 ± 1.5	62.5 ± 14.6	43.9 ± 3.9	64.3 ± 7.5	2.2 ± 0.7
		M	10.9 ± 1.9	21.2 ± 5.1	41.2 ± 13.4	46.3 ± 2.9	62.4 ± 5.1	2.2 ± 0.7
	t/*p*-values		1.07/0.342	1.75/0.153	2.30/0.082	-0.72/0.509	0.16/0.873	-
	X̄ Median	F + M	10.7 ± 1.59	14.1 ± 3.38	41.2 ± 19.66	45.4 ± 6.5	63.1 ± 4.51	2.2 ± 0.37
	A. serpentina	F	1.7 ± 0.3	13.6 ± 1.3	82.2 ± 13.3	66.9 ± 7.6	41.2 ± 4.0	3.2 ± 0.7
		M	1.8 ± 0.5	12.5 ± 0.6	49.0 ± 7.7	70.4 ± 5.6	37.4 ± 4.6	2.6 ± 0.4
	t/*p*-values		0.85/-0.201	1.16/0.307	1.95/0.122	-0.53/0.622	0.95/0.393	1.62/0.179
	X̄ Median	F + M	1.2 ± 0.2	12.9 ± 0.99	52.6 ± 8.8	64.1 ± 10.6	39.5 ± 2.6	2.9 ± 0.55
	A. striata	F	3.6 ± 0.4	11.4 ± 1.0	62.3 ± 5.7	78.9 ± 5.9	36.8 ± 1.2	3.5 ± 0.3
		M	2.5 ± 0.2	16.4 ± 1.3	75.9 ± 6.4	80.3 ± 9.0	42.1 ± 1.4	3.1 ± 0.3
	t/*p*-values		2.04/0.110	-2.50/0.066	-1.86/0.136	-0.12/0.909	-6.77/**0.002**	0.79/0.469
	X̄ Median	F + M	2.3 ± 0.3	11.3 ± 0.62	63.1 ± 13.3	82.2 ± 9.83	39.5 ± 2.2	2.7 ± 0.37
	H/*p* value		15.64/**0.001**	11.28/**0.007**	11.9/**0.007**	10.13/**0.017**	10.93/**0.012**	3.6/0.3074
Minimum and maximum	**Species**	**Sex**	**5 °C**	**10 °C**	**15 °C**	**20 °C**	**30 °C**	**40 °C**
	A. ludens	F	2–36	11–186	6–376	1–226	6–105	1–4
		M	1–37	7–183	7–344	1–196	2–132	1–6
	A. obliqua	F	3–30	1–96	1–162	1–135	4–126	1–3
		M	3–27	1–89	1–156	1–118	3–154	1–3
	A. serpentina	F	1–8	1–37	1–226	1–164	1–99	2–7
		M	1–7	1–35	5–176	3–159	1–97	2–6
	A. striata	F	1–9	1–45	1–176	6–181	1–71	1–9
		M	1–9	1–70	2–176	2–194	3–84	3–7

46.2042°N, Longitude: 6.1431°E), Switzerland, from the POWER Project CERES/MERRA2 Native Resolution Monthly and Annual on 2022/07/01, National Aeronautics and Space Administration (NASA) Langley Research Center (LaRC) Prediction of Worldwide Energy Resource (POWER) Project funded through the NASA Earth Science/Applied Science Program. The reason for choosing these two sites in Switzerland was based on having represented two regions (Basel in the northwestern and Geneva in the southwest) in which apples (*M.* × *domestica*) and pears (*P. communis*) are produced (Bravin, 2013). Apples and pears are naturally infested by *A. ludens* in Mexico (M.A. personal observation; Norrbom, 2004). We estimated the spring (April-June), summer (July-September), fall (October-December) and winter (January-March) mean temperatures of each site and considered a 1.3°C increase in temperature for the next 100 years based on Begert et al. (2019). Then, based on the fitted models, we predicted the mean life expectancy of females, the number of eggs per female per day and egg hatch for each of the hypothetical temperatures considered in the 100-year period projection. We coupled this information with the natural history theory and physiological understanding of *A. ludens* to surmise whether *A. ludens* could invade and establish in Switzerland.

Results

Kaplan-Meier survival curves of four *Anastrepha* spp. under laboratory conditions

We found clear statistical differences in the survival of the four fly species studied at the different temperatures tested (Table 1; Figure 2). At 5°C, *A. ludens* and *A. obliqua* had a longer lifespan than *A. serpentina* and *A. striata* (Figures 2A,B). While *A. ludens* at 10 and 15°C had a longer lifespan than the other three fly species (Figures 2C–F), with a mean (±SE) maximal survival of 340 ± 17.62 days at 15°C

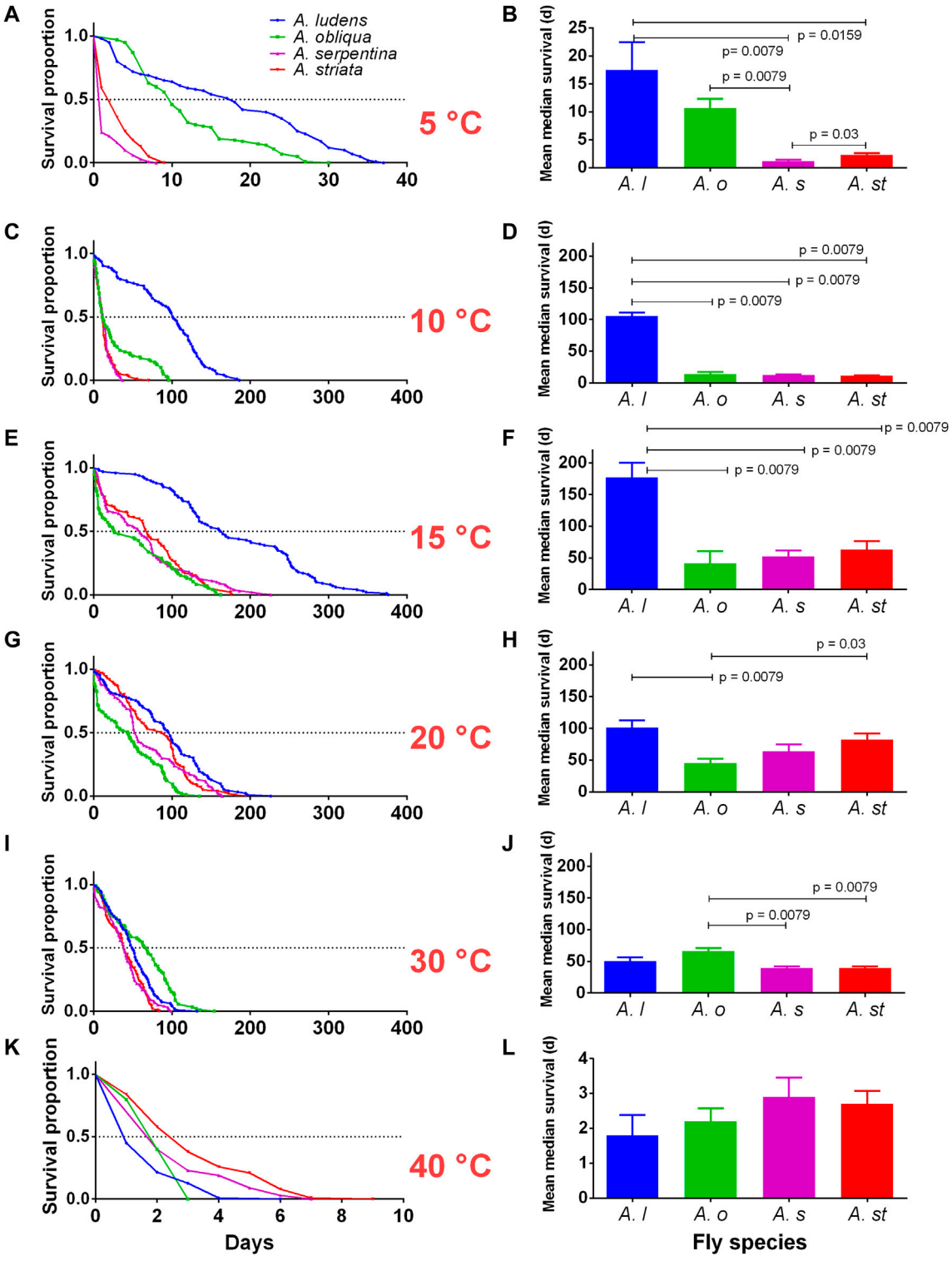

FIGURE 2
Adult survival (days) of four *Anastrepha* species (*A. ludens, A. obliqua, A. serpentina,* and *A. striata*) exposed to different temperatures (5, 10, 15, 20, 30,40°C) in bioclimatic chambers. **(A,C,E,G,I,K)** Kaplan-Meier survival curves by temperature; the dotted horizontal line represents the mean of the medians of all replicates. **(B,D,F,H,J,L)** Means ± SE of median survival (days) of five replicates (cage with flies) per species. Horizontal bars represent pairwise comparations with Mann-Whitney tests when clear differences were noticed. We left the data for 45°C out as in all species no adult survived more than 24 h.

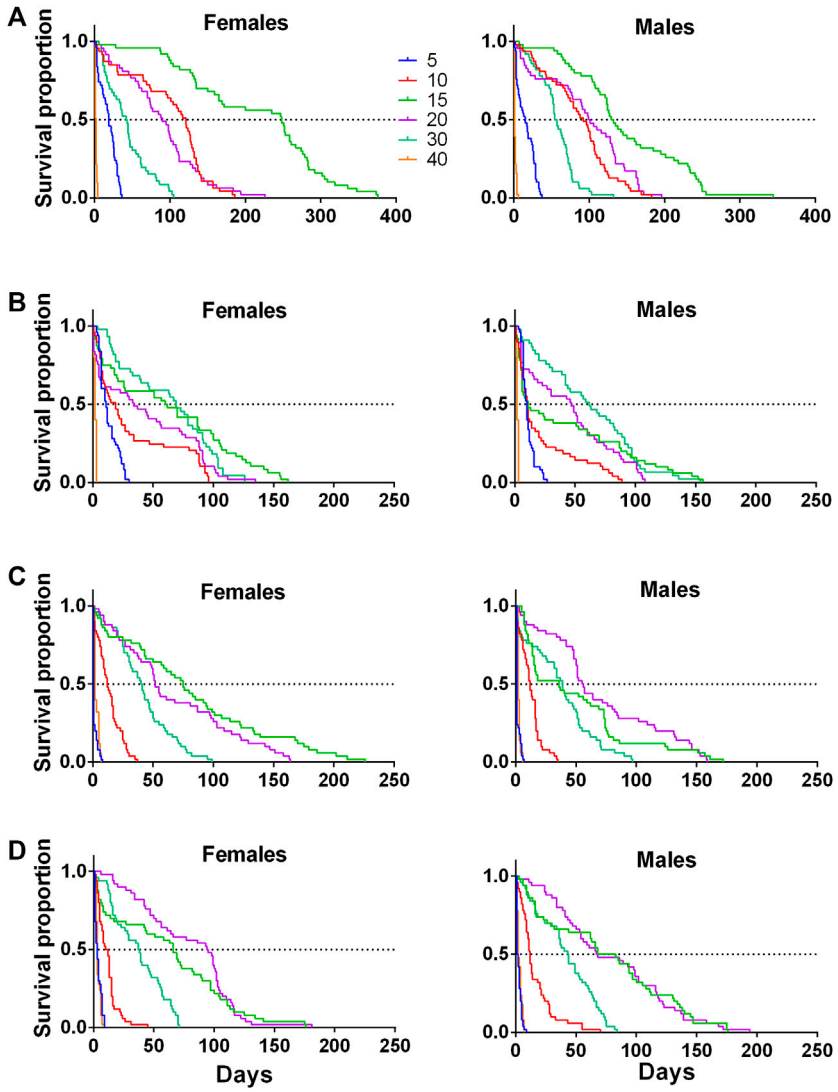

FIGURE 3
Kaplan-Meier survival curves of females and males of four pestiferous *Anastrepha* species exposed to different temperatures (5, 10, 15, 20, 30,40°C) in bioclimatic chambers **(A)** *A. ludens,* **(B)** *A. obliqua* **(C)** *A. serpentina* and, **(D)** *A. striata*).

(Figure 2E; Table 1). All fly species reached maximal survival at 15°C, although lifespan was clearly different in each one of them (Table 1; Figure 2E). At 20°C, *A. obliqua* had the shortest lifespan (45.4 ± 6.5 days), unlike *A. serpentina,* which had the longest mean lifespan (82.2 ± 9.83 days) at this temperature (Figures 2G,H), although its mean maximal survival (170 ± 23.6 days) was reached at 15°C (Figure 2G; Table 1). At 30°C, *A. obliqua* and *A. ludens* exhibited similar lifespans (Figure 2J), but *A. obliqua* at this temperature had its longest lifespan (63.1 ± 4.51 days) (Figures 2I,J). Finally, at 40°C, the lifespan of all fly species was similar, although *A. striata* and *A. serpentina* lived more days than *A. ludens* (Figures 2K,L). The lifespan of all fly species was affected by extreme low and high temperatures (Figure 2; Table 1). *Anastrepha ludens* and *A. obliqua* resisted colder temperatures, and *A. serpentina* and *A. striata* hotter ones (Figure 2; Table 1).

Females lived more than males at 15°C in all species, except for *A. striata,* where females and males had similar lifespans (Table 1; Figures 3D). Approximately 50% of *A. ludens* females and males reached 100 days of age at 10 and 20°C (Figure 3A), while at 30°C the 50% of the lifespan of both sexes was almost half than at 15°C, i.e., 50 days (Figure 3A; Table 1). In *A. obliqua,* females and males lived longer at 30°C, but 50% of the population perished around day 62, practically a month less than *A. ludens* (Figure 3B; Table 1). In the case of *A.*

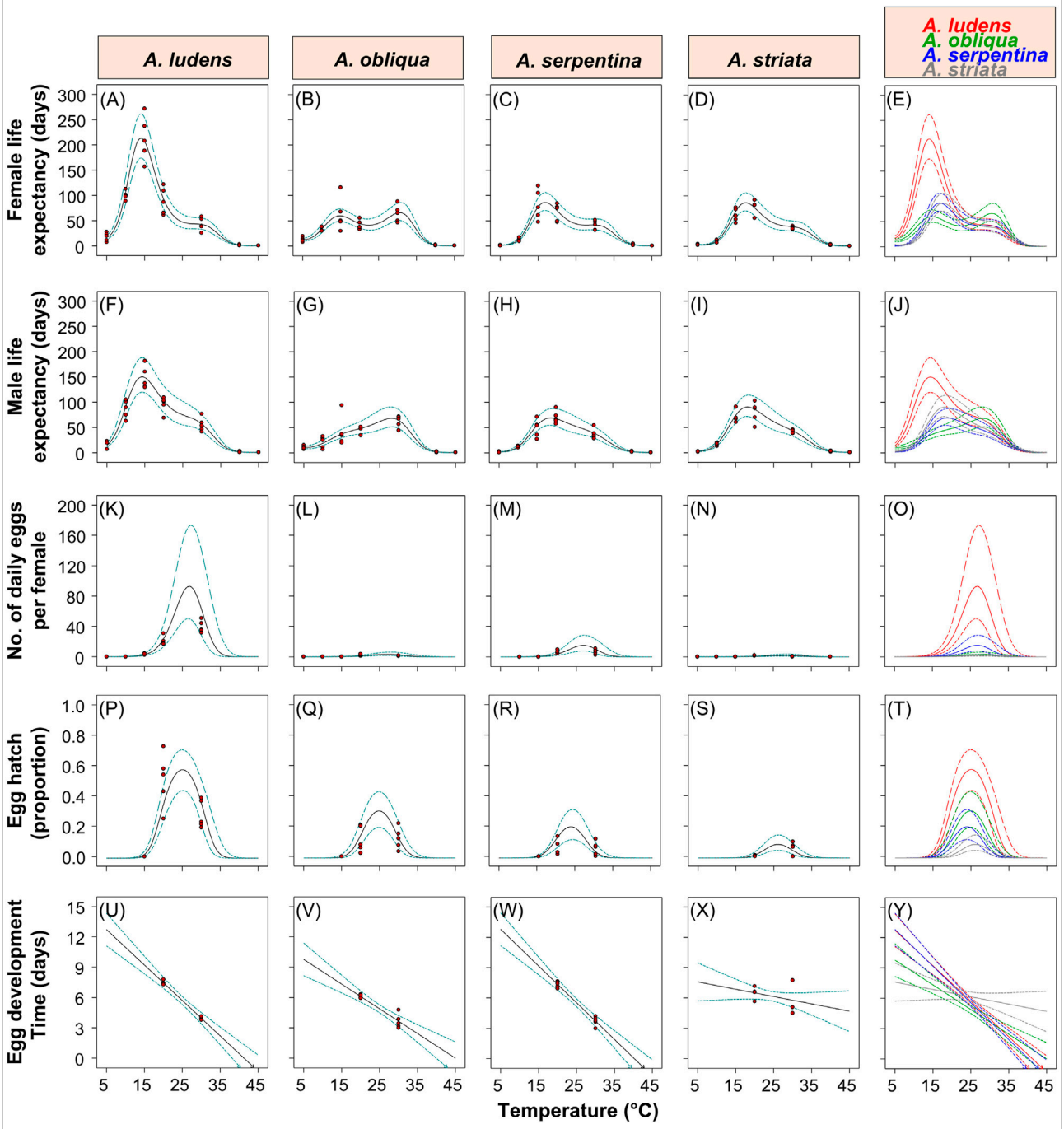

FIGURE 4
Polynomial models fitted to data on female **(A–E)** and male **(F–J)** life expectancy, the estimated daily egg production per female **(K–O)**, egg hatch **(P–T)** and egg development time **(U–Y)** of four *Anastrepha* species (from left to right *A. ludens*, *A. obliqua*, *A. serpentina* and *A. striata*) in response to an extreme increase in temperature. Solid lines indicate the models fitted to the data, and the dotted lines the 95% confidence intervals. Red points indicate the data points to which the models were fitted.

serpentina, females exhibited a larger lifespan (around 80 days) than males at 15°C with a 50% lifespan when they reached 75 days, while males had the 50% of longest lifespan when they reached approximately 60 days (Figure 3C). Finally, *A. striata* females reached the highest 50% lifespan (approximately 100 days) at 20°C, while males only survived about 75 days at 15 and 20°C (Figure 3D; Table 1).

Life expectancy/lifespan of female flies under laboratory conditions

A sixth-order polynomial model indicated clear main and interaction effects of temperature and fly species on the average life expectancy of female flies (ANOVA full model: F = 195.69; df = 24, 115; $p = 2.07^{-76}$; Supplementary Table S1). On average, females of *A. ludens* and *A. obliqua* lived longer periods (16.97 days in the case of *A. ludens* and 13.06 days in *A. obliqua*) than *A. serpentina* (1.68 days) and A. striata (3.71 days) at low temperatures (5°C) (Figures 4A–E). Females of *A. ludens* had the longest life expectancy of all four species, with an estimated maximum of ca. 214 days between 11 and 16°C (Figures 4A,E). *Anastrepha serpentina* and *A. striata* had similar estimated maximum life expectancies of ca. 87 days at temperatures between 14 and 20°C (Figures 4C–E), whereas the life expectancy of *A. obliqua* resembled a bimodal distribution in response to temperature with two estimated maximums of 60 and 66 days at temperatures between 12–17 and 27–33°C, respectively (Figures 4B,E). At 40°C, the species that lived the longest was *A. striata* with an estimated mean of 3.6 days of life expectancy, whereas at 45°C no fly species lived longer than an average of 1.1 days.

Life expectancy/lifespan of male flies under laboratory conditions

A sixth-order polynomial model showed clear main and interaction effects of temperature and fly species on the average life expectancy of male flies (ANOVA full model: F = 156.21; df = 24, 115; $p = 7.39^{-82}$; Supplementary Table S2). As was the case with female flies, males of *A. ludens* and *A. obliqua* lived longer periods (estimated mean of 14.56 days in *A. ludens* and 11.18 days in *A. obliqua*) than *A. serpentina* (1.67 days) and *A. striata* (2.63 days) at low temperatures (5°C) (Figures 4F–J). *Anastrepha ludens* males had the longest life expectancy of all four fly species with an estimated maximum of ca. 150.6 days between 11 and 18°C (Figures 4F,J). *Anastrepha serpentina* and *A. striata* had estimated maximum life expectancies of ca. 70–90 days at temperatures between 15 and 22°C (Figures 4H–J), whereas *A. obliqua* an estimated maximum of 80 days at temperatures between 26–31°C (Figures 4G,J). At 40°C, the species that lived the longest was *A. striata* with an average of 3.3 days of life expectancy, whereas at 45°C no species lived more than an average of 1.1 days (Figure 4J).

Daily egg production per female under laboratory conditions

A cubic model indicated clear main and interaction effects of temperature and species on the daily mean egg production per female fly (ANOVA full model: F = 45.08; df = 12, 82; $p = 5.4^{-31}$; Supplementary Table S3). No species laid eggs at temperatures between 5 and 10°C, and only *A. ludens* and *A. obliqua* laid eggs at 15°C with estimated means of 2.7 and 0.21 eggs per female per day, respectively (Figures 4K–O). *Anastrepha ludens* was the species that laid the largest number of eggs with an estimated maximum of 93 eggs per day per female at a temperature close to 25–27°C, whereas the maximums estimated for *A. obliqua*, *A. serpentina* and *A. striata* were ~3.5, 15.3 and 2.4 eggs per day per female, respectively (Figures 4K–O).

Figure 5A presents the pattern of laid eggs by *A. ludens* females exposed to different temperatures showing that females only lay eggs at temperatures 15, 20, and 30°C. It stands out that the females exposed to 15°C regularly laid eggs from day 40 until day 335 (Figure 5A), although eggs did not hatch (Figure 5B). At 20°C, females laid eggs from day ten until day 209 with a peak between days 11 and 91 (Figure 5B). At this temperature, the percentage of eggs hatching fluctuated between 0 and 100 (Figure 5B). Finally, females exposed to a constant temperature of 30°C began to lay eggs at 8 days of age and finished at 102, 3 days before the last female of this treatment died.

Egg hatch under laboratory conditions

A quadratic model indicated clear main and interaction effects of temperature and species on egg hatch (ANOVA full model: F = 17.06; df = 8, 41; $p = 8.07^{-11}$; Supplementary Table S4). There was no hatching of *A. ludens*, *A. obliqua* and *A. serpentina* eggs at 15°C (in the case of *A. striata* there were no eggs to evaluate at this temperature). In the four fly species, the models fitted to data on egg hatch had an inverted "u" shape with the highest proportion of hatched eggs predicted by the models at temperatures between 21–29°C for *A. ludens* (proportion of 0.57) and *A. obliqua* (proportion of 0.30), 20–27°C for *A. serpentina* (proportion of 0.19), and 22–30°C for *A. striata* (proportion of 0.08) (Figures 4P–T).

Egg development time under laboratory conditions

A two-factor interaction model (F = 33.94; df = 7, 29; $p = 2.62^{-12}$) showed clear main and interaction effects of temperature and the fly species on egg development time (Supplementary Table S5). In *A. ludens*, *A. obliqua* and *A. serpentina*, egg development time decreased markedly as temperature increased from 20 to 30°C (Figures 4U–W), whereas in *A. striata* the same change in temperature had an unclear effect on egg development time (Figure 4X).

Predicted life expectancy, egg production and egg hatch of *A. ludens* in hypothetical temperature conditions

Spring, summer, fall, and winter 2021 temperature estimates for Basel and Geneva are shown in Table 2 along

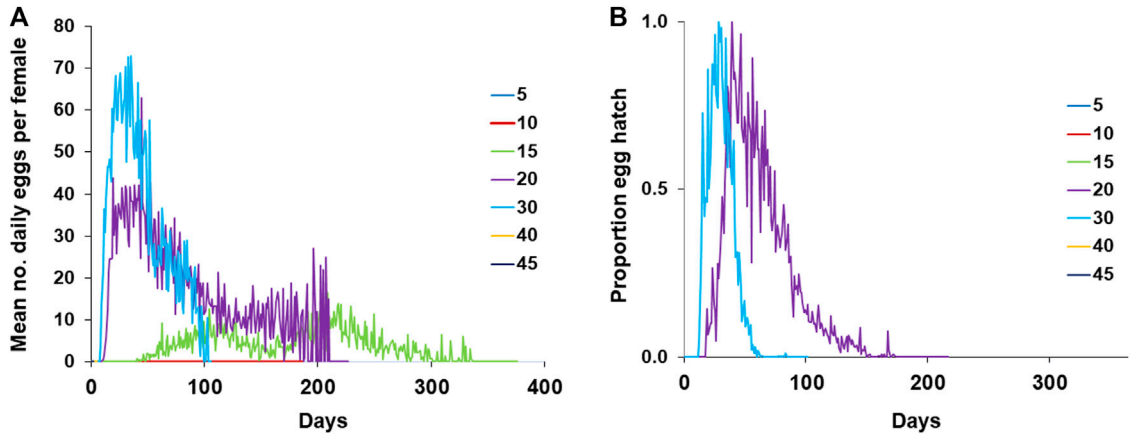

FIGURE 5
Reproduction parameters of *A. ludens* females exposed to different temperatures in climatic chambers **(A)** Fecundity; **(B)** Fertility.

TABLE 2 The 2021 real temperature and predicted temperature for 2121 in two sites in Switzerland and the predicted life expectancy, egg production and egg hatch of *A. ludens* in such predicted temperatures.

Season	Site	Estimated temperature for 2021 (°C)	Predicted temperature for 2121 (°C)	Predicted life expectancy of female flies for 2121 temperature (Days)	Predicted production of eggs/female/day for 2121 temperature (Days)	Predicted egg hatch for 2121 temperature (proportion)
Spring	Basel	10.14	11.44	160.42	0.74	0.0
Spring	Geneva	11.42	12.72	198.32	1.25	0.0
Summer	Basel	15.44	16.74	170.63	5.23	0.07
Summer	Geneva	17.08	18.38	128.02	8.69	0.19
Fall	Basel	3.25	4.55	16.05	0.0	0.0
Fall	Geneva	4.44	5.74	20.30	0.01	0.0
Winter	Basel	0.14	1.44	ND	ND	ND
Winter	Geneva	1.71	3.01	ND	ND	ND

with the hypothetical average temperature estimate for 2121 and predictions of life expectancy, egg production and egg hatch of *A. ludens* females for each predicted temperature. *Anastrepha ludens* females could live up to 170.62 days at an estimated summer temperature of 16.74°C in Basel, whereas at a spring temperature of 12.72 °C in Geneva the flies could reach a maximum lifespan of 198.32 days. Maximum egg production per female was estimated for summer temperatures of 16.74°C in Basel with an average of 5.23 eggs per female per day and 8.69 eggs per female per day at 18.38°C in Geneva (Table 2). Spring, fall, and winter temperatures were predicted to inhibit egg hatch in *A. ludens* (Table 2).

Adult survival of four *Anastrepha* spp. under field conditions

The mean lifespan of *A. ludens* in the field (Table 3) compared with the longest lifespan in the laboratory (15 °C treatment) (Table 1; Figures 2E,F) was ca. 70% lower for *A. ludens* stemming from mango and 46% lower than flies originating from grapefruit (Figures 6A,B). In the case of *A. obliqua*, the average lifespan in the field was 31% higher than the longest lifespan in the laboratory at 30°C (Table 1; Figures 2I,J and Figure 6C). Field and laboratory lifespans of *A. serpentina* were similar; laboratory flies at 20°C lived 5% more than field flies (Tables 1 and 3). Field *A. striata* lived 48% more than the

TABLE 3 Means of median, maximum, and minimum survival days ±SEM of the different *Anastrepha* spp. in the field (females and males together).

Survival parameters in days	*A. ludens* (mango)	*A. ludens* (grapefruit)	*A. obliqua* (mango)	*A. serpentina* (sapodilla)	*A. striata* (guava)	$F_{4, 30}$ (*p*-value)
Median (±SE)	53.6 ± 3.7	95.2 ± 4.7	92.3 ± 5	60.8 ± 8.3	159 ± 8.27	23.58 (0.0001)
Maximum (±SE)	173.8 ± 38	190 ± 10.6	167.4 ± 22.8	127 ± 6	211.5 ± 11.1	
Minimum (±SE)	8.6 ± 3.1	18.1 ± 5	14.4 ± 8	30.3 ± 6	49 ± 16	

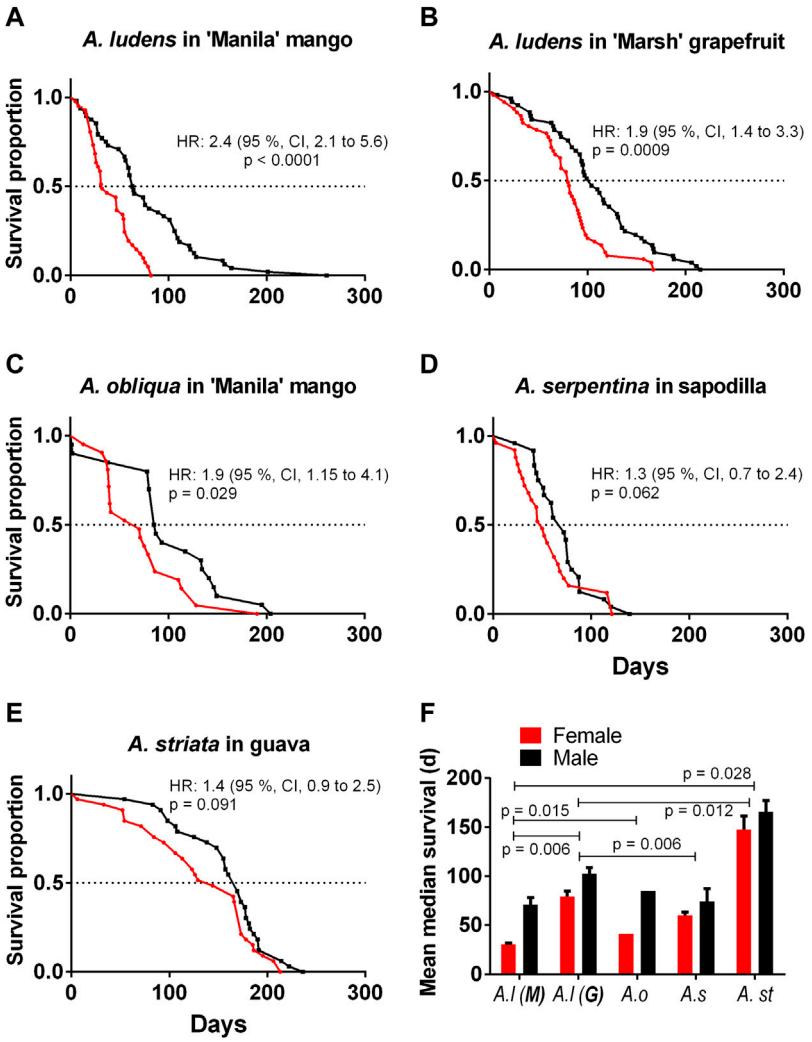

FIGURE 6
Kaplan-Meier survival curves of four pestiferous *Anastrepha* spp. under field conditions **(A)** *A. ludens* reared in mango in Apazapan, **(B)** *A. ludens* reared in grapefruit in Tolome; **(C)** *A. obliqua* reared in mango in Actopan; **(D)** *A. serpentina* reared in sapodilla in Apazapan; **(E)** *A. striata* reared in guava. The red lines show female survival, and the black ones male survival. **(F)** Mean ± SE of median survival (days) of females and males of the four *Anastrepha species*.

laboratory flies at 20°C (Table 1 and Table 3; Figures 2G–H and Figure 6E). The lifespan of *A. ludens* females and males from 'Marsh' grapefruit in the field was higher than that observed in *A. ludens* from mango, and *A. serpentina* (Table 3). The lifespan of *A. ludens* developed in grapefruit was 87.7% higher than that observed in flies that developed in mango (Table 3, Figure 7). We found a statistically clear difference between the lifespan of males and females in all the studied species (Figure 6); all hazard ratios comparing survival curves show that females lived less than males in the field.

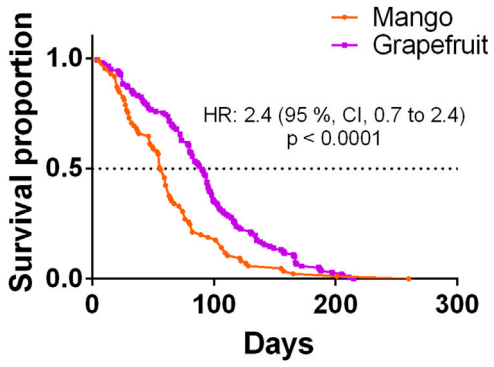

FIGURE 7
Kaplan-Meier survival curves of *Anastrepha ludens* females and males originating from two host plants (mango cv. 'Manila' and grapefruit cv. 'Marsh') under field conditions.

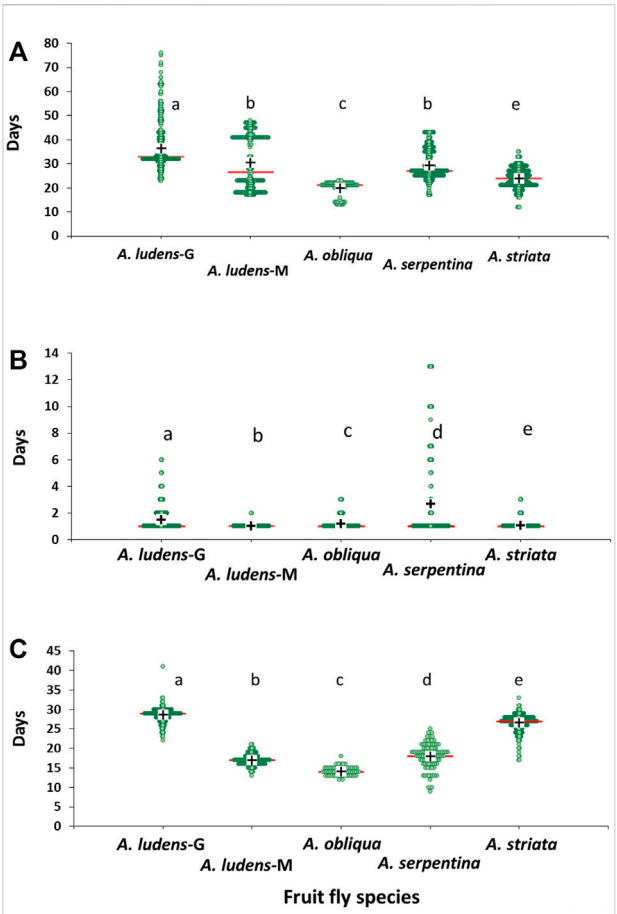

FIGURE 8
Development time in days of immature stages of four *Anastrepha* species reared under field conditions **(A)** Egg-third instar larvae; **(B)** Third instar larvae-pupae; **(C)** Pupation period. Green points show dispersion data, red horizontal lines show the median and black crosses the mean of days. *A. ludens*-G (from grapefruit), *A. ludens*-M (from mango).

Development time of *Anastrepha* spp. immature stages under natural field conditions

We found statistically clear differences in the development time from egg to third instar larva among the studied *Anastrepha* species (H = 922.38; df = 4, 2,101; $p < 0.0001$; Figure 8A). *Anastrepha obliqua* had the shortest development time with an estimated mean (±SE) of 19.8 ± 0.34 days, whereas the longest development time was observed in *A. ludens* from grapefruit with an estimated mean of 36.4 ± 0.32 days, followed by *A. ludens* from mango with 30.5 ± 0.64 days (Table 4; Figure 8).

We found statistically clear differences in the time that the larvae of the different *Anastrepha* species took to pupate (H = 210.02; df = 4, 1971, $p < 0.0001$). *Anastrepha serpentina* larvae took an average (±SE) of 2.7 ± 0.20 days to pupate with a maximum of 13 days, followed by *A. ludens* reared on grapefruit (1.5 ± 0.03 days) (Table 4; Figure 8B).

Finally, we found statistically clear differences in pupation time among the four *Anastrepha* species studied (H = 1,032.77; df = 4, 1,552; $p < 0.0001$). *Anastrepha ludens* reared in grapefruit had the longest pupation time (28.64 ± 0.06) whereas the shortest time was observed in *A. obliqua* (14.18 ± 0.14) (Table 4; Figure 8C).

Temperature and humidity patterns in the field

There was a clear difference in temperature and relative humidity (RH) across time among hours in any given day and over days (Figure 9; Table 5). Temperature and relative humidity patterns were contrasting: when the highest temperatures were measured, relative humidity values dropped to their lowest points. In all sites, the temperature and RH patterns were similar, with variations along the day and the season (Figure 9). The lower temperatures were recorded between 00:00–07:00 h, and between 20:00 and 23:00 h at Tolome and Actopan (Figures 9C,E). In the case of Apazapan, the lower temperature occurred from 00:00 to 09:00 h and between 20:00 and 23:00 h (Figure 9A). In Tolome, the place where *A. ludens* naturally infests grapefruit, recorded temperatures reached more than 40°C at 15:00 h in April, but in February, the temperature was 11°C at 07:00 h (Figure 9C). In Actopan, the site where *A. obliqua* and *A. ludens* infest mangoes, the maximum temperature reached 36°C in October, whereas the minimum was 12°C in January (Figure 9E). At this site, the temperature pattern presented two peaks, one in October and the

TABLE 4 Mean (±SE), minimum and maximum values for development times (in days) of immature stages of four *Anastrepha* species reared under field conditions *A. ludens*-G (from grapefruit) and *A. ludens*-M (from mango).

Fruit fly species	Eggs-third instar larvae			Larve-pupae			Pupation		
	Mean	Min	Max	Mean	Min	Max	Mean	Min	Max
***A. ludens*-G**	36.41 ± 0.32	23.00	76.00	1.48 ± 0.03	1	6.00	28.64 ± 0.06	22.00	41.00
***A. ludens*-M**	30.54 ± 0.64	17.00	48.00	1.01 ± 0.00	1	2.00	16.96 ± 0.10	13.00	21.00
A. obliqua	19.81 ± 0.34	13.00	23.00	1.19 ± 0.05	1	3.00	14.18 ± 0.14	12.00	18.00
A. serpentina	29.40 ± 0.33	17.00	43.00	2.66 ± 0.20	1	13.00	18.06 ± 0.31	9.00	25.00
A. striata	23.89 ± 0.15	12.00	35.00	1.07 ± 0.01	1	3.00	26.70 ± 0.09	17.00	33.00

TABLE 5 Climatic data of field study sites in Veracruz, Mexico.

Climatic data	Apazapan (mango, guava and sapodilla area)			Tolome (citrus area)			Actopan (mango area)		
	Mean	Min	Max	Mean	Min	Max	Mean	Min	Max
Temperature (°C)	23.5	11.8	34.4	25.16	11.6	40.92	23.9	11.3	36.0
RH (%)	92.4	38.4	100	82.8	21.4	100	83.1	29.5	100
Altitude (masl)	408	40	96						

other in September (Figure 9E). In Apazapan, a mango and sapodilla producing area, the temperatures fluctuated between 11°C (November) and 38°C (September) (Figure 9A). In Tolome, the site with the highest temperatures recorded, the RH dropped to 21% in April, which is the dry season (Figure 9D). In general, the lowest humidity percentages fluctuated between 40 and 80% and occurred between 10:00 and 17:00 h, which coincides with the hours of the day when temperatures were at their highest peaks. In Apazapan and Actopan, the highest percentages of RH (80–100%) were recorded between 00:00 and 09:00 h and between 20:00 and 23:00 h for the case of Actopan (Figures 9B,F). In the case of HR, Apazapan presented a very variable pattern between 09:00 and 20:00 h.

Discussion

In this study, we addressed a key topic of research in insect developmental biology and physiology that is critical for decision-making in the management of pestiferous insect invasions and the understanding of insect ecology in the face of global warming (Wagner et al., 1984; Samayoa et al., 2018; Lisbôa et al., 2020; Schneider et al., 2021). Our results show clear patterns indicating that some of the four species studied will suffer more under a global warming scenario and that as predicted, *A. ludens* lived significantly longer under controlled laboratory conditions when compared to highly variable field conditions exerting metabolic challenges (Table 1 and Table 3; Figure 9). Interestingly, the two species belonging to the more basal *serpentina* species group (*A. striata* and *A. serpentina*, Norrbom, 2002) survived more days as adults under the constant and extreme temperature of 40°C (Figures 2K,L), and in the case of *A. striata*, it was the species in which adults lived more time under variable conditions in the field (Table 3), implying that these species will better cope with rising temperatures granted their host plants also adapt to these temperatures. Individuals of these two species also suffered the most when exposed to the low temperatures of 5 and 10°C (Figures 2A–D). Contrary patterns were observed in the two representatives of the *fraterculus* species group (*A. ludens* and *A. obliqua*). At a constant temperature of 45°C, adults, independent of species, only managed to survive a single day, likely due to thermal shock. We note however that in nature adult flies can move to cooler places during the hottest hours of the day (Aluja and Birke, 1993) and that the air temperature is not the same as the temperature in the pulp and thus could likely survive for longer periods as adults. In the case of *A. ludens*, the species exhibiting the widest distribution margin in nature when considering altitude above sea level, our data clearly show that its adult survival rate peaked at 15°C (Figures 4A,F), which means that under a global warming scenario, it is likely that the altitudinal distribution range of this species will shift from

10.3389/fphys.2022.991923

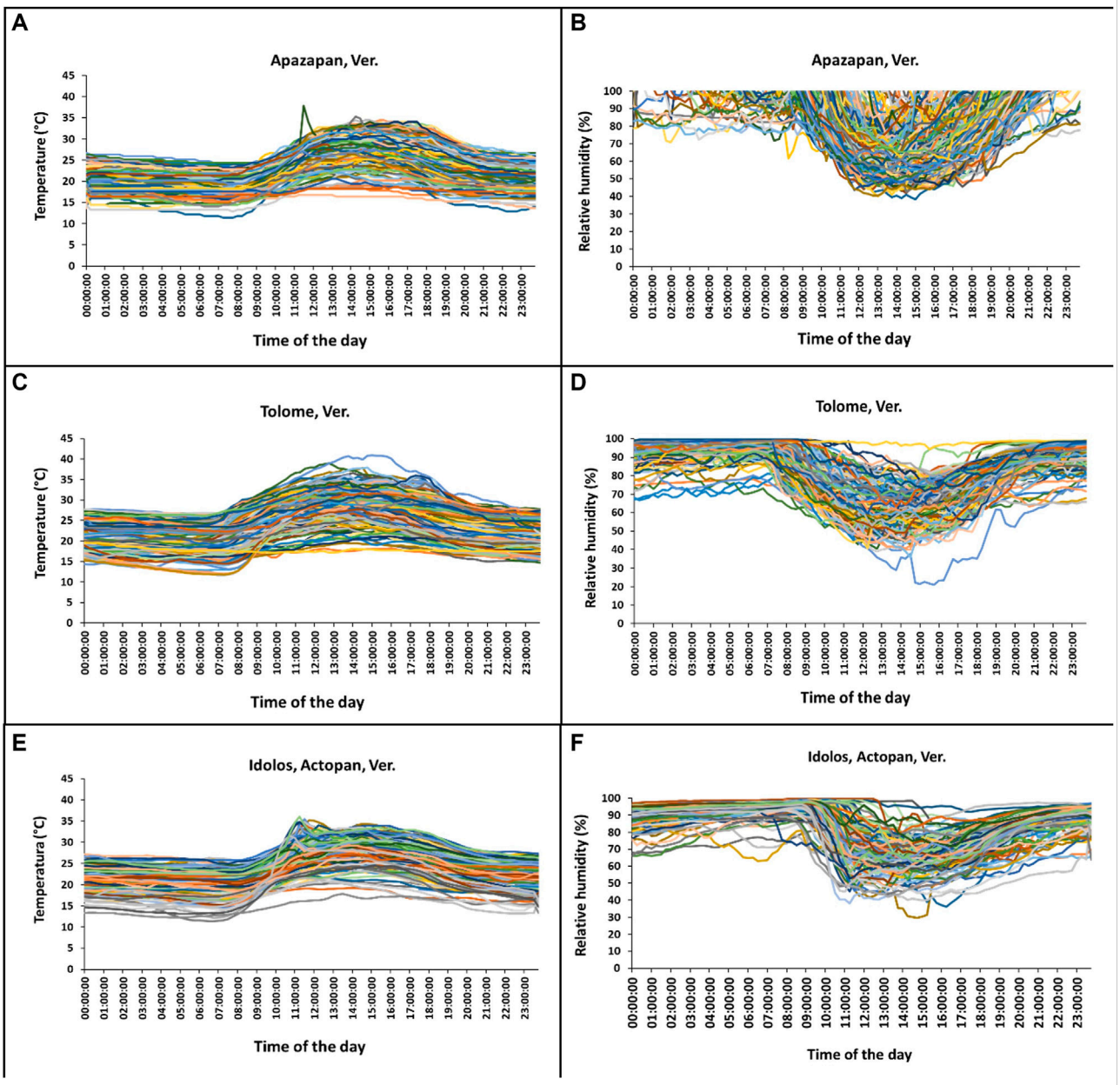

FIGURE 9
Mean temperature and RH per hour of each day throughout the experiment in **(A–B)** Apazapan (mango, sapodilla, and guava area) **(C–D)** Tolome (citrus area), and **(E–F)** Idolos, Actopan (mango area) in Veracruz, Mexico.

lowland tropical regions to higher altitude ones, using new hosts along the way. At the same low temperature, females laid large numbers of eggs, but none hatched. In contrast to *A. striata* and *A. serpentina*, *A. ludens* survived for up to 40 and 185 days, respectively, at 5 and 10 °C degrees. Surprisingly, *A. obliqua*, a species that is found in warm, tropical environments, fared much better than *A. striata* and *A. serpentina* at 5 and 10°C degrees, respectively (e.g., females survived up to 30 and 125 days, respectively). In all species, egg hatch was first recorded at 20°C but it is possible that the eggs that did not hatch at 15°C were viable and would have hatched if temperature conditions changed (i.e., if eggs were moved from an environmental chamber under 15°C to one under 20 or 30°C). Importantly, field data, under highly variable temperature and relative humidity conditions (Figure 9), yielded similar overall patterns among the four species studied (compared to the laboratory studies), but with significantly shorter survival rates in the cases of *A. ludens* and *A. serpentina* (Table 1 and Table 3).

The latter, likely due to an increased metabolic wear/exhaustion caused by the need to cope with the highly variable environmental conditions (e.g., Moloń et al., 2020). Also, field conditions, flushed out an interesting difference in survival between sexes in *A. ludens*. In what follows, we expand on the results of our modelling approach and their implications related to global warming, and discuss our findings considering the physiological/metabolic processes possibly regulating adaptation to varying temperatures.

Our modelling approach allowed us to determine how the life expectancy, fecundity, fertility, and egg development time in four *Anastrepha* species, some of which infest the fruit of various plant species including commercial mango and citrus, differentially vary as a function of a wide range of temperatures from 5 to 45°C (Figure 4). The same approach allowed us to make predictions on the life expectancy, fecundity, and fertility of *A. ludens* females in hypothetical invasion scenarios to temperate areas as a consequence of global warming. We used Switzerland as an illustration of a European country which already has been invaded by an American tephritid fruit fly (Walnut Husk Fly, *R. completa*, Aluja et al., 2011), and where commercial apple (*Malus* × *domestica* Borkh.) production could be severely affected by an *A. ludens* invasion (Birke et al., 2013; Aluja et al., 2014). Based on our models and analyses, we calculated that in the case of a future increase in temperature and expansion of *A. ludens* to temperate areas, females could potentially live more than six months in spring and summer temperatures of 11.44–18.38°C (Figure 4A, Table 2). Over three months at such temperatures, a single *A. ludens* female could potentially oviposit up to 792 eggs and leave an estimated larval offspring of 150 individuals (i.e., 8.69 eggs per day and a hatching rate of 19%, Table 2). Although our study did not directly evaluate the effects of temperature on larval development time, it is well known that in *A. ludens* (Messenger and Flitters, 1957; Thomas, 1997; Aluja et al., 2010) and other tephritid pest species (Samayoa et al., 2018; Huang et al., 2020) temperature is a critical factor that affects development. In this study, we observed that *A. ludens* larvae could live almost three months inside grapefruit (Figure 8A) in a field site where the overall mean temperature was ca. 25.16°C, but that during winter can drop to 10°C. Cold winter temperatures are known to extend pupal development time of *A. ludens* (Thomas, 1997), and the minimal lethal time (LT) for 99.9968% mortality of phanerocephalic pupae and pharate adults at a constant temperature of 1.1°C was estimated to be 20.8 and 20.2 days, respectively (Hallman, 1999). This means that *A. ludens* individuals likely activate physiological mechanisms that allow them to extend developmental periods in response to cold temperatures (a topic discussed later). In fact, our study showed that the egg development time of *A. ludens*, *A. obliqua* and *A. serpentina*, takes longer at low temperatures than at high temperatures (Figures 4U–W). This could help flies to withstand cold winters in the case they invade temperate areas. But given that temperature and RH conditions in nature fluctuate significantly (Figure 9) caution should be applied when reaching conclusions from experimental data using constant temperatures. However, our study provides a valuable way to address the issue of thermal thresholds in insects using predictive models generated from experimental data under controlled laboratory conditions, which together with climatic predictions and life history theory of the studied species, contributes to improving our understanding of insect developmental physiology. But as underlined by Hagstrum and Milliken (1991) and Fischer et al. (2011), future studies in the laboratory should consider varying temperatures to predict life histories of insects more accurately in nature.

Our results confirm old findings (Messenger and Flitters, 1957) on the negative effect of high temperatures on the survival of adult flies (Figures 2–4). An extreme increase in temperature in the current range of distribution of flies could force them to move to temperate zones. In fact, recently, we have been documenting infestations of *A. ludens* in commercial apple orchards growing in temperate areas of Mexico where they were not found before (MA, pers. obs.). In addition, extremely hot temperatures were recorded in Mexico last year (2021) in Hermosillo, Sonora, reaching more than 45 °C in some places (NASA, 2022). Hermosillo is currently a fruit fly pest-free zone (Gutiérrez-Ruelas et al., 2013), therefore our data will help managers gauge strategic decisions in this area of the country as we now have reliable information on the upper thermal limits of *A. ludens*. The same applies to other areas of the world such as for example Northern Africa, many parts of Asia and Australia where temperatures easily reach 45°C. We note however, and as documented by Aluja and Birke (1993) in the case of *A. obliqua*, adult flies move back and forth during the day between habitat units, in this case, a tropical plum tree (*Spondias purpurea* L.) devoid of leaves at the time of study, and a densely foliated mango tree, using the latter as a refuge to deal with the extremely hot temperatures at midday (close to 45°C). So adult flies will likely live for much longer periods as observed here in the laboratory at 40 and 45°C as there they had no place to escape. In addition, it must be considered that as is the case with extremely low temperatures (discussed before), the temperature inside fruit is lower than the air temperature where the tree grows. So, the survival of larvae will be higher when protected by the fruit, compared to adults exposed to very high air temperatures granted they do not find refuge in a densely foliated tree or crevice in for example rocky walls or dry riverbeds. But the latter depends on the size to the fruit and the degree of leaf cover in the tree because Aluja and Birke (1993) also documented the fact that *S. purpurea* fruit, which have a very large seed and as a result very little pulp and a thin skin, can heat up considerably forcing larvae to jump out of the fruit dropping up to 10 m to the ground to bury themselves and pupate (if an ant does not kill them before (Aluja et al., 2005)). In the case of immature stages, surviving at high temperatures can be more complex. Pucci et al. (1981)

concluded that most of the eggs and larvae of *B. oleae* die when the olive fruits reach maximum temperatures of 36°C for 1 week. The air temperature, the size of the fruit and its location on the tree or the ground influence the internal temperature of the fruit and the survival of immature stages (Sivinski et al., 2007). Eggs cannot avoid high and mortal temperatures inside some fruit, but females can diminish the risk of desiccation by avoiding laying eggs in sun-exposed sites on the fruit (Guillén et al., 2022) and larvae can move to fresher areas within the fruit (Sivinski et al., 2007), or as noted before crawl out of the fruit and jump to the ground.

One of the strengths of our experimental approach is that we studied all four species under controlled conditions using a fixed temperature regime that spanned over a wide range of temperatures, as well as under highly variable natural conditions. This approach enabled us to flush out interesting differences between males and females in most species (Figure 6) that point to physiological mechanisms that differ between the sexes (details follow). It also allowed us to determine that, for example, *A. ludens* individuals, can survive as adults up to 200 days in the field and up to 370 days in the laboratory under a constant temperature regime of 15°C. Notably, females of this species can lay viable eggs after 150 days of age (Figure 5B) at 20°C and lay many eggs at 15°C but that do not eclose (Figures 5A,B). Low and high temperatures are known to decrease sperm production and viability in *Drosophila*, which can lead to sterility in males (David et al., 2005). Perhaps *Anastrepha* flies maintained at low temperatures in our study suffered from damage to the male reproductive system, which in turn could have reduced mating frequency or sperm quality (Meats and Fay, 2000; Walsh et al., 2019). In contrast, when flies were subjected to high temperatures, the production of eggs in the ovaries was accelerated as was the case with the olive fly, *B. oleae* (Wang et al., 2009), but likely at the cost of high energy expenditure (Novoseltsev and Novoseltseva, 2013) and a reduction in lifespan. All this has important implications for the management of fruit flies applying the Sterile Insect Technique as adults are many times chilled prior to release in the field (Hernández et al., 2010). Another relevant effect of temperature on the biological traits of flies is related to the size of the eggs. Three different scenarios have been observed in insects: 1) at constant temperatures, the size of the eggs remains without significant changes; 2) at low temperatures, females generally produce fewer numbers of eggs, but the size of the eggs is larger (Fox and Czesak, 2000; Fischer et al., 2011; Xu et al., 2012); 3) at high temperatures females produce a greater number of eggs but with a relatively small size (Fox and Czesak, 2000; Fischer et al., 2011). Under field conditions, egg size is expected to be highly variable because of the influence of fluctuating temperatures and food availability (Xu et al., 2012). Finally, we would like to highlight the differences observed in the field in the case of *A. ludens* infesting two different hosts (grapefruit and mango). Given that these fruits do not overlap because of their different fruiting phenologies, we were not able to conduct the study simultaneously and thus attribute a definitive host effect under equal environmental conditions. But the patterns observed were very interesting. Both sites had overall similar temperatures and RH (Figure 9; Table 5) and, in both sites, insects were exposed to low (ca. 11°C) and high temperatures (ca. 38°C). However, the lifespan of adults and development time of immatures were significantly longer in grapefruit than mango (Figure 8). The difference, independent of host type, was the moment at which immature stages experienced the cold stress. In grapefruit, immature stages experienced cold temperatures from December to February. Notably, the development time from egg to larvae extended for some individuals over almost 80 days. Under more favorable environmental conditions, this period covers ca. 12 days (five for egg incubation and seven for larvae development; Aluja, 1994). In contrast to what occurred in grapefruit, in mango, insects were exposed to cold temperatures at the end of their adult life (not as eggs or larvae). In other Diptera with facultative diapause, it has been reported that early-instar larvae, depending on the environmental cues received, prolong the duration of larval or pupal stages (Denlinger, 2002). In *A. ludens* a facultative diapause has not been reported, but our observations here (i.e., extremely long egg to larvae periods), suggest that it could be a mechanism triggered to deal with adverse (i.e., cold) temperatures. We note too that subtle changes in temperature or relative humidity can have subtle effects on immature development time as recently documented by Manenti et al. (2021) and references therein working with five *Drosophila* species with different thermal niches. These authors were able to document the fact that several species of the same genus "can show substantial differences when developing at fluctuating temperatures not always predictable by development at comparable constant temperature (25°C)". These results relate nicely to ours as we also observed different development patterns in for example *A. ludens* developing in different fruit in two times of the year, highlighting the fact that studies under variable environmental conditions are crucial to fully understand the abiotic factors driving immature development. For further discussion on this critical issue, please see Parmesan (2006), Jaworski and Hilszczański (2013) and Ketola and Saarinen (2015).

Among the most critical physiological responses to temperature changes in insects, the following stand out: 1) sensory responses, 2) changes in metabolic rates, 3) responses to heat stress mediated by HSP proteins, and 4) modulation of hormones that culminate in modifications in development time and behavior (González-Tokman et al., 2020). In addition, phenotypic attributes such as foraging, regurgitation and mating behavior, abdominal ventilation, cuticular biopolymers, and body size help insects to deal with extreme temperatures (Perez and Aron, 2020). Some plastic physiological responses can counteract the mechanical, structural, and functional challenges in cells, mainly in cell structure, protein activity, and energetic

balance. Changes in cell membrane composition have been described to avoid fluidity modifications and interchange of proteins that have higher flexibility in response to extreme temperatures (Koštál et al., 2007). Besides, dehydration has been described as a response to extreme temperatures. The water loss in the insect body can decrease the risk of ice crystallization and damage to cell structure (Toxopeus and Sinclair, 2018). In the case of flies depending on the species, the crystallization temperature is between 0 and -65°C (Lee, 1991). The synthesis of bioamines and other small molecules with cryoprotectant qualities as well as glycerol and trehalose can counteract the protein stress response to heat shock. In this respect, there is evidence of significant effects in transcriptome and metabolome organization from *Drosophila melanogaster* Meigen during cold acclimation (MacMillan et al., 2016). Under laboratory conditions, the effects observed on primary functions may be due to the consequence of phenotypic qualities and the physiological and metabolic plasticity that each species have. In *Drosophila* an increase in temperature causes the energy stored in the form of fat in adipose tissue cells to be metabolized much faster and once the energy reserves are depleted, cells get damaged by apoptosis (i.e., programmed cell death) (Klepsatel et al., 2016). In our study, *A. ludens* and *A. obliqua* were the species that lived shorter periods at high temperatures, which may reflect a depletion of their adipose tissue reserves and cellular damage. Our results point to a division between the *fraterculus* (*A. ludens* and *A. obliqua*) and *serpentina* (*A. serpentina* and *A. striata*) groups in their resistance to survive extreme temperatures (Figure 2). Thus, identifying the biochemical and physiological mechanisms behind such responses promises to be a fruitful endeavor.

We found that *A. ludens* and *A. obliqua* adults kept under experimental laboratory conditions, tolerated low temperatures of 5 and 10°C for longer periods than *A. striata* and *A. serpentina* (Figure 2; Table 1). Causes of cold injury include dehydration, osmolyte concentration, disturbance in homeostasis, oxidative stress, energy loss, protein dissociation and/or denaturation, and cell damage (Privalov, 1990; MacMillan and Sinclair, 2011; MacMillan et al., 2015a; MacMillan et al., 2015b; Koštál et al., 2016). There are several molecular mechanisms that insects exhibit in response to cold stress, including synthesis of cryoprotective molecules such as polyhydric alcohols (glycerol, sorbitol, mannitol, erythritol, and myo-inositol), sugars (glucose and trehalose) (Koštál et al., 2007; Doucet et al., 2009; Toxopeus et al., 2019) and aminoacids (arginine, asparagine, glutamine, and proline) (Michaud and Denlinger, 2007; MacMillan et al., 2016; Olsson et al., 2016). Other mechanisms include changes in the profile of membrane phospholipids (Enriquez and Colinet, 2019; Trenti et al., 2022), induction of antioxidant enzyme activities (Joanisse and Storey, 1996), and the gene expression induced by cold such as heat shock proteins (HSP: HSP22, HSP23, HSP26, HSP67, and HSP70Bbb, *etc.*), circadian rhythm and metabolism related genes (*Frost*, *smp-30, Starvin* and *hsr-omega*) (Sejerkilde et al., 2003; Sinclair et al., 2007; Colinet et al., 2010; Vesala et al., 2012; King and MacRae, 2015; MacMillan et al., 2016). The function of HSPs is dependent on the physiology of a particular insect and environmental conditions. In response to stress, small HSPs bind to denaturing proteins and prevent the irreversible protein aggregation, while ATP-dependent HSPs are focused on the protein refolding and/or degrading and restoration of homeostasis (Basha et al., 2012; Clare and Saibil, 2013; King and MacRae, 2015). Directed studies are needed to determine if the species of the *fraterculus* group studied here activate some of these mechanisms to tolerate cold temperatures for longer periods, and if the representatives of the *serpentina* group lack them.

The constant temperature of 15°C prevented egg hatch (Figure 5B). In places where seasonality is pronounced, *D. melanogaster* females inhibit egg production in cold temperatures activating an "ovarian diapause", characterized by the reduction of vitellogenin in the eggs and the absence of ovarian development (Denlinger, 2002; Williams and Sokolowski, 2009). We note that the absence of egg hatch observed at 15°C in *A. ludens*, does not necessarily imply that females were infertile as it is known that a short exposure to optimal temperatures after a cold shock can allow the recovery of insects from possible injuries caused by extreme cold (Colinet et al., 2015).

On the other hand, *A. striata* and *A. serpentina* were more tolerant to high temperatures than *A. ludens* and *A. obliqua* (Figure 2K; Table 1). Several studies have shown that tropical ectotherms, which are faced with almost permanent high temperatures, have a lower tolerance for heat than temperate ectotherms and tend to seek shelter or move to places that protect them from heat stress (Kearney et al., 2009; Sunday et al., 2014). In Mexico, *A. ludens* and *A. obliqua* are found from 0–2000 masl and 0–1,400 masl, respectively, a much wider altitudinal distribution range when compared to *A. striata* and *A. serpentina*, which occupy ranges between 0–1,200 masl (M.A, unpublished data). In a comparative study between *B. correcta* and *B. dorsalis*, two species with partially overlapping distributions in China, it was shown that *B. correcta* exhibited higher survival rates at 39–41°C, or after short exposures to 45°C than *A. dorsalis*. Consistent with this, HSP70 and HSP90 transcripts were identified in *B. correcta*, but not in *B. dorsalis* (Hu et al., 2014). HSP70 was also overexpressed after heat stress in *R. mendax* (Teixeira and Polavarapu, 2005), and both, HSP70 and HSP90, were involved in the heat response of *R. pomonella* (López-Martínez and Denlinger, 2008). Interestingly, differences between the sexes have been found. For example, Bauerfeind et al. (2018) found higher levels of HSP proteins in females than in males of the yellow dung flies (*Scathophaga stercoraria* (L); Diptera: Scathophagidae), but males performed better than females in response to extreme temperatures. Our results show that the mean lifespan of males in the field was

significantly longer than the one of females in the case of species of the *fraterculus* group (Figure 6). In the case of our laboratory studies, we found differences between females and males of *A. ludens* at 15°C and, in *A. ludens* and *A. striata* at 30°C (Table 1). At 15°C, *A. ludens* females lived more than males, and at 30°C in both *A. ludens* and *A. striata*, males lived more than females. Perhaps *A. ludens* females triggered a faster response to thermic stress *via* a more robust expression of HSP´s compared to males. This could explain the longer survival of *A. ludens* females at a constant temperature of 15°C. Under highly variable field conditions, *A. ludens* females lived for significantly shorter periods than males (independent of host origin) possibly due to a higher energetic and physiological cost in activating response mechanisms to thermal stress. Energy costs associated with tolerance to heat have been studied in *D. melanogaster* larvae. For example, transgenic flies with overexpression of HSP70 are more tolerant to higher temperatures but with the cost of reduced growth, survival, and egg hatch when compared to wild-type flies (Krebs and Feder, 1997). More recently, Moloń et al. (2020) documented an inverse relationship between metabolic rate and lifespan in the same fly species (also see Menail et al., 2022). In our case, *A. ludens* females are known to invest significantly in costly ovary development and oogenesis (Aluja et al., 2001) which added to the activation to heat stress response mechanisms, may explain why they lived for shorter periods than males.

In conclusion, among the most interesting findings the unexpected cold hardiness of *A. obliqua* stands out, a species found in very hot environments. But this species belongs to the same *fraterculus* species group where *A. ludens* is placed, the other species that proved better adapted to lower temperatures. In contrast, representatives of the *serpentina* species group withstood better extreme hot temperatures, which means that they may be better adapted to the rising temperatures related to global warming. In the field, we found significant differences in *A. ludens* between female and male survival, likely related to the metabolic cost of dealing with highly variable environmental conditions (differences of almost 30°C between the hottest and coldest temperatures were recorded) and ovary development/egg production. Our findings, of ecological nature, demand an in depth look into the physiological/molecular mechanisms behind the patterns observed, although we can rely on the vast literature on *Drosophila* and the few studies on tephritid flies we cite here to infer the types of metabolic processes at play as thermal responses trigger highly conserved metabolic routes in insects (González-Tokman et al., 2020). An area that definitively deserves closer attention is the possible role that bacteria play in aiding tephritid flies in dealing with thermal stress as recently Ayyasamy et al. (2021) identified various bacteria (e.g., *Acinetobacter*, *Brevibacillus*, *Bacillus*, *Enterobacter*, *Enterococcus*, *Pseudomonas* and *Staphylococcus*) associated with resistance to thermal stress in the tefritid fly *B. dorsalis*. Another topic worthy of investigation is the one related to the effect of temperature stress and insect immunity (Wojda, 2017), as pestiferous flies are mass reared and sometimes larvae experience high temperatures in their rearing medium caused by metabolic heat which could compromise their immune system and render them more prone to infections by pathogenic bacteria and fungi.

Data availability statement

The raw data supporting the conclusions of this article are available on request to the corresponding authors.

Author contributions

Design research: MA, LG, and AA-M; experimental procedures, RO-C, OV, EE-O, and LG; writing—original draft preparation: MA, LG, CP-V, IO-P, AA-M, and EE-O; writing—review and editing, MA, LG, CP-V, IO-P, AA-M, and EE-O; data base preparation: RO-C, EE-O, and OV; data analysis: LG, CP-V, IO-P, and EE-O; editing: MA, CP-V, and LG; project administration, MA, LG, and AA-M; supervising and funding resources, MA. All authors have read and agreed to the published version of the manuscript.

Funding

This study was funded by the Mexican Campaña Nacional Contra Moscas de la Fruta (Convenio SAGARPA (currently SADER)—CONACOFI—INECOL) through projects 10545-2015, 10601-2016, 41011-2017, 41012-2018, 41013-2019, 80124-2020 and 80147-2021 and from the Fondo Mixto (FOMIX- CONACyT)—Gobierno del Estado de Veracruz de Ignacio de la Llave (Grant FOMIX-VER-2017-01-292397) both awarded to MA. Additional funds were provided by the Instituto de Ecología, A. C. (INECOL) in the form of salaries to scientists and technicians and facilities/equipment and their maintenance.

Acknowledgments

We thank Emilio Acosta, Gabriel Hernández, Lizbeth González, Adriana Santos, Juan Carlos Conde and Gregorio Juárez for technical assistance. We also thank the farmers in Apazapan, Tolome and Actopan Veracruz for allowing us to work in their orchads. Finally, we gratefully acknowledge the contribution of three anonymous referees for their constructive criticisms and suggestions for improvement that allowed to produce a better quality final product.

Conflict of interest

The authors declare that the research was conducted in the absence of any commercial or financial relationships that could be construed as a potential conflict of interest.

Publisher's note

All claims expressed in this article are solely those of the authors and do not necessarily represent those of their affiliated organizations, or those of the publisher, the editors and the reviewers. Any product that may be evaluated in this article, or claim that may be made by its manufacturer, is not guaranteed or endorsed by the publisher.

Supplementary material

The Supplementary Material for this article can be found online at: https://www.frontiersin.org/articles/10.3389/fphys.2022.991923/full#supplementary-material

References

Adly, D. (2016). Thermal requirements of the peach fruit fly, *Bactrocera zonata* (Saunders) (Diptera: Tephritidae), and its exotic parasitoid species *Aganaspis daci* (Weld) (Hymenoptera: Eucoilidae). *Egypt. Acad. J. Biol. Sci. A Entomology* 9, 89–96. doi:10.21608/eajbsa.2016.12848

Aluja, M. (1994). Bionomics and management of *Anastrepha*. *Annu. Rev. Entomol.* 3, 155–178. doi:10.1146/annurev.en.39.010194.001103

Aluja, M., Birke, A., Ceymann, M., Guillén, L., Arrigoni, E., Baumgartner, D., et al. (2014). Agroecosystem resilience to an invasive insect species that could expand its geographical range in response to global climate change. *Agric. Ecosyst. Environ.* 186, 54–63. doi:10.1016/j.agee.2014.01.017

Aluja, M., and Birke, A. (1993). Habitat use by *Anastrepha obliqua* (Diptera: Tephritidae) in a mixed mango and tropical plum orchard. *Ann. Entomol. Soc. Am.* 86, 799–812. doi:10.1093/aesa/86.6.799

Aluja, M., Díaz-Fleischer, F., Arredondo, J., Valle-Mora, J., and Rull, J. (2010). Effect of cold storage on larval and adult *Anastrepha ludens* (Diptera: Tephritidae) viability in commercially ripe, artificially infested *Persea americana* 'Hass'. *J. Econ. Entomol.* 103, 2000–2008. doi:10.1603/ec09425

Aluja, M., Díaz-Fleischer, F., Papaj, D. R., Lagunes, G., and Sivinski, J. (2001). Effects of age, diet, female density, and the host resource on egg load in *Anastrepha ludens* and *Anastrepha obliqua* (Diptera: Tephritidae). *J. Insect Physiol.* 47, 975–988. doi:10.1016/s0022-1910(01)00072-5

Aluja, M., Guillén, L., Rull, J., Höhn, H., Frey, J., Graf, B., et al. (2011). Is the alpine divide becoming more permeable to biological invasions? – insights on the invasion and establishment of the walnut husk fly, *Rhagoletis completa* (Diptera: Tephritidae) in Switzerland. *Bull. Entomol. Res.* 101, 451–465. doi:10.1017/S0007485311000010

Aluja, M., and Mangan, R. L. (2008). Fruit fly (Diptera: Tephritidae) host status determination: Critical conceptual, methodological, and regulatory considerations. *Annu. Rev. Entomol.* 53, 473–502. doi:10.1146/annurev.ento.53.103106.093350

Aluja, M., Sivinski, J., Rull, J., and Hodgson, P. J. (2005). Behavior and predation of fruit fly larvae (*Anastrepha* spp.) (Diptera: Tephritidae) after exiting fruit in four types of habitats in tropical Veracruz, Mexico. *Environ. Entomol.* 34, 1507–1516. doi:10.1603/0046-225x-34.6.1507

Anderson, M. J., and Whitcomb, P. J. (2005). *RSM simplified: Optimizing processes using response surface methods for design of experiments*. Boca Raton, FL: CRC Press.

Ayyasamy, A., Kempraj, V., and Pagadala Damodaram, K. J. (2021). Endosymbiotic bacteria aid to overcome temperature induced stress in the oriental fruit fly, *Bactrocera dorsalis*. *Microb. Ecol.* 82, 783–792. doi:10.1007/s00248-021-01682-2

Basha, E., O'Neill, H., and Vierling, E. (2012). Small heat shock proteins and α-crystallins: Dynamic proteins with flexible functions. *Trends Biochem. Sci.* 37, 106–117. doi:10.1016/j.tibs.2011.11.005

Bauerfeind, S. S., Sorensen, J. G., Loeschcke, V., Berger, D., Broder, E. D., Geiger, M., et al. (2018). Geographic variation in responses of European yellow dung flies to thermal stress. *J. Therm. Biol.* 73, 41–49. doi:10.1016/j.jtherbio.2018.01.002

Bayoumy, M. H., Michaud, J. P., Badr, F. A. A., and Ghanim, N. M. (2021). Validation of degree-day models for predicting the emergence of two fruit flies (Diptera: Tephritidae) in northeast Egypt. *Insect Sci.* 28, 153–164. doi:10.1111/1744-7917.12750

Begert, M., Stöckli, R., and Croci-Maspoli, M. (2019). Climate evolution in Switzerland – preindustrial reference period and change since 1864 on the basis of temperature monitoring. *Tech. Rep. MeteoSwiss* 274, 23.

Birke, A., Guillén, L., Midgarden, D., and Aluja, M. (2013). "Fruit flies, *Anastrepha ludens* (Loew), *A. obliqua* (Macquart) and *A. grandis* (Macquart) (Diptera: Tephritidae): Three pestiferous tropical fruit flies that could potentially expand their range to temperate areas," in *Potential invasive pests*. Editor J. E. Peña (Wall Ingford, UK: CAB International), 192–213.

Bolzan, A., Nava, D. E., Smaniotto, G., Valgas, R. A., and Garcia, F. R. M. (2017). Development of *Anastrepha grandis* (Diptera: Tephritidae) under constant temperatures and field validation of a laboratory model for temperature requirements. *Crop Prot.* 100, 38–44. doi:10.1016/j.cropro.2017.06.001

Boullis, A., Detrain, C., Francis, F., and Verheggen, F. J. (2016). Will climate change affect insect pheromonal communication? *Curr. Opin. Insect Sci.* 17, 87–91. doi:10.1016/j.cois.2016.08.006

Bravin, E. (2013). *Apple production in Switzerland*. Switzerland: Federal Department of Economy, Education and Research of Switzerland. Retrived from: http://www.agribenchmark.org/fileadmin/Dateiablage/B-Horticulture/CountryInformation_Apple/Apple_Switzerland.pdf.

Brooks, A., Lithgow, G., and Johnson, T. E. (1994). Mortality rates in a genetically heterogeneous population of *Caenorhabditis elegans*. *Science* 263, 668–671. doi:10.1126/science.8303273

Byrne, M. P., and O'Gorman, P. A. (2016). Understanding decreases in land relative humidity with global warming: Conceptual model and GCM simulations. *J. Clim.* 29, 9045–9061. doi:10.1175/jcli-d-16-0351.1

Carnicer, J., Stefanescu, C., Vives-Ingla, M., López, C., Cortizas, S., Wheat, C., et al. (2018). Phenotypic biomarkers of climatic impacts on declining insect populations: A key role for decadal drought, thermal buffering and amplification effects and host plant dynamics. *J. Anim. Ecol.* 88, 376–391. doi:10.1111/1365-2656.12933

Chang, X.-N., Gao, H.-J., Chen, F.-J., and Zhai, B.-P. (2008). Effects of environmental moisture and precipitation on insects: A review. *Chin. J. Ecol.* 27, 619–625.

Chapman, R. R. (1998). *The insects: Structure and function*. 4th Ed. UK: Cambridge University Press, 770.

Chung, H., and Carroll, S. B. (2015). Wax, sex and the origin of species: Dual roles of insect cuticular hydrocarbons in adaptation and mating. *BioEssays* 37, 822–830. doi:10.1002/bies.201500014

Clare, D. K., and Saibil, H. R. (2013). ATP-driven molecular chaperone machines. *Biopolymers* 99, 846–859. doi:10.1002/bip.22361

Colinet, H., Lee, S. F., and Hoffmann, A. (2010). Knocking down expression of Hsp22 and Hsp23 by RNA interference affects recovery from chill coma in *Drosophila melanogaster*. *J. Exp. Biol.* 213, 4146–4150. doi:10.1242/jeb.051003

Colinet, H., Sinclair, B. J., Vernon, P., and Renault, D. (2015). Insects in fluctuating thermal environments. *Annu. Rev. Entomol.* 60, 123–140. doi:10.1146/annurev-ento-010814-021017

Darby, H. H., and Kapp, E. M. (1933). *Observations on the thermal death points of Anastrepha ludens* (Loew) *(No. 1488-2016-124445)*. Washington, DO: United States Department of Agriculture.

David, J. R., Araripe, L. O., Chakir, M., Legout, H., Lemos, B., Petavy, G., et al. (2005). Male sterility at extreme temperatures: A significant but neglected phenomenon for understanding *Drosophila* climatic adaptations. *J. Evol. Biol.* 18, 838–846. doi:10.1111/j.1420-9101.2005.00914.x

Denlinger, D. L. (2002). Regulation of diapause. *Annu. Rev. Entomol.* 47, 93–122. doi:10.1146/annurev.ento.47.091201.145137

Doucet, D., Walker, V. K., and Qin, W. (2009). The bugs that came in from the cold: Molecular adaptations to low temperatures in insects. *Cell. Mol. Life Sci.* 66, 1404–1418. doi:10.1007/s00018-009-8320-6

Drummond, F. A., and Collins, J. A. (2019). Dispersal from overwintering sites, action thresholds for blueberry maggot fly (Diptera: Tephritidae), and factors that can influence variation in predicted fruit infestation levels in maine wild blueberry: Part I. *J. Econ. Entomol.* 113, 851–859.

Duyck, P. F., and Quilici, S. (2002). Survival and development of different life stages of three *Ceratitis* spp. (Diptera: Tephritidae) reared at five constant temperatures. *Bull. Entomol. Res.* 92, 461–469. doi:10.1079/ber2002188

Enriquez, T., and Colinet, H. (2019). Cold acclimation triggers lipidomic and metabolic adjustments in the spotted wing drosophila *Drosophila suzukii* (Matsumara). *Am. J. Physiol. Regul. Integr. Comp. Physiol.* 316, R751–R763. doi:10.1152/ajpregu.00370.2018

Fischer, K., Kolzow, N., Holtje, H., and Karl, I. (2011). Assay conditions in laboratory experiments: Is the use of constant rather than fluctuating temperatures justified when investigating temperature-induced plasticity? *Oecologia* 166, 23–33. doi:10.1007/s00442-011-1917-0

Flitters, N. E., and Messenger, P. S. (1965). *Effect of temperature and humidity on development and potential distribution of the Mexican fruit fly in the United States*. Washington D.C: USDA Tech., 36.

Fox, C. W., and Czesak, M. E. (2000). Evolutionary ecology of progeny size in arthropods. *Annu. Rev. Entomol.* 45, 341–369. doi:10.1146/annurev.ento.45.1.341

Genç, H., and Nation, J. L. (2008). Survival and development of *Bactrocera oleae* Gmelin (Diptera: Tephritidae) immature stages at four temperatures in the laboratory. *Afr. J. Biotechnol.* 7, 14. doi:10.5897/AJB08.395

González-Tokman, D., Córdoba-Aguilar, A., Dáttilo, W., Lira-Noriega, A., Sánchez-Guillén, R. A., and Villalobos, F. (2020). Insect responses to heat: Physiological mechanisms, evolution, and ecological implications in a warming world. *Biol. Rev.* 95, 802–821. doi:10.1111/brv.12588

Guillén, L., Monribot-Villanueva, J. L., Guerrero-Analco, J. A., Ortega, R., Altúzar-Molina, A., Mena, V., et al. (2022). Influence of sunlight incidence and fruit chemical features on oviposition site selection in mango by *Anastrepha obliqua*: Implications for management. *Insects* 13, 141. doi:10.3390/insects13020141

Gutiérrez Ruelas, J. M., Santiago Martínez, G., Villaseñor Cortés, A., and Hernández López, F. (2013). *Los Programas de Moscas de la Fruta en México: su historia reciente*. Mexico: IICA.

Hagstrum, D. W., and Milliken, G. A. (1991). Modeling differences in insect developmental times between constant and fluctuating temperatures. *Ann. Entomol. Soc. Am.* 84, 369–379. doi:10.1093/aesa/84.4.369

Hallman, G. J. (1999). Lethality of cold to third instars, pupae, and pharate adults of the Mexican fruit fly (Diptera: Tephritidae). *J. Econ. Entomol.* 92, 480–484. doi:10.1093/jee/92.2.480

Hallman, G. J., Wang, S., and Tang, J. (2005). Reaction orders for thermal mortality of third instars of Mexican fruit fly (Diptera: Tephritidae). *J. Econ. Entomol.* 98, 1905–1910. doi:10.1603/0022-0493-98.6.1905

Hernández, E., Escobar, A., Bravo, B., and Montoya, P. (2010). Chilled packing systems for fruit flies (Diptera: Tephritidae) in the sterile insect technique. *Neotrop. Entomol.* 39, 601–607. doi:10.1590/s1519-566x2010000400021

Hollander, M., and Wolfe, D. A. (1999). *Nonparametric statistical methods*. New York, USA: J. Wiley.

Hu, J. T., Chen, B., and Li, Z. H. (2014). Thermal plasticity is related to the hardening response of heat shock protein expression in two *Bactrocera* fruit flies. *J. Insect Physiol.* 67, 105–113. doi:10.1016/j.jinsphys.2014.06.009

Huang, Y., Gu, X., Peng, X., Tao, M., Chen, G., and Zhang, X. (2020). Effect of short-term high-temperatures on the growth, development and reproduction in the fruit fly, *Bactrocera tau* (Diptera: Tephritidae). *Sci. Rep.* 10, 6418. doi:10.1038/s41598-020-63502-w

Jaworski, T., and Hilszczański, J. (2013). The effect of temperature and humidity changes on insects development their impact on forest ecosystems in the expected climate change. *For. Res. Pap.* 74, 345–355. doi:10.2478/frp-2013-0033

Jiang, R., Gan, T. Y., Xie, J., Wang, N., and Kuo, Ch-Ch. (2015). Historical and potential changes of precipitation and temperature of alberta subjected to climate change impact: 1900–2100. *Theor. Appl. Climatol.* 127, 725–739. doi:10.1007/s00704-015-1664-y

Joanisse, D., and Storey, K. (1996). Oxidative stress and antioxidants in overwintering larvae of cold-hardy goldenrod gall insects. *J. Exp. Biol.* 199, 1483–1491. doi:10.1242/jeb.199.7.1483

Kasana, A., and AliNiazee, M. T. (1994). Effect of constant temperatures on development of the walnut husk fly, *Rhagoletis completa*. *Entomol. Exp. Appl.* 73, 247–254. doi:10.1111/j.1570-7458.1994.tb01862.x

Kearney, M., Shine, R., and Porter, W. P. (2009). The potential for behavioral thermoregulation to buffer "cold-blooded" animals against climate warming. *Proc. Natl. Acad. Sci. U. S. A.* 106, 3835–3840. doi:10.1073/pnas.0808913106

Ketola, T., and Saarinen, K. (2015). Experimental evolution in fluctuating environments: Tolerance measurements at constant temperatures incorrectly predict the ability to tolerate fluctuating temperatures. *J. Evol. Biol.* 28, 800–806. doi:10.1111/jeb.12606

King, A. M., and MacRae, T. H. (2015). Insect heat shock proteins during stress and diapause. *Annu. Rev. Entomol.* 60, 59–75. doi:10.1146/annurev-ento-011613-162107

Klepsatel, P., Gáliková, M., Xu, Y., and Kühnlein, R. P. (2016). Thermal stress depletes energy reserves in *Drosophila*. *Sci. Rep.* 6, 33667. doi:10.1038/srep33667

Koštál, V., Korbelová, J., Štětina, T., Poupardin, R., Colinet, H., Zahradníčková, H., et al. (2016). Physiological basis for low-temperature survival and storage of quiescent larvae of the fruit fly *Drosophila melanogaster*. *Sci. Rep.* 6, 32346–32411. doi:10.1038/srep32346

Koštál, V., Zahradnícková, H., Simek, P., and Zeleny´, J. (2007). Multiple component system of sugars and polyols in the overwintering spruce bark beetle, *Ips typographus*. *J. Insect Physiol.* 53, 580–586. doi:10.1016/j.jinsphys.2007.02.009

Krebs, R. A., and Feder, M. E. (1997). Deleterious consequences of Hsp70 overexpression in *Drosophila melanogaster* larvae. *Cell Stress Chaperones* 2, 60–71. doi:10.1379/1466-1268(1997)002<0060:dcohoi>2.3.co;2

Lee, R. E. (1991). "Principles of insect low temperature tolerance," in *Insects at low temperature*. Editors R. E. Lee, Jr. and D. L. Denlinger (New York: Chapman & Hall), 17–46.

Leyva-Vazquez, J. L. (1988). Temperatura umbral y unidades calor requeridas por los estados inmaduros de *Anastrepha ludens* (Loew) (Diptera: Tephritidae). *Folia Entomol. Mex.* 74, 189–196.

Lisbôa, H., Grutzmacher, A. D., Wrege, M. S., Garcia, F. R. M., and Nava, D. E. (2020). Impact of global warming on the distribution of *Anastrepha grandis* (Diptera: Tephritidae) in Brazil. *Arq. Inst. Biol.* 87, e0882018. doi:10.1590/1808-1657000882018

Liu, X., and Ye, H. (2009). Effect of temperature on development and survival of *Bactrocera correcta* (Diptera: Tephritidae). *Sci. Res. Essays* 4, 467–472.

López-Martínez, G., and Denlinger, D. L. (2008). Regulation of heat shock proteins in the apple maggot *Rhagoletis pomonella* during hot summer days and overwintering diapause. *Physiol. Entomol.* 33, 346–352. doi:10.1111/j.1365-3032.2008.00639.x

MacMillan, H. A., Andersen, J. L., Davies, S. A., and Overgaard, J. (2015a). The capacity to maintain ion and water homeostasis underlies interspecific variation in *Drosophila* cold tolerance. *Sci. Rep.* 5, 18607. doi:10.1038/srep18607

MacMillan, H. A., Ferguson, L. V., Nicolai, A., Donini, A., Staples, J. F., and Sinclair, B. J. (2015b). Parallel ionoregulatory adjustments underlie phenotypic plasticity and evolution of *Drosophila* cold tolerance. *J. Exp. Biol.* 218, 423–432. doi:10.1242/jeb.115790

MacMillan, H. A., Knee, J. M., Dennis, A. B., Udaka, H., Marshall, K. E., Merritt, T. J., et al. (2016). Cold acclimation wholly reorganizes the *Drosophila melanogaster* transcriptome and metabolome. *Sci. Rep.* 6, 28999–29014. doi:10.1038/srep28999

MacMillan, H. A., and Sinclair, B. J. (2011). The role of the gut in insect chilling injury: Cold-induced disruption of osmoregulation in the fall field cricket, *Gryllus pennsylvanicus*. *J. Exp. Biol.* 214, 726–734. doi:10.1242/jeb.051540

Manenti, T., Kjærsgaard, A., Schou, T. M., Pertoldi, C., Moghadam, N. N., and Loeschcke, V. (2021). Responses to developmental temperature fluctuation in life history traits of five *Drosophila* species (Diptera: Drosophilidae) from different thermal niches. *Insects* 12, 925. doi:10.3390/insects12100925

McPhail, M., and Bliss, C. I. (1933). *Observations on the Mexican fruit fly and some related species in Cuernavaca, Mexico, in 1928 and 1929*. Washington D.C: U.S. Dept. of Agriculture, 24.

Meats, A. (1976). Thresholds for cold-torpor and cold-survival in the Queensland fruit fly, and predictability of rates of change in survival threshold. *J. Insect Physiol.* 22, 1505–1509.

Meats, A. (1984). Thermal constraints to successful development of the Queensland fruit fly in regimes of constant and fluctuating temperature. *Entomol. Exp. Appl.* 36, 55–59.

Meats, A. (1989). "Abiotic mortality factors: temperature," in *Fruit Flies: Biology, Natural Enemies and Control*. Editors A. S. Robinson and G. H. S. Hooper (Amsterdam: Elsevier), 231–234.

Meats, A., and Fay, F. A. C. (2000). Distribution of mating frequency among males of the Queensland fruit fly, *'Bactrocera tryoni'* (Froggatt), in relation to temperature, acclimation and chance. *Gen. Appl. Entomol.* 29, 27–30.

Menail, H. A., Cormier, S. B., Ben Youssef, M., Jorgensen, L. B., Vickruck, J. L., Morin, P., Jr., et al. (2022). Flexible thermal sensitivity of mitochondrial oxygen consumption and substrate oxidation in flying insect species. *Front. Physiol.* 13, 897174. doi:10.3389/fphys.2022.897174

Mengual, M., Kerr, P., Norrbom, A. L., Barr, N. B., Lewis, M. L., Stapelfeldt, A. M., et al. (2017). Phylogenetic relationships of the tribe Toxotrypanini (Diptera: Tephritidae) based on molecular characters. *Mol. Phylogenet. Evol.* 113, 84–112. doi:10.1016/j.ympev.2017.05.011

Menzel, F., Zumbusch, M., and Feldmeyer, B. (2018). How ants acclimate: Impact of climatic conditions on the cuticular hydrocarbon profile. *Funct. Ecol.* 32, 657–666. doi:10.1111/1365-2435.13008

Messenger, P. S., and Flitters, N. E. (1957). Bioclimatic studies of the Mexican fruit fly. *Calif. Avocado Soc. Yearb.* 41, 119–127.

Michaud, M. R., and Denlinger, D. L. (2007). Shifts in the carbohydrate, polyol, and amino acid pools during rapid cold hardening and diapause-associated cold-hardening in flesh flies (*Sarcophaga crassipalpis*): A metabolomic comparison. *J. Comp. Physiol. B* 177, 753–763. doi:10.1007/s00360-007-0172-5

Moloń, M., Dampc, J., Kula-Maximenko, M., Zebrowski, J., Moloń, A., Dobler, R., et al. (2020). Effects of temperature on lifespan of *Drosophila melanogaster* from different genetic backgrounds: Links between metabolic rate and longevity. *Insects* 11, E470. doi:10.3390/insects11080470

Motswagole, R., Gotcha, N., and Nyamukondiwa, C. (2019). Thermal biology and seasonal population abundance of *Bactrocera dorsalis* Hendel (Diptera: Tephritidae): Implications on pest management. *Int. J. Insect Sci.* 11, 1179543319863417. doi:10.1177/1179543319863417

NASA (2022). *POWER project CERES/MERRA2 native resolution monthly and annual on 2022/07/01, national Aeronautics and Space administration (NASA) Langley research center (LaRC) prediction of worldwide energy resource (POWER) project funded through the NASA Earth science/applied science program.*

Norrbom, A. L. (2002). A revision of the *Anastrepha serpentina* species group (Diptera: Tephritidae). *Proc. Entomol. Soc. Wash.* 104, 390–436.

Norrbom, A. L. (2004). *Host plant database for Anastrepha and Toxotrypana (Diptera: Tephritidae: Toxotrypanini).* Diptera Data Dissemination Disk.

Novoseltsev, V. N., and Novoseltseva, J. A. (2013). Why is individual reproduction in *Drosophila* flies stochastic? *Front. Genet.* 3, 324. doi:10.3389/fgene.2012.00324

Nyamukondiwa, C., and Terblanche, J. S. (2009). Thermal tolerance in adult Mediterranean and Natal fruit flies (*Ceratitis capitata* and *Ceratitis rosa*): Effects of age, gender and feeding status. *J. Therm. Biol.* 34, 406–414. doi:10.1016/j.jtherbio.2009.09.002

Olsson, T., MacMillan, H. A., Nyberg, N., Staerk, D., Malmendal, A., and Overgaard, J. (2016). Hemolymph metabolites and osmolality are tightly linked to cold tolerance of *Drosophila* species: A comprehensive study. *J. Exp. Biol.* 219, 2504–2513. doi:10.1242/jeb.140152

Parmesan, C. (2006). Ecological and evolutionary responses to recent climate change. *Annu. Rev. Ecol. Evol. Syst.* 37, 637–669. doi:10.1146/annurev.ecolsys.37.091305.110100

Pascacio-Villafán, C., Williams, T., Birke, A., and Aluja, M. (2016). Nutritional and non-nutritional food components modulate phenotypic variation but not physiological trade-offs in an insect. *Sci. Rep.* 6, 29413. doi:10.1038/srep29413

Perez, R., and Aron, S. (2020). Adaptations to thermal stress in social insects: Recent advances and future directions. *Biol. Rev. Cambridge Philosophic Soc.* 95, 1535–1553. doi:10.1111/brv.12628

Privalov, P. (1990). Cold denaturation of proteins. *Crit. Rev. Biochem. Mol. Biol.* 25, 281–305. doi:10.3109/10409239009090612

Pucci, C., Porcina, A., and Salmistraro, D. (1981). Effects of temperature on the death rate of larvae, pupation, and activities of parasites for *Dacus oleae* (Gmel.). *Frustula Entomol.* 16, 143–155.

Qin, Y., Paini, D. R., Wang, C., Fang, Y., and Li, Z. (2015). Global establishment risk of economically important fruit fly species (Tephritidae). *PLoS One* 10, e0116424. doi:10.1371/journal.pone.0116424

Rashmi, M. A., Verghese, A., Rami Reddy, P. V., Kandakoor, S., and Chakravarthy, A. K. (2020). Effect of climate change on biology of oriental fruit fly, *Bactrocera dorsalis* Hendel (Diptera: Tephritidae). *J. Entomol. Zool.* 8, 935–940.

Ratajczak, M. G. (2020). "Frequency and trends in cold and warm spells in Norway in relation to large-scale atmospheric circulation," (Norway: University Of OSLO). (Master's thesis).

Reissig, W. H., Barnard, J., Weires, R. W., Glass, E. H., and Dean, R. W. (1979). Prediction of apple maggot Fly emergence from thermal unit accumulation. *Environ. Entomol.* 8, 51–54. doi:10.1093/ee/8.1.51

Richter, K., Haslbeck, M., and Buchner, J. (2010). The heat shock response: Life on the verge of death. *Mol. Cell* 40, 253–266. doi:10.1016/j.molcel.2010.10.006

Ruiz-Montoya, L., Vallejo, R. V., Haymer, D., and Liedo, P. (2020). Genetic and ecological relationships of *Anastrepha ludens* (Diptera: Tephritidae) populations in southern Mexico. *Insects* 11, 815. doi:10.3390/insects11110815

Rull, J., Tadeo, E., Lasa, R., and Aluja, M. (2016). The effect of winter length on survival and duration of dormancy of four sympatric species of *Rhagoletis* exploiting plants with different fruiting phenology. *Bull. Entomol. Res.* 106, 818–826. doi:10.1017/S0007485316000717

Samayoa, A. C., Choi, K. S., Wang, Y. S., Hwang, S. Y., Huang, Y. B., and Ahn, J. J. (2018). Thermal effects on the development of *Bactrocera dorsalis* (Hendel) (Diptera: Tephritidae) and model validation in Taiwan. *Phytoparasitica* 46, 365–376. doi:10.1007/s12600-018-0674-6

Schneider, L., Comte, V., and Rebetez, M. (2021). Increasingly favourable winter temperature conditions for major crop and forest insect pest species in Switzerland. *Agric. For. Meteorol.* 298, 108315. doi:10.1016/j.agrformet.2020.108315

Sejerkilde, M., Sørensen, J. G., and Loeschcke, V. (2003). Effects of cold-and heat hardening on thermal resistance in *Drosophila melanogaster*. *J. Insect Physiol.* 49, 719–726. doi:10.1016/s0022-1910(03)00095-7

Sentis, A., Ramon-Portugal, F., Brodeur, J., and Hemptinne, J. L. (2015). The smell of change: Warming affects species interactions mediated by chemical information. *Glob. Chang. Biol.* 21, 3586–3594. doi:10.1111/gcb.12932

Shaw, J. G., and Starr, D. F. (1946). Development of the immature stages of *Anastrepha serpentina* in relation to temperature. *J. Agric. Res.* 72, 265.

Silva, M. A., Bezerra-Silva, G. C. D., Vilanova, E. S., Cunha, M. G., and Santos, M. G. S. (2019). Establishment probability of *Anastrepha grandis* and *Zeugodacus cucurbitae* (Diptera: Tephritidae) in Brazilian semiarid based on thermal requirements. *Neotrop. Entomol.* 48, 853–862. doi:10.1007/s13744-019-00701-9

Sinclair, B. J., Gibbs, A. G., and Roberts, S. P. (2007). Gene transcription during exposure to, and recovery from, cold and desiccation stress in *Drosophila melanogaster*. *Insect Mol. Biol.* 16, 435–443. doi:10.1111/j.1365-2583.2007.00739.x

Sivinski, J., Holler, T., Pereira, R., and Romero, M. (2007). The thermal environment of immature Caribbean fruit flies, *Anastrepha suspensa* Diptera: Tephritidae. *Fla. Entomol.* 90, 347–357. doi:10.1653/0015-4040(2007)90[347:tteoic]2.0.co;2

Smith-Caldas, M. R. B., McPheron, B. A., Silva, J. G., and Zucchi, R. A. (2001). Phylogenetic relationships among species of the *fraterculus* group (*Anastrepha*: Diptera: Tephritidae) inferred from DNA sequences of mitochondrial cytochrome oxidase I. *Neotrop. Entomol.* 30, 565–573. doi:10.1590/s1519-566x2001000400009

Stat Soft, Inc. (2011). STATISTICA (data analysis software system), version 10, Available at: www.statsoft.com.

Sunday, J. M., Bates, A. E., Kearney, M. R., Colwell, R. K., Dulvy, N. K., Longino, J. T., et al. (2014). Thermal-safety margins and the necessity of thermoregulatory behavior across latitude and elevation. *Proc. Natl. Acad. Sci. U. S. A.* 111, 5610–5615. doi:10.1073/pnas.1316145111

Teixeira, L. A. F., and Polavarapu, S. (2005). Evidence of a heat-induced quiescence during pupal development in *Rhagoletis mendax* (Diptera: Tephritidae). *Environ. Entomol.* 34, 292–297. doi:10.1603/0046-225x-34.2.292

Teixeira, C. M., Peter Krüger, A., Nava, D. E., and Mello Garcia, F. R. (2021). Potential global distribution of the south American cucurbit fruit fly *Anastrepha grandis* (Diptera: Tephritidae). *Crop Prot.* 145, 105647. doi:10.1016/j.cropro.2021.105647

Teixeira, C. M., Peter Krüger, A., Nava, D. E., and Mello Garcia, F. R. (2022). Global potential distribution of *Anastrepha grandis* (Diptera, Tephritidae) under climate change scenarios. *Crop Prot.* 151, 105836. doi:10.1016/j.cropro.2021.105836

Telles-Romero, R., Toledo, J., Hernández, E., Quintero-Fong, J. L., and Cruz-López, L. (2011). Effect of temperature on pupa development and sexual maturity of laboratory *Anastrepha obliqua* adults. *Bull. Entomol. Res.* 101, 565–571. doi:10.1017/S0007485311000150

Thomas, D. B. (1997). Degree-day accumulations and seasonal duration of the pre-imaginal stages of the Mexican fruit fly (Diptera: Tephritidae). *Fla. Entomol.* 80, 71–79. doi:10.2307/3495978

Toxopeus, J., Koštál, V., and Sinclair, B. J. (2019). Evidence for non-colligative function of small cryoprotectants in a freeze-tolerant insect. *Proc. R. Soc. B-Biol. Sci.* 286, 20190050. doi:10.1098/rspb.2019.0050

Toxopeus, J., and Sinclair, B. J. (2018). Mechanisms underlying insect freeze tolerance. *Biol. Rev. Cambridge Philosophic Soc.* 93, 1891–1914. doi:10.1111/brv.12425

Trenberth, K. E. (2011). Changes in precipitation with climate change. *Clim. Res.* 47, 123–138. doi:10.3354/cr00953

Trenti, F., Sandron, T., Guella, G., and Lencioni, V. (2022). Insect cold-tolerance and lipidome: Membrane lipid composition of two chironomid species differently adapted to cold. *Cryobiology* 106, 84–90. doi:10.1016/j.cryobiol.2022.03.004

Vesala, L., Salminen, T. S., Laiho, A., Hoikkala, A., and Kankare, M. (2012). Cold tolerance and cold-induced modulation of gene expression in two *Drosophila virilis* group species with different distributions. *Insect Mol. Biol.* 21, 107–118. doi:10.1111/j.1365-2583.2011.01119.x

Wagner, T. L., Wu, H. I., Sharpe, P. J., Schoolfield, R. M., and Coulson, R. N. (1984). Modeling insect development rates: A literature review and application of a biophysical model. *Ann. Entomol. Soc. Am.* 77, 208–220. doi:10.1093/aesa/77.2.208

Walsh, B. S., Parratt, S. R., Hoffmann, A. A., Atkinson, D., Snook, R. R., Bretman, A., et al. (2019). The impact of climate change on fertility. *Trends Ecol. Evol.* 34, 249–259. doi:10.1016/j.tree.2018.12.002

Wang, G., and Schimel, D. (2003). Climate change, climate modes, and climate impacts. *Annu. Rev. Environ. Resour.* 28, 1–28. doi:10.1146/annurev.energy.28.050302.105444

Wang, X. G., Johnson, M. W., Daane, K. M., and Nadel, H. (2009). High summer temperatures affect the survival and reproduction of olive fruit fly (Diptera: Tephritidae). *Environ. Entomol.* 38, 1496–1504. doi:10.1603/022.038.0518

Wang, X., Levy, K., Son, Y., Johnson, M. W., and Daane, K. M. (2012). Comparison of the thermal performance between a population of the olive fruit fly and its co-adapted parasitoids. *Biol. Control* 60, 247–254. doi:10.1016/j.biocontrol.2011.11.012

Weng, C., Fu, Y., Jiang, H., Zhuang, S., and Li, H. (2015). Binding interaction between a queen pheromone component HOB and pheromone binding protein ASP1 of *Apis cerana*. *Int. J. Biol. Macromol.* 72, 430–436. doi:10.1016/j.ijbiomac.2014.08.046

Williams, K. D., and Sokolowski, M. B. (2009). Evolution: How fruit flies adapt to seasonal stresses. *Curr. Biol.* 19, R63–R64. doi:10.1016/j.cub.2008.11.035

Wojda, I. (2017). Temperature stress and insect immunity. *J. Therm. Biol.* 68, 96–103. doi:10.1016/j.jtherbio.2016.12.002

Xu, L., Zhou, C., Xiao, Y., Zhang, P., Tang, Y., and Xu, Y. (2012). Insect oviposition plasticity in response to host availability: The case of the tephritid fruit fly *Bactrocera dorsalis*. *Ecol. Entomol.* 37, 446–452. doi:10.1111/j.1365-2311.2012.01383.x

Yan, Z., Jones, P. D., Davies, T. D., Moberg, A., Bergström, H., Camuffo, D., et al. (2002). "Trends of extreme temperatures in Europe and China based on daily observations," in *Improved understanding of past climatic variability from early daily European instrumental sources* (Dordrecht: Springer), 355–392.

Yu, M., Ma, S., and Zhu, C. (2022). The alternating change of cold and warm extremes over North Asia during winter 2020/21: Effect of the annual cycle anomaly. *Geophys. Res. Lett.* 49, e2021GL097233. doi:10.1029/2021gl097233

frontiers | Frontiers in Physiology

TYPE Original Research
PUBLISHED 23 November 2022
DOI 10.3389/fphys.2022.1024136

OPEN ACCESS

EDITED BY
Pankaj Kumar Tyagi,
Noida Institute of Engineering and Technology (NIET), India

REVIEWED BY
Arvind Arya,
Noida Institute of Engineering and Technology (NIET), India
Tianbo Ding,
Qingdao Agricultural University, China

*CORRESPONDENCE
Chang-Zhong Liu,
liuchzh@gsau.edu.cn

SPECIALTY SECTION
This article was submitted to Invertebrate Physiology, a section of the journal Frontiers in Physiology

RECEIVED 21 August 2022
ACCEPTED 02 November 2022
PUBLISHED 23 November 2022

CITATION
Li C, Ul Haq I, Khurshid A, Tao Y, Quandahor P, Zhou J-J and Liu C-Z (2022), Effects of abiotic stresses on the expression of chitinase-like genes in *Acyrthosiphon pisum*. *Front. Physiol.* 13:1024136. doi: 10.3389/fphys.2022.1024136

Effects of abiotic stresses on the expression of chitinase-like genes in *Acyrthosiphon pisum*

Chunchun Li[1], Inzamam Ul Haq[1], Aroosa Khurshid[1], Yan Tao[1], Peter Quandahor[1,2], Jing-Jiang Zhou[1,3] and Chang-Zhong Liu[1]*

[1]Biocontrol Engineering Laboratory of Crop Diseases and Pests of Gansu Province, College of Plant Protection, Gansu Agricultural University, Lanzhou, China, [2]CSIR-Savanna Agricultural Research Institute, Tamale, Ghana, [3]State Key Laboratory of Green Pesticide and Agricultural Bioengineering, Guizhou University, Guiyang, China

Insect chitinases play a crucial part to digest chitin in the exoskeleton during the molting process. However, research on insect chitinase related to the environmental stress response is very limited. This study was the first conducted to expression analysis of chitinase- related genes in *A. pisum* under abiotic stresses. Here, we identified five chitinase-like proteins (ApIDGF, ApCht3, ApCht7, ApCht10 and ApENGase), and clustered them into five groups (group II, III, V, X, and ENGase). Developmental expression analysis revealed that the five *A. pisum* chitinase-related genes were expressed at whole developmental stages with different relative expression patterns. When aphids were exposed to various abiotic stresses including temperature, insecticide and the stress 20-hydroxyecdysone (20E), all five chitinase genes were differentially expressed in *A. pisum*. The results showed that insecticide such as imidacloprid down-regulated the expression of these five Cht-related genes. Analysis of temperature stress of *A. pisum* chitinase suggested that *ApCht7* expression was high at 10°C, which demonstrates its important role in pea aphids under low temperature. Conversely, *ApCht10* was more active under high temperature stress, as it was significantly up-regulated at 30°C. Besides, 20E enhanced *ApCht3* and *ApCht10* expression in *A. pisum*, but reduced *ApCht7* expression. These findings provide basic information and insights for the study of the role of these genes under abiotic stress, which advances our knowledge in the management of pea aphids under multiple stresses.

KEYWORDS

***Acyrthosiphon pisum*, chitinase, expression profiles, phylogenetic analysis, 20hydroxyecdysone**

1 Introduction

Chitin is a polysaccharide of *N*-acetylglucosamine (GlcNAc) residues joined by -1, 4-glycosidic links (Merzendorfer, 2006). It is widely distributed in fungus, arthropod, nematodes, and marine organism (Rudall and Kenchington, 1973; Tharanathan and Kittur, 2003). Insect chitin is the major components of the exoskeletons. It also forms the trachea lining and the peritrophic matrix (PM), which protect insects from physical

abrasion, chemical erosion, and pathogenic invasion (Merzendorfer and Zimoch, 2003). The cuticular chitin is periodically degraded by the efficient chitin degradation system secreted by epithelial cells, due to the rigid cuticle structure that restricts the growth and development of the insect (Arakane and Muthukrishnan, 2010; Moussian, 2010; Arakane et al., 2012).

Chitinase is the main enzyme involved in the degradation of chitin. Insects chitinases are present mainly in the moulting fluid and midgut to enable periodic shedding of old exoskeleton and turnover of the midgut lining, which belongs to the 18 glycosyl hydrolases family and has the potential to degrade chitin and also controls the degradation of chitin into low-molecular-weight chitooligosaccharides (Kramer and Muthukrishnan, 1997; Chen et al., 2018). Commonly, according to sequence homology and phylogenetic analysis, insects chitinases have been classified into 11 groups with different relative expression levels (Arakane and Muthukrishnan, 2010). *Nilaparvata lugens* expressed *NlCht2*, *NlIDGF*, and *NlENGase* at all stages with slight periodical changes, especially in the adult female reproductive organs, whereas *NlCht4* was highly expressed only at the adult stage in the male reproductive organs (Xi et al., 2014). In *Bactrocera dorsalis*, expressions of *BdChts*, *BdIDGF4*, and *BdIDGF6* were up-regulated from eggs to adults, *BdCht5*, *BdCht8*, and *BdCht10* were also up-regulated at larvae-pupae metamorphosis stages, whereas *BdCht11* was low regulated at all developmental stages (Liu et al., 2018).

Insect chitinase genes play a major role in the physiological process of insect growth and development, as well as their adaptation to environmental stress. *B. dorsalis* showed high heat tolerance by up-regulating *IDGF* gene (Gu et al., 2019). At 45°C for 1 h, the expression of *BdIDGF4* in *B. dorsalis* was 3.15-fold higher, compared with the control, whereas the expressions of *BdIDGF1* and *BdIDGF2* were significantly up-regulated at 40°C (Gu et al., 2019). Insect steroid hormone and 20-hydroxyecdysone (20E) influence insect development and chitinase. In *Bombyx mori*, 20E induced the up-regulation of *BmCht5* at the larval–larval and larval-pupa stage (Zhang and Zheng, 2016). The expression of chitinase genes by 20E has been reported, especially in *Manduca sexta* (Kramer et al., 1993), *Tenebrio molitor* (Royer et al., 2002), *Choristoneura fumiferana* (Zheng et al., 2003), *Locusta migratoria manilensisand* (Li et al., 2015). Collectively, these effects change the expression of the chitinase gene, thus disrupting normal chitin metabolism, which may play crucial roles in insect defense against abiotic stresses.

The pea aphid, *Acyrthosiphon pisum* Harris, is one of the major agricultural pests, which inhibits crop production not just by directly feeding on plant phloem sap but also acts as a vector to various viral diseases (Ryalls et al., 2013). Globally, pea aphid management has become a major challenge, due to its small size, high fecundity, and plasticity. Consequently, wide range of synthetic insecticides is continuously used to control of pea aphids. This type of strategy is seriously increasing environmental contamination, insecticide resistance, and endangering the health of farm operators, animals, and food consumers. Therefore, there is an urgent need to find other effective and friendly methods to control *A. pisum*. Fortunately, the completion of *A. pisum* whole genome sequence has provided an opportunity to develop new strategies with molecular tools for aphid control (International Aphid Genomics Consortium, 2010). *In silico* screening of the entire genome of *A. pisum*, detected nine genes encoding putative chitinase-like proteins, including six enzymatically active chitinases, one imaginal disc growth factor, and one endo-beta-N-acetylglucosaminidase in 2010 (Nakabachi et al., 2010). Still, only a few were revised as Cht genes after the Gene Bank database update in 2017. Moreover, Nakabachi et al. (2010) demonstrated that the expression of four and two distinct chitinase-like genes of *A. pisum* to be highly up-regulated in the embryo and the midgut, respectively, suggesting specific roles in these pea aphid tissues. However, whether there are differences in chitinase gene expression in different developmental stages of *A. pisum* has not been reported. Based on previous research, we further accurately studied on the identification of chitinase- related genes in *A. pisum* in this study. We also described gene expression patterns of the chitinase- related genes in different stages. Besides, the expression pattern with qRT-PCR of the chitinase gene on environmental stress in the development stage was investigated for the first time in *A. pisum*, and understanding the chitin degradation of the pea aphid under stress conditions can help in developing a safer molecular strategy for their control.

2 Materials and methods

2.1 Insect culture

The green pea aphid *Acyrthosiphon pisum* was cultured from a single parthenogenetic female collected from an alfalfa field in Gansu Province, China. They were maintained in the greenhouse at 20 ± 1°C, 60 ± 10% relative humidity, and a photoperiod of 16 h:8 h (L:D).

2.2 Gene identification and phylogenetic analysis

The chitinase genes (*Chts*) were identified by searching against the genome of *A. pisum* (Ap) (https://bipaa.genouest.org/sp/acyrthosiphon_pisum/). To compare the chitinase sequences of *A. pisum* with those of other different species and explore the evolutionary relationship of chitinase identified in *A. pisum*, the protein sequences of *Phenacoccus solenopsis* (Ps), *Anopheles gambiae* (Ag), *Bombyx mori* (Bm), *Drosophila melanogaster* (Dm), *Tribolium castaneum* (Tca),

Aphis gossypii (Ago), *Apis mellifera* (Am), *Bactrocera dorsalis* (Bd), *Nilaparvata lugens* (Nl) were downloaded from the NCBI database and listed in Supplementary Table S1. The phylogenetic tree was generated using the Maximum Likelihood method with 1,000 bootstrap tests using the MEGA 6.0 software.

2.3 Domain analysis

The online ExPASy Proteomics website (https://web.expasy.org/protparam/) was used to predict the theoretical parameters of the proteins. The domain architecture and signal peptide were identified from the protein sequences using the Pfam (http://pfam.wustl.edu/) and SMART search. The exon-intron organization of chitinase-like genes were predicted by sequence comparison between genomic sequences and putative cDNA sequences.

2.4 Sample collection at different developmental stages

To clarify the development time required for different instar stages of *A. pisum*, we observed the entire developmental stages of the pea aphid under our laboratory condition in pre-experiments. Based on the pre-experiment information, ten wingless adult aphids from the same cultural batch were inoculated on the broad bean leaves in a 9 cm diameter Petri dish and then removed after 6 h of reproduction. These primiparous aphids were allowed to grow on the broad bean leaves, and then the 1st-, 2nd-, 3rd-, 4th-instar nymphs and adults were sampled. The broad bean leaves used for the experiments were replaced after every 3 days. The sample collection process was independently repeated three times, and all samples were placed in liquid nitrogen immediately after collection and then stored at −80°C.

2.5 Stress treatments

2.5.1 Temperature treatment

The primiparous aphids were inoculated on the leaves until they reached 2nd instars. Four hundred fifty 2nd instar nymphs were randomly selected and transferred to new Petri dishes. These selected nymphs were divided into 3 groups (150 per group) and reared at different temperatures in three incubators as "low temperature group (10°C)", "normal temperature group (20°C)" and "high temperature group (30°C)" (Du et al., 2015) at 60 ± 10% relative humidity and a photoperiod of 16L: 8D. Ten aphids were randomly collected at 12 h, 24 h, 36 h, and 48 h from each temperature group as experimental samples and placed in a 1.5 ml sterile centrifuge tube. These samples were immediately frozen in liquid nitrogen and stored at −80°C. This collection procedure was repeated 3 times, so there were 360 2nd instar nymphs were used in the temperature treatment experiment.

2.5.2 Insecticide treatment

The leaf dipping method was used in this experiment (Ministry of Agriculture of the PRC, 2008). Newly emerged and healthy wingless adult aphids from the same batch were used in the insecticide treatments. Based on the LC_{50} results determined in the previous study (Wang et al., 2014), imidacloprid (Shanghai Yuelian Chemical Co., Ltd. China) was dissolved in double distilled H_2O at 5.34 mg/L as the working solution. The broad bean leaves with 60 wingless adult aphids were immersed in the working solution for 10 s and placed on filter paper in a 9 cm petri dish for natural air drying, and then kept for 24 h and 48 h in the condition of 20 ± 1°C, a light cycle of L:D = 16 h:8 h, and relative humidity of RH 60 ± 10%. Adult aphids treated with clean water were used as the control group. After that, five live adults were randomly selected from each treated group (24 h and 48 h) and the control group and placed separately in three 1.5 ml sterile centrifuge tubes. The samples were immediately frozen in liquid nitrogen and stored in a refrigerator at −80°C for later use. Three biological replicates were set for each treatment group and the control group.

2.5.3 20E treatment

The 20E (20-hydroxyecdysone) (Sigma Co., St Louis, MO, United States) was dissolved in 95% ethanol as the stock solution. It was diluted to 12 mg/mL with double distilled H_2O and used as the working solution (Ma et al., 2021). Newly emerged (<6 h) nymphs were placed into 9 cm Petri dishes and fed on the leaves with their back facing up and moist absorbent cotton around the petioles until they reached the 2nd instar stage. Fifty 2nd instar nymphs were collected and soaked in the 20E working solution for 10 min. Similarly, fresh broad bean leaves were also treated with the 20E working solution. Then the nymphs and the treated leaves were placed on sterile filter paper to dry. The nymphs were inoculated on the treated leaves (moist absorbent cotton around the petioles) in Petri dishes at 20 ± 1°C, a light cycle of L:D = 16 h: 8 h, and the relative humidity of 60 ± 10%. The nymphs treated with 5% alcohol were used as the control group. Ten aphids were randomly sampled at 24 h, 48 h, and 72 h after the treatments from each treatment group and the control group, and placed separately in a 1.5 ml sterile centrifuge tube. The samples were immediately frozen in liquid nitrogen and stored in a refrigerator at -80°C for later use. Three independent repeats were set in the treatment group and the control group.

2.6 Total RNA extraction and cDNA synthesis

The total RNA of the *A. pisum* samples from different developmental stages and the 2nd instar nymphs under each

TABLE 1 List of the chitinase genes characterization in the *Acyrthosiphon pisum* genome.

Gene name	Gene IDs	RefSeq mRNA	Protein length (aa)	MW (kDa)[1]	pI[1]
ApIDGF	LOC100160032	NM_001168671	442	48.65	8.66
ApCht3	LOC100169240	X0M_001952683	473	53.52	5.84
ApCht7	LOC100165452	XM_001950345	998	112.75	6.64
ApCht10	LOC100169480	XM_001943003	2,274	257.99	6.76
ApENGase	LOC100168559	XM_001949910	528	60.75	5.49

[1]Mw, molecular weight; pI, isoelectric point.

emergency stress (temperatures, insecticide and 20E) were isolated using TRIzol reagent (Invitrogen, Carlsbad, CA, United States) as recommended by the manufacturer. The RNA purity was determined by measuring the absorbance ratio 260/280. The gDNA was removed with the RQ1 RNase-Free DNase kit (Promega, United States), and the first-strand complementary DNA (cDNA) was synthesized using the PrimerScript RT Reagent Kit (TAKARA, Dalian, China) with 1 μg of total RNA template in a 20 μL reaction following the manufacturer's protocol. The synthesized cDNA was stored at −20°C.

2.7 Real-time quantitative reverse transcription-PCR

Primer 3.0 (http://bioinfo.cu.ee/primer3-0.4.0) was used to design gene specific primers (Supplementary Table S2) and synthesized by Qinke Biotech (Beijing, China). All RT-qPCR was carried out in a 10 μL reaction mixture consisting of 5 μL of 2×SuperReal PreMix Plus (Tiangen, Beijing, China), 0.5 μL of each primer (0.2 mM), 0.5 μL of cDNA template, 0.2 μL of 50 × ROX Reference DyeΔ, and 3.3 μL of nuclease-free water. The real-time qPCR program consisted of an initial denaturation step at 95°C for 15 s followed by 40 cycles at 95°C for 10 s and 60°C for 30 s. Two reference genes, the *Elongation factor 1 alpha* (*EF1α*) and *Ribosomal protein S20* (*RPS20*) (Supplementary Table S2), were used to normalize the expression levels of targeted genes through qBase+ (Hellemans et al., 2007) based on the $2^{-\Delta\Delta CT}$ method (Pfaffl, 2001). The relative expression level of Cht-related genes was presented as mean ± SE of three biological replicates.

2.8 Statistical analyses

Parameters measured in different stages and under abiotic stresses (temperature, Insecticide and 20E) were analysed using one-way analysis of variance (one-way ANOVA), followed by Tukey's HSD tests to detect statistically significant differences ($p < 0.05$) between these parameters using SPSS 22.0 software.

3 Results

3.1 Identification and characterization of chitinase genes in *A. pisum*

Five chitinase genes were identified from the *A. pisum* genome, and their basic information are listed in Table 1. Among the 5 Cht-related genes, 3 genes encode for chitinases. The protein length of *ApCht3*, *ApCht7* and *ApCht10* is 473 aa, 998 aa and 2,274 aa, respectively, with the predicted MW and pI of 53.52 and 5.84, 112.75 and 6.64, 257.99 and 6.76, respectively. One *ApIDGF* (Imaginal disc growth factor) belongs to GH18 Cht-like superfamily, and encodes for a protein with 442 aa, predicted MW of 48.65 kDa and theoretical pI of 8.66. One *ApENGase* (Endobeta-N-acetylglucosaminidase) gene belongs to the glycosyl hydrolase family 85 (GH85) with deduced amino acids of 528 aa, and theoretical pI of 5.49 (Table 1).

The chitinase from *A. pisum* and other nine insect species were used to construct a phylogenetic tree based on their protein sequence (Figure 1). The phylogenetic analysis showed ApCht10, ApCht7, ApIDGF, ApCht3, and ApENGase belong to groups II, III, V, X, and ENGase, respectively. ApCht3 had a higher homology with AgoCht3-2 (100%) and PsCht3 (76%). Both ApCht10 had a higher homology with the genes of PsCht10 (83%) and NlCht10 (100%). ApIDGF also shared higher homology with PsIDGF (93%). ApCht7 shared higher homology with NlCht7 (52%). Besidess, ApENGase shared high similarities with TcENGase (100%) and AmENGase (86%).

3.2 Gene structure of chitinase in *A. pisum*

The domain architectures of the predicted chitinases in *A. pisum* are shown in Figure 2. All chitinases contain the catalytic domain of insect chitinases. Among them, ApIDGF and ApCht3 have one copy of the GH18 chitinase-like domain, ApCht7 and ApCht10 have two and four copies of this domain, respectively. Whereas ApENGase has a single copy of the GH85 domain (Figure 2). Multiple sequence alignments showed that each of these 8 catalytic regions had four

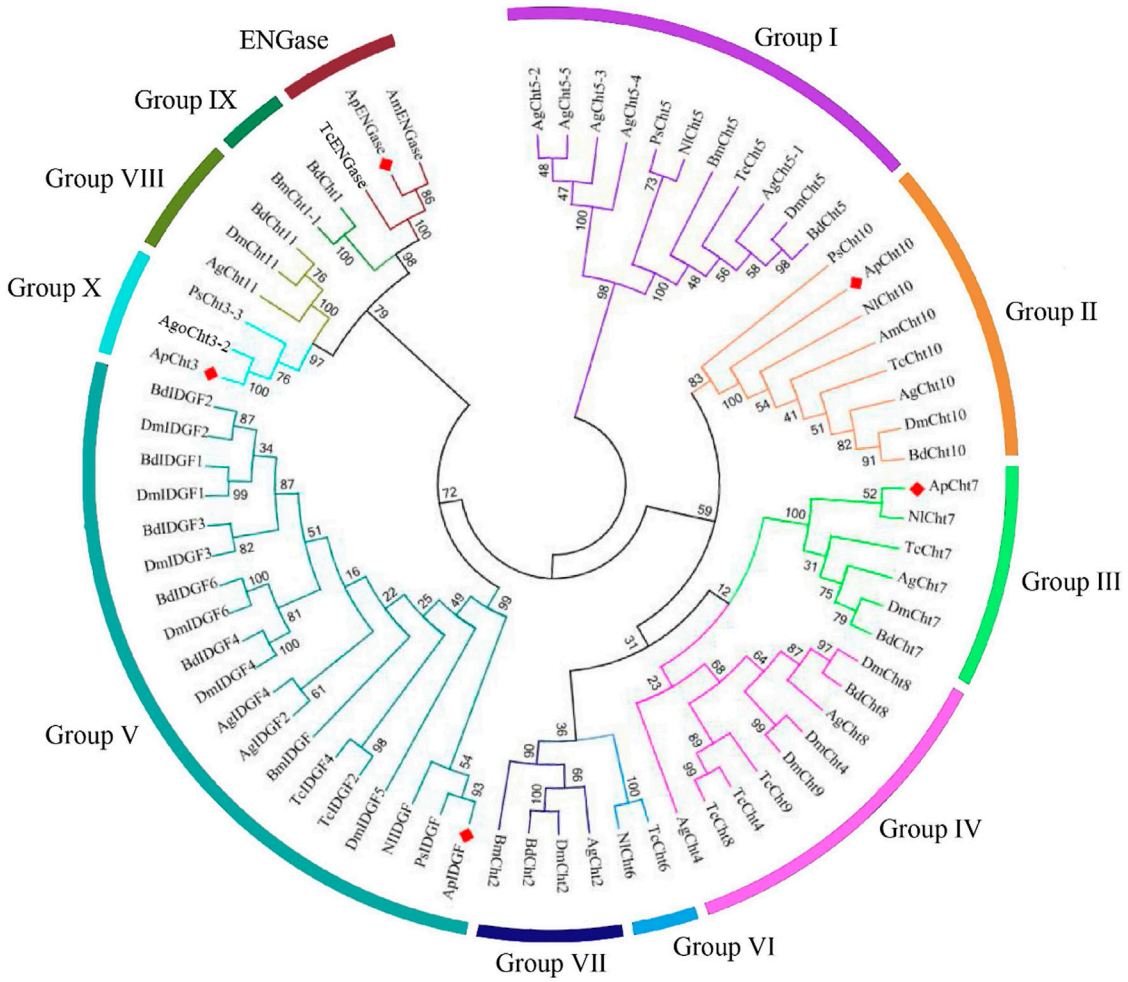

FIGURE 1
Phylogenetic analysis of chitinase genes from 10 different insects. *Acyrthosiphon pisum* (Ap), *Anopheles gambiae* (Ag), *Drosophila melanogaster* (Dm), *Tribolium castaneum* (Tc), *Bombyx mori* (Bm), *Phenacoccus solenopsis* (Ps), *Aphis gossypii* (Ago), *Apis mellifera* (Am), *Bactrocera dorsalis* (Bd), *Nilaparvata lugens* (Nl).

conserved mofits with the sequences KxxxxxGGW (Mofit Ⅰ), FDGxDLDWEYP (Mofit Ⅱ), MxYDxxG (Mofit Ⅲ), and GxxxWxxDxDD (Mofit Ⅳ), respectively (Supplementary Figure S1). The conserved sequence in Mofit Ⅱ, DWEYP, is an essential characteristic of a putative chitinase. In ApIDGF and ApENGase, most of the amino acids in the four domains are different from the corresponding four conserved mofits, suggesting all four regions were poorly conserved (Supplementary Figure S1). Moreover, ApCht7 and ApCht10 have one and four chitin-binding domains (CBD), respectively, while other three genes have no CBD. Besides, one transmembrane region was detected in ApCht3 and ApCht10. One signal peptide was detected in ApCht7 (Figure 2).

The exon/intron organization of 5 chitinase genes within the *A. pisum* genome is shown in Figure 3. There is a clearly diverged organization among the chitinase genes in the number of exons-introns and the gene sizes. *ApIDGF*, *ApCht3,* and *ApENGase* had six, eight, and two exons, whereas *ApCht7* and *ApCht10* had 16 and 37 exons respectively. The sizes of their introns ranged from 57 bp to 3,381 bp (Supplementary Table S3).

3.3 Developmental expression patterns of chitinase genes

We used RT-qPCR to examine the specific expression patterns of chitinase genes at different developmental stages (1^{st}-, 2^{nd}-, 3^{rd}-, 4^{th}-nymph and adults) (Figure 4). *ApCht10* was mainly expressed in 1^{st}- and 2^{nd}-instar nymphs. *ApCht7* expression was abruptly increased at the 4^{th} instar stage and then decreased until adult stage. The expressions of *ApIDGF* and *ApCht10* had similar patterns, and were significantly higher at

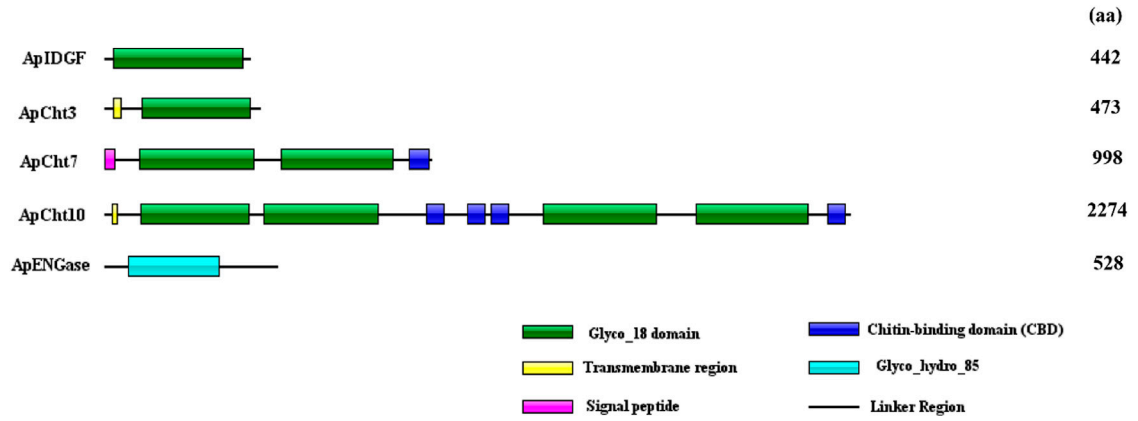

FIGURE 2
Domain analysis of 5 chitinase genes in *A. pisum*. The deduced amino acid sequences and domain architectures of 5 *A. pisum* chitinase genes were predicted by SMART software.

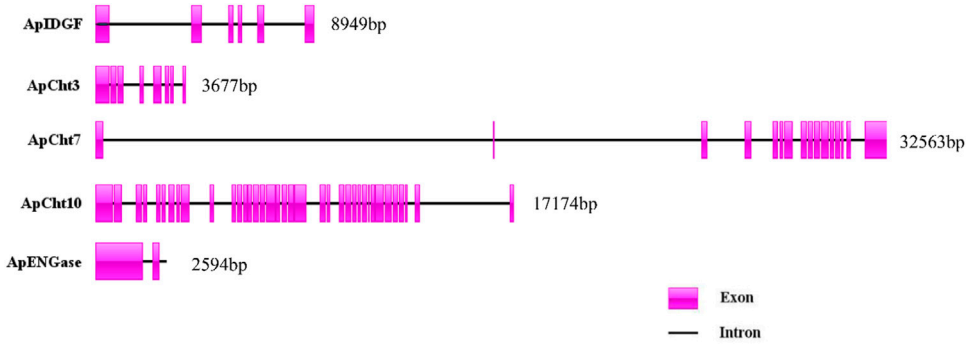

FIGURE 3
Exon-intron organization in 5 chitinase genes in *A. pisum*. The exons Exons are displayed as red box areas. The lines between the boxes represent introns.

the 4th instar stage than at the 3rd instar and adult stages ($p < 0.05$). The expression level of *ApENGase* was stable at all stages. Moreover, *ApCht3* had a special expression pattern that was confined to the adult stage and was increased by a great margin in the adult stage relative to those of other chitinase genes (Figure 4).

3.4 Effect of temperature stress on the expression of the chitinase genes

To examine the expression of these chitinase genes in response to temperatures, the *A. pisum* at the 2nd instar nymph stage were treated at 10°C, 20°C, and 30°C for various periods. At 10°C, the expression of *ApCht3*, *ApCht10*, *ApIDGF*, and *ApENGase* was lower than those at 20°C (Figure 5). While the expression of *Ap*Cht7 was higher by 0.4-, 1.1-, 0.7- and 0.6-fold at 12 h, 24 h, 36 h and 48 h at 10°C than at 20°C ($p < 0.05$). At 30°C, the expression of *ApIDGF* was significantly reduced by 0.3 to 0.6-fold relative to those at 20°C ($p < 0.05$). Similarly, the expression of *ApCht7* was reduced at 12 h and 24 h at 30°C, but it gradually increased with the treatment time and peaked at 48 h with a 1.3-fold higher at 30°C than that at 20°C ($p < 0.05$) (Figure 5). *ApCht3* and *ApCht10* had contrary expression patterns to *ApCht7*, the treatment at 30°C for 12 h and 24 h increased their expression but the treatment for 48 h decreased their expression by1.1-fold for *ApCht3* and 0.9-fold for *ApCht10* than their expression under the 20°C treatment ($p < 0.05$). The *ApENGase* expression was up-regulated by the 10°C treatment at 12 h and 24 h, but decreased with the extension of exposure time, and reached the lowest level at 48 h (Figure 5; Supplementary Figure S2).

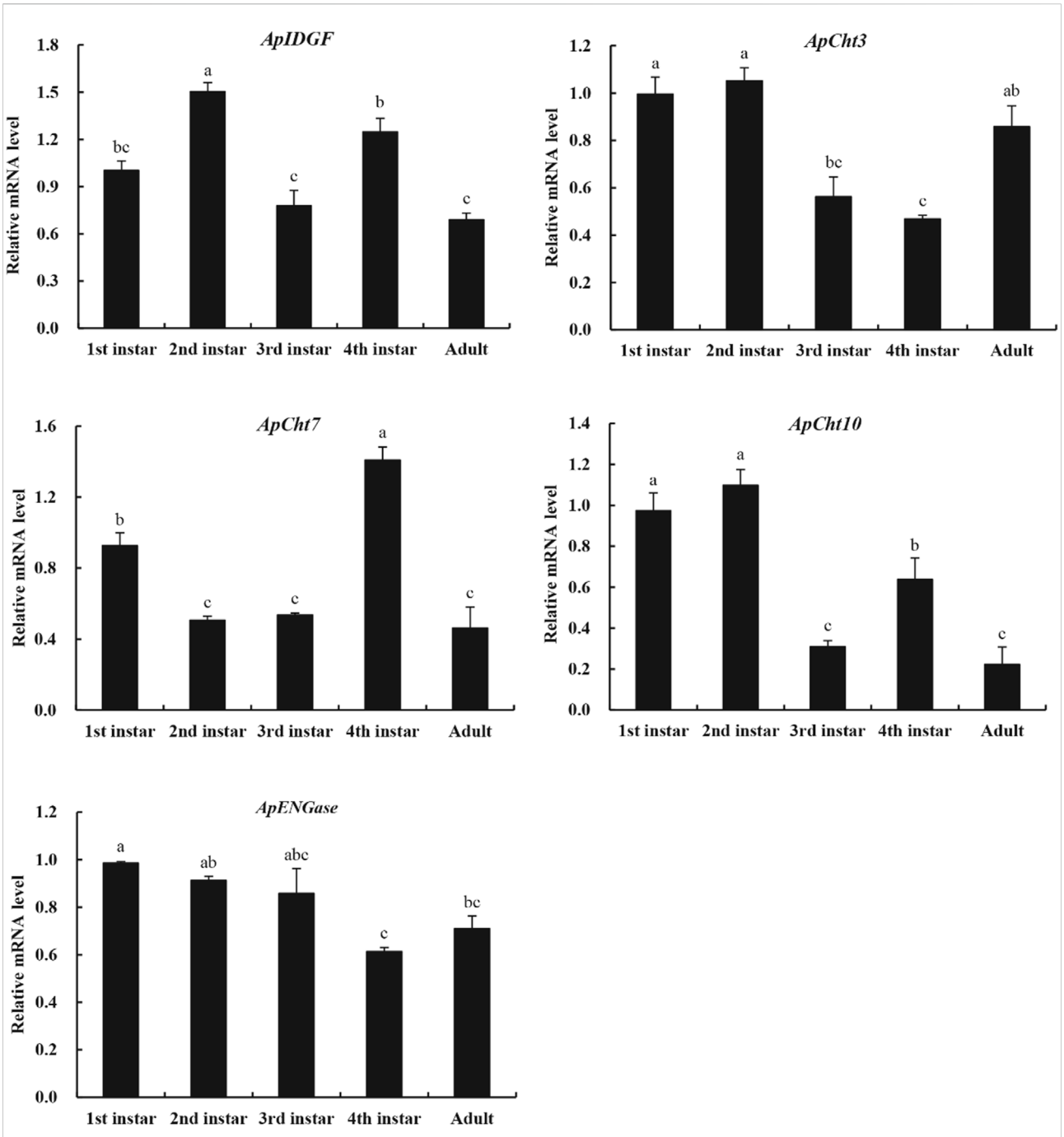

FIGURE 4
Developmental expression patterns of chitinase genes. Different letters on the top of the columns indicate significance in the difference of expression levels by Tukey's HSD test ($p < 0.05$).

3.5 Effect of insecticide stress on the expression of the cht-related genes

The expression of chitinase-related genes was significantly reduced by the imidacloprid treatment relative to that of the control (Figure 6). Furthermore, the expression of *ApIDGF* and *ApCht10* gradually reduced by 0.8 and 0.3-fold at 48 h than that of 24 h, respectively ($p < 0.05$) (Figure 6). The imidacloprid treatment also significantly reduced the expression of *ApCht3* during 24 h

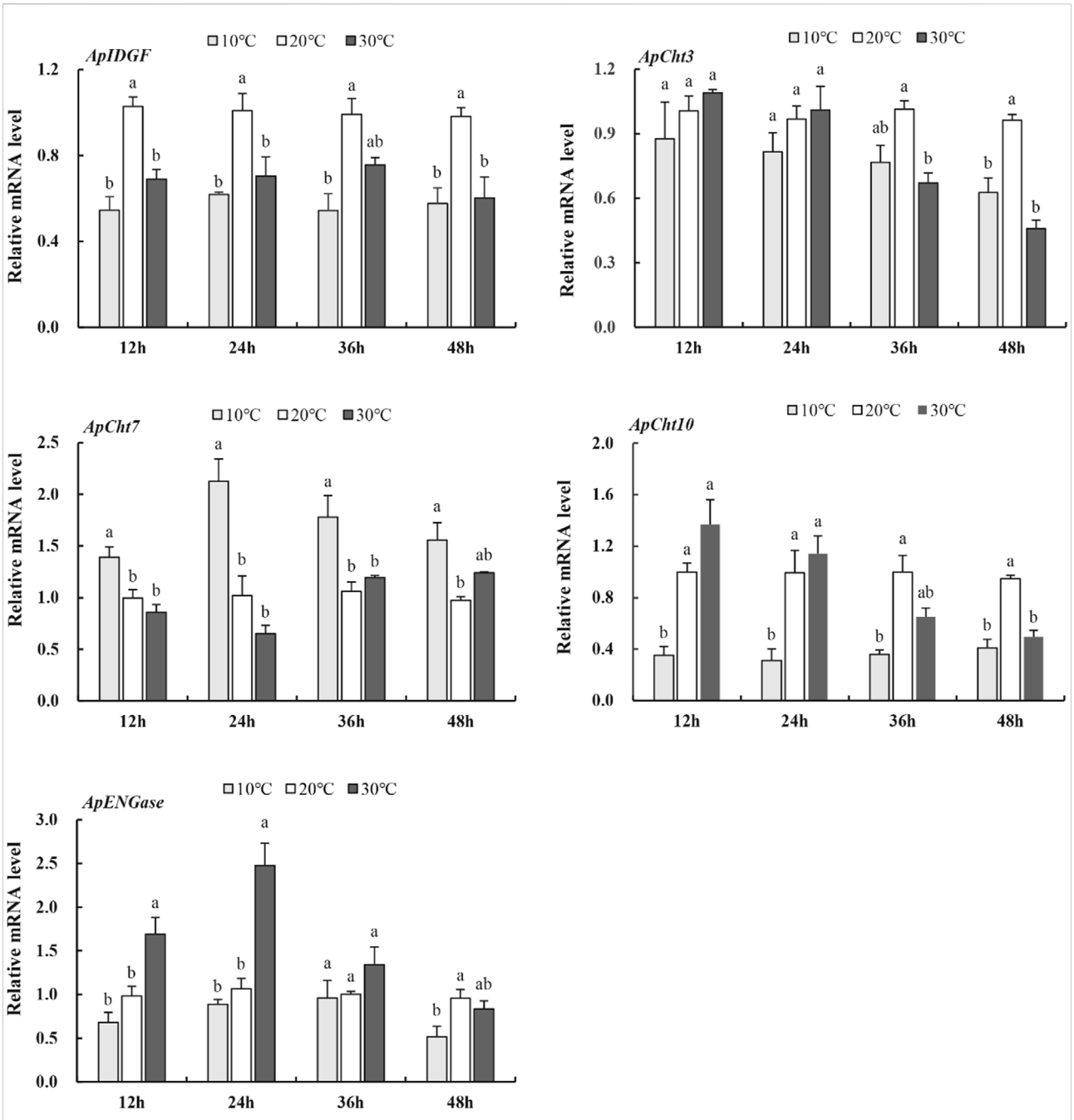

FIGURE 5
Expression of the chitinase genes in response to temperature stress. Different letters on the top of the columns indicate significance in the difference of expression levels by Tukey's HSD test at same treatment time ($p < 0.05$).

and 48 h relative to the control treatment, however, stable expression levels were observed during this time under the imidacloprid treatment (Figure 6). The expression of *ApCht7* and *ApENGase* was increased by the imidacloprid treatment with prolonged time, and significantly lower than that of the control ($p < 0.05$) (Figure 6; Supplementary Figure S3).

3.6 Effect of 20E treatment on the expression of the cht-related genes

The 20E treatment upregulated the expression of *ApCht3* and *ApCht10* at 24 h compared with the control, and the highest expression occurred at 48 h (Figure 7). The 20E treatment

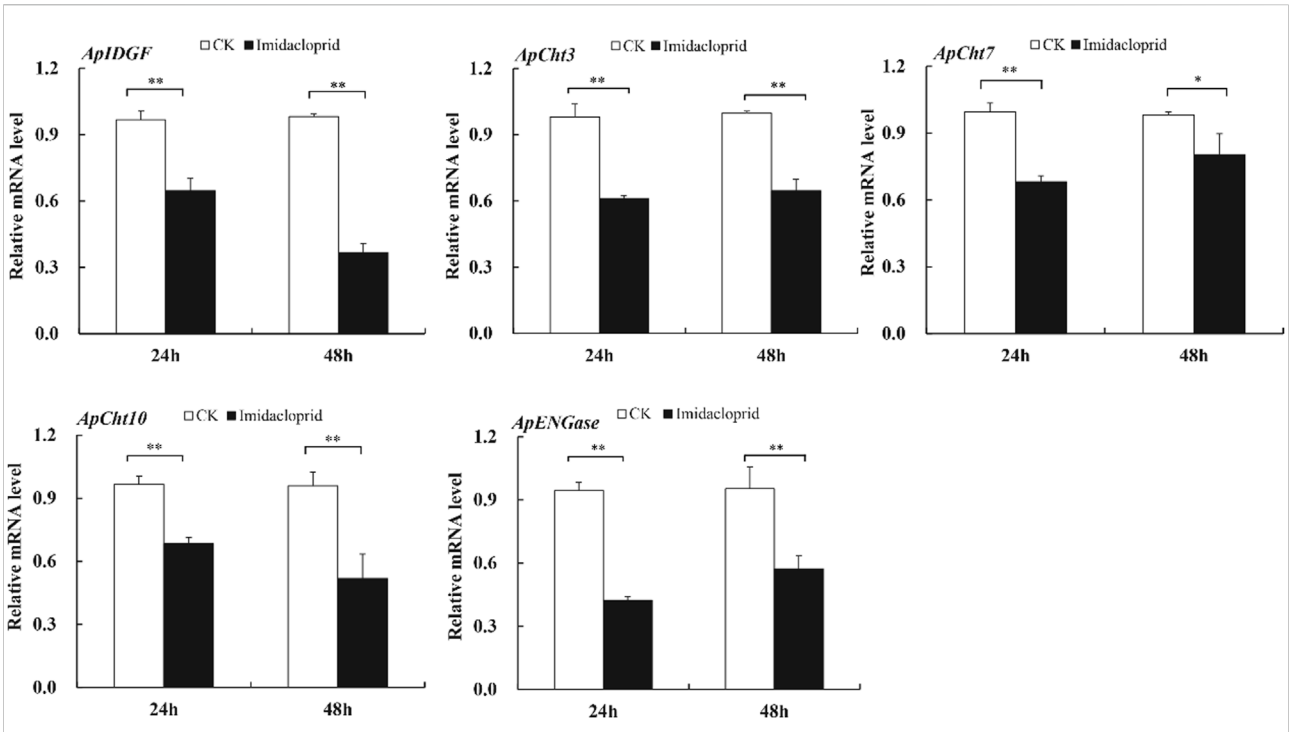

FIGURE 6
Expression of the Cht-related genes in response to insecticide stress. Different letters on the top of the columns indicate significance in the difference of expression levels by Tukey's HSD test at same treatment time (*$p < 0.05$ and **$p < 0.01$ compared with the control group).

significantly reduced *ApCht7* expression by between 0.63-fold and 0.48-fold compared with the control ($p < 0.05$). The 20E treatment for 24 h inhibited the expression of *ApIDGF*, but as time prolonged after 48 h the expression of *ApIDGF* was gradually increased by 0.1- and 0.8-fold than that of the control at 48 h and 72 h, respectively ($p > 0.05$). Contrary to *ApIDGF*, the expression of *ApENGase* gradually declined as the treatment time was prolonged (Supplementary Figure S4). Still, its expression level was higher than that of the control at 24 h and 48 h under the 20E treatment (Figure 7).

4 Discussion

Identification of Cht-related genes by bioinformatic approaches is valid and reliable due to the publications of insect whole genome sequences. This study identified five chitinases and chitinase-like proteins genes from the *A. pisum* genome. Among these, three *Chts* genes were encoded true chitinases and closely related to those chitinases with chitinolytic activities, while the remaining two genes appeared to encode an *IDGF* and an *ENGase*, respectively. The previous report also identified 9 Cht-related genes in *A. pisum* (Nakabachi et al., 2010). However, four of those Cht-related genes (IDs: LOC100160065, LOC100169337, LOC100164767, and LOC100162732) were not identified in the present study. Moreover, *A. pisum* has fewer chitinase-like genes as reported for other hemimetabolous insects such as *N. lugens* and *P. solenopsis* (Xi et al., 2014; Omar et al., 2019) than insect species especially Coleoptera and Diptera. This was speculated as the expansion of chitinase genes in dipteran and coleopteran insects (Nakabachi et al., 2010).

Based on the similarities in amino acids and phylogenetic analysis, the classification of insect Chts and Cht-like proteins has been increased from 8 groups (I-VIII) to 11 groups (I-X and H), which can provide consistent classification and nomenclature of chitinase and chitinase-like genes in different insect species (Arakane and Muthukrishnan, 2010; Tetreau et al., 2015). Compared with previous results from *A. pisum* (Nakabachi et al., 2010), we have determined that the previously assigned four genes previously named *ApCht1*, *ApCht2*, *ApCht4*, and *ApCht6*, were renamed as *ApIDGF*, *ApCht10*, *ApCht7*, and *ApCht3*, and all of the five chitinase and chitinase-like proteins were identified in group II (ApCht10), III (ApCht7), V (ApIDGF), X (ApCht3) and ENGase (ApENGase), respectively. Among them, ApENGase is closely related to *A. mellifera* and *T. castaneum* ENGase, and the other four chitinases have very high homology with Chts of *P. solenopsis* and *N. lugens*. Previous studies have shown that there are four conserved regions in the amino acid sequence of the catalytic domain of

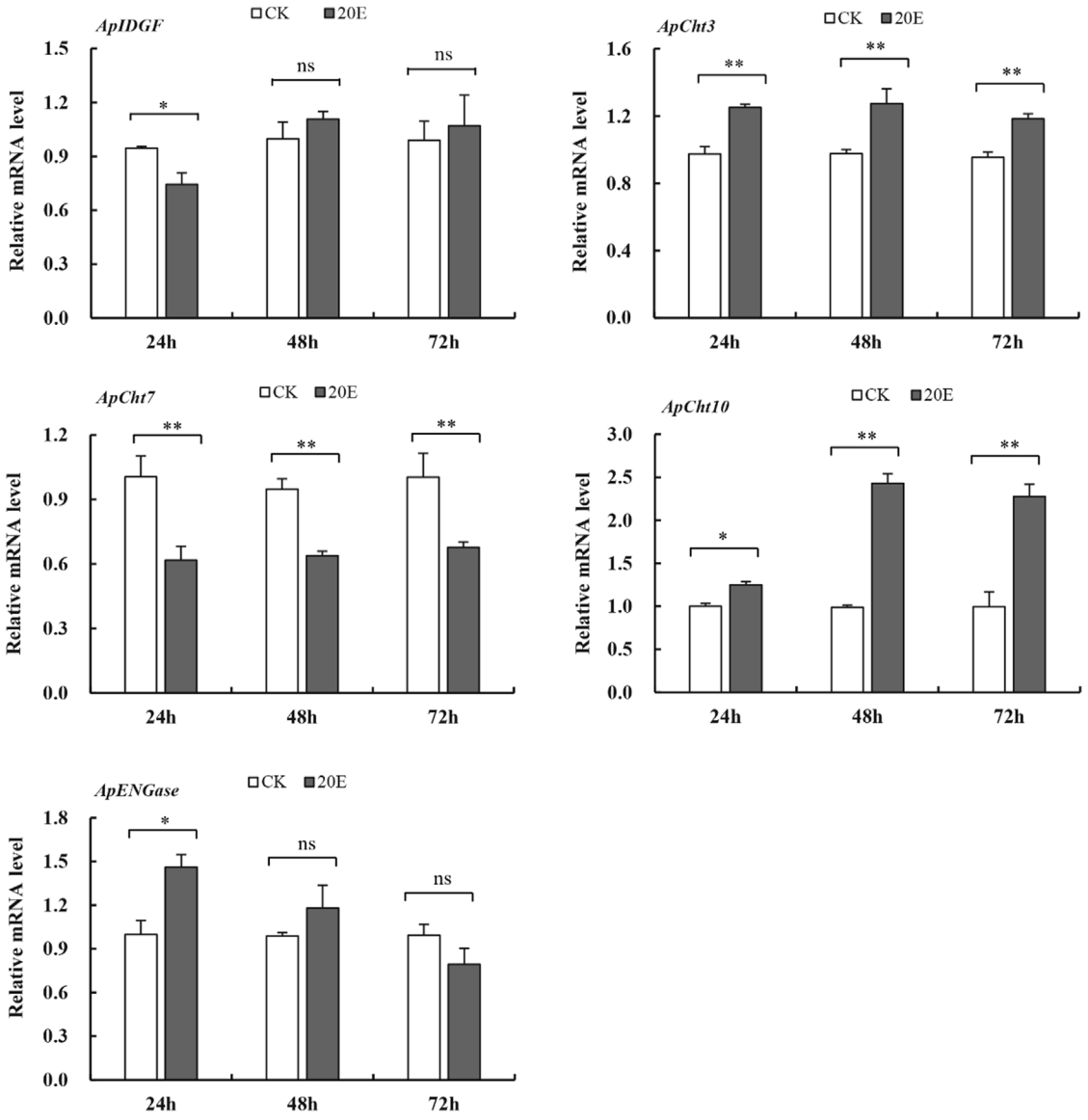

FIGURE 7
Expression of the Cht-related genes in response to 20E treatment. Different letters on the top of the columns indicate significance in the difference of expression levels by Tukey's HSD test at same treatment time (*$p < 0.05$ and **$p < 0.01$ compared with the control group).

insect chitinase GH18. The conserved sequence in Mofit II, DWEYP, is an essential characteristic of a putative chitinase, and the residue E is a putative protein donor essential for catalytic activity (Zhu et al., 2008a). While the Mofit II regions were observed to be poorly conserved in ApIDGF and ApENGase, indicating that these proteins lack chitinase activity. Although IDGF lacks chitinase activity. They may be used as a receptor binding to a cell surface (Kawamura et al., 1999; Bryant, 2001; Varela et al., 2002), and indispensable for adult eclosion (Zhu et al., 2008b). ApCht10 is the longest chitinase gene in the pea aphid and has 4 catalytic domains and 4 CBDs identical to that of *B. dorsalis* (Liu et al., 2018). ApCht7 has two catalytic domains and one CBD, and ApCht3 contains one catalytic domain. An interesting finding is that chitin-binding domains can bind chitinase to insoluble substrates with a high degradation efficiency (Arakane et al., 2003). Our data show that the domain II is well conserved in ApCht3, ApCht7, and ApCht10, suggesting they all have chitinase activity. ApCht7 and ApCht10 also have one and four chitin-binding domains respectively, which further shows that ApCht7 and ApCht10 have the degradation activity of chitinase.

The studies on the expression profiles of chitinase-related genes in the pea aphid at different developmental stages mainly focus on chitin synthesis pathway genes (Wang et al., 2021a; Wang et al.,2021b; Ye et al., 2019), but there are relatively few studies on chitin metabolism- related genes. Insect chitinases not only play a very important function in the degradation of old exoskeleton and turnover of the gut lining, but are also involve in the formation of barrier tissues, detoxification and immunity (Pesch et al., 2016; Broz et al., 2017), and these genes showed specific developmental expression pattern in insects. In *A. gambiae*, the study of stage-specific gene expression showed that most chitinase genes were expressed at the larval stages, while *AgCht8* was mainly expressed at pupal and adult stages (Zhang et al., 2011). In this study, real-time qPCR demonstrated that the five *A. pisum* chitinase-related genes were expressed at all developmental stages with different relative expression patterns. This result fully reflects the diversity and complexity of the chitinase regulation mechanism. Previous research has shown that Group I and II chitinases are involved in molting by digesting cuticular chitin, whereas Group III chitinases have a morphogenetic role in insect development (Zhu et al., 2008b). In the present study, the group II *ApCht10* showed a high expression level at both the first and second instar nymph stages in *A. pisum*, which is a similar to *P. solenopsis* (Omar et al., 2019) and *B. dorsalis* (Liu et al., 2018). This indicates that *Cht10* probably play an active role at the early developmental stages of *A. pisum*. Conversely, the group III gene *ApCht7* was highly expressed in the fourth instar nymph, suggesting that *ApCht7* may be involved in the process of insect emergence and molting. The expression of *Cht7* was upregulated during pupa-adult molts of *Drosophila meloganster* (Pesch et al., 2016) and significantly changed at the molting stage in *Sogatella furcifera* (Chen et al., 2017) and *Mythimna separata* (Yang and Fan, 2018).

The development and growth of insects are greatly affected by environmental temperatures due to their poor ability to adjust and maintain their body temperature as poikilotherms (Hu et al., 2014). Research has found that the inadequate environment of high temperature leads to an increased expression of *IDGF4* in *B. dorsalis*, and reveal its involvement in heat tolerance (Gu et al., 2019). In the desert beetle *Microdera punctipennis*, low temperature such as 4°C and −4°C both upregulate the expression of six chitinase genes, including *IDGF2* (Lu et al., 2014). We showed the different results; that both high and low temperature can down-regulate the expression of *ApIDGF*, which indicates that this gene was negatively regulated under temperature stress in *A. pisum*. Meanwhile, the expression of *ApCht3* and *ApCht10* was also significantly decreased at 36 h under the high temperature (30°C). Noticeably, the expression level of *ApCht7* was increased at 10°C than to 20°C compared to the other genes, which is similar to the study on *DcCht6* in *Diaphorina citri* (Liu, 2021). The increasing expression pattern of *ApCht7* might reveal its involvement in low temperature. In contrast, the expression of *ApCht10* was lower at 10°C than 20°C. This indicates that *ApCht7* and *ApCht10* are more sensitive to 10°C rather than 30°C. Interestingly, Liu found that CBD in chitinase gene interacts with heat shock chaperone in response to low temperature stress (Liu, 2021). *ApCht7* and *ApCht10* have one and four CBD, respectively, which may play a role in the responses to the low temperature.

Neonicotinoid imidacloprid are nicotinic acetylcholine receptor agonists which disrupt the function of insect neurons and cause paralysis and death (Bebane et al., 2019). Imidacloprid is the most effective insecticides for controlling pea aphids. The previously reported the fecundity and longevity were affected significantly when green pea aphids were exposed to sublethal doses of imidacloprid (Wang et al., 2014). Using the same insect, insecticide, and doses, here we showed that the down-regulation the expression of all the five chitinase genes when *A. pisum* were exposed to sublethal concentrations of imidacloprid. Similarly, Liu found that the expressions of *BdIDGF1*, *BdIDGF2* and *BdCht7* were significantly down-regulated compared with the control group when the adults of *B. dorsalis* were treated with the insecticide malathion (Liu et al., 2018). These results suggest that these insecticides could disturb the metabolic balance of chitin in addition to their actions on nerve systems, this may have been associated with reduced fecundity/reproduction in *A. pisum*.

Moreover, 20E is an insect hormone and has been reported to contribute to many insect physiological processes including molting (Jindra et al., 2013). Treatment with 20E enhanced the transcription level of *BdCht2* in *B. dorsalis* (Yang et al., 2013) and *MsCht5* in *M. sexta* (Kramer et al., 1993). In the present study, the 20E treatment up-regulated *ApCht3* and *ApCht10* expression over a prolonged time. Similarly, the expression of *TmCht10* gene in *Tenebrio molitor* was significantly upregulated with 20E treatment (Royer et al., 2002). Whereas 20E significantly reduced *ApCht7* expression compared with the control. This indicates that *ApCht7* is negatively regulated by 20E, which is analogous to chitinases in *M. separata*, which was reported that 20E could induce the expression of *MsCht7* of *M. separata*, and advance the molting time (Yang and Fan, 2018). Our results indicate that the expression levels of chitinase genes can be induced by 20E in pea aphids.

In conclusion, we identified five genes encoding Cht-related proteins in *A. pisu*m with different expression patterns during development and under stress. The differential expression of these chitinase genes in response to stresses confirms that each gene may function differently under stress conditions. The developmental-specific and stress-inducible expressions suggest that the insect chitinases may have diverse functions and play roles in response to environmental stress. We therefore speculate that *A. pisum* chitinases may be one of the potential signal molecules in the cross tolerance and cross-talk to a changing environment.

Data availability statement

The original contributions presented in the study are included in the article/Supplementary material, further inquiries can be directed to the corresponding author.

Author contributions

CL, IUK, and AK conducted data acquisition and analysis; CL, IUK, and YT conducted Methodology and sampling; CL, CZL, JJZ, and PQ written-original draft preparation; CL and JJZ made critical editing and proofreading. All authors read and approved manuscript.

Funding

This research was funded by the National Science Foundation of China (No. 31960351, 31960227). Gansu Province excellent graduate "Innovation Star" project of China (2021CXZX-379) to CL. Program of Introducing Talents to Chinese Universities (111 Program no. D20023) to JZ.

Acknowledgments

We would like to thank all of the participants who volunteered their time in the study. We appreciate very much the valuable comments and suggestion by the Reviewers and Editors.

Conflict of interest

The authors declare that the research was conducted in the absence of any commercial or financial relationships that could be construed as a potential conflict of interest.

Publisher's note

All claims expressed in this article are solely those of the authors and do not necessarily represent those of their affiliated organizations, or those of the publisher, the editors and the reviewers. Any product that may be evaluated in this article, or claim that may be made by its manufacturer, is not guaranteed or endorsed by the publisher.

Supplementary material

The Supplementary Material for this article can be found online at: https://www.frontiersin.org/articles/10.3389/fphys.2022.1024136/full#supplementary-material

References

Arakane, Y., and Muthukrishnan, S. (2010). Insect chitinase and chitinase-like proteins. *Cell. Mol. Life Sci.* 67, 201–216. doi:10.1007/s00018-009-0161-9

Arakane, Y., Taira, T., Ohnuma, T., and Fukamizo, T. (2012). Chitin-related enzymes in agro-biosciences. *Curr. Drug Targets* 13, 442–470. doi:10.2174/138945012799499721

Arakane, Y., Zhu, Q., Matsumiya, M., Muthukrishnan, S., and Kramer, K. J. (2003). Properties of catalytic, linker and chitin-binding domains of insect chitinase. *Insect biochem. Mol. Biol.* 33, 631–648. doi:10.1016/s0965-1748(03)00049-3

Bebane, P. S. A., Hunt, B. J., Pegoraro, M., Jones, A. R. C., Marshall, H., Rosato, E., et al. (2019). The effects of the neonicotinoid imidacloprid on gene expression and DNA methylation in the buff-tailed bumblebee *Bombus terrestris*. *Proc. Biol. Sci.* 286, 20190718. doi:10.1098/rspb.2019.0718

Broz, V., Kucerova, L., Rouhova, L., Fleischmannova, J., Strnad, H., Bryant, P. J., et al. (2017). *Drosophila* imaginal disc growth factor 2 is a trophic factor involved in energy balance, detoxification, and innate immunity. *Sci. Rep.* 7, 43273. doi:10.1038/srep43273

Bryant, P. J. (2001). Growth factors controlling imaginal disc growth in Drosophila. In: *Book Growth factors controlling imaginal disc growth in Drosophila*. Vol., pp. 182–202. Chichester New York John Wiley City.

Chen, C., Yang, H., Tang, B., Yang, W. J., and Jin, D. C. (2017). Identification and functional analysis of chitinase 7 gene in white-backed planthopper, *Sogatella furcifera*. *Comp. Biochem. Physiol. B Biochem. Mol. Biol.* 208-209, 19–28. doi:10.1016/j.cbpb.2017.03.002

Chen, W., Qu, M., Zhou, Y., and Yang, Q. (2018). Structural analysis of group II chitinase (ChtII) catalysis completes the puzzle of chitin hydrolysis in insects. *J. Biol. Chem.* 293, 2652–2660. doi:10.1074/jbc.RA117.000119

Du, J. L., Wu, D. G., Lv, N., and Liu, C. Z. (2015). Population parameters of two pea aphid (*Acyrthosiphon pisum*) color morphs at different temperatures. *Acta Prataculturae Sin.* 124, 91–99.

Gu, X., Li, Z., Su, Y., Zhao, Y., and Liu, L. (2019). Imaginal disc growth factor 4 regulates development and temperature adaptation in *Bactrocera dorsalis*. *Sci. Rep.* 9, 931. doi:10.1038/s41598-018-37414-9

Hellemans, J., Mortier, G., De Paepe, A., Speleman, F., and Vandesompele, J. (2007). qBase relative quantification framework and software for management and automated analysis of real-time quantitative PCR data. *Genome Biol.* 8, R19. doi:10.1186/gb-2007-8-2-r19

Hu, J. T., Chen, B., and Li, Z. H. (2014). Thermal plasticity is related to the hardening response of heat shock protein expression in two *Bactrocera* fruit flies. *J. Insect Physiol.* 67, 105–113. doi:10.1016/j.jinsphys.2014.06.009

International Aphid Genomics Consortium (2010). Genome sequence of the pea aphid *Acyrthosiphon pisum*. *PLoS Biol.* 8, e1000313. doi:10.1371/journal.pbio.1000313

Jindra, M., Palli, S. R., and Riddiford, L. M. (2013). The Juvenile hormone signaling pathway in insect development. *Annu. Rev. Entomol.* 58, 181–204. doi:10.1146/annurev-ento-120811-153700

Kawamura, K., Shibata, T., Saget, O., Peel, D., and Bryant, P. J. (1999). A new family of growth factors produced by the fat body and active on *Drosophila* imaginal disc cells. *Development* 126, 211–219. doi:10.1242/dev.126.2.211

Kramer, K. J., Lolita, C., Choi, H. K., and Muthukrishinan, S. (1993). Sequence of a cDNA and expression of the gene encoding epidermal and gut chitinases of *Manduca sexta*. *Insect biochem. Mol. Biol.* 23, 691–701. doi:10.1016/0965-1748(93)90043-r

Kramer, K. J., and Muthukrishnan, S. (1997). Insect chitinases: Molecular biology and potential use as biopesticides. *Insect biochem. Mol. Biol.* 27, 887–900. doi:10.1016/s0965-1748(97)00078-7

Li, D. Q., Zhang, J. Q., Wang, Y., Liu, X., Ma, E., Sun, Y., et al. (2015). Two chitinase 5 genes from *Locusta migratoria*: Molecular characteristics and functional differentiation. *Insect biochem. Mol. Biol.* 58, 46–54. doi:10.1016/j.ibmb.2015.01.004

Liu, S. H., Li, H. F., Yang, Y., Yang, R. L., Yang, W. J., Jiang, H. B., et al. (2018). Genome-wide identification of chitinase and chitin deacetylase gene families in the oriental fruit fly. *Bactrocera dorsalis (Hendel)*. Comparative Biochemistry and Physiology. 27D, 13–22.

Liu, Y. (2021). *Identification of chitinase genes and function of DcCht5 and DcCht10 in eclosion stage of Diaphorina citri*. Chongqing: Southwest University.

Lu, X. Y., Li, J. Q., Liu, X. N., Li, X. B., and Ma, J. (2014). Characterization and expression analysis of six chitinase genes from the desert beetle Microdera punctipennis in response to low temperature. *Cryo Letters*. 35, 438–448.

Ma, T. T., Yang, Z. L., Chang, M. L., Luo, C. Y., Kan, Y. C., and Li, D. D. (2021). Response of miRNAs related to wing differentiation and their predicted target genes to ecdysone and the confirmation of target gene of miR-92a-1-p5 in the pea aphid, *Acyrthosiphon pisum* (Hemiptera: Aphidae). *Acta Entomol. Sin.* 64, 419–427.

Merzendorfer, H. (2006). Insect chitin synthases: A review. *J. Comp. Physiol. B* 176, 1–15. doi:10.1007/s00360-005-0005-3

Merzendorfer, H., and Zimoch, L. (2003). Chitin metabolism in insects: Structure, function and regulation of chitin synthases and chitinases. *J. Exp. Biol.* 206, 4393–4412. doi:10.1242/jeb.00709

Ministry of Agriculture of the Prc (2008). *NY/T1154. 14-2008 pesticide indoor bioassay test criteria for pesticides. Part 14: Leaf soaking method*. Beijing: China Agriculture Publishing House Society.

Moussian, B. (2010). Recent advances in understanding mechanisms of insect cuticle differentiation. *Insect biochem. Mol. Biol.* 40, 363–375. doi:10.1016/j.ibmb.2010.03.003

Nakabachi, A., Shigenobu, S., and Miyagishima, S. (2010). Chitinase-like proteins encoded in the genome of the pea aphid, *Acyrthosiphon pisum*. *Insect Mol. Biol.* 19, 175–185. doi:10.1111/j.1365-2583.2009.00985.x

Omar, M. A. A., Ao, Y., Li, M., He, K., Xu, L., Tong, H. J., et al. (2019). The functional difference of eight chitinase genes between male and female of the cotton mealybug, *Phenacoccus solenopsis*. *Insect Mol. Biol.* 28, 550–567. doi:10.1111/imb.12572

Pesch, Y. Y., Riedel, D., Patil, K. R., Loch, G., and Behr, M. (2016). Chitinases and Imaginal disc growth factors organize the extracellular matrix formation at barrier tissues in insects. *Sci. Rep.* 6, 18340. doi:10.1038/srep18340

Pfaffl, M. W. (2001). A new mathematical model for relative quantification in real-time RT-PCR. *Nucleic Acids Res.* 29, e45–e2007. doi:10.1093/nar/29.9.e45

Royer, V., Fraichard, S., and Bouhin, H. (2002). A novel putative insect chitinase with multiple catalytic domains: Hormonal regulation during metamorphosis. *Biochem. J.* 366, 921–928. doi:10.1042/BJ20011764

Rudall, K. M., and Kenchington, W. (1973). The chitin system. *Biol. Rev. Camb. Philosophical Soc.* 48, 597–636.

Ryalls, J. M. W., Riegler, M., Moore, B. D., and Johnson, S. N. (2013). Biology and trophic interactions of lucerne aphids. *Agric. For. Entomol.* 15, 335–350. doi:10.1111/afe.12024

Tetreau, G., Dittmer, N. T., Cao, X. L., Agrawal, S., Chen, Y. R., Muthukrishnan, S., et al. (2015). Overview of chitin metabolism enzymes in *Manduca sexta*: Identification, domain organization, phylogenetic analysis and gene expression. *Insect biochem. Mol. Biol.* 62, 114–126. doi:10.1016/j.ibmb.2015.01.006

Tharanathan, R. N., and Kittur, F. S. (2003). Chitin-The undisputed biomolecule of great potential. *Crit. Rev. Food Sci. Nutr.* 43, 61–87. doi:10.1080/10408690390826455

Varela, P. F., Llera, A. S., Mariuzza, R. A., and Tormo, J. (2002). Crystal structure of imaginal disc growth factor-2 A member of a new family of growth-promoting glycoproteins from *Drosophila melanogaster*. *J. Biol. Chem.* 277, 13229–13236. doi:10.1074/jbc.M110502200

Wang, G., Guo, Y. P., Guo, S. F., Zhou, J. J., and Liu, C. Z. (2021a). RNA interference of trehalose-6-phosphate synthase and trehalase genes regulates chitin metabolism in two color morphs of *Acyrthosiphon pisum* Harris. *Sci. Rep.* 11, 948. doi:10.1038/s41598-020-80277-2

Wang, G., Zhou, J. J., Yan, L., Guo, Y. P., Quandahor, P., and Liu, C. Z. (2021b). Trehalose and glucose levels regulate feeding behavior of the phloem-feeding insect, the pea aphid *Acyrthosiphon pisum* Harris. *Sci. Rep.* 11, 15864. doi:10.1038/s41598-021-95390-z

Wang, X. Q., Liu, C. Z., Xin, Y. T., and Shi, Z. (2014). Effects of sublethal dosage of imidacloprid, abamectin and beta-cypermethrin on the development and reproduction of green of the morph of pea aphid (*Acyrthosiphon pisum*). *Acta Prataculturae Sin.* 23, 279–286.

Xi, Y., Pan, P. L., Ye, Y. X., Yu, B., Xu, H. J., and Zhang, C. X. (2014). Chitinase-like gene family in the Brown planthopper, *Nilaparvata lugens*. *Insect Mol. Biol.* 24, 29–40. doi:10.1111/imb.12133

Yang, W. J., Xu, K. K., Zhang, R. Y., Dou, W., and Wang, J. J. (2013). Transcriptional regulation of a chitinase gene by 20-hydroxyecdysone and starvation in the oriental fruit fly, *Bactrocera dorsalis*. *Int. J. Mol. Sci.* 14, 20048–20063. doi:10.3390/ijms141020048

Yang, W. Q., and Fan, D. (2018). Cloning, expression and ecdysone regulation of chitinase *MsCHT7* from the oriental armyworm, *Mythimna separata* walker. *Chin. J. Biol. Control* 34, 354–363.

Ye, C., Jiang, Y. D., An, X., Li, Y., Shang, F., Niu, J. Z., et al. (2019). Effects of RNAi-based silencing of chitin synthase gene on moulting and fecundity in pea aphids (*Acyrthosiphon pisum*). *Sci. Rep.* 9, 3694. doi:10.1038/s41598-019-39837-4

Zhang, J., Zhang, X., Arakane, Y., Muthukrishnan, S., Kramer, K. J., Ma, E., et al. (2011). Comparative genomic analysis of chitinase and chitinase-like genes in the African malaria mosquito (*Anopheles gambiae*). *PLoS One* 6, e19899. doi:10.1371/journal.pone.0019899

Zhang, X., and Zheng, S. (2016). 20-hydroxyecdysone enhances the expression of the chitinase 5 via Broad-Complex Zinc-Finger 4 during metamorphosis in silkworm, *Bombyx mori*. *Insect Mol. Biol.* 26, 243–253. doi:10.1111/imb.12288

Zheng, Y. P., Retnakaran, A., Krell, P. J., Arif, B. M., Primavera, M., and Feng, Q. L. (2003). Temporal, spatial and induced expression of chitinase in the spruce budworm, *Choristoneura fumiferana*. *J. Insect Physiol.* 49, 241–247. doi:10.1016/s0022-1910(02)00271-8

Zhu, Q., Arakane, Y., Banerjee, D., Beeman, R. W., Kramer, K. J., and Muthukrishnan, S. (2008a). Domain organization and phylogenetic analysis of the chitinase-like family of proteins in three species of insects. *Insect biochem. Mol. Biol.* 38, 452–466. doi:10.1016/j.ibmb.2007.06.010

Zhu, Q., Arakane, Y., Beeman, R. W., Kramer, K. J., and Muthukrishnan, S. (2008b). Functional specialization among insect chitinase family genes revealed by RNA interference. *Proc. Natl. Acad. Sci. U. S. A.* 105, 6650–6655. doi:10.1073/pnas.0800739105

frontiers | Frontiers in Physiology

TYPE Original Research
PUBLISHED 13 January 2023
DOI 10.3389/fphys.2022.1097459

OPEN ACCESS

EDITED BY
Divya Singh,
Chandigarh University, India

REVIEWED BY
Tiantao Zhang,
Chinese Academy of Agricultural Sciences (CAAS), China
Habib Ali,
Khwaja Fareed University of Engineering and Information Technology (KFUEIT), Pakistan

*CORRESPONDENCE
Mritunjoy Barman,
mritubarman@gmail.com
Jayanta Tarafdar,
jayanta94bckv@gmail.com
Deepayan Roy,
deepayan.roy@gdgu.org

†These authors have contributed equally to this work and share first authorship

SPECIALTY SECTION
This article was submitted to Invertebrate Physiology, a section of the journal Frontiers in Physiology

RECEIVED 13 November 2022
ACCEPTED 23 December 2022
PUBLISHED 13 January 2023

CITATION
Barman M, Samanta S, Ahmed B, Dey S, Chakraborty S, Deeksha MG, Dutta S, Samanta A, Tarafdar J and Roy D (2023), Transcription dynamics of heat-shock proteins (Hsps) and endosymbiont titres in response to thermal stress in whitefly, *Bemisia tabaci* (Asia-I).
Front. Physiol. 13:1097459.
doi: 10.3389/fphys.2022.1097459

Transcription dynamics of heat-shock proteins (Hsps) and endosymbiont titres in response to thermal stress in whitefly, *Bemisia tabaci* (Asia-I)

Mritunjoy Barman[1,2*†], Snigdha Samanta[1†], Bulbul Ahmed[2], Soumik Dey[3], Swati Chakraborty[4], M.G. Deeksha[5], Subham Dutta[4], Arunava Samanta[1], Jayanta Tarafdar[4*] and Deepayan Roy[2*]

[1]Department of Agricultural Entomology, B.C.K.V, Mohanpur, West Bengal, India, [2]GD Goenka University, Gurgaon, Haryana, India, [3]Faculty Centre for Agriculture Rural and Tribal Development (ARTD), RKMVERI, Ranchi, India, [4]Department of Plant Pathology, B.C.K.V, Nadia, West Bengal, India, [5]Division of Entomology, I.C.A.R-Indian Agricultural Research Institute, New Delhi, India

The sweet potato whitefly, *Bemisia tabaci* (Gennadius), is one of the several species complexes of whitefly that are currently significant agricultural pests. *Bemisia tabaci* infests more than 600 plant species and thrives under a wide range of temperature conditions. In addition to the direct damage caused by sucking plant sap, it vectors several plant viruses. Heat-shock proteins play a pivotal role in enabling the insect to extend its geographical location, survival, and reproduction under different stress conditions. *B. tabaci* harbours several endosymbionts under the genera *Portiera*, *Rickettsia*, *Hamiltonella*, *Wolbachia*, *Arsenophonus*, *Cardinium*, and *Fritschea* that directly or indirectly affect its fitness. By accelerating cuticle biosynthesis and sclerotisation, symbiotic microbes can reduce or enhance tolerance to extreme temperatures and detoxify heavy metals. Thus, symbionts or microbial communities can expand or constrain the abiotic niche space of their host and affect its ability to adapt to changing conditions. The present study delineates the effect of thermal stress on the expression of heat-shock genes and endosymbionts in *B. tabaci*. Studies of the expression level of heat-shock proteins with the help of quantitative real-time polymerase chain reaction (qRT-PCR) showed that heat- and cold-shock treatment fuels the increased expression of heat-shock proteins (Hsp40 and Hsp70). However, Hsp90 was not induced by a heat- and cold-shock treatment. A significant decrease in the relative titre of secondary endosymbionts, such as *Rickettsia*, *Arsenophonus*, and *Wolbachia*, were recorded in *B. tabaci* upon heat treatment. However, the titre of the primary symbiont, *C. Portiera*, was relatively unaffected by both cold and heat treatments. These results are indicative of the fact that Hsp genes and endosymbionts in *B. tabaci* are modulated in response to thermal stress, and this might be responsible for the adaptation of whitefly under changing climatic scenario.

KEYWORDS

whitefly, endosymbionts, qRT-PCR, heat-shock protein, stress

1 Introduction

The whitefly, *Bemisia tabaci*, is an economically important agricultural pest causing huge damage to crops worldwide. They inflict damage to plants directly and as a vector of several hundred viruses, most of which belong to the genus *Begomovirus* (>320 species), and other economically important viruses belonging to the genera *Ipomovirus*, *Carlavirus*, *Crinivirus*, *Torradovirus*, and *Polerovirus* (Bedford et al., 1994; Jones, 2003; Mugerwa et al., 2021; Navas-Castillo et al., 2011). There are many species and/or biotypes of whiteflies, each with its own preferences for host plants, virus-transmitting abilities, and insecticide resistance (Barman et al., 2022a; De Barro et al., 2011; Gilbertson et al., 2015; Perring, 2001). A wide host adaptability and virus transmission ability make it one of the 100 most dreadful alien invasive species (Barman et al., 2022b; Hogenhout et al., 2008; Lowe et al., 2000). This polyphagous pest has adapted easily to varied temperature regimes across the world, such as in India, ranging from chilling cold temperatures in the hills to oppressively high temperatures in the deserts (Barro et al., 2011; Singh et al., 2012).

Temperature is one of the important determinants of abundance and geographical distribution of every ectotherm including insects (Huey and Kingsolver, 1993). When it comes to the invasive trait of *B. tabaci*, its heat-resistance ability is considered to be one of the underlying reasons (Cui et al., 2008; Lü and Wan 2008; Wan et al., 2009). Insects in general respond to elevated temperatures and other stresses with increase in synthesis of heat-shock proteins (Hsps) (Zhao and Jones, 2012). The role of Hsps in heat/cold stress adaptation, metamorphosis, and developmental responses in other insects is well documented (Waters and Rioflorido, 2007; Aevermann and Walters, 2008; Waters et al., 2008; Pan et al., 2017; Qin et al., 2018; Xiong et al., 2018; Yu et al., 2018; Parsell and Lindquist, 1993). Based on their molecular weight and homologous relationship, the Hsps are divided into five families and they are Hsp100, Hsp90, Hsp70, Hsp60, and small heat-shock proteins (sHsps) (Li et al., 2009). Stress proteins, such as the Hsps, are a potential candidate responsible for the wide adaptability of whitefly across different geographical niches (Wolfe et al., 1999; Salvucci et al., 2000; Lin et al., 2007; Cui et al., 2008; Lü and Wan, 2008; Mahadev et al., 2009). The mechanism by which the Hsps acts as molecular chaperones is quite distinctive; they stabilize proteins to enable host survival under heat-stress conditions by safeguarding the integrity of the host cell and their homeostasis (Jakob et al., 1993).

Considering the change in the climatic scenario of the Indian subcontinent due to imperious human activities, it is rational to detect the differentially expressed genes under thermal stress condition for better understanding of the tolerance capacity of *B. tabaci* to varying temperature conditions, thus delineating the underlying mechanism for niche expansion of this pest across India. In addition, symbiotic bacteria also have an important role to play in improving the fitness of their host, enabling it to sustain under novel climatic conditions (Wernegreen and Moran 2001). In accordance with other plant-sucking insects, *B. tabaci* harbours a diversity of symbionts, which enrich hosts' nutrient-poor diet by synthesizing essential amino acids (Douglas 1989; Baumann 2005; Barman et al., 2020). Endosymbionts are generally classified into two major classes: primary symbionts/P-symbionts and secondary symbionts/S-symbionts (Baumann 2005; Feldhaar 2011). *Candidatus Portiera aleyrodidarum* (hereafter, *Portiera*), being a primary symbiont, occurs in all individuals. Secondary symbionts like *Hamiltonella, Arsenophonus*, *Cardinium*, *Wolbachia*, and *Fritschea* participate in functions that may not be necessary for the survival of the host but renders noticeable influence on its biological adaptation and ecological requirements (Ali et al., 2018; Feldhaar 2011; Khan et al., 2020). *Portiera* is described to be involved in the synthesis of nutrients such as essential amino acids (EAAs) and carotenoids, which are not present in a phloem diet (Cheng et al., 2016; Ferrari and Vavre, 2011; Su et al., 2014). Symbionts like *Hamiltonella* and *Arsenophonus* have been reported to be associated with the transmission of plant viruses (Gottlieb et al., 2010; Rana et al., 2012). *Rickettsia* is also reported to induce genes required for thermo tolerance in whitefly (Brumin et al., 2011). Reference has also been drawn indicating the obligate symbionts as "Achilles' heel" from the perspective of temperature change (Corbin et al., 2017). Variations in the symbiont titre also have a significant impact on the insect fitness (Ali et al., 2019). For example, in *Aphis craccivora*, the quantity of *Buchnera* decreases under both low- and high-temperature conditions, which in turn negatively influences aphid reproduction (Chen et al., 2009).

The effect of heat stress in *B. tabaci* has been explored in the viewpoint of survival and reproduction (Byrne and Bellows 1991; Cui et al., 2008; Wolfe et al., 1999). Keeping these points in mind, the present research experiment was envisioned to assess the survivability of whitefly under sub-optimal and supra-optimal temperature conditions. In particular, we discussed certain key research priorities to shed light on the complex interaction between insect functioning, their microbial communities, and the Hsps gene. Primarily, the following questions were addressed: 1) what are the changes in the expression pattern of three Hsps (Hsp40, Hsp70, and Hsp90) under temperature stress conditions? 2) What are the relative changes in the symbiont titre harboured in *B. tabaci* after exposure to a temperature shock? And 3) is any sort of relation between symbiont titres and the Hsp gene expression? Many studies indicate such complex interactions in insects worldwide; however, this study represents an important step in emphasizing possible mechanisms for developing thermal resistance in *B. tabaci*, which is responsible for its sudden outbreak and wide spread in the country, and suggesting new management strategies.

2 Materials and methods

2.1 Whitefly rearing

Whitefly adults were collected from a research farm (C-Block) in B.C.K.V, India, and reared on brinjal seedlings (Samrat), and the population was maintained in insect-proof rearing cages in the glasshouse under controlled environmental conditions at 26°C ± 1°C with 60% R.H and 16 h light/8 h dark condition and maintained for two generations.

2.2 Genetic identification of whitefly and their symbiont

The genetic purity was verified by every generation by molecular analyses. An mt-COI gene was used for the confirmation of whitefly by

TABLE 1 Primers used in the current study. The primer name, accession number, primer sequence, and annealing temperature are listed in the table.

Organism	Accession number	Primer name	Primer sequence (5′→3′)	Annealing temperature (°C)
PCR primers				
"*Candidatus Portiera aleyrodidarum*"	OK036339, OK036338	Por-F	CGTACGGAAACGTACGCTAA	60
		Por-R	TAAGCATAGGGCTTTCACATAAA	
Rickettsia sp.	OK036575, OK044137	Ric-F	GCTCAGAACGAACGCTGG	56
		Ric-R	GAAGGAAAGCATCTCTGC	
Wolbachia	OK042301, OK042302	Wol-F	CGGGGGAAAATTTATTGCT	56
		Wol-R	AGCTGTAATACAGAAAGGAAA	
Arsenophonus	OK042289, OK042290	Arse-F	CGTTTGATGAATTCATAGTCAAA	54
		Arse_R	GGTCCTCCAGTTAGTGTTACCCAAC	
B. tabaci	MZ973007, MZ973008	C1-J-2195	TTGATTTTTTGGTCATCCAGAAGT	53
		L2-N-3014	TCCAATGCACTAATCTGCCATATTA	
qPCR	**Target gene**	**Primer name**	**Primer sequence (5′→3′)**	**Annealing temperature (°C)**
"*Candidatus Portiera aleyrodidarum*"	16S rDNA	Port73-F	TAGTCCACGCTGTAAACG	60
		Port266-R	AGGCACCCTTCCATCT	
Rickettsia sp.	gltA	glt375-F	AAAGGTTGCTCATCATGCGTT	60
		glt574-R	GCCATAGGATGCGAAGAGCT	
Arsenophonus	23S rDNA	23S-F	CGTTTGATGAATTCATAGTCAAA	60
		23S-R	GGTCCTCCAGTTAGTGTTACCCAAC	
Wolbachia	Wsp	Wsp-F	TGGTCCAATAAGTGATGAAGAAAC	60
		Wsp-R	AAAAATTAAACGCTACTCCA	
B. tabaci	Hsp40	Hsp40-F	AGATGAGGCTCATGGTCAA	60
		Hsp40-R	TGAGAAGCGCATTGCATTGT	
B. tabaci	Hsp70	Hsp70-F	ATTGAAAAGTCCACTGGTAAAGAA	60
		Hsp70-R	GCTTGTACTTTTCAGCATCAGAC	
B. tabaci	Hsp90	Hsp90-F	TGGAAATCAACCCTGACCACCCTG	60
		Hsp90-R	TCACTGACTTGTCGTTCTTC	
B. tabaci	β-actin	Actin-F	ACCGCAAGATTCCATACCC	60
		Actin-R	CGCTGCCTCCACCTCATT	

using forward primer C1-J-2195 (5′-TTGATTTTTTGGTCATCCAGAAGT-3′) and reverse primer L2-N-3014 (5′ TCCAATGCACTAATCTGCCATATTA-3′) (Simón et al., 1994). After the confirmation of the species, samples were drawn from these pure cultures. Total DNA was extracted using GSure® Insect DNA Mini Kit (GCC Biotech, India) from whitefly samples. The presence of four endosymbionts (*Candidatus Portiera*, *Wolbachia*, *Arsenophonus*, and *Rickettsia*) was detected in the reared whitefly populations using their specific primers (Raina et al., 2015). The presence of these endosymbionts in the field population of whitefly was confirmed with the findings of Singh et al., (2012). A polymerase chain reaction (PCR) program was carried out in a total volume of 25 µl, containing 2 µl of template DNA, 12.5 µl PCR Master Mix, 8.5 µl molecular grade water, and 1 µl each of a forward and reverse primer specific to the symbiont. A thermal cycler programmed a denaturation at 94°C for 5 min, followed by 40 cycles of 94°C for 30 s, annealing at different temperature specific to the endosymbiont (60°C for *Portiera*, 54°C for *Arsenophonus*, and 56°C for *Wolbachia* and *Rickettsia*) for 30 s. An extension was carried out at 72°C for 40 s with a final extension at 72°C for 5 min.

2.3 Thermal stress on whitefly

Whitefly adults collected from brinjal plants were placed in small glass tubes of 50 × 5 mm and covered with gauze at the top for smooth breathing. They were subjected to different temperature treatments (T1 = 12°C, T2 = 18°C, T3 = 44°C, and C = 26°C) in a Merck incubator for 3 h, with C being the control for the

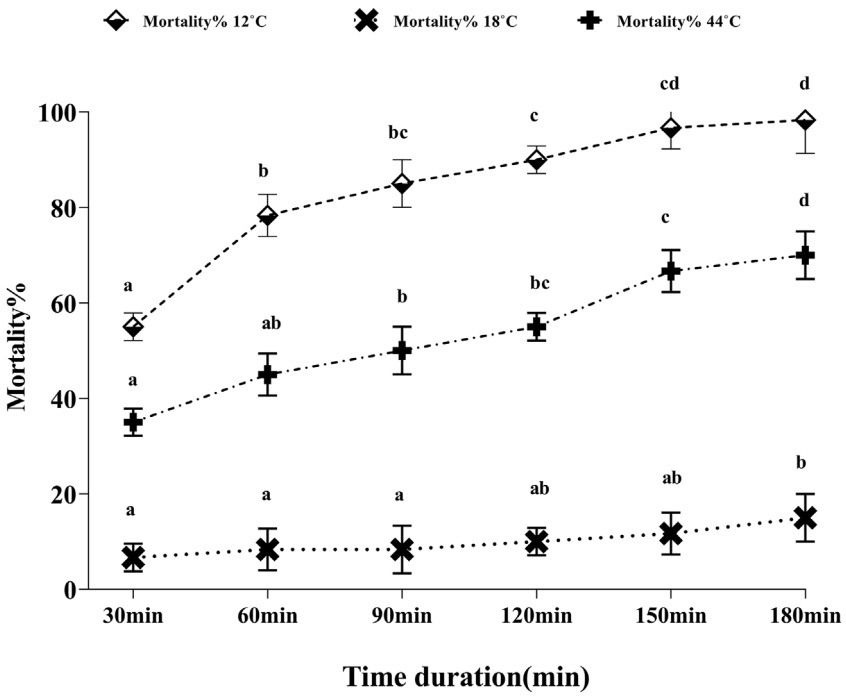

FIGURE 1
Percentage mortality of whitefly adults in response to thermal stress (12°C, 18°C, and 44°C). Whitefly adults from each treatment were incubated for 30, 60, 90, 120, 150, and 180 min in three replicates, and the mortality rates were measured after each incubation time.

experiment. Each treatment consisted of three replicates with 20 adult whiteflies in each replicate. The mortality rate of whitefly adults in each replicate was calculated at an interval of 30 min up to 3 h. The tubes were simultaneously transferred at room temperature (26°C) to allow the adult whiteflies to recover the heat shock. The treated samples were henceforth stored at −80°C for further experimentation.

2.3 RNA isolation and cDNA synthesis

RNAs were extracted from treated whitefly using the insect RNA isolation kit (Thermo Fisher Scientific) following the manufacturer's protocol (Morin et al., 2017). For each treatment, the RNA templates consist of 40 individual whiteflies that were eluted in 30 µl of molecular-grade water. RNA quality was evaluated using Invitrogen ™ Qubit ™ four Fluorometer (Thermo Fisher Scientific) to determine the quality and quantity with high precision per µl of RNA, and the eluted templates were stored at −80°C until use.

The synthesis of complementary DNA was performed by using GeneSure H-Minus First-Strand cDNA Synthesis Kit (Genetix Biotech Asia Pvt. Ltd.) by mixing 2.5 µl of total RNA with 1 µl of oligo dT, 1 µl 10 mM dNTPs, and DEPC-treated water to a volume of 12 µl. The solution was incubated at 65°C for 5 min, and the following reagents were added: 4 µl 5X First-Strand buffer, 1 µl ribonuclease inhibitor (40 units/µl), and 4 µl DEPC-treated water. This mixture was placed at 25°C for 5 min before adding 1 µl M-MLV RT. A final incubation at 42°C for 60 min, followed by 70°C for 15 min was performed for terminating the reaction.

2.4 DNA extraction

Heat shock-treated whitefly samples (20 individuals/treatments) were subjected to a DNA extraction with the help of the insect DNA extraction kit (GCC Biotech, India). The purified DNA template was eluted in 40 µl of nuclease-free water supplied with the kit. The final products were assessed with the help of Invitrogen ™ Qubit ™ 4 Fluorometer (Thermo Fisher Scientific) to determine the quality and quantity with high precision per µl of DNA.

2.5 Quantitative PCR and quantitive RT-PCR analysis

The expression of Hsp genes and the relative amount of different symbionts were examined using the qPCR and qRT-PCR protocol. 2X SYBR Green qPCR Master Mix (Applied Biosystems, United States) was used. Primers name, annealing temperature, and sequences are shown in Table 1. The DNA and cDNA samples were run in triplicate to ensure the validity of the data using the Agilent Technologies Stratagene Mx3000P sequence detection system. Amplification was carried out in 20 µl reaction containing 10 µl 2X SYBR Green PCR Master Mix, 1 µl of each primer (10 µM each), 2 µl template DNA, 0.4 µl ROX, and 5.6 µl molecular-grade water. The cycling condition was as follows: 3 min activation at 95°C, followed by 40 cycles of 40 s at 95°C, 40 s at 60°C, and 45 s at 72°C. The relative expression of each target was calculated using the $2^{-\Delta\Delta CT}$ method (Livak and Schmittgen, 2001). The β-actin (nuclear gene) level, which did not reflect any significant difference across treatments, was used as an endogenous control.

2.6 Data analysis

The differences in the relative expression of Hsp genes and the amount of different symbionts in *B. tabaci* treated under different heat stress conditions were analysed using one-way analysis of variance (ANOVA). The means were compared using Tukey's test at p-value < 0.05. The statistical analysis was performed using SPSS 14.0 (SPSS Inc. Chicago, IL). The error bars present in the graphs represented the standard error.

3 Results

3.1 Effect of heat stress on adult mortality

To evaluate the direct effect of temperature stress in whiteflies, the mortality rate of the whitefly adults was counted every 30 min of exposure for 3 h (Figure 1). Upon the exposure of whitefly to 44°C, the initial mortality rate was noted to be 35%, which steadily increased to 66.67% and 70% at 2.5 and 3 h, respectively. On the contrary, at an extremely low temperature (12°C), the mortality rate was calculated to be as high as 55% within the initial 30 min that rapidly increased to 78% after 1 h of continuous heating, and finally reached 98.33% until 3 h. However, at a moderately low temperature (18°C), the calculated mortality rate was low, 6.67% in the initial 30 min to only 15% until 3 h.

3.2 Characterization of cryptic species of *B. tabaci* and the endosymbionts

Several DNA-based techniques have been exploited for proper identification of *B. tabaci* cryptic species (Simón et al., 1994). Nonetheless, sequence analysis of the mitochondrial cytochrome oxidase I (mt-COI) gene has been the most widely accepted (Barman et al., 2022c). In the current study, running culture is one homogenous population of *B. tabaci* that was identified by using the primer pair (C1-J-2195 F/L2-N-3014 R) of the universal mt-COI gene. Based on the previously known sequences in the GenBank database, a phylogenetic tree was constructed by using the maximum likelihood phylogram (Figure 2A). The phylogenetic analysis of the determined COI sequences assured that the populations belonged to Asia-I cryptic species. The sequence can be retrieved using the GenBank Accession No. MZ973007 and MZ973008.

Subsequently, a diagnostic PCR confirmed the presence of primary endosymbiont *Portiera* and secondary endosymbionts *Wolbachia*, *Arsenophonus*, and *Rickettsia* in the selected whitefly population. The sequencing results of the products could generate 1,350, 580, 560, and 800 nt sequences for *Portiera*, *Arsenophonus*, *Wolbachia*, and *Rickettsia*, respectively. From BLASTn analysis, we obtained 100% similarity with other sequences available in NCBI (Figure 3).

3.3 Effect of temperature treatments on an Hsp transcript level

After the exposure of whitefly at 12°C, 18°C, and 44°C for 3 h (hours), the transcript level of Hsp40, Hsp70, and Hsp90 displayed mercurial changes in their expression pattern. The transcript level of Hsp70 showed significant ($F_{3,\ 8}$ = 2.687, p = 0.017) upregulation under all the three temperature conditions with an increase of 2.90-, 2.09-, and 3.34-fold (Figure 2B), whereas the transcript level of Hsp40 was not upregulated at all three temperature regimes but only at 12°C and 44°C with an increase of 32.85- and 89.62-fold, respectively. Moreover, Hsp40 showed noticeable downregulation of the transcript level at 18°C ($F_{3,8}$ = 10.71, p = 0.003) (Figure 2C). On the contrary, the expression level of Hsp90 was downregulated at extremely low (12°C) and high (44°C) temperatures with an elevation of 1.78 times, observed at 18°C which showed statistical significance ($F_{3,8}$ = 7.83, p = 0.009) (Figure 2D).

3.4 Relative density of endosymbionts in whitefly after different temperature treatments

After exposing whitefly to different temperature treatments (12°C, 18°C, and 44°C), the relative titre of four endosymbionts (*Candidatus Portiera*, *Arsenophonus*, *Wolbachia*, and *Rickettsia*) was measured. It was observed that the primary and secondary symbiont titre were markedly different in terms of relative quantity (Figures 4A–D). In the presence of extremely high temperatures (44°C), the primary endosymbiont (*Portiera*) was 2.04-fold greater in the relative amount, whereas the three secondary endosymbionts, namely, *Arsenophonus*, *Wolbachia*, and *Rickettsia*, had a reduction in the relative density (0.62-, 0.68-, and 0.58-folds, respectively) as compared to the control. Significant differences were observed for all the secondary symbionts (*Arsenophonus*: $F_{3,\ 8}$ = 13.39, p = 0.0017; *Wolbachia*: $F_{3,\ 8}$ = 4.34, p = 0.041; and *Rickettsia*: $F_{3,8}$ = 19.27, p = 0.0005) except the primary symbiont *Portiera* ($F_{3,\ 8}$ = 1.07, p = 0.41). There was an increase in relative densities of 1.35-fold in *Portiera*, 3.29-fold in *Arsenophonus*, and 1.05-fold in *Rickettsia* at 18°C, whereas the relative densities of *Wolbachia* exhibited a decrease of 0.39-fold. Alternatively, at extremely low temperatures (12°C), all aforementioned endosymbionts showed an increase in the relative density.

3.5 Correlation of a relative endosymbionts titre with Hsp gene expression at different temperature treatments

Hsp gene expression correlated positively or negatively with the relative endosymbiont titre at different temperatures (Table 2). There was a strong uphill linear relationship between all the endosymbionts and Hsp40 at extremely low temperatures (12°C) (Figures 5A–D), whereas both Hsp70 and Hsp90 expression showed a downward linear relationship with all four endosymbionts. The *Wolbachia* titre is highly influenced at extremely low temperatures (12°C) by Hsp expression, while the *Arsenophonus* titre is least affected, either positively or negatively. At moderately low temperature (18°C), *Arsenophonus* and *Wolbachia* displayed a positive relationship with Hsp40, whilst *Portiera* exhibited a negative relation. In a similar manner, all the secondary symbionts (*Arsenophonus*, *Wolbachia*, and *Rickettsia*) except *Portiera* exhibited a positive relation with Hsp70. Nonetheless, primary symbiont, *Portiera*, exhibited a strong

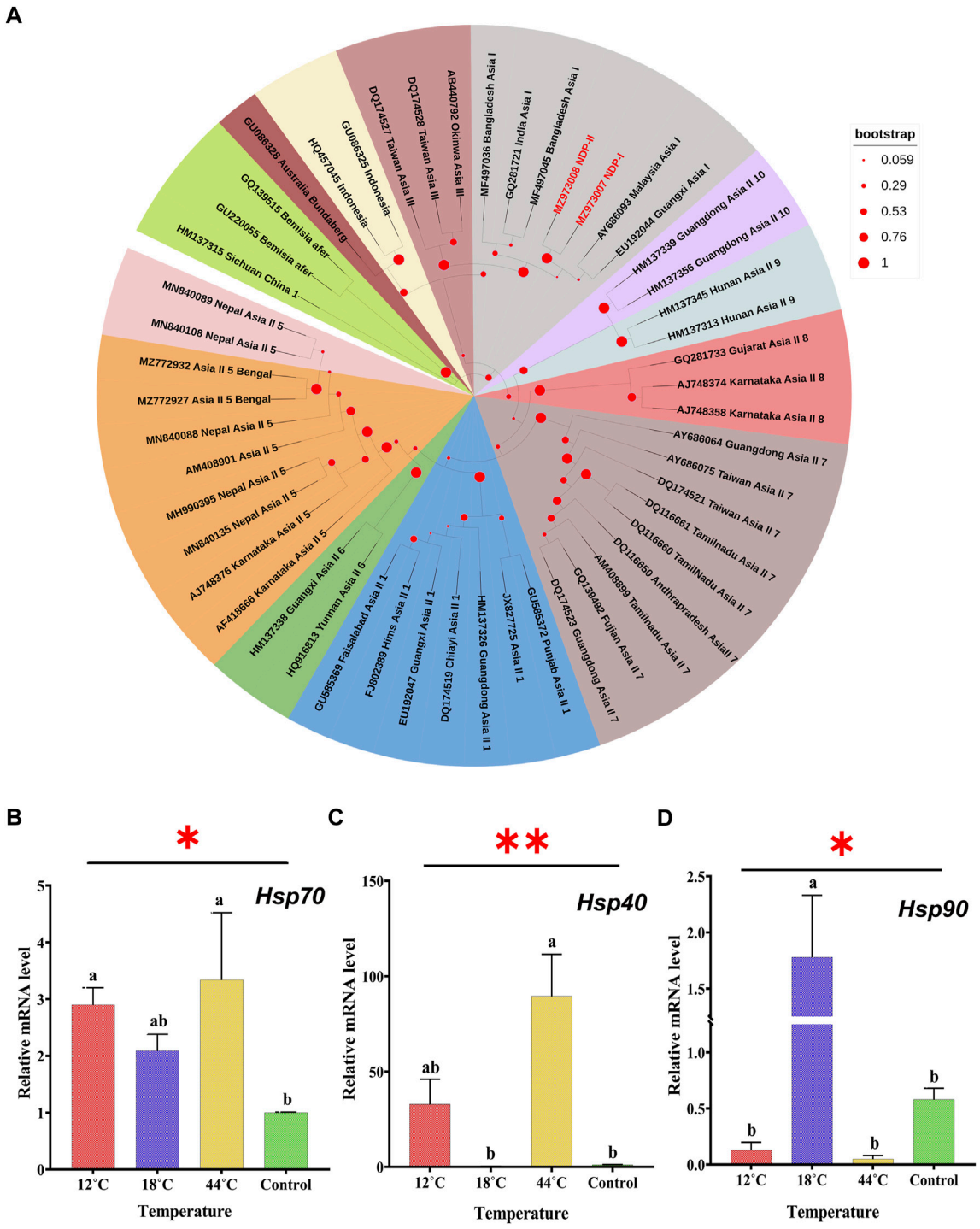

FIGURE 2
(A) Phylogenetic tree of *B. tabaci* cryptic species is identified based on cytochrome oxidase subunit I (COI) sequences. The samples from the study are indicated by bold text (red) in the tree; all other sequences were obtained from the GenBank database. *Bemisia afer* sequences were taken as an out-group. Effect of thermal stress (12°C, 18°C, 26°C, and 44°C) on the transcript level of Hsp70 **(B)**, Hsp40 **(C)**, and Hsp90 **(D)**. Adult whitefly exposed to 26°C was considered as control. Relative mRNA expression levels measured by qRT-PCR with β- actin are used as a reference gene. The different letters indicate statistically significant differences between the treatments. $p \leq 0.05$ is indicated by *, and $p \leq 0.01$ is indicated by **.

uphill linear relationship with Hsp90. Thus, at a moderately low temperature (18°C), the relationship between symbiont titres and Hsp gene expression varied significantly (Figures 5E–H). Lastly, at an extremely high temperature (44°C), the relative titre of *Portiera*, *Arsenophonus*, and *Wolbachia* showed a positive relationship with Hsp40, whereas *Rickettsia* exhibited a negative relation. On the contrary, the relative titre of *Rickettsia* exhibited a positive correlation with Hsp70 and Hsp90, while *Arsenophonus* and *Wolbachia* displayed an opposite trend (Figure 5I–L).

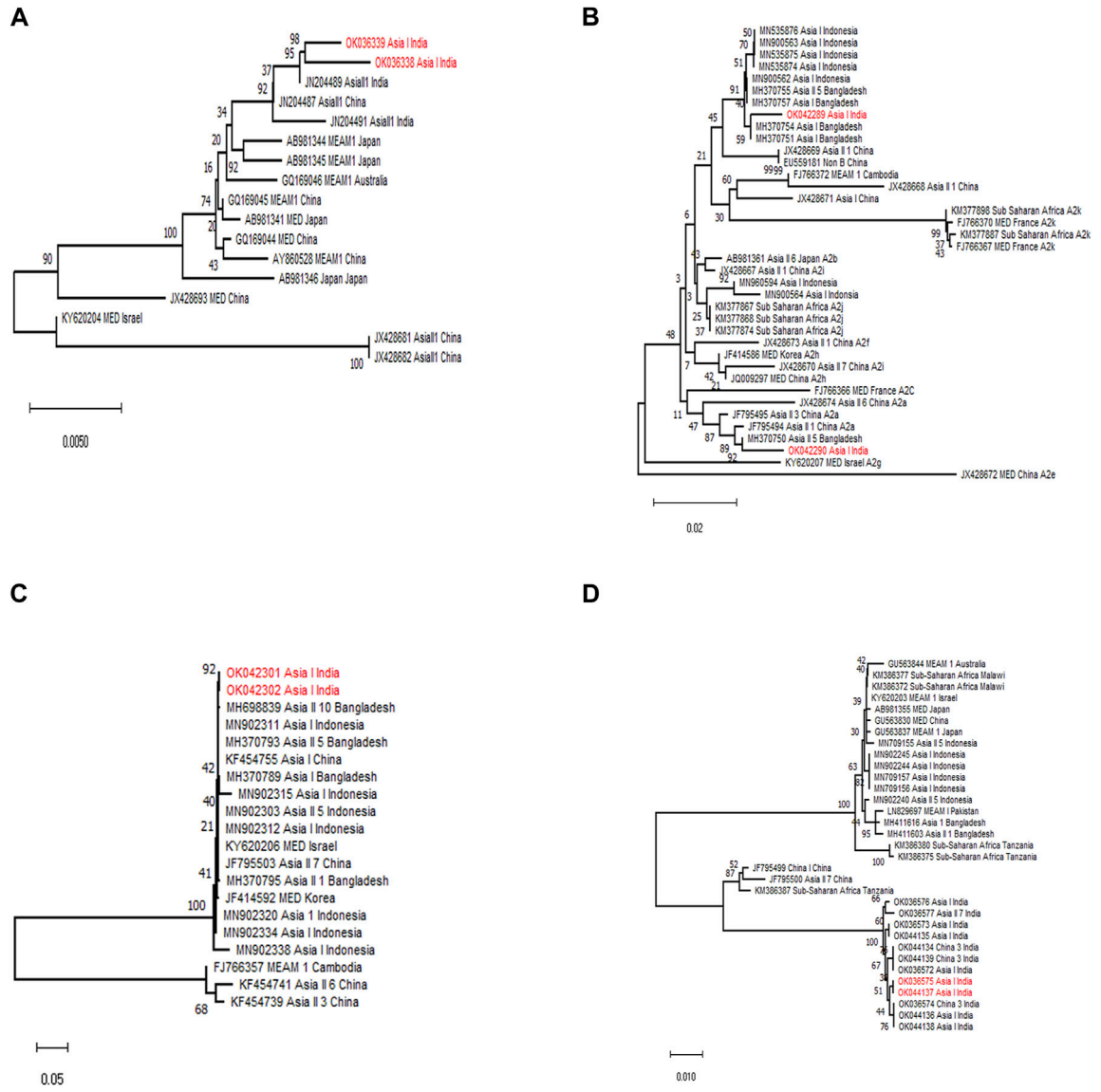

FIGURE 3
Phylogenetic tree of primary and secondary endosymbionts of *B. tabaci* based on 16S rDNA (*Portiera*, *Wolbachia*, and *Rickettsia*) and 23S rDNA (*Arsenophonus*) gene segments. The samples from the study are indicated by bold text (red) in the tree; all other sequences were obtained from the GenBank database. **(A)** Maximum likelihood phylogenetic tree of the 16S rDNA sequences of *Portiera* sp. infecting different whitefly populations. **(B)** Maximum likelihood phylogenetic tree of the 23S rDNA sequences of *Arsenophonus* sp. infecting different whitefly populations. **(C)** Maximum likelihood phylogenetic tree of the 16S rDNA sequences of *Wolbachia* sp. infecting different whitefly populations. **(D)** Maximum likelihood phylogenetic tree of the 16S rDNA sequences of *Rickettsia* sp. infecting different whitefly populations.

4 Discussion

Temperature is one of the important determinants of an organism's distribution and abundance (Colinet et al., 2010). The ability to tolerate thermal stress is a vital parameter enabling the survival of *B. tabaci* under varying temperature conditions, thus playing a pivotal role in its wide distribution pattern in the Indian sub-continent (Samanta et al., 2021). In the current study, we determined the mortality rate of whitefly adults on the exposure to thermal stress and highlighted the molecular aspects underlying the heat responsive mechanism in *B. tabaci*. The varying mortality percentage of whitefly on subjection to different temperature stress conditions was observed with a higher mortality rate at 12°C than the mortality rate noted at 44°C. Cui et al. (2008) also reported a low mortality rate of whitefly at higher temperatures (40°C). A possible reason for this variation may be the differential expression pattern of Hsp genes that are reported to play a vital role in protecting organisms under heat stress conditions (Salvucci et al., 2000; Hoffmann et al., 2003; Wang et al., 2019).

Hsp genes are a central protagonist in helping organisms to cope with different environmental challenges, such as pathogen infection, xenobiotic substances, and thermal stress conditions (Chakraborty et al., 2021; Derecka et al., 2013; Somero, 1995; Sun and MacRae 2005; Tissiêrs et al., 1974). The present study puts forward the differential expression of three Hsp genes (Hsp40,

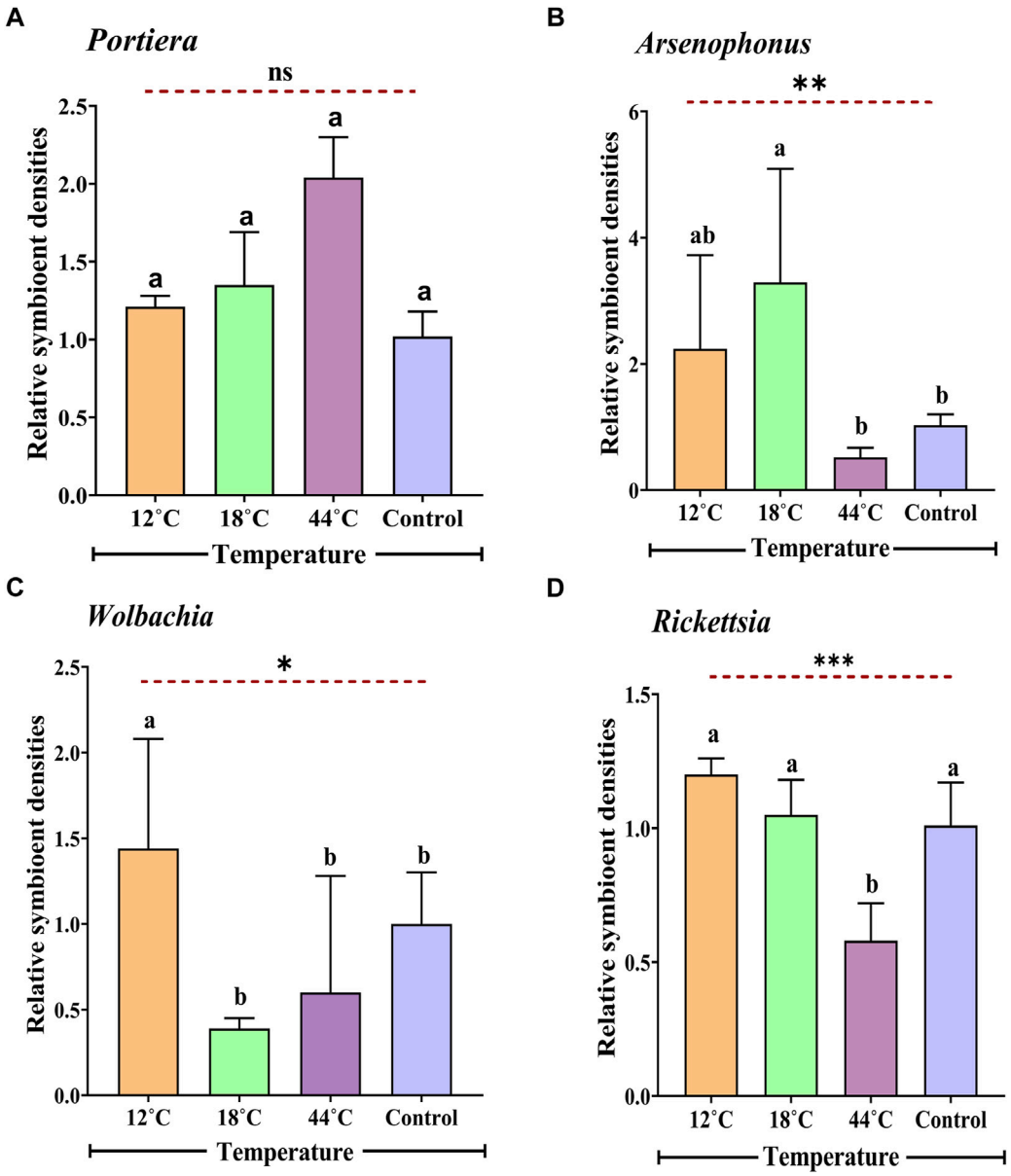

FIGURE 4
Relative titre of *Portiera* **(A)**, *Arsenophonus* **(B)**, *Wolbachia* **(C)**, and *Rickettsia* **(D)** in four different temperatures (12°C, 18°C, 26°C, and 44°C) *B. tabaci* populations as determined by quantitative PCR (normalized according to the amount of an actin gene). Adult whitefly exposed to 26°C was considered as control. Values for the relative amount of symbionts are means ± SEM of three replicates for each treatment. The data were analysed with one-way ANOVA. The different letters indicate statistically significant differences between the treatments. *ns* = non-significant, $p \leq 0.05$ is indicated by *, $p \leq 0.01$ is indicated by **, and $p \leq 0.001$ is indicated by ***.

Hsp70, and Hsp90) in *B. tabaci* under a heat-shock condition. The temperature treatment of whitefly resulted in an induced expression of Hsp70 under all the three conditions (12°C, 18°C, 44°C, and 26°C acting as control) with maximum expression observed at 44°C. The elevation of Hsp70 at extremes of temperature suggests its involvement in both heat and cold adaptation (Xiao et al., 2019). Reports suggest that the optimal expression level of Hsp70 is critical to the maintenance of cell function and homeostasis (Wheeler et al., 1999; Kristensen et al., 2002) and for chaperons to bind peptide chains (Fink, 1999). The transcript level of Hsp40 was also significantly upregulated upon the exposure of whitefly to extreme cold (12°C) and hot (44°C) conditions with a much higher expression level at 44°C, indicating the possible involvement of Hsp40 in heat adaptation of whitefly. Previous studies mentioned the association of Hsp genes in insects with important functions such as the regulation of growth and reproduction that, henceforth, increased their ability to fit under adverse environmental conditions (Lu et al., 2015; Quan et al., 2022). Work pertaining to the role of Hsp40 in whitefly seems limited; however, there are unequivocal indications regarding the role of Hsp40 in Hymenoptera, wherein, upon protein denaturation, Hsp40 delivers unfolded protein to Hsp70, and they together facilitate refolding by ATP binding and hydrolysis (Nguyen et al., 2016; Rinehart et al., 2007). Upregulation of the two

TABLE 2 Correlation of relative endosymbiont titres and Hsp gene expression, under different temperature treatments.

Temperature	r	P	R^2	r	P	R^2	r	P	R^2
Treatment	Hsp40			Hsp70			Hsp90		
Relationship with *Portiera* titre									
12°C	0.74	0.46	0.54	−0.52	0.65	0.26	−0.48	0.67	0.23
18°C	−0.18	0.88	0.03	−0.98	0.03*	0.95	0.89	0.04*	0.78
44°C	0.66	0.54	0.43	0.40	0.73	0.16	−0.11	0.93	0.01
Relationship with *Arsenophonus* titre									
Temperature	r	P	R^2	r	P	R^2	r	P	R^2
Treatments	Hsp40			Hsp70			Hsp90		
12°C	0.53	0.64	0.28	−0.26	0.82	0.07	−0.23	0.85	0.05
18°C	1.00	0.04*	0.99	0.47	0.68	0.22	0.20	0.86	0.04
44°C	0.28	0.81	0.08	−0.99	0.09	0.97	−0.78	0.42	0.61
Relationship with *Wolbachia* titre									
Temperature	r	P	R^2	r	P	R^2	r	P	R^2
Treatments	Hsp40			Hsp70			Hsp90		
12°C	0.95	0.19	0.90	−0.83	0.38	0.68	−0.80	0.40	0.64
18°C	0.42	0.72	0.17	0.99	0.02*	0.99	−0.74	0.46	0.55
44°C	0.95	0.02*	0.90	−0.11	0.92	0.012	−0.59	0.59	0.35
Relationship with *Rickettsia* titre									
Temperature	r	P	R^2	r	P	R^2	r	P	R^2
Treatments	Hsp40			Hsp70			Hsp90		
12°C	0.57	0.61	0.32	−0.32	0.79	0.10	−0.28	0.82	0.07
18°C	−0.26	0.83	0.06	0.79	0.42	0.62	−1.00	0.02*	0.99
44°C	−0.44	0.70	0.19	1.00	0.01*	0.99	0.88	0.31	0.77

r, correlation coefficient; R^2, coefficient of determination; and *, significant level ($p < 0.05$).

Hsps (Hsp40 and Hsp70) under thermal stress conditions are indicative of their role in preventing cell damage under such stress conditions.

Contrary to the upregulation of most Hsp genes subjected to heat stress, a low basal expression of Hsp90 was observed, when exposed to extremes of temperature. Hence, it would not be wrong to say that the expression of Hsp90 is less dependent upon temperature stress than other Hsps. However, in the case of Hsp90, the transcript level attained a peak at 18°C. This clearly suggests that Hsps might have evolved from different expression patterns under different temperature conditions. Reports indicate the participation of Hsp90 in the negative regulation of proteins (Lindquist and Craig, 1988). The susceptibility of *B. tabaci* to temperature has been reported to vary according to geography and genetic groups (Pusag et al., 2012). This highlights the importance of thermal tolerance for insects including whitefly to thrive under such a diverse climatic condition as that of India.

In addition to determining the role of Hsp genes in adaptation and survivability of whitefly, an important dynamic which remains unattended is the host–microbe association or to say symbiont-mediated modulation of host traits such as thermal tolerance. Thermal variation has a strong influence on host metabolism, and any deviation from optimum environmental conditions could have a deleterious influence on the hosts' survival and fecundity (Macmillan, 2019). To shed light on this aspect, we evaluated the change in the relative amount of four endosymbionts in whitefly when subjected to thermal stress. Although we are aware that many host–microbe interactions protect their host partners from pathogens or predators (Flórez et al., 2015), less is acknowledged regarding the influence of these symbionts on insects' thermal tolerance. However, reports suggest that temperature has a significant influence in the abundance of endosymbionts harboured in insects and their interaction (Bensadia et al., 2006; Burke et al., 2010.; Dunbar et al., 2007.; Montllor et al., 2002). Microbes can either expand or restrict the abiotic niche of their host partners, thus influencing their ability

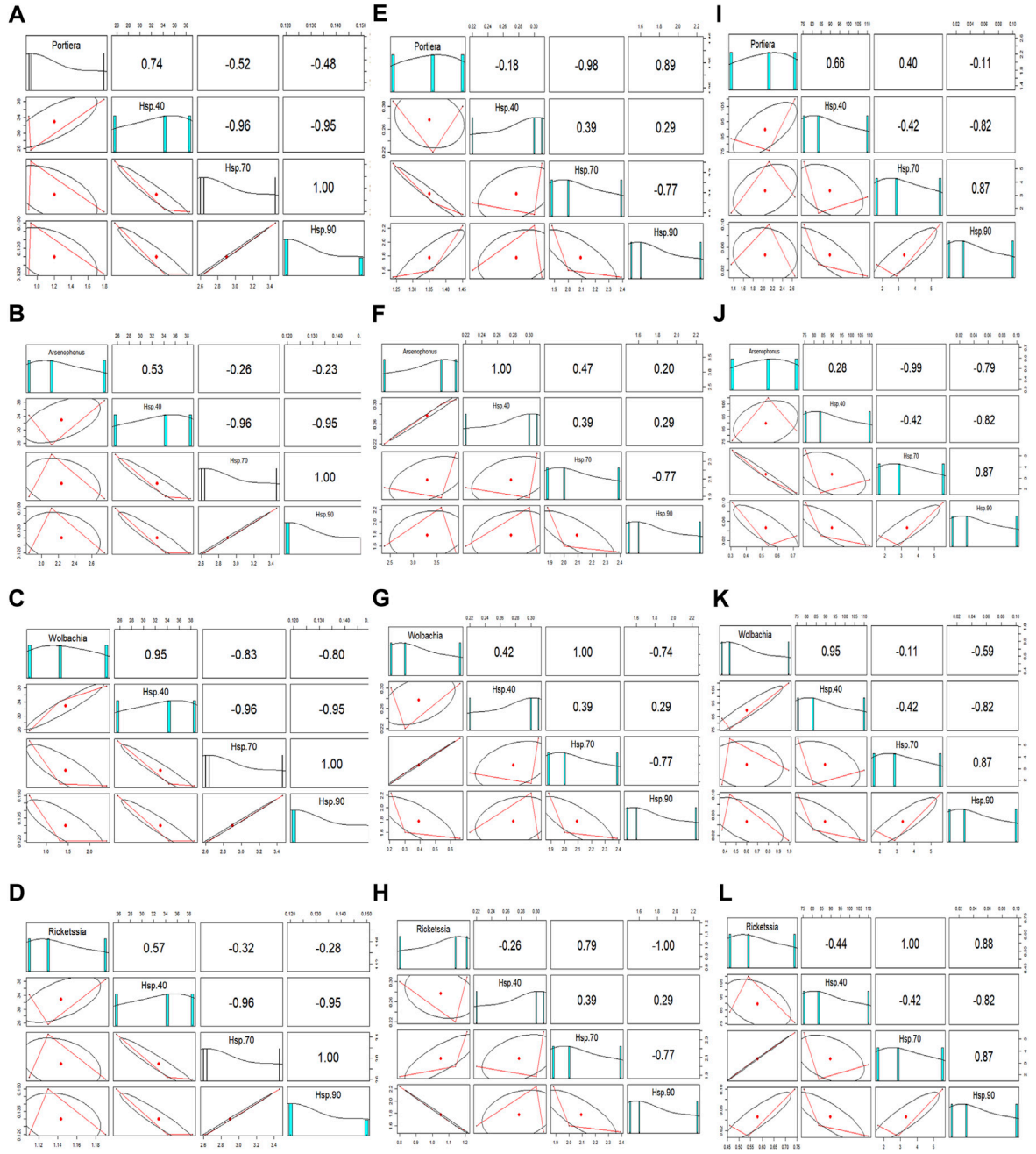

FIGURE 5
Correlation of relative endosymbiont (*Portiera, Arsenophonus, Wolbachia*, and *Rickettsia*) titres and Hsp gene (Hsp40, Hsp70, and Hsp90) expression, at **(A–D)** 12°C, **(E–H)** 18°C, and **(I–L)** 44°C.

to adapt to the fluctuating environmental condition (Lemoine et al., 2020; Zaynab et al., 2019).

Our findings revealed multiple patterns in the relative abundance of primary and secondary symbionts upon subjection to thermal stress. The primary endosymbiont, *Portiera*, was relatively unaffected by temperature treatment. Localization of *Portiera* inside the bacteriosome might be held accountable for their limited response to temperature stress (Su et al., 2014; Li et al., 2017; Caspi-Fluger et al., 2011). On the contrary, depletion in the quantity of the three secondary symbionts (*Arsenophonus*, *Wolbachia*, and *Rickettsia*) was measured at 44°C. This indicates a possible involvement of the facultative symbionts in enhanced thermo-tolerance of *B. tabaci* at extremely high temperatures and hence the low mortality rates at this temperature. Experiments carried out in the pea aphid also demonstrated the involvement of facultative symbionts in protecting hosts from detrimental effects of thermal stress (Oliver et al., 2010). Brumin et al. (2011) reported the spatial location of *Rickettsia* outside the bacteriosome, resulting in a significant decrease of the endosymbiont when subjected to thermal stress. Shan et al. (2014) also observed a reduction in *Rickettsia* population in heat-treated whitefly, although the reduction was non-significant. Disturbances in gut symbionts

when exposed to high temperature were noted in many insects. A possible explanation to this could be that an escalation in temperature upsets the stability of some protein that is involved in the transportation of metabolite, thereby restricting supplementation of the metabolites between the partners. It was also seen that titres of *Wolbachia* were depleted in *Aedes albopictus* when exposed to elevated temperature conditions (Mouton et al., 2007; Wiwatanaratanabutr and Kittayapong, 2009). Such depletion does not essentially indicate host extinction. Hence, the primary symbionts are reported to be directly involved in vital metabolic functions of insect host, and on the flip side, the secondary symbionts are reported to mitigate the effect of heat stress on the primary symbionts, thus aiding the hosts' survival (Lemoine et al., 2020). Thus, it would not be wrong to say that host–microbial association has a key role in temperature acclimation; however, the exact dynamics vis-à-vis direct effect of an abiotic factor on any sort of symbiotic interactions still remains unknown and will require further exploration.

Deleterious effects of thermal stress on symbiont quantity may be allayed *via* other mechanism such as gene expression (Brumin et al., 2011) or modulation of the host behaviour (Truitt et al., 2019). In the current study, the expression of the Hsp genes and relative symbionts titre were highly variable under different temperature conditions. Based on the correlation studies, we assumed that endosymbionts infection modulate host gene expression by altering the expression of specialized Hsp genes or by affecting the activities of transcription factors (Moon et al., 2021; Brennan et al., 2008). In addition, further investigation is required in this direction.

In the light of current disturbances in the ecological and environmental balance caused by human activities, the present investigation can be considered an important step in predicting the potential factors responsible for the adaptation of whitefly in such a diverse temperature regime. However, few vital questions that arise on our way stem from the basic evolution of symbiont-mediated thermal resistance/heat tolerance and the precise molecular interactions occurring between symbionts and host genes. Particularly, through proper clarification of these vital issues, a symbiont-targeted pest management will prove to be an effective control component for the future agricultural community. However, detailed work needs to be carried out before the large-scale application of symbiont-targeted pest management strategies.

Data availability statement

The datasets presented in this study can be found in online repositories. The names of the repository/repositories and accession number(s) can be found in the article/Supplementary Material.

Author contributions

MB: conceptualization, data curation, and software. SC: checking of manuscript and software. DM: checking of manuscript, analysis, and correction of manuscript, AS: supervision. JT: supervision, validation, reviewing, and editing. SS: conceptualization, methodology, and writing—original draft preparation. SD: writing—original draft preparation. DR: Reviewing and Editing. BA: Analysis, Reviewing and Editing. SD: Analysis, Reviewing and Editing

Acknowledgments

The first author thankfully acknowledges Bidhan Chandra Krishi Viswavidyalaya (ICAR-accredited State Agricultural University) for providing the university research scholarship to carry out the research work.

Conflict of interest

The authors declare that the research was conducted in the absence of any commercial or financial relationships that could be construed as a potential conflict of interest.

Publisher's note

All claims expressed in this article are solely those of the authors and do not necessarily represent those of their affiliated organizations, or those of the publisher, the editors, and the reviewers. Any product that may be evaluated in this article, or claim that may be made by its manufacturer, is not guaranteed or endorsed by the publisher.

References

Aevermann, B. D., and Waters, E. R. (2008). A comparative genomic analysis of the small heat shock proteins in *Caenorhabditis elegans* and briggsae. *Genetica* 133, 307–319. doi:10.1007/s10709-007-9215-9

Ali, H., Muhammad, A., Islam, S. U., Islam, W., and Hou, Y. (2018). A novel bacterial symbiont association in the hispid beetle, *Octodonta nipae* (Coleoptera: Chrysomelidae), their dynamics and phylogeny. *Microb. Pathog.* 118, 378–386. doi:10.1016/j.micpath.2018.03.046

Ali, H., Muhammad, A., Sanda, N. B., Huang, Y., and Hou, Y. (2019). Pyrosequencing uncovers a shift in bacterial communities across life stages of *Octodonta nipae* (Coleoptera: Chrysomelidae). *Front. Microbiol.* 10, 466. doi:10.3389/fmicb.2019.00466

Barman, M., Chakraborty, S., Das, S., Samanta, S., Samanta, A., and Tarafder, J. (2020). Molecular characterization of the endosymbiont *Candidatus portiera aleyrodidarum* collected from West Bengal.

Barman, M., Samanta, S., Upadhyaya, G., Thakur, H., Chakraborty, S., Samanta, A., et al. (2022c). Unraveling the basis of neonicotinoid resistance in whitefly species complex: Role of endosymbiotic bacteria and insecticide resistance genes. *Front. Microbiol.* 13, 901793. doi:10.3389/fmicb.2022.901793

Barman, M., Samanta, S., Chakraborty, S., Samanta, A., and Tarafdar, J. (2022a). Copy number variation of two begomovirus acquired and inoculated by different cryptic species of whitefly, *Bemisia tabaci* in Okra. *PloS one* 17 (3), e0265991. doi:10.1371/journal.pone.0265991

Barman, M., Samanta, S., Thakur, H., Chakraborty, S., Samanta, A., Ghosh, A., et al. (2022b). Effect of neonicotinoids on bacterial symbionts and insecticide-resistant gene in whitefly, *Bemisia tabaci*. *Insects* 12, 742. doi:10.3390/insects12080742

Barro, P. J. D., Liu, S. S., Boykin, L. M., and Dinsdale, A. B. (2011). *Bemisia tabaci*: A statement of species status. *Annu. Rev. Entomol.* 56, 1–19. doi:10.1146/annurev-ento-112408-085504

Baumann, P. (2005). Biology bacteriocyte-associated endosymbionts of plant sap sucking insects. *Annu. Rev. Microbiol.* 59, 155–189. doi:10.1146/annurev.micro.59.030804.121041

Bedford, I. D., Briddon, R. W., Brown, J. K., Rosell, R. C., and Markham, P. G. (1994). Gemini virus transmission and biological characterisation of *Bemisia tabaci* (Gennadius) bio-types from different geographic regions. *Ann. Appl. Biol.* 125, 311–325. doi:10.1111/j.1744-7348.1994.tb04972.x

Bensadia, F., Boudreault, S., Guay, J. F., Michaud, D., and Cloutier, C. (2006). Aphid clonal resistance to a parasitoid fails under heat stress. *J. Insect Physiol.* 52, 146–157. doi:10.1016/j.jinsphys.2005.09.011

Brennan, L. J., Keddie, B. A., Braig, H. R., and Harris, H. L. (2008). The endosymbiont Wolbachia pipientis induces the expression of host antioxidant proteins in an Aedes albopictus cell line. *PLoS One* 3 (5), e2083.

Brown, J. K., and Czosnek, H. (2002). Whitefly transmission of plant viruses. *Adv. Bot. Res. J.* 36, 65–100.

Brumin, M., Kontsedalov, S., and Ghanim, M. (2011). Rickettsia influences thermotolerance in the whitefly *Bemisia tabaci* B biotype. *Insect Sci.* 18, 57–66. doi:10.1111/j.1744-7917.2010.01396.x

Burke, G., Fiehn, O., and Moran, N. (2010). Effects of facultative symbionts and heat stress on the metabolome of pea aphids. *ISMEJ* 4, 242–252. doi:10.1038/ismej.2009.114

Byrne, D. N., and Bellows, T. S., Jr. (1991). Whitefly biology. *Annu. Rev. Entomol.* 36, 431–457. doi:10.1146/annurev.en.36.010191.002243

Caspi-Fluger, A., Inbar, M., Mozes-Daube, N., Mouton, L., Hunter, M. S., and Zchori-Fein, E. (2011). Rickettsia 'in' and 'out': Two different localization patterns of a bacterial symbiont in the same insect species. *PLoS ONE* 6, e21096. doi:10.1371/journal.pone.0021096

Chakraborty, S., Barman, M., Samanta, S., Roy, M., and Tarafdar, J. (2021). Effect of banana bunchy top virus on the heat shock protein genes of *Pentalonia nigronervosa* during temperature susceptibility and its effect on virus transmission. *Agronomy* 11 (9), 1866. doi:10.3390/agronomy11091866

Chen, C. Y., Lai, C. Y., and Kuo, M. H. (2009). Temperature effect on the growth of Buchnera endosymbiont in *Aphis craccivora* (Hemiptera: Aphididae). *Symbiosis* 49, 53–59. doi:10.1007/s13199-009-0011-4

Cheng, W., Li, D., Wang, Y., Liu, Y., and Zhu-Salzman, K. (2016). Cloning of heat shock protein genes (hsp70, hsc70 and hsp90) and their expression in response to larval diapause and thermal stress in the wheat blossom midge, *Sitodiplosis mosellana*. *J. Insect Physiol.* 95, 66–77. doi:10.1016/j.jinsphys.2016.09.005

Colinet, H., Lee, S. F., and Hoffmann, A. (2010). Temporal expression of heat shock genes during cold stress and recovery from chill coma in adult *Drosophila melanogaster*. *FEBS J.* 277, 174–185. doi:10.1111/j.1742-4658.2009.07470.x

Corbin, C., Heyworth, E. R., Ferrari, J., and Hurst, G. D. D. (2017). Heritable symbionts in a world of varying temperature. *Heredity* 118, 10–20. doi:10.1038/hdy.2016.71

Cui, X. H., Wan, F. H., Xie, M., and Liu, T. X. (2008). Effects of heat shock on survival and reproduction of two whitefly species, *Trialeurodes vaporariorum* and *Bemisia tabaci* biotype B. *J. Insect. Sci.* 24, 1–10. doi:10.1673/031.008.2401

De Barro, P. J., Liu, S. S., Boykin, L. M., and Dinsdale, A. B. (2011). Bemisia tabaci: A statement of species status. *Annu. Rev. Entomol.* 56, 1–19. doi:10.1146/annurev-ento-112408-085504

Derecka, K., Blythe, M. J., Malla, S., Genereux, D. P., Guffanti, A., Pavan, P., et al. (2013). Transient exposure to low levels of insecticide affects metabolic networks of honeybee larvae. *PLoS ONE* 8, e68191. doi:10.1371/journal.pone.0068191

Douglas, A. E. (1989). Mycetocyte symbiosis in insects. *Biol. Rev.* 64, 409–434. doi:10.1111/j.1469-185x.1989.tb00682.x

Dunbar, H. E., Wilson, A. C. C., Ferguson, N. R., and Moran, N. A. (2007). Aphid thermal tolerance is governed by a point mutation in bacterial symbionts. *PLoS Bio* l5, e96. doi:10.1371/journal.pbio.0050096

Feldhaar, H. (2011). Bacterial symbionts as mediators of eco-logically important traits of insect hosts. *Ecol. Entomol.* 36, 533–543. doi:10.1111/j.1365-2311.2011.01318.x

Ferrari, J., and Vavre, F. (2011). Bacterial symbionts in insects or the story of communities affecting communities. *Biol. Sci.* 366 (1569), 1389–1400. doi:10.1098/rstb.2010.0226

Fink, A. K. (1999). Chaperone-mediated protein folding. *Physiol. Rev.* 79, 425–449. doi:10.1152/physrev.1999.79.2.425

Flórez, L. V., Biedermann, P. H., Engl, T., and Kaltenpoth, M. (2015). Defensive symbioses of animals with prokaryotic and eukaryotic microorganisms. *Nat. Prod. Rep.* 32, 904–936. doi:10.1039/c5np00010f

Gilbertson, R. L., Batuman, O., Webster, C. G., and Adkins, S. (2015). Role of the insect supervectors *Bemisia tabaci* and *Frankliniella occidentalis* in the emergence and global spread of plant viruses. *Annu. Rev. Virol.* 2 (1), 67–93. doi:10.1146/annurev-virology-031413-085410

Gottlieb, Y., Zchori-Fein, E., Mozes-Daube, N., Kontsedalov, S., Skaljac, M., Brumin, M., et al. (2010). The transmission efficiency of Tomato yellow leaf curl virus by the whitefly *Bemisia tabaci* is correlated with the presence of a specific symbiotic bacterium species. *J. Virol.* 8, 9310–9317. doi:10.1128/JVI.00423-10

Hoffmann, A. A., Sφrensen, J. G., and Loeschcke, V. (2003). Adaptation of Drosophila to temperature extremes: Bringing together quantitative and molecular approaches. *J. Therm. Biol.* 28, 175–216. doi:10.1016/s0306-4565(02)00057-8

Hogenhout, A., Ammar, E. D., Whitfield, A. E., and Redinbaugh, M. G. (2008). Insect vector interactions with persistently transmitted viruses. *Annu. Rev. Entomol.* 46, 327–359. doi:10.1146/annurev.phyto.022508.092135

Huey, R. B., and Kingsolver, J. G. (1993). Evolution of resistance to high temperature in ectotherms. *Am. Nat.* 142, 21–46. doi:10.1086/285521

Jakob, U., Gaestel, M., Engel, K., and Buchner, J. (1993). Small heat-shock proteins are molecular chaperones. *J. Biol. Chem.* 268, 1517–1520. doi:10.1016/s0021-9258(18)53882-5

Jones, D. R. (2003). Plant viruses transmitted by whiteflies. *Eur. J. Plant Pathol.* 109, 195–219. doi:10.1023/a:1022846630513

Khan, K. A., Al-Ghamdi, A. A., Ghramh, H. A., Ansari, M. J., Ali, H., Alamri, S. A., et al. (2020). Structural diversity and functional variability of gut microbial communities associated with honey bees. *Microb. Pathog.* 138, 103793. doi:10.1016/j.micpath.2019.103793

Kristensen, T. N., Dahlgaard, J., and Loeschcke, V. (2002). Inbreeding affects Hsp70 expression in two species of *Drosophila* even at benign temperatures. *Evol. Ecol. Res.* 4, 1209–1216.

Lemoine, M. M., Engl, T., and Kaltenpoth, M. (2020). Microbial symbionts expanding or constraining abiotic niche space in insects. *Curr. Opin. Insect. Sci.* 39, 14–20. doi:10.1016/j.cois.2020.01.003

Li, S. J., Ahmed, M. Z., Lv, N., Shi, P. Q., Wang, X. M., Huang, J. L., et al. (2017). Plant mediated horizontal transmission of Wolbachia between whiteflies. *ISME J.* 11 (4), 1019–1028. doi:10.1038/ismej.2016.164

Li, Z. W., Li, X., Yu, Q. Y., Xiang, Z. H., Kishino, H., and Zhang, Z. (2009). The small heat shock protein (sHSP) genes in the silkworm, *Bombyx mori*, and comparative analysis with other insect sHSP genes. *BMC Evol. Biol.* 9, 1–14. doi:10.1186/1471-2148-9-215

Lin, K., Wu, K., Zhang, Y., and Guo, Y. (2007). Overwintering and population dynamics of *Bemisia tabaci* biotype B in greenhouse during the spring in northern China. *J. Crop Prot.* 26, 1831–1838. doi:10.1016/j.cropro.2007.04.002

Lindquist, S. L., and Craig, E. A. (1988). The heat-shock proteins. *Annu. Rev. Genet.* 22, 631–677. doi:10.1146/annurev.ge.22.120188.003215

Livak, K. J., and Schmittgen, T. D. (2001). Analysis of relative gene expression data using realtime quantitative PCR and the $2^{-\Delta\Delta CT}$ method. *Methods* 25, 402–408. doi:10.1006/meth.2001.1262

Lu, M. X., Xu, J., and Du, Y. Z. (2015). Progress in research on insect small heat shock proteins. *J. Appl. Entomol.* 52, 1326–1332.

Lü, Z. C., and Wan, F. H. (2008). Differential gene expression in whitefly (*Bemisia tabaci*) Bbiotype females and males under heat-shock condition. *Comp. Biochem. Physiol.* 3, 257–262. doi:10.1016/j.cbd.2008.06.003

MacMillan, H. A. (2019). Dissecting cause from consequence: A systematic approach to thermal limits. *J. Exp. Biol.* 222, jeb191593. doi:10.1242/jeb.191593

Mahadav, A., Kontsedalov, S., Czosnek, H., and Ghanim, M. (2009). Thermotolerance and gene expression following heat stress in the whitefly *Bemisia tabaci* B and Q biotypes. *Insect biochem. Mol. Biol.* 39, 668–676. doi:10.1016/j.ibmb.2009.08.002

Moon, E. K., Park, S. M., Chu, K. B., Quan, F. S., and Kong, H. H. (2008). Differentially Expressed Gene Profile of Acanthamoeba castellanii Induced by an Endosymbiont Legionella pneumophila. *The Korean Journal of Parasitology* 59 (1), 67.

Montllor, C. B., Maxmen, A., and Purcell, A. H. (2002). Facultative bacterial endosymbionts benefit pea aphids *Acyrthosiphon pisum* under heat stress. *Ecol. Entomol.* 27, 189–195. doi:10.1046/j.1365-2311.2002.00393.x

Morin, M. D., Frigault, J. J., Lyons, P. J., Crapoulet, N., Boquel, S., Storey, K. B., et al. (2017). Amplification and quantification of cold-associated micro RNAs in the Colorado potato beetle (*Leptinotarsa decemlineata*) agricultural pest. *Insect Mol. Biol.* 26, 574–583. doi:10.1111/imb.12320

Mouton, L., Henri, H., Charif, D., Boule´treau, M., and Vavre, F. (2007). Interaction between host genotype and environmental conditions affects bacterial density in Wolbachia symbiosis. *Biol. Lett.* 3, 210–213. doi:10.1098/rsbl.2006.0590

Mugerwa, H., Colvin, J., Alicai, T., Omongo, C. A., Kabaalu, R., Visendi, P., et al. (2021). Genetic diversity of whitefly (Bemisia spp.) on crop and uncultivated plants in Uganda: Implications for the control of this devastating pest species complex in Africa. *J. Pest Sci.* 94, 1307–1330. doi:10.1007/s10340-021-01355-6

Navas-Castillo, J., Fiallo-Olivé, E., and Sánchez-Campos, S. (2011). Emerging virus diseases transmitted by whiteflies. *Ann. Rev. Phytopathol.* 49, 219–248. doi:10.1146/annurev-phyto-072910-095235

Nguyen, A. D., Gotelli, N. J., and Cahan, S. H. (2016). The evolution of heat shock protein sequences, cis-regulatory elements, and expression profiles in the eusocial Hymenoptera. *BMC Evol. Biol.* 16, 15–13. doi:10.1186/s12862-015-0573-0

Oliver, K. M., Degnan, P. H., Burke, G. R., and Moran, N. A. (2010). Facultative symbionts in aphids and the horizontal transfer of ecologically important traits. *Ann. Rev. Entomol.* 55, 247–266. doi:10.1146/annurev-ento-112408-085305

Pan, D. D., Lu, M. X., Li, Q. Y., and Du, Y. Z. (2017). Characteristics and expression of genes encoding two small heat shock protein genes lacking introns from *Chilo suppressalis*. *Cell Stress Chaperones* 23, 55–64. doi:10.1007/s12192-017-0823-8

Parsell, D. A., and Lindquist, S. (1993). The function of heat shock proteins in stress tolerance: Degradation and reactivation of damaged proteins. *Ann. Rev. Genet.* 27, 437–496. doi:10.1146/annurev.ge.27.120193.002253

Perring, T. M. (2001). The *Bemisia tabaci* species complex. *J. Crop Prot.* 20, 725–737. doi:10.1016/s0261-2194(01)00109-0

Pusag, J. C. A., Jahan, S. H., Lee, K. S., Lee, S., and Lee, K. Y. (2012). Upregulation of temperature susceptibility in *Bemisia tabaci* upon acquisition of Tomato yellow leaf curl virus (TYLCV). *J. Insect Physiol.* 58, 1343–1348. doi:10.1016/j.jinsphys.2012.07.008

Qin, J., Gao, P., Zhang, X. X., Lu, M. X., and Du, Y. Z. (2018). Characterization of two novel heat shock protein70s and their transcriptional expression patterns in response to thermal stress in adult of *Frankliniella occidentalis* (Thysanoptera: Thripidae). *J. Integr. Agric.* 17, 1023–1031. doi:10.1016/s2095-3119(17)61725-8

Quan, Y., Wang, Z., Wei, H., and He, K. (2022). Transcription dynamics of heat shock proteins in response to thermal acclimation in Ostrinia furnacalis. *Front. Phys.*, 13.

Raina, H. S., Rawal, V., Singh, S., Daimei, G., Shakarad, and M., and Rajagopal, R. (2015). Elimination of Arsenophonus and decrease in the bacterial symbionts diversity by antibiotic treatment leads to increase in fitness of whitefly, *Bemisia tabaci*. *Infect. Genet. Evol.* 32, 224–230. doi:10.1016/j.meegid.2015.03.022

Rana, V. S., Singh, S. T., Priya, N. G., Kumar, J., and Rajagopal, R. (2012). *Arsenophonus* GroEL interacts with CLCuV and is localized in midgut and salivary gland of whitefly *B. tabaci*. *PLoS One* 7, e42168. doi:10.1371/journal.pone.0042168

Rinehart, J. P., Li, A., Yocum, G. D., Robich, R. M., Hayward, S. A., and Denlinger, D. L. (2007). Up-regulation of heat shock proteins is essential for cold survival during insect diapause. *Proc. Natl. Acad. Sci.* 104, 11130–11137. doi:10.1073/pnas.0703538104

Salvucci, M. E., Stecher, D. S., and Henneberry, T. J. (2000). Heat shock proteins in whiteflies, an insect that accumulates sorbitol in response to heat stress. *J. Therm. Biol.* 25, 363–371. doi:10.1016/s0306-4565(99)00108-4

Samanta, S., Barman, M., Chakraborty, S., Banerjee, A., and Tarafdar, J. (2021). Involvement of small heat shock proteins (sHsps) in developmental stages of fall armyworm, *Spodoptera frugiperda* and its expression pattern under abiotic stress condition. *Heliyon* 7, e06906. doi:10.1016/j.heliyon.2021.e06906

Shan, H. W., Lu, Y. H., Bing, X. L., Liu, S. S., and Liu, Y. Q. (2014). Differential responses of the whitefly *Bemisia tabaci* symbionts to unfavourable low and high temperatures. *Microb. Ecol.* 68, 472–482. doi:10.1007/s00248-014-0424-3

Simón, C., Frati, F., Beckenbach, A., Crespi, B., Liu, H., and Flook, P. (1994). Evolution, weighting, and phylogenetic utility of mitochondrial gene sequences and a compilation of conserved polymerase chain reaction primers. *Ann. Entomol. Soc. Am.* 87, 651–701. doi:10.1093/aesa/87.6.651

Singh, S. T., Priya, N. G., Kumar, J., Rana, V. S., Ellango, R., Joshi, A., et al. (2012). Diversity and phylogenetic analysis of endosymbiotic bacteria from field caught Bemisia tabaci from different locations of North India based on 16S rDNA library screening. *Infect. Genet. Evol.* 12, 411–419. doi:10.1016/j.meegid.2012.01.015

Somero, G. N. (1995). Proteins and temperature. *Annu. Rev. Physiol.* 57, 43–68. doi:10.1146/annurev.ph.57.030195.000355

Su, Q., Xie, W., Wang, S., Wu, Q., Ghanim, M., and Zhang, Y. (2014). Location of symbionts in the whitefly *Bemisia tabaci* affects their densities during host development and environmental stress. *PloS one* 9, e91802. doi:10.1371/journal.pone.0091802

Sun, Y., and MacRae, T. H. (2005). Small heat shock proteins: Molecular structure and chaperone function. *Cell. Mol. Life Sci.* 62, 2460–2476. doi:10.1007/s00018-005-5190-4

Tissières, A., Mitchell, H. K., Tracy, U. M., and Tissieres, A. (1974). Protein synthesis in salivary glands of *Drosophila melanogaster*: Relation to chromosome puffs. *J. Mol. Biol.* 84, 389–398. doi:10.1016/0022-2836(74)90447-1

Truitt, A. M., Kapun, M., Kaur, R., and Miller, W. J. (2019). Wolbachia modifies thermal preference in *Drosophila melanogaster*. *Environ. Microbiol.* 21, 3259–3268. doi:10.1111/1462-2920.14347

Wan, F., Zhang, G., Liu, S., Luo, C., Chu, D., Zhang, Y., et al. (2009). Invasive mechanism and management strategy of *Bemisia tabaci* (Gennadius) biotype B: Progress report of 973 Program on invasive alien species in China. *Sci. China Life Sci.* 52, 88–95. doi:10.1007/s11427-008-0135-4

Wang, X. R., Wang, C., Ban, F. X., Zhu, D. T., Liu, S. S., and Wang, X. W. (2019). Genome-wide identification and characterization of HSP gene superfamily in whitefly (Bemisia tabaci) and expression profiling analysis under temperature stress. *Insect Sci.* 26 (1), 44–57. doi:10.1111/1744-7917.12505

Waters, E. R., Aevermann, B. D., and Sanders-Reed, Z. (2008). Comparative analysis of the small heat shock proteins in three angiosperm genomes identifies new subfamilies and reveals diverse evolutionary patterns. *Cell Stress Chaperones* 13, 127–142. doi:10.1007/s12192-008-0023-7

Waters, E. R., and Rioflorido, I. (2007). Evolutionary analysis of the small heat shock proteins in five complete algal genomes. *J. Mol. Evol.* 65, 162–174. doi:10.1007/s00239-006-0223-7

Wernegreen, J. J., and Moran, N. A. (2001). Vertical transmission of biosynthetic plasmids in aphid endosymbionts (Buchnera). *J. Bacteriol.* 183, 785–790. doi:10.1128/JB.183.2.785-790.2001

Wheeler, J. C., King, V., and Tower, J. (1999). Sequence requirements for upregulating expression of *Drosophila* hsp70 transgenes during aging. *Neurobiol. Aging.* 20, 545–553. doi:10.1016/s0197-4580(99)00088-3

Wiwatanaratanabutr, I., and Kittayapong, P. (2009). Effects of crowding and temperature on Wolbachia infection density among life cycle stages of *Aedes albopictus*. *J. Invertebr. Pathol.* 102, 220–224. doi:10.1016/j.jip.2009.08.009

Wolfe, G. R., Hendrix, D. L., and Salvucci, M. E. (1999). A thermoprotective role for sorbitol in the silverleaf whitefly, Bemisia argentifolii. *J. Insect Physiol.* 44, 597–603. doi:10.1016/s0022-1910(98)00035-3

Xiao, C., Hull, D., Qiu, S., Yeung, J., Barwell, T., and Seroude, L. (2019). Expression of heat shock protein 70 is insufficient to extend Drosophila melanogaster longevity. *G3: Genes, Genomes, Genetics* 9 (12), 4197–4207.

Xiong, W. F., Xie, J., Wei, L. T., Zhang, S. S., Song, X. W., Gao, S. S., et al. (2018). Transcriptome analysis of hsp18.3 functions and regulatory systems using RNA-sequencing in the red flour beetle, Tribolium castaneumflour beetle. *Tribolium Castaneum. J. Integr. Agric.* 17, 1040–1056. doi:10.1016/s2095-3119(17)61886-0

Yu, T. Y., Lu, M. X., and Cui, Y. D. (2018). Characterization of T-complex polypeptide 1 (TCP-1) from the *Chilo suppressalis* HSP60 family and its expression in response to temperature stress. *J. Integr. Agric.* 17, 1032–1039. doi:10.1016/s2095-3119(17)61775-1

Zaynab, M., Fatima, M., Sharif, Y., Zafar, M. H., Ali, H., and Khan, K. A. (2019). Role of primary metabolites in plant defense against pathogens. *Microb. Pathog.* 137, 103728. doi:10.1016/j.micpath.2019.103728

Zhao, L., and Jones, W. A. (2012). Expression of heat shock protein genes in insect stress responses. *Invertebr. Surviv. J.* 9, 93–101.

frontiers | Frontiers in Physiology

TYPE Original Research
PUBLISHED 09 February 2023
DOI 10.3389/fphys.2023.1063601

OPEN ACCESS

EDITED BY
Divya Singh,
Chandigarh University, India

REVIEWED BY
Karan Singh,
Grossman School of Medicine, New York University, United States
Meena Yadav,
University of Delhi, India
HABIB ALI,
Khwaja Fareed University of Engineering and Information Technology (KFUEIT), Pakistan

*CORRESPONDENCE
Fei Lyu,
haimolv@foxmail.com

†These authors have contributed equally to this work

SPECIALTY SECTION
This article was submitted to Invertebrate Physiology, a section of the journal Frontiers in Physiology

RECEIVED 07 October 2022
ACCEPTED 31 January 2023
PUBLISHED 09 February 2023

CITATION
Jiang X-l, Ren Z, Hai X-x, Zhang L, Wang Z-g and Lyu F (2023), Exposure to artificial light at night mediates the locomotion activity and oviposition capacity of *Dastarcus helophoroides* (Fairmaire). *Front. Physiol.* 14:1063601. doi: 10.3389/fphys.2023.1063601

Exposure to artificial light at night mediates the locomotion activity and oviposition capacity of *Dastarcus helophoroides* (Fairmaire)

Xiang-lan Jiang[1†], Zhe Ren[1†], Xiao-xia Hai[1], Ling Zhang[2], Zhi-gang Wang[1] and Fei Lyu[1*]

[1]Key Laboratories for Germplasm Resources of Forest Trees and Forest Protection of Hebei Province, College of Forestry, Agricultural University of Hebei, Baoding, Hebei, China, [2]Chengde Academy of Agriculture and Forestry Sciences, Chengde, Hebei, China

Light entrains the endogenous circadian clocks of organisms to synchronize their behavioral and physiological rhythms with the natural photoperiod. The presence of artificial light at night disrupts these photoperiodic cues and is currently considered to be a major threat to key fitness-related behaviors, including sleep disruption and physiological stress. Research on the ecological influence of forest pest and their natural enemies is lacking. The wood-boring insects significantly damage forest and urban forest ecosystem functions. The parasitic beetles, *Dastarcus helophoroides* is an important natural enemy of wood-boring insects, especially those in the Cerambycidae family. However, the effect of artificial light at night on the locomotor rhythms and oviposition capacity of *D. helophoroides* has received little attention. To address this gap, diel changes in the locomotor activity and number of eggs laid by female *D. helophoroides* was analyzed under different light-dark (LD) cycles and temperatures. The results showed that the 24-h rhythmic of locomotor activity in these beetles was elevated in darkness and reduced under illumination, indicating that they are nocturnal insects. This activity has two major peaks, the evening (1–8 h after lights off) and morning (3.5–12.5 h after lights off) components, reflecting that light mediate regular changes in locomotor activity. Moreover, the circadian rhythms and active percentage were influenced by the illumination duration and temperature, especially constant light and 40°C. Females laid more eggs under the 16 L: 8 D cycles at 30°C than under the other combinations of photoperiod (including constant light and darkness) and temperature. Finally, the potential influence of exposure to four ecologically relevant intensities of artificial light at night (0, 1, 10 or 100 lx) on oviposition capacity was studied. The results showed that lifetime exposure to bright artificial light (1–100 lx) at night decreased the number of eggs laid relative to those laid with no lighting at night. These results demonstrate that chronic exposure to bright artificial light at night may influence the locomotor activity and oviposition capacity of this parasitic beetle.

KEYWORDS

Dastarcus helophoroides, locomotor activity, circadian rhythms, oviposition, light pollution

Introduction

Before the invention of electric lighting, mammals and invertebrates spent nearly all of their time during the day exposed to natural daylight (>300 lx) and nearly all of their time after sunset exposed to dim sources of light (<30 lx), including moonlight, starlight and small fires (Phillips et al., 2019). Earth's rotation produces daily cycles of light and dark, influencing the behaviors, physiological functions, metabolic regulation, and hormone secretion of organisms, and even plant rhizosphere microbial communities (Zhao et al., 2021; Liu et al., 2022; Mason et al., 2022; Sanders et al., 2022). As a result, these behaviors and physiological processes show an inherent ability to follow the change in light/dark cycles (LD cycles) at approximately a circa 24-h scale. Therefore, an organism's behavioral and physiological processes, such as locomotor activity, food intake, and sleep, display rhythmic oscillations in response to the internal circadian clocks (Brüning et al., 2015; Mason et al., 2022). Circadian clock is significantly influenced by the alteration of natural light environment, for example, the daily LD cycle (Brüning et al., 2015).

With rapid urbanization, natural light regimes have been widely disrupted by artificial light at night, such as streetlights, industrial and domestic lighting and vehicle lighting (Sanders et al., 2022). Artificial light has transformed the nighttime environment of large areas of the Earth; 23% of the world's land surfaces, 88% of Europe, and almost half of the United States are estimated to be exposed to light pollution, which includes light sources such as small night lights indoors, television light indoors, streetlights, industrial lighting and vehicle lighting (Falchi et al., 2016). Exposure to light at night has been reported to influence the circadian clock and health of humans and animals. Compared to the absence of light exposure during sleep, exposure to any artificial light in the bedroom during sleep was associated with obesity (in women and older age groups), cardiometabolic syndrome, type 2 diabetes (in an elderly population), and depression (in young people) (Park et al., 2019; Obayashi et al., 2020; Crouse et al., 2021; Kim et al., 2022; Mason et al., 2022). In birds, mammals, and fruit flies, individual fitness traits, such as reproduction and juvenile growth, were reduced by chronic exposure to light at an intensity less than 10 lx (Kempenaers et al., 2010; McLay et al., 2017).

Comparatively, few studies have investigated whether fitness in invertebrates is impacted by exposure to dim nighttime lighting (McLay et al., 2017). Previous studies have shown a negative effect of constant light exposure on fecundity and longevity in a model species (*Drosophila melanogaster*) relative to a normal day-night environment (Kouser et al., 2014). Female *D. melanogaster* chronically exposed to light at night (light intensities of 1, 10 and 100 lx) were less likely to commence oviposition than females exposed to 0 lx light at night (McLay et al., 2017). However, knowledge of how the reproductive capacity of non-model invertebrates is influenced by light exposure at night remains limited.

The beetle *Dastarcus helophoroides* (Fairmaire) is an important generalist or polyphagous parasitoid of several longhorn beetle species in China, Korea, and Japan, including *Anoplophora glabripennis* Motschulsky, *Monochamus alternatus* (Hope), *Massicus raddei* Blessig and *Batocera horsfieldi* (Hope), and has been widely used to control Cerambycidae beetles (Wei et al., 2013; Lyu et al., 2014; Yang et al., 2014; Kaitlin et al., 2018; Shen et al., 2022). Under natural LD cycles at a temperature of 27°C ± 1°C, the locomotor activity of *D. helophoroides* showed an obvious circadian rhythm, peaking within 0.5–2.5 h after lights off during the dark period (Lyu et al., 2015a). A similar rhythm of locomotor activity was revealed under a LD cycles of 16:8 h at 23°C ± 1°C in an artificial climate chamber (Lyu et al., 2015b), but the locomotor active percentage of adults at 27°C ± 1°C was approximately equal to 1.5 to 2 times that at 23°C ± 1°C at peak time. However, the influence of exposure to different illumination durations at night and temperatures on the locomotor activity of this beetle is still unknown.

The beetle *D. helophoroides* is an ideal model species for examining the influences of artificial light on behavioral and physiological traits. Because it is a nocturnal insect and its prey (Cerambycidae beetles) is widely distributed in different urban and rural habitats (Lyu et al., 2014), these beetles are affected by different intensities of artificial night lighting in urban and rural environments. Moreover, recent studies have revealed decreased parasitic efficiency of *D. helophoroides* in controlling *M. alternatus* in southern pine forests, especially in forests containing dying *Pinus massoniana* (Lamb.) caused by the longhorn beetle (Shen et al., 2022). The number of eggs laid by insects is often negatively affected by several ecological factors, such as exposure to light at night and extreme temperatures (Yang et al., 2012; McLay et al., 2017). Therefore, a series of experiments were performed to investigate the effects of different illumination durations at night and different temperatures on the two key life history traits (locomotor activity and oviposition capacity) in a non-model invertebrate, *D. helophoroides*. In addition, the potential effect on the number of eggs was determined when adults were exposed to four different ecologically relevant intensities of artificial light at night.

Materials and methods

Insects

Adults of the beetle *D. helophoroides* were sourced from the Department of Entomology, Agriculture Vocational College of Beijing. The first generation of the wild population was collected from parasitized larvae and pupae of *A. glabripennis*. Larvae were reared on a substitute host (*Thyestilla gebleri* (Fald.). Adults used in the experiment were the second generation of beetles and maintained in white plastic cages in the laboratory at 25°C ± 1°C and 50% ± 10% relative humidity under an LD cycle of 16:8 h (light: 500 lx and dark 0 lx) in an artificial climate chamber (RXZ-500D, Jiangnan Instrument Factory, Ningbo, China). Plastic centrifuge tubes (diameter: 10 mm and length: 50 mm) were plugged with a cotton ball to provide water, and *Tenebrio molitor* (L.) larvae oven-dried at 60°C served as food for the adults. The water and food were changed every 5 days. Female adults were used in behavioral tests and distinguished by the end angle of the anal plate and the length and width of the anal plate under a dissecting microscope (Olympus SZ51, Tokyo, Japan) according to Tang et al. (2007). All adults that did not differ in body size were used in our experiment at 60–70 days after emergence, and all of the individuals were able to mate and oviposit normally in our experiment.

Locomotor activity recording

Based on the behavioral characteristics of *D. helophoroides* adults in a previous experiment (Lyu et al., 2015a), equipment was designed

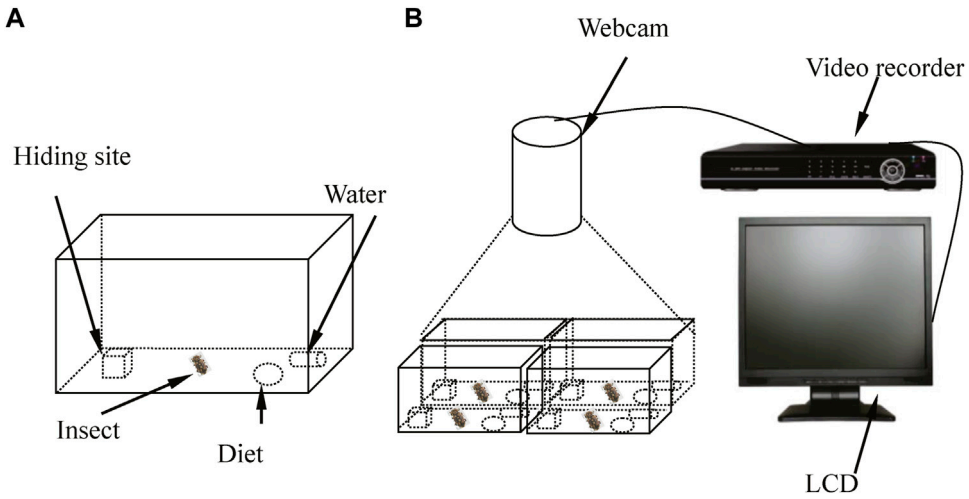

Figure 1
Schematic of the behavioral bioassay chamber used to monitor the circadian rhythms of locomotor activity by female adults under different conditions. **(A)** Females *D. helophoroides* were placed in the breeding box during the experiment. **(B)** The equipment used to observe the locomotor activity of female adults during the experiment. LCD: liquid crystal display.

to observe and record the circadian rhythm of locomotor activity under different temperatures and LD cycles (Figure 1). The experimental equipment comprised four artificial breeding boxes, a video camera (high definition 720P), a liquid crystal display, a hard disk video recorder and a coaxial cable (Figure 1). The artificial breeding box was designed as shown in Figure 1A. The breeding box consisted of a polyvinyl box (18.5 cm × 12.5 cm × 7.5 cm), wooden block with a concave trough (3 cm × 3 cm × 3 cm), artificial diet and water resource. In a previous study (Lyu et al., 2015a), 55%–100% of adults hid under the wooden block during the light period; thus, a wooden block with a concave trough was placed in a polyvinyl box to provide a resting site. To prevent the test insects from escaping and to observe their activity, a layer of odorless plastic wrap with 50–100 pinholes was placed on the top of a breeding box to allow air circulation. The video camera in the artificial climate chamber, hard disk video recorder and liquid crystal display were connected by the coaxial cable to record locomotor activity.

Locomotor activity

Effect of LD cycle on the locomotor activity

The beetle *D. helophoroides* is a nocturnal insect. These beetles show characteristic clock-controlled evening locomotor activity at temperatures of 23°C ± 1°C and 27°C ± 1°C (Lyu et al., 2015a; Lyu et al., 2015b). However, whether the rhythm of locomotor activity is influenced by the duration of illumination at night remains unclear. The previous study showed no significant difference in locomotor activity between females and males under different conditions (Lyu et al., 2015a; Lyu et al., 2015b). In addition, the effect of different microhabitat conditions on the oviposition capacity of beetles was measured in the second section. Therefore, the locomotor activity of female beetles, which is more correlated with oviposition behavior (relative to that of male beetles), was monitored at a temperature of 25°C under seven different LD cycles to examine how illumination duration at night affects the rhythm of locomotor activity (in hours, from constant darkness to constant light), including constant darkness (0 L/24 D), 4 L/20 D, 8 L/16 D, 12 L/12 D, 16 L/8 D, 20 L/4 D, and constant light (24 L/0 D), all measured in hours. Locomotor activity mainly includes the moving, foraging and drinking behavior of beetles. The recorded data was observed every 30 min, and locomotor activity at a time point was confirmed if the beetle was found at a different location from the previous location. Individual female beetles were placed in an artificial breeding box under the different LD cycles, and locomotor activity under these different conditions was recorded for continuous 10 days. Twenty individual beetles were tested per LD cycles.

Effect of temperature on the locomotor activity

Previous studies also showed that at the peak time of locomotor activity, the percentage of adult beetles displaying this behavior at 27°C ± 1°C was approximately 75% of the total beetles; however, at a temperature of 23°C ± 1°C, this percentage decreased considerably to 35% (Lyu et al., 2015a; Lyu et al., 2015b). To determine how different temperatures affect the rhythm of locomotor activity, the locomotor activity of females was monitored under the LD cycle of 16:8 at six temperature treatments, including 15°C, 20°C, 25°C, 30°C, 35°C, and 40°C. Individual female beetles were placed in an artificial breeding box under these different conditions, and then their locomotor activity was recorded for continuous 10 days. Twenty individual beetles were tested per temperature condition.

Oviposition capability

Effect of the LD cycle and temperature on the number of eggs laid

A series of experiments were conducted to establish the effect of exposure to different illumination duration at night and different temperatures on the number of eggs laid by female beetles in closed arenas (i.e., glass Petri dishes), including the above mentioned seven different LD cycles and six different temperatures (10°C, 15°C, 20°C,

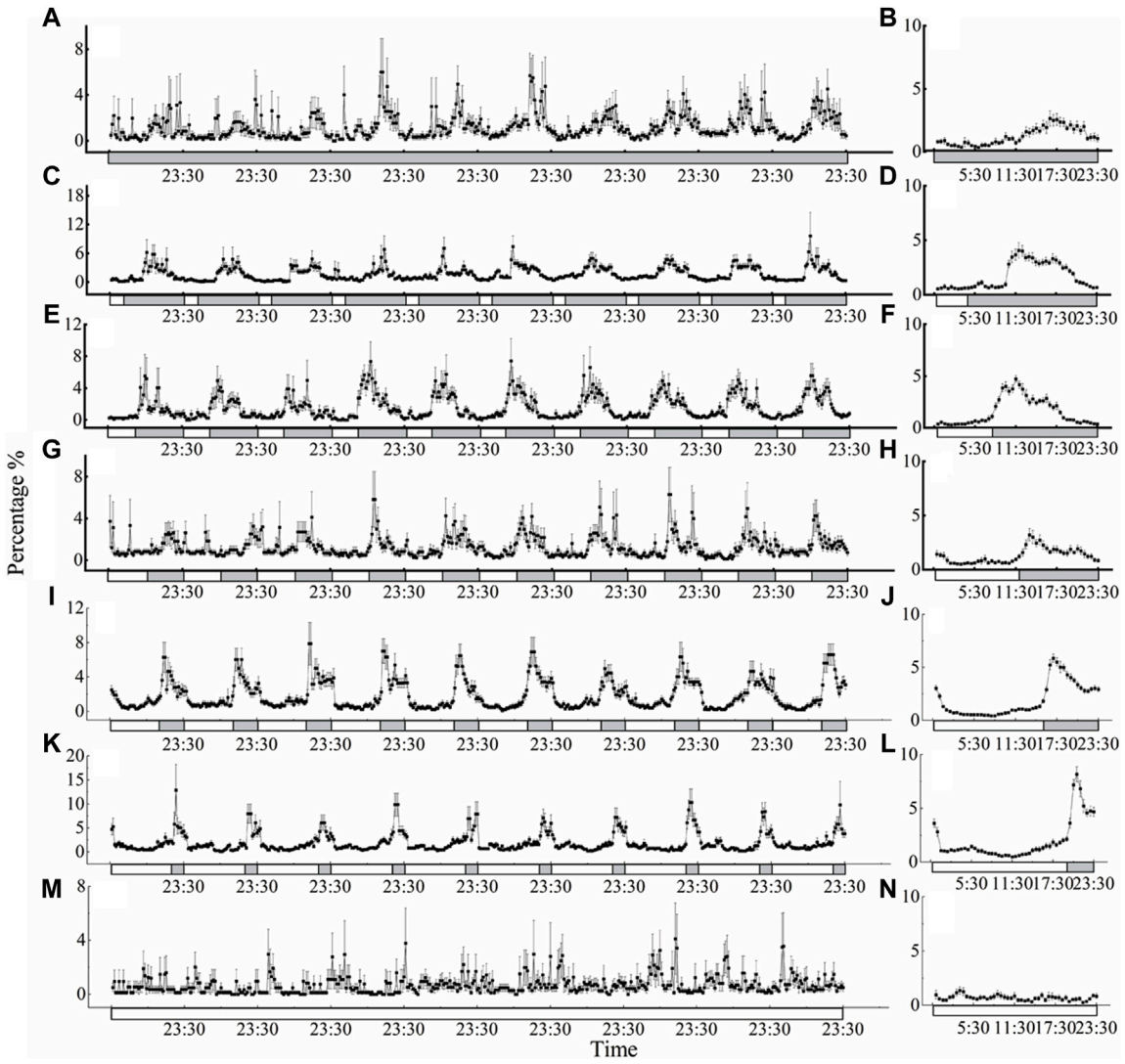

Figure 2
Circadian rhythms of locomotor activity of *D. helophoroides* under different LD cycles at a temperature of 25°C. LD cycles: **(A, B)** 0L/24D; **(C, D)** 4L/20D; **(E, F)** 8L/16D; **(G, H)** 12L/12D; **(I, J)** 16L/8D; **(K, L)** 20L/4D; **(M, N)** 24L/0D. Data (n = 20) shown are the mean ± standard error of the mean (SEM). The percentages in the figure indicate the occurrence frequency of single behaviors of individual insects at 30 min various time intervals within 1 day. Black and white bars represent the LD cycle, black = subject night, white = subject day.

25°C, 30°C, 35°C). Glass Petri dishes (14 cm diameter, 2.5 cm height) were used in the experiment. We pasted white filter paper to the wall and bottom of each glass Petri dish to visually isolate individuals, and thereby prevent the different groups from influencing each other. Wooden blocks (1.5 cm high × 1.5 cm wide × 1.5 cm long), each with a carved trough, were placed on top of the filter paper to provide a microhabitat for oviposition. The glass Petri dishes were then placed in an artificial climate chamber under the previously described microhabitat conditions. Three female and three male beetles were introduced in the center of the experimental arena (the glass Petri dishes) to determine female oviposition. The adults remained in glass Petri dishes for a period of 30 successive days to allow oviposition to occur. Female *D. helophoroides* usually laid clusters of eggs on the filter paper beneath the wood blocks. Every 24 h, the number of eggs on the filter paper was counted under a dissecting microscope (Olympus SZ51, Tokyo, Japan). Then, the frass of adults and food debris were cleared from the glass Petri dishes to decrease their influence on the next count. Fifteen groups (15 replicates × 3 male-female adult pairs) were tested per condition.

Effect of light intensity at night on the number of eggs laid

To determine the influence of light at night on oviposition, four light conditions were created in an artificial climate chamber, each with identical daytime lighting conditions (500 lx) but varying in the intensity of nighttime lighting as follows: 0 lx (control, complete darkness at night), 1 lx (10 times full moonlight on a clear night), 10 lx (similar to nighttime street illumination), and 100 lx (similar to bright urban lighting) (Brüning et al., 2015; Botha et al., 2017). The results of the experiment described in section *"Effect of LD cycle and temperature on the number of eggs laid"* indicated that beetles laid more eggs under an LD cycle of 16:8 at 30°C than under the other

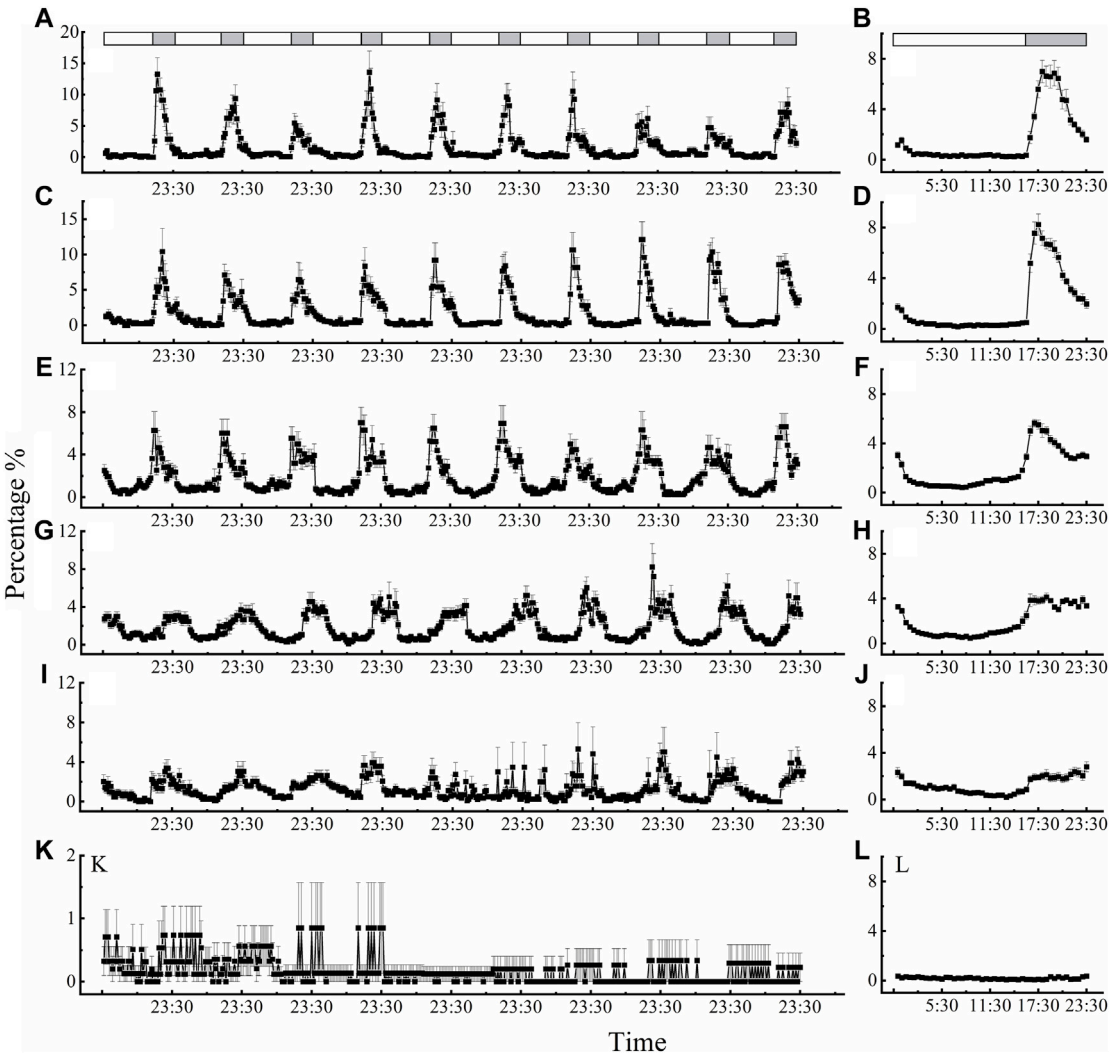

Figure 3
Circadian rhythms of locomotor activity of *D. helophoroides* at different temperatures. **(A, B)** 15°C; **(C, D)** 20°C; **(E, F)** 25°C; **(G, H)** 30°C; **(I, J)** 35°C; **(K, L)** 40°C. Data (n = 20) shown are the mean ± SEM. The percentages indicate the occurrence frequency of single behaviors of individual test insects in various time intervals within 1 day. The light-dark cycle was 16 h L/8 h D. Black and white bars represent the LD cycle, black = subject night, white = subject day.

treatments (Figure 5); therefore, an LD cycle of 16:8 and a temperature of 30°C were selected to evaluate the effect of the intensity of light at night on the number of eggs laid. The number of eggs laid on the filter paper was counted each day. Fifteen groups (15 replicates × 3 pairs of adults) were tested per treatment.

Statistical analyses

In each set of experiments, to assess the influence of the LD cycle and temperature on locomotor activity, the means of the activity percentage during the light or dark phases were compared using one-way analyses of variance (ANOVAs) and Duncan's *post hoc* tests. The mean activity percentages between the light and dark periods in the different treatments were compared by means of a two-tailed independent-samples Student's t-test or Mann-Whitney test if the data displayed severe heteroscedasticity. Moreover, one-way ANOVAs were used to assess differences in the average number of eggs laid under the seven different LD cycles, six different temperatures and four different light intensities at night. Duncan's *post hoc* test was used to determine significant differences between groups. All statistical analyses were performed using IBM SPSS Statistics 21.00 for Windows (IBM SPSS Inc., Boston, MA, United States).

Results

Locomotor activity

Effect of LD cycle on the locomotor activity

The locomotor activity of *D. helophoroides* was monitored under seven different LD cycles at a temperature of 25°C (Figure 2). Under the different LD cycles at 25°C, there were two major peaks in

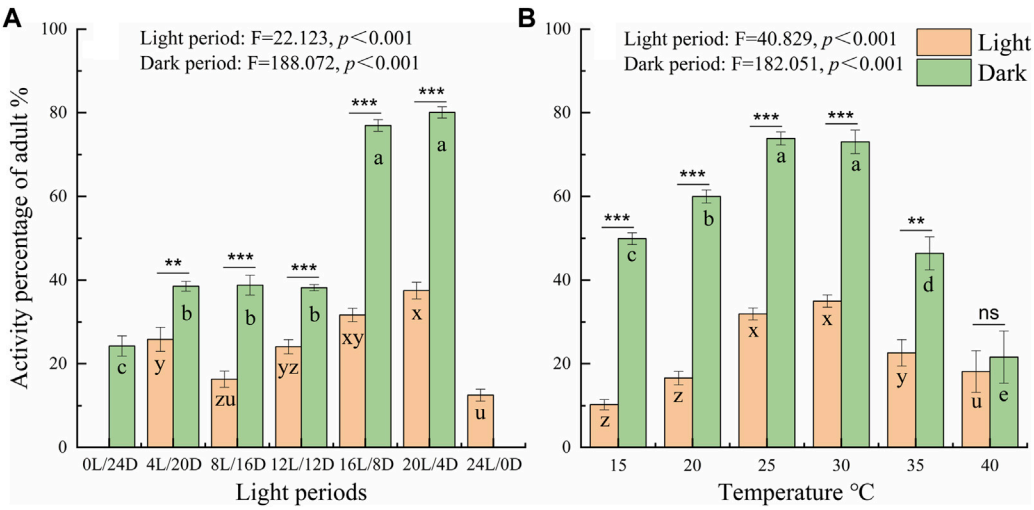

Figure 4
Comparison of the locomotor active percentages of *D. helophoroides* between the light and dark phases under different LD cycles **(A)** and temperatures **(B)**. The difference in active percentage between the light and dark phases under the different conditions was determined by two-tailed Student's t tests (***$p < 0.001$, **$p < 0.01$). a, b, and c indicate significant differences in the active percentages of during the dark phase at different temperatures according to Duncan's post hoc test, one-way analysis of variance (α = 0.05). x, y, and z indicate significant differences in the active percentage during the light phase at different temperatures according to Duncan's post hoc test, one-way analysis of variance (α = 0.05). Data shown are the mean ± SEM (n = 10).

locomotor behavior in the morning and evening, except for the constant light condition (Figure 2). The highest peak in locomotor activity occurred in the dark period from 2 h to 16.5 h after lights off signal, and the second peak in locomotor activity occurred at ZT = 16:00–23:30 before "lights on signal" (ZT0 = lights on; Figure 2 B, D, F, H, J, and L). There was a direct correlation between the locomotor activity peak after lights off signal and the duration of the light period, with the peak activity moving progressively later with increasing durations of the light phase (Figure 2 D, F, H, J, and L). The locomotor activity peak of female occurred 16.5 h after lights off signal under the constant darkness condition. When the duration of illumination was increased, the timing of the first peaking in the locomotor activity were shifted forward relative to that under the constant darkness condition; for example, under the LD 4:20 cycle, the timing of the first peak in locomotor activity was 8.5 h after lights off signal; whereas the timing of the first peak under the LD cycles of 8:16, 12:12, 20:4 was 2.5 h, 2 h, and 2 h after lights off signal, respectively (Figures 2B, D, F, H, J, L). In contrast, the beetles showed no circadian regulation of locomotor activity under the constant light condition (Figures 2M, N).

To further probe the influence of different LD cycles, the locomotor active percentages was analyzed in the light and dark phases under the different conditions (Figure 4 A). The average active percentages of adults in the dark phase were significantly higher than that in the light phase (Supplementary Table S1 $4.089 < t < 21.411$, $p < 0.001$), except under the constant light and darkness conditions. Furthermore, the active percentages of adults were significantly higher under the LD cycles of 16:8 and 20:4 than under the other LD cycles at a temperature of 25°C (Figure 4A). The active percentages of adults in the dark phase were 80.06% and 76.94% under the LD cycles of 16:8 and 20:4, respectively, and there was no significant difference in the active percentages in the light phase and dark phase between the LD cycles of 16:8 and 20:4 (Figure 4A; Supplementary Table S1).

Effect of temperature on the locomotor activity

Locomotor activity also displayed regular rhythms under the LD 16:8 cycle at different temperatures, except for 40°C (Figure 3). The beetles showed characteristic clock-controlled evening locomotor activity, peaking between ZT 17:00 and ZT 18:30 (ZT0 = lights on; Figure 3 B, D, F, H and J). The first peak in locomotor activity occurred approximately 2.5 h, 2 h, 1.5 h, 3 h after lights off signal at 15°C, 20°C, 25°C and 30°C, respectively. Compared with performance of adults under dark phase at 15, 20, 25, 30, 35°C (Figures 3B, D, F, H, J), the rhythm of locomotor activity at 40°C was irregular, smooth, and exhibited only slight changes (Figure 3L). Moreover, we also found a subtle small peak in activity before "lights on" (ZT = 23:00–23:30 after lights on) at temperatures of 15°C, 20°C, 25°C, 30°C, and 35°C, which was labeled the "morning peak" (Figures 3A, C, E, G, I, K).

At the different temperatures under the LD cycle of 16:8, the active percentages in the dark phase were significantly higher at 25°C and 30°C than at the other temperatures (Figure 4B). The active percentages of females in the dark phase at temperature of 30°C and 25°C were 79.56% and 75.38%, respectively. There was no significant difference in the active percentages of females between 30°C and 25°C (Figure 4B; Supplementary Table S2). The average active percentages of adults in the dark phase were significantly higher than those in the light phase (Supplementary Table S2 $3.507 < t < 26.809$, $p < 0.003$), except at 40°C (Supplementary Table S2 $t = 0.194$, $p = 0.848$).

Oviposition capability

Effect of LD cycle and temperature on oviposition capacity

To investigate the oviposition capacity of female beetles, a series of bioassays were conducted under the different treatments, The number of eggs laid on the glass Petri dishes was affected by the LD cycle and

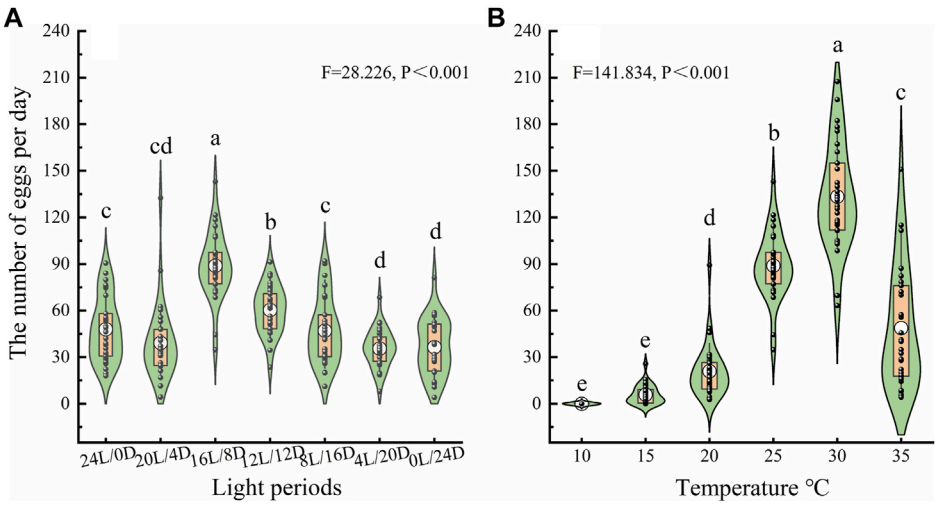

Figure 5
Number of eggs laid by ovipositing females under different LD cycles **(A)** and temperatures **(B)**. The lower and upper vertex of lines within the violin plots and the lines of the lower and upper edges of the box indicate the 10%, 90%, 25% and 75%, respectively; the middle circles in the boxes indicate the mean number of eggs laid. a, b, and c indicate a significant difference in the number of eggs laid among different conditions according to Duncan's post hoc test and one-way analysis of variance (α = 0.05).

temperature (Figure 5). The average numbers of eggs laid by females were 47.97 ± 3.76, 39.20 ± 4.43, 88.94 ± 3.93, 60.04 ± 2.79, 47.04 ± 3.95, 35.59 ± 2.26 and 36.44 ± 3.29 under LD cycles of 24:0, 20:4, 16:8, 12:12, 8:12, 4:20 and 0:24, respectively. Females laid far more eggs under LD cycle 16:8 than under the other cycles at 25°C (Figure 5A). The average numbers of eggs laid by females were 0, 5.89 ± 1.11, 20.93 ± 3.13, 88.94 ± 3.93, 133.38 ± 6.21, and 48.76 ± 7.16at 10°C, 15°C, 20°C, 25°C, 30°C and 35°C, respectively, under the LD cycle 16:8. Females laid significantly more eggs under LD cycle 16:8at 30°C than at the other temperatures (Figure 5B).

Light exposure at night decreases the number of eggs laid

To explore the effects of light intensity at night on oviposition, the number of eggs laid was evaluated under light intensities of 0 lx, 1 lx, 10 lx, and 100 lx (Figure 6). The results showed that the number of eggs laid was significantly affected by light intensity ($F = 17.528$, $df = 3$, $p < 0.001$); specifically, the average number of eggs laid per three pairs of adults was 133.38 ± 6.21, 96.23 ± 6.29, 76.27 ± 4.52, and 107.03 ± 5.54 under light intensities of 0 lx, 1 lx, 10 lx, and 100 lx, respectively. Females exposed to light at night (1, 10, and 100 lx) laid fewer eggs than those exposed to no light (0 lx) at night (Figure 6). There was no significant difference in the number of eggs laid between the 1 lx and 10 lx conditions or between the 1 lx and 100 lx conditions. Females exposed to light at night laid fewer eggs with increases in the light intensity. However, females exposed to100 lx light at night laid more eggs than those exposed to 10 lx light at night.

Discussion

The experiments revealed a surprising and intriguing change in the circadian rhythms of locomotor activity and the oviposition capacity of *D. helophoroides* under different LD cycles and temperatures. First, the beetles displayed rhythmic oscillation of locomotor activity under different conditions, except under the constant light and 40°C. Locomotor activity elevated in darkness and reduced under illumination, indicating that this species is nocturnal insect. Across LD cycles, the active rhythm of females was 38.53%–80.06% at dark phase in the different LD cycles and 25.81%–37.50% in the light phase (Figure 4A; Supplementary Table S1). Similar active percentages were observed under the LD 16:8 cycle at different temperatures (Figure 4B; Supplementary Table S2). The active percentage was also influenced by the LD cycle and temperature (Figure 3). Second, the fecundity of the beetles (provided with sufficient nutrient supply) was highest under LD cycle 16:8at a temperature of 30°C rather than 25°C. Finally, and perhaps most importantly, chronic exposure to dim nighttime lighting significantly reduced the oviposition capacity of *D. helophoroides*. Taken together, these findings suggest a negative impact of dim nighttime illumination in terms of both duration and intensity on the locomotor activity and oviposition capacity of the beetle *D. helophoroides*.

The beetle *D. helophoroides* is a widely distributed in China (Lyu et al., 2014), and its circadian rhythms may be influenced by the complex natural cycle in environment. For example, in fruit flies, rhythmic locomotor activity shows a more complex oscillation under natural environments than under laboratory LD cycles (Vanin et al., 2012). Although various combinations of LD cycles and temperatures were used to determine locomotor activity rhythm in this study, it remains unclear how the complex natural cycles in the environment affect locomotor activity.

Moreover, previous studies have shown that the active percentage decreased significantly after three consecutive days under constant darkness but increased to normal levels after the adults were transferred to another laboratory and maintained under a natural LD cycle (Wei et al., 2008). The results of the present study corroborate those of previous research (Wei et al., 2008), which showed that approximately 24% of beetles per 30 min interval exhibited locomotor activity under the constant darkness condition and that the active percentage was significantly lower under the

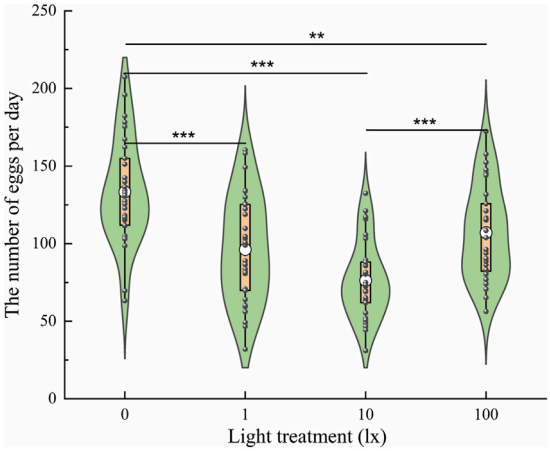

Figure 6
Number of eggs laid by ovipositing females the four light intensities at night. The lower and upper vertex of lines within the violin plots, the lines of lower and upper edges of boxes indicate 10%, 90%, 25% and 75%, respectively; the middle circles in the box indicate the mean number of eggs laid. An asterisk (*) indicates a significant difference in the number of eggs laid among the different conditions according to Duncan's *post hoc* test and one-way analysis of variance ($\alpha = 0.05$, ***$p < 0.001$, **$p < 0.01$).

constant darkness than under the other LD cycles (Figure 4); in contrast 77%–80% of adults showed locomotor activity behavior in the dark phase under LD cycles of 16:8 and 20:4, suggesting that the illumination (lights on and off signals) mediates locomotor activity.

The experiments showed that the 24-h rhythmic of locomotor activity of *D. helophoroides* adults peaked twice, once in the evening (1–8 h after lights off, or 16,5 h under the constant darkness condition) and once in the morning (3.5–12.5 h after lights off), indicating a regular circadian rhythm. These results corroborate those of a previous study that reported two major locomotor activity peaks in the evening and forenoon (before 11:00) under a natural light-dark environment (Wei et al., 2008). However, the subtle smaller peak in locomotor activity before "lights on" was not observed at high temperature (35°C and 40°C) (Figures 3K, M), suggesting that temperature can also impact the locomotor activity rhythm. Notably, there was a very high mortality rate at 40°C after 3 days. Therefore, this temperature was excluded from the following oviposition test. Furthermore, recent research has shown that the parasitic efficiency of *D. helophoroides* on longhorn beetles is decreased in southern pine forests; this decrease may have been caused by extreme temperatures because high temperatures have frequently occurred in southern China (Shen et al., 2022). In present study, we found that the number of eggs laid by females at 35°C was significantly lower than that at 25°C and 30°C (Figure 5); thus, high temperatures may lead to a decrease in the oviposition capacity of beetles, thereby reducing parasitic efficiency.

Circadian rhythms driven by biological clocks are expected to enhance organism fitness by adjusting their locomotor activity and metabolism to adapt to the external environment (Zhao et al., 2021). Importantly, the endogenous circadian clock depends on light to synchronize behavior and physiological activity of organisms with the external daily environment (Bumgarner and Nelson, 2021). It is therefore reasonable to infer that synchronicity of these rhythms would be less advantageous to organisms living under conditions of constant light or darkness (Zhao et al., 2021). In the present study, beetles maintained under constant light or darkness appeared to lose the rhythmicity of locomotor activity. Although locomotor activity showed a certain rhythmicity, the active percentage of beetles was significantly lower under constant light or constant darkness conditions than under the other LD cycles, suggesting that constant darkness or light can derange temporal adaptation and decrease organism fitness (Figure 4). Indeed, in the oviposition experiment, females laid fewer eggs under constant light or constant darkness conditions than under other LD cycles (Figure 5).

Chronic exposure to dim artificial light at night impacted locomotor activity and also decreased the oviposition capacity of the *D. helophoroides* (Figure 6). On average, the presence of dim lighting at night resulted in a 20%–43% reduction in the number of eggs laid per three pairs of beetles (Figure 6: three pairs of beetles laid an average of 134 eggs per day under the 0 lx condition at night compared to an average of 94 eggs laid by females exposed to light at night). Dim lighting at night represents a suboptimal mating environment, as variation in oviposition with light conditions has been observed in moths, fruit flies and fireflies (Van Geffen et al., 2015; Firebaugh and Haynes, 2016; McLay et al., 2017). A previous study found that mating behavior occurred at 19:00–22:00 (Wei et al., 2008); therefore, the presence of night lighting is likely to have a direct influence on the rhythm of mating, in turn, affecting oviposition capacity.

Multiple physiological mechanisms have been proposed to explain the relationships of nighttime light exposure with altered locomotor activity and fecundity *via* changes in sleep. Robust evidence from experimental studies indicates that nighttime light exposure has negative impacts on the activity of enzymes in the juvenile hormone (JH) biosynthetic pathway and on the circadian secretion of melatonin and biogenic amines (Zera and Cisper, 2001; Guy et al., 2013; Zera, 2016). The circadian rhythms of reproductive functions, such as courtship, mating, and gamete production, were regulated by oscillations in JH titers. In cockroaches and bark beetles, oscillations in JH titers mediated the production or release of sex pheromones to influence female or male calling signals (Kang et al., 2019; Fang et al., 2021; Chen et al., 2022). Moreover, melatonin has been identified in many insect tissues, including the head, brain, and compound eyes (Guy et al., 2013). In mammals, the circadian secretion of melatonin is important for the timing of circadian and seasonal rhythms, influencing sleep quality (Mason et al., 2022). Because melatonin levels exhibit a circadian rhythms with peaks during the dark phase, nighttime light exposure can suppress melatonin secretion, and several studies have suggested a link between the suppression of nighttime melatonin and the incidence of type 2 diabetes (Kim et al., 2022) and impaired cardiometabolic function (Mason et al., 2022). In silkworms, neuroanatomical evidence suggested that melatonin may influence JH signaling and is likely to regulate reproduction (Guy et al., 2013). Moreover, lighting at night suppresses melatonin secretion and may contribute to higher levels of oxidative stress, influencing gamete production. The potential physiological mechanism underlying these associations needs to be determined by future studies.

Furthermore, this experiment may indicate optimal lighting and temperature conditions for mass rearing of *D. helophoroides*, including those that postponing or increasing oviposition. The *D. helophoroides* is the most important natural parasitoid of wood borers, including longhorn and buprestid beetles, and mass rearing is quite challenging (Yang et al., 2014). Emerging evidence has indicated that temperature

influences the fecundity of this beetle, which reaches a maximum under sufficient nutrient supply at 22–25°C (Yang et al., 2012). However, the present study shows that females laid more eggs under LD cycle 16:8at 30°C than under the other conditions. In previous research, the conditions contained of four different temperatures of 16°C, 19°C, 22°C, and 25°C (Yang et al., 2012); in contrast, the present study included six different temperature conditions (10°C, 15°C, 20°C, 25°C, 30°C and 35°C). Different gradients and ranges utilized in various studies may lead to discrepant results. Previous studies have reported that constant darkness disturbs the normal behavioral rhythms of beetles and suggested that appropriate illumination should be considered for mass rearing (Wei et al., 2008). Indeed, in the present study, females laid fewer eggs under constant light or constant darkness conditions than under the other LD cycle treatments, suggesting that LD cycles are key to mass rearing. Moreover, the results showed that females laid an average of 0 and six eggs at 10°C and 15°C, respectively; and thus, these temperatures may be used to prolong the shelf life of this beetle. Overall, the present study established a foundation for the mass rearing of *D. helophoroides*, the natural enemy of the trunk-boring pests.

Conclusion

Overall, our experiment highlights that locomotor activity and oviposition capacity are influenced by the LD cycle and temperature and that chronic exposure to dim artificial light at night decreased the oviposition capacity of the beetle *D. helophoroides*. These findings enhance our understanding of the behavioral responses of *D. helophoroides* to different microhabitat environment. These finding also establish optimal microhabitat conditions for mass rearing of *D. helophoroides*, thus prolonging the shelf life or increasing the number of eggs laid.

Data availability statement

The raw data supporting the conclusion of this article will be made available by the authors, without undue reservation.

Author contributions

FL and Z-GW conceived of and designed the work; X-LJ, X-XH, ZR, LZ, and FL collected and analyzed the data; X-LJ, X-XH, ZR, LZ, and FL wrote the manuscript. All authors read and approved the manuscript.

Funding

This research was funded by the National Natural Science Foundation of China (No. 32171800), the National Natural Science Foundation of Hebei Province of China (No. C2019204276) and the Basic Scientific Research of Universities in Hebei Province of China (No. KY202008).

Acknowledgments

We thank the personnel at the Agricultural University of Hebei (Fan Xinyue, Jia Yuheng, Wang Pengwen, Huang Chen, Chen Peng) for their assistance with data collection. We also thank the National Natural Science Foundation of China (No. 32171800), the Natural Science Foundation of Hebei Province of China (No. C2019204276), and the Basic Scientific Research of Universities in Hebei Province of China (No. KY202008) for their generous support.

Conflict of interest

The authors declare that the research was conducted in the absence of any commercial or financial relationships that could be construed as a potential conflict of interest.

Publisher's note

Supplementary material

The Supplementary Material for this article can be found online at: https://www.frontiersin.org/articles/10.3389/fphys.2023.1063601/full#supplementary-material

References

Botha, L. M., Jones, T. M., and Hopkins, G. R. (2017). Effects of lifetime exposure to artificial light at night on cricket (*Teleogryllus commodus*) courtship and mating behaviour. *Anim. Behav.* 129, 181–188. doi:10.1016/j.anbehav.2017.05.020

Brüning, A., Hölker, F., Franke, S., Preuer, T., and Kloas, W. (2015). Spotlight on fish: Light pollution affects circadian rhythms of European perch but does not cause stress. *Sci. Total Environ.* 511, 516–522. doi:10.1016/j.scitotenv.2014.12.094

Bumgarner, J. R., and Nelson, R. J. (2021). Light at night and disrupted circadian rhythms alter physiology and behavior. *Integr. Comp. Biol.* 61, 1160–1169. doi:10.1093/icb/icab017

Chen, N., Liu, Y. J., Fan, Y. L., Pei, X. J., Yang, Y., Liao, M. T., et al. (2022). A single gene integrates sex and hormone regulators into sexual attractiveness. *Nat. Ecol. Evol.* 6, 1180–1190. doi:10.1038/s41559-022-01808-w

Crouse, J. J., Carpenter, J. S., Song, Y. J. C., Hockey, S. J., Naismith, S. L., Grunstein, R. R., et al. (2021). Circadian rhythm sleep–wake disturbances and depression in young people: Implications for prevention and early intervention. *Lancet Psychiat* 8, 813–823. doi:10.1016/S2215-0366(21)00034-1

Falchi, F., Cinzano, P., Dan, D., Kyba, C., Furgoni, R., Baugh, K., et al. (2016). The new world atlas of artificial night sky brightness. *Sci. Adv.* 2, e1600377. doi:10.1126/sciadv.1600377

Fang, J. X., Du, H. C., Shi, X., Zhang, S. F., Liu, F., Zhang, Z., et al. (2021). Monoterpenoid signals and their transcriptional responses to feeding and juvenile hormone regulation in bark beetle *Ips hauseri*. *J. Exp. Biol.* 224, jeb238030. doi:10.1242/jeb.238030

Firebaugh, A., and Haynes, K. J. (2016). Experimental tests of light-pollution impacts on nocturnal insect courtship and dispersal. *Oecologia* 182, 1203–1211. doi:10.1007/s00442-016-3723-1

Guy, B., Esther, H., and Ada, R. (2013). Circadian rhythms and endocrine functions in adult insects. *J. Insect Physiol.* 59, 56–69. doi:10.1016/j.jinsphys.2012.10.012

Kaitlin, R., Golec, J. R., and Duan, J. J. (2018). Host selection and potential non-target risk of *Dastarcus helophoroides*, a larval parasitoid of the Asian longhorned beetle, *Anoplophora glabripennis*. *Biol. Control* 123, 120–126. doi:10.1016/j.biocontrol.2018.05.012

Kang, L., Jia, Q. Q., and Sheng, L. (2019). Juvenile hormone signaling – A mini review. *Insect Sci.* 26, 600–606. doi:10.1111/1744-7917.12614

Kempenaers, B., Borgstrom, P., Loes, P., Schlicht, E., and Valcu, M. (2010). Artificial night lighting affects dawn song, extra-pair siring success, and lay date in songbirds. *Cur. Biol.* 20, 1735–1739. doi:10.1016/j.cub.2010.08.028

Kim, M., Vu, T. H., Maas, M. B., Braun, R. I., Wolf, M. S., Roenneberg, T., et al. (2022). Light at night in older age is associated with obesity, diabetes, and hypertension. *Sleep*, zsac130. doi:10.1093/sleep/zsac130

Kouser, S., Palaksha, P., and Shakunthala, V. (2014). Study on fitness of *Drosophila melanogaster* in different light regimes. *Biol. Rhythm Res.* 45, 293–300. doi:10.1080/09291016.2013.817138

Liu, Y., Speisser, B., Knop, E., and Van Kleunen, M. (2022). The Matthew effect: Common species become more common and rare ones become more rare in response to artificial light at night. *Glob. Change Biol.* 28, 3674–3682. doi:10.1111/gcb.16126

Lyu, F., Hai, X. X., Wang, Z. G., Liu, B. X., Yan, A. H., and Bi, Y. G. (2015a). Circadian behaviors of the parasitic beetles, *Dastarcus helophoroides* (Fairmaire) (Coleptera: Bothrideridae) under artificial light/dark conditions. *Acta Entomol. Sin.* 58, 658–664. doi:10.16380/j.kcxb.2015.06.010

Lyu, F., Hai, X. X., Wang, Z. G., Liu, B. X., Yan, A. H., and Bi, Y. G. (2014). Research progress in *Dastarcus helophoroides* Fairmaire(Bothrideridae), an important natural enemy of the longhorn beetle pests. *Sci. Seric.* 40, 1107–1113. doi:10.13441/j.cnki.cykx.2014.06.026

Lyu, F., Hai, X. X., Wang, Z. G., Yan, A. H., Bi, Y. G., and Liu, B. X. (2015b). Diurnal rhythm of adult behavior of *Dastarcus helophoroides* Fairmaire, the parasitic natural enemy of *Apriona germari*. *Sci. Seric.* 41, 239–246. doi:10.13441/j.cnki.cykx.2015.02.007

Mason, I. C., Grimaldi, D., Reid, K. J., Warlick, C. D., Malkani, R. G., Abbott, S. M., et al. (2022). Light exposure during sleep impairs cardiometabolic function. *Proc. Natl. Acad. Sci. U. St. A* 119, e2113290119. doi:10.1073/pnas.2113290119

Mclay, L. K., Green, M. P., and Jones, T. M. (2017). Chronic exposure to dim artificial light at night decreases fecundity and adult survival in *Drosophila melanogaster*. *J. Insect Physiol.* 100, 15–20. doi:10.1016/j.jinsphys.2017.04.009

Obayashi, K., Yamagami, Y., Kurumatani, N., and Saeki, K. (2020). Bedroom lighting environment and incident diabetes mellitus: A longitudinal study of the HEIJO-KYO cohort. *Sleep. Med.* 65, 1–3. doi:10.1016/j.sleep.2019.07.006

Park, Y. M. M., White, A. J., Jackson, C. L., Weinberg, C. R., and Sandler, D. P. (2019). Association of exposure to artificial light at night while sleeping with risk of obesity in women. *JAMA Intern. Med.* 179, 1061–1071. doi:10.1001/jamainternmed.2019.0571

Phillips, A. J. K., Vidafar, P., Burns, A. C., Mcglashan, E. M., Anderson, C., Rajaratnam, S. M. W., et al. (2019). High sensitivity and interindividual variability in the response of the human circadian system to evening light. *Proc. Natl. Acad. Sci. U. S. A.* 116, 12019–12024. doi:10.1073/pnas.1901824116

Sanders, D., Baker, D. J., Cruse, D., Bell, F., Van Veen, F. J. F., and Gaston, K. J. (2022). Spectrum of artificial light at night drives impact of a diurnal species in insect food web. *Sci. Total Environ.* 831, 154893. doi:10.1016/j.scitotenv.2022.154893

Shen, H., He, H., Lu, C., Liang, Y., Wu, H., Zheng, L., et al. (2022). Comparative transcriptome analysis of two populations of *Dastarcus helophoroides* (Fairmaire) under high temperature stress. *Forests* 13, 13. doi:10.3390/f13010013

Tang, H., Yang, Z. Q., and Zhang, Y. N. (2007). Technical researches on distinguishing female and male alive adults of the main parasite of longhorn beetles, *Dastarcus helophoroides* (Coleoptera: Bothrideridae) without injuring. *Acta Zootaxonomica Sin.* 32, 649–654. doi:10.3969/j.issn.1000-0739.2007.03.032

Van Geffen, K. G., Van Eck, E., De Boer, R. A., Van Grunsven, R. H. A., Salis, L., Berendse, F., et al. (2015). Artificial light at night inhibits mating in a Geometrid moth. *Insect Conserv. diver.* 8, 282–287. doi:10.1111/icad.12116

Vanin, S., Bhutani, S., Montelli, S., Menegazzi, P., Green, E. W., Pegoraro, M., et al. (2012). Unexpected features of *Drosophila* circadian behavioural rhythms under natural conditions. *Nature* 484, 371–375. doi:10.1038/nature10991

Wei, J. R., Lu, X. P., and Jiang, L. (2013). Monoterpenes from larval frass of two Cerambycids as chemical cues for a parasitoid, *Dastarcus helophoroides*. *J. Insect Sci.* 13, 59–12. doi:10.1673/031.013.5901

Wei, J. R., Yang, Z. Q., Tang, H., Ma, J. H., and Du, J. W. (2008). Behavior of a Cerambycid parasitiod beetle (*Dastarcus helophoroides*). *Sci. silvae Sin.* 44, 50–55. doi:10.3321/j.issn:1001-7488.2008.07.009

Yang, Z. Q., Li, M. L., Lei, Q., and Wang, X. Y. (2012). Effects of temperature on development and reproduction of *Dastarcus helophoroides* (Coleoptera: Bothrideridae). *Chin. J. Biol. Control* 28, 9–24. doi:10.16409/j.cnki.2095-039x.2012.01.004

Yang, Z. Q., Wang, X. Y., and Zhang, Y. N. (2014). Recent advances in biological control of important native and invasive forest pests in China. *Biol. Control* 68, 117–128. doi:10.1016/j.biocontrol.2013.06.010

Zera, A. J., and Cisper, G. (2001). Genetic and diurnal variation in the juvenile hormone titer in a wing-polymorphic cricket: Implications for the evolution of life histories and dispersal. *Physiol. Biochem. Zool.* 74, 293–306. doi:10.1086/319664

Zera, A. J. (2016). Juvenile hormone and the endocrine regulation of wing polymorphism in insects: New insights from circadian and functional-genomic studies in *Gryllus* crickets. *Physiol. Entomol.* 41, 313–326. doi:10.1111/phen.12166

Zhao, K., Ma, B., Xu, Y., Stirling, E., and Xu, J. (2021). Light exposure mediates circadian rhythms of rhizosphere microbial communities. *ISME J.* 15, 2655–2664. doi:10.1038/s41396-021-00957-3

frontiers | Frontiers in Physiology

TYPE Original Research
PUBLISHED 10 February 2023
DOI 10.3389/fphys.2023.1036397

OPEN ACCESS

EDITED BY
Seema Ramniwas,
Chandigarh University, India

REVIEWED BY
Karan Singh,
New York University, United States
Meena Yadav,
University of Delhi, India
Geetanjali Mishra,
University of Lucknow, India

*CORRESPONDENCE
Guo-Hua Chen,
chenghkm@126.com
Xiao-Ming Zhang,
zxmalex@126.com

SPECIALTY SECTION
This article was submitted to Invertebrate Physiology, a section of the journal Frontiers in Physiology

RECEIVED 04 September 2022
ACCEPTED 30 January 2023
PUBLISHED 10 February 2023

CITATION
Li M, Wei X-M, Li J, Wei S-M, Zhang J-L, Chen G-H and Zhang X-M (2023), Effect of short-term exposure to high temperatures on the reproductive behavior and physiological enzyme activities in the fruit fly *Zeugodacus tau* (Walker). *Front. Physiol.* 14:1036397. doi: 10.3389/fphys.2023.1036397

Effect of short-term exposure to high temperatures on the reproductive behavior and physiological enzyme activities in the fruit fly *Zeugodacus tau* (Walker)

Mao Li, Xiao-Man Wei, Juan Li, Shi-Ming Wei, Jin-Long Zhang, Guo-Hua Chen* and Xiao-Ming Zhang*

College of Plant Protection, Yunnan Agricultural University, Kunming, China

Zeugodacus tau is an economically important invasive pest of various vegetables and fruits. In this study, we evaluated the effects of short-term (12 h) exposure to high temperatures on the reproductive behaviors and physiological enzyme activities of adult *Z. tau* flies. When compared to the control group, the mating rate in the treated group increased significantly after exposure to 34°C and 38°C. After 34°C exposure, the mating rate of the control♀-treated♂ mating was the highest (60.0%). The use of high temperatures for a short period reduced the pre-mating period and lengthened the duration of copulation. After 38°C exposure, the mating between treated♀ and treated♂ had the shortest pre-mating period of 39.0 min and the longest copulation duration of 67.8 min. Mating after a brief exposure to high temperatures had a negative impact on female reproduction, whereas mating with males who previously had a brief exposure to 34°C and 38°C significantly increased female fecundity. After 40 °C exposure, the mating between treated♀ and control♂ showed the lowest fecundity and hatching rate of 293.25 eggs and 25.71%, respectively. The mating between control♀ and treated♂ showed the highest fecundity of 1,016.75 eggs after exposure to 38°C. The SOD, POD, and CAT activities exhibited significant changes (increase or decrease) after the short-term exposure of *Z. tau* adults to high temperatures. After being exposed to 38°C, SOD activity increased by 2.64 and 2.10 times in females and males in the treated group, respectively, compared to the SOD activity in the control group. The AchE, CarE, and GST activities first increased and then decreased with the increase in temperature. CarE activity changed the most after exposure to 38°C, with females and males in the treated group increasing by 7.81 and 1.69 times, respectively, compared to the activity in the control group. In conclusion, mating strategy and physiological stress are important adaptive mechanisms of *Z. tau* for adapting to short-term heat stress in a sex-specific manner.

KEYWORDS

***Zeugodacus tau*, short-term high temperatures, mating behavior, oviposition, physiological enzyme**

1 Introduction

The fruit fly *Z. tau* Walker (Diptera: Tephritidae) is an economically important agricultural pest of various fruits and vegetables. They are widely distributed in Southeast Asia and the South Pacific regions (Jaleel et al., 2018). It is classified as a complex species consisting of nine sibling species (*Zeugodacus tau* A, B, C, D, E, F, G, I, and J) (Baimai et al., 2000; Zaelor and Kitthawee, 2018). The females of *Z. tau* lay eggs beneath the skin of fruits and cause irreversible damage. Additionally, *Z. tau* larvae exhibit an innate feeding behavior of tunneling into the core of fruits, which allows them to escape insecticides (Zheng and Wei, 2019; Canhanga et al., 2020). Temperature is a critical factor in limiting the distribution of ectotherms (Santana et al., 2019). The abnormal changes in climate caused by global warming have a negative impact on pest survival and reproduction (García-Robledo et al., 2016; Ma et al., 2021). Therefore, understanding the impact of short-term high-temperature episodes on *Z. tau* is critical.

High-temperature and low-temperature stress irreversibly damages the function and structure of the reproductive system, thus, affecting the mating behavior of ectotherms (Singh et al., 2015; Enos and Kozak, 2021). High and low temperatures affect the mating behavior of fruit flies, including the mating-related traits of mating latency, duration of copulation, mating frequency, the number of progeny produced, *etc.* (Dev et al., 2013; Stazione et al., 2019; Singh et al., 2022). For example, keeping individuals of *Z. cucurbitae* for 1 h at 45 °C significantly stimulated the mating of *Zeugodacus cucurbitae* (Zeng et al., 2018). Females of *Drosophila melanogaster* recovered faster from cold shock in terms of mating latency, mating success, and progeny production; males recovered faster in terms of mating latency, fertility, sperm competitive ability, and progeny production (Singh and Prasad, 2016; Singh et al., 2017). At 25°C, however, *A. ipsilon* had the highest mating percentage. Calling and mating behaviors were prevent in females of *Agrotis ipsilon* at temperatures lower or higher than 25°C (Xiang et al., 2018). This effect of high and low temperatures on the reproductive behavior of ectotherms altered reproductive fitness. This alteration manifested mainly as a delay in the pre-oviposition and peak period of oviposition, a reduction in egg production and hatching rate, a gradual shortening of the life span in both males and females, and an increase in the female-to-male offspring ratio (Zhou et al., 2011; Stazione et al., 2021). However, the evolution of reproductive traits was found to have no apparent life-history associated cost for cold shock resistance (Singh et al., 2021). Huang et al. (2020) reported that short-term exposure to temperatures above 42°C was unsuitable for the development of *Z. tau* individuals, while short-term treatment with temperatures above 40°C was unsuitable for reproduction in *Z. tau*. However, more research on the reproductive behavior of *Z. tau* under short-term high-temperature exposure is needed.

Under high temperatures, several stress reactions occur in ectotherms. Under stress, ectotherms accumulate toxic metabolites and generate high levels of free radicals. To overcome this problem, protective enzyme systems, including antioxidant and detoxification systems, have evolved in ectotherms (Guo et al., 2018; Shankarganesh et al., 2022). Superoxide dismutase (SOD), catalase (CAT), and peroxidase (POD) are the three main antioxidant enzymes found in ectotherms (Cai et al., 2018). The three main detoxification enzymes in ectotherms are acetylcholinesterase (AchE), carboxylesterase (CarE), and glutathione S-transferase (GST) (Li et al., 2022). Abiotic stresses can have an impact on both enzyme activity and insect reproduction (Roma et al., 2021; Cai et al., 2022). According to previous research, elevated CO_2 affects the population development of thrips as well as the activities of detoxification enzymes. The fecundity of *Frankliniella occidentalis* and *Thrips hawaiiensis* increased and decreased significantly as CO_2 concentration increased. This could be due to the activity of detoxifying enzymes (Cao et al., 2020). The effects of sodium fluoride (NaF) on the reproduction and antioxidant enzyme activities of *Bombyx mori* larvae revealed that NaF in mulberry leaves fed to *B. mori* larvae would cause reproductive damage, a disorder of the antioxidant system in the gonads, and oxidative stress (Tang et al., 2016). External stress-induced oxidative stress may be an important factor in determining their toxicity to insects (Paweł and Grzegorz, 2021). There is, however, little direct evidence of a link between insect enzyme activity and reproduction. In other organisms, particularly marine organisms, oxidative stress caused by abiotic stresses has been linked to impaired reproduction (Han et al., 2014). According to recent research, harmful environments may cause reproduction toxicity by disrupting the expression of reproduction and detoxification-related genes and inducing oxidative stress in organisms (Liu et al., 2022).

The courtship and mating of *Z. tau* occur mainly in the evening (Shamshir and Wee, 2019). Although global warming is characterized primarily by an increase in daytime temperatures (Ma et al., 2021), exposure to such high-temperature conditions affects the subsequent mating activities of the individuals of *Z. tau* in the evening. Few studies have investigated the effect of temperature on the behavior of fruit flies concerning finding a mate and coordinating during mating (Singh et al., 2015; Singh et al., 2021; Singh et al., 2022). Furthermore, male and female behavior and physiology differ, particularly in terms of thermal sensitivity and physiological enzyme activities (Brandt et al., 2018; Macchiano et al., 2019; Singh et al., 2022). Therefore, at higher temperatures, females and males may exhibit behavioral mismatches when seeking or being receptive to potential mates (Singh and Prasad, 2016; Singh et al., 2017; Leith et al., 2020). In this context, we hypothesized that *Z. tau* males and females would use different mating strategies and physiological response mechanisms to adapt to high-temperature stress after a brief high-temperature exposure, and that mating immediately following a brief high-temperature exposure would affect subsequent oviposition behavior at 25°C. The experiment was carried out in an artificial climate chamber, and the mating behaviors of the animals on the same day were evaluated after they were exposed to high temperatures for a short period during the day and then returned to 25°C at dusk. The mating rate, pre-mating period, duration of copulation, and number of offspring produced by mating were all assessed. The activities of antioxidant and detoxification enzymes were determined immediately after exposing individuals of *Z. tau* to high temperatures for a short period of time. By conducting these experiments, we investigated the adaptation of mating behavior and the mechanism of physiological enzyme regulation in *Z. tau* after short-term exposure to high temperatures. The findings of this study could provide a theoretical foundation for the comprehensive management of *Z. tau* in future climate scenarios caused by global warming.

2 Materials and methods

2.1 Rearing and temperature settings

Individuals of *Z. tau* were collected during 2021 from a field of *Cucurbita pepo* in Mengzi City (103.24°E, 23.30°N), Yunnan Province, South China. The study area has an annual average temperature of 17°C–26°C, and extreme summer heat waves (≥34°C) occur in Mengzi City (https://lishi.tianqi.com/mengzi/202207.html). We collected samples of *Z. tau* adults (n = 3–5) from the study area to confirm their identity. These individuals were tested in the laboratory using their mtCOI sequences (Kitthawee and Julsirikul, 2019). The results of the identification revealed that the *Z. tau* individuals belonged to *Z. tau* A. (the identity of the sample deposited in GenBank, no. OP735533). Under laboratory conditions of 25°C ± 1°C, 70% ± 5% RH, and a 14 h:10 h (light: dark) photoperiod, a stable experimental population of *Z. tau* was established. Adults and larvae were fed a synthetic diet (Huang et al., 2020). Individuals of *Z. tau* were reared for more five generations.

The experiments were conducted in an artificial climate chamber (model BIC-300, Shanghai Boxun Medical Biological Instrument Co., Ltd., China) at 25°C ± 1°C, 70% ± 5% RH, and 14 h: 10 h (light: dark) photoperiod (Abraham et al., 2016). Previous research has shown that keeping *Z. tau* adults at 34°C for 12 h does not effect on their survival; however, no individuals can survive for 12 h at 44°C (Huang et al., 2020). Therefore, the temperature exposure groups were evaluated 12 h after being exposed to 34, 36, 38, 40, 42, and 44 °C, while the control group was evaluated at 25°C.

2.2 Effects of short-term exposure to high temperatures on *Z. tau* adults' survival

The adults that emerged within 24 h were selected. Male and female adults were separated and transferred to plastic cages for rearing (35 cm × 35 cm × 35 cm). The sexually mature virgin females and males were chosen after 30 days of rearing at 25°C, and each group of 300 females or males was considered one replicate. The adults were placed in an artificial climate chamber and subjected to temperature of 34, 36, 38, 40, 42, and 44°C for 12 h (light period). After 12 h, the number of dead *Z. tau* adults, survival rate, semi-lethal temperature (LT_{50}), and lethal temperature were calculated. Each recorded temperature was then chosen as a treatment, and four such treatments were established, each with four replicates.

2.3 Effects of short-term exposure to high temperatures on *Z. tau* mating

The experiment was carried out at a temperature of 25°C, and the surviving adult females and males from the previous step were chosen as test insects. After 12 h of exposure at 34, 38, 40, and 42°C, the mating behavior was evaluated within 12 h at 25 °C on the same day because the survival rate test revealed no difference in adult survival at 34°C and 36°C. Three short-term high-temperature exposure conditions were used: a) females were exposed to short-term high-temperature stress before mating with unexposed males (treated♀-control♂); b) males were exposed to short-term high-temperature stress before mating with unexposed females (control♀-treated♂), and c) both females and males were exposed to short-term high-temperature stress before mating (treated♀-treated♂). The control group (control♀-control♂) were formed when females and males were mated at 25 °C without short-term high temperature exposure (control♀-control♂). To allow mating, each pair of female and male in the various combinations was placed inside a 180-mL disposable plastic cup (inverted). To form the base, a suitable cylinder of flower mud was cut out at the mouth of the cup. During the dark period, the disposable plastic cup containing the female-male pair was placed in the artificial climate box at 25 °C. Every 15 min, mating was observed. The mating rate, pre-mating period, and duration of copulation were calculated. A mating combination after exposure to different short-term high temperatures was treated as one treatment, with a total of four short-term high temperatures, three mating combinations, and forming 12 treatments. One replicate consisted of 30 pairs of adults, and four replicates were performed.

2.4 Effects of mating after short-term exposure to high temperatures on *Z. tau* oviposition

The experiments were carried out at a temperature of 25°C. The mated females in the previous step were chosen for the oviposition experiment, and each female was raised in a 180-mL disposable plastic cup. Cotton balls, artificial feed, and a piece of *C. pepo* (1 cm^3) were placed in the plastic cup to provide water and food, as well as to aid in oviposition. All materials were replaced every 24 h. The fecundity and number of eggs laid by females were observed and recorded until they died. Four replicates were performed, each with 20 females.

2.5 Effects of short-term exposure to high temperatures on the physiological enzyme activities of *Z. tau* individuals

Since the survival rate test revealed that only a few adults survived at 42 °C, physiological enzyme activity was measured only at 34, 38, and 40 °C. Virgin females and males (30 days old) were chosen at random and exposed to one of the above temperatures for 12 h, while the control group was kept at 25 °C. The activities of SOD, POD, CAT, AchE, GST, and CarE were determined using the kit's instructions (Beijing Solarbio Science & Technology Co., Ltd., Beijing, China). The enzyme activity was measured using UV-Vis spectrophotometry based on the sample mass (Zhang et al., 2020). Each treatment received three replicates.

2.6 Statistical analysis

Based on linear regression, the semi-lethal temperature (LT_{50}), 95% confidence intervals, regression equation, and correlation coefficient for *Z. tau* were calculated. One-way ANOVA was used to evaluate the reproductive behaviors and activity tests of the physiological enzymes of *Z. tau*. The LSD multiple comparison method was used to compare significant differences between different mating combinations and between females and males at different temperatures. The SPSS software was used for all analyses (version 25.0; SPSS, Chicago, IL, United States). Origin software was used to draw the figures (version 9.1 pro; OriginLab, Northampton, MA, United States).

TABLE 1 The survival rate of *Z. tau* adults exposed to different high-temperature treatments for 12 h.

Temperature (°C)	Females	Males
25	100.0 ± 0.0a	100.0 ± 0.0a
34	99.02 ± 0.98a	96.80 ± 1.62a
36	98.89 ± 0.11a	95.89 ± 0.48a
38	75.28 ± 4.31 b	58.91 ± 8.12 b
40	33.14 ± 3.95c	20.01 ± 3.49c
42	5.44 ± 0.72 d	5.16 ± 1.85 d
44	0.0 ± 0.0 d	0.0 ± 0.0 d

Data are presented as mean ± SE. The different lowercase letters within the same column indicate significant differences ($p < 0.05$).

TABLE 2 The LT_{50} values of *Z. tau* adults after 12 h of exposure to different high-temperature treatments.

	Regression equation	Correlation coefficient r)	LT50 (95% confidence interval)
Females	Y = 51.953 X-82.753	0.920	39.161 (38.544–39.774)
Males	Y = 44.891 X-71.155	0.912	38.464 (38.071–38.855)

3 Results

3.1 The survival rate of *Z. tau* adults exposed to high temperatures for a short duration

The different short-term high-temperature treatments affected the survival rate of *Z. tau* adults. The survival rate of females and males was significantly lower after 38, 40, and 42 °C exposure than that at the control temperature (females: $F_{6,27}$ = 398.1320, p = 0.0001; males: $F_{6,27}$ = 168.5890, p = 0.0001). Male and female survival rates decreased as treatment temperature increased, and the female survival rate was higher than the male survival rate (Table 1). The LT_{50} value for the males was 38.46°C, which was 0.70 °C lower than that of females (Table 2).

3.2 Effect of different short-term high-temperature treatments on reproductive behaviors in *Z. tau*

3.2.1 The mating rate of *Z. tau* adults exposed to different short-term high-temperature treatments

Exposure to high temperatures for a short duration significantly affected the subsequent mating rate of *Z. tau* individuals that day. The mating rate of females was different from that of males after the same temperature exposure. The mating rate was significantly higher after 34 °C and 38 °C exposure compared to that at 25 °C (34 °C: $F_{3,15}$ = 24.4930, p = 0.0001; 38 °C: $F_{3,15}$ = 14.1660, p = 0.0003). After these two temperatures exposure, the control♀-treated♂ combination increased the mating rate by the most (60.0% and 53.25%, respectively), followed by the treated♀- treated♂ and treated♀-control♂ combinations. After short-term exposure to 40 °C, the mating rates of all mating combinations were lower than those of the control, except for the treated♀-control♂ combination ($F_{3,15}$ = 0.4980, p = 0.6908). After short-term exposure to 42 °C, no mating occurred between males and females (Figure 1).

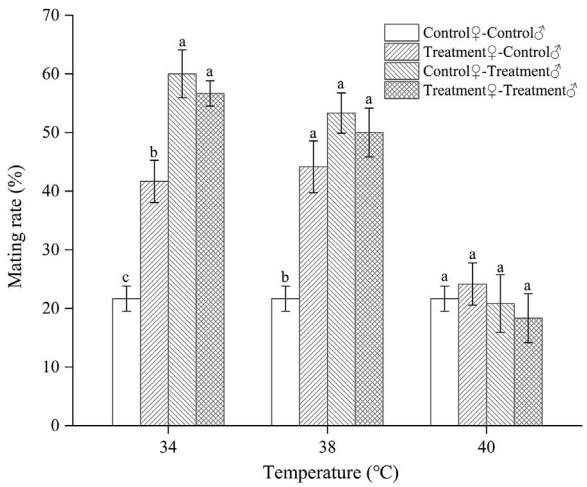

FIGURE 1
The mating rate of *Z. tau* individuals exposed to different high-temperature treatments for 12 h. Data are presented as the mean ± SE. Different lowercase letters above the bars indicate significant differences between different mating combinations at the same temperature ($p < 0.05$). No mating occurred within 24 h after the individuals were exposed to 42°C for 12 h.

3.2.2 The pre-mating period in *Z. tau* adults exposed to different short-term high-temperature treatments

The pre-mating period of *Z. tau* individuals was shortened after a brief exposure to high temperatures. The pre-mating period became shorter at first, then longer as the treatment temperature increased. For all mating combinations, the shortest pre-mating period occurred after 38 °C exposure ($F_{3,15}$ = 9.290, p = 0.0001). The order was as follows: treated♀-treated♂ (39.0 min), treated♀-control♂ (66.47 min), control♀-treated♂ (78.59 min), and control♀-control♂ (123.40 min). Among all mating

TABLE 3 The pre-mating period of *Z. tau* adults exposed to different high-temperature treatments for 12 h.

Temperature (°C)	Pre-mating period (min)			
	Treated♀-control♂	Control♀-treated♂	Treated♀-treated♂	Control♀-control♂
34	97.27 ± 7.79ABab	109.67 ± 11.82ABab	85.0 ± 10.05BCb	123.40 ± 12.91a
38	66.47 ± 6.67Bb	78.59 ± 7.15Bb	39.0 ± 9.76Cc	123.40 ± 12.91a
40	98.75 ± 12.77ABa	100.0 ± 8.66ABa	93.75 ± 9.87ABa	123.40 ± 12.91a
25	123.40 ± 12.91A	123.40 ± 12.91A	123.40 ± 12.91A	—

Data are mean ± SE. the different lowercase letters after the same row data indicate significant differences between different mating combinations at the same temperature, and the different uppercase letters after the same column data indicate significant differences between the same mating combinations at different temperatures ($p < 0.05$). The same is below.

TABLE 4 The duration of copulation of *Z. tau* adults exposed to different short-term high-temperature treatments for 12 h.

Temperature (°C)	Duration of copulation (min)			
	Treated♀-control♂	Control♀-treated♂	Treated♀-treated♂	Control♀-control♂
34	627.42 ± 16.87ABa	640.0 ± 18.43Aa	622.47 ± 11.29Ba	595.47 ± 16.23a
38	648.07 ± 14.82Aa	637.81 ± 9.03Aa	678.0 ± 18.67Aa	595.47 ± 16.23b
40	609.50 ± 12.75ABa	626.0 ± 14.33Aa	599.83 ± 15.95Ba	595.47 ± 16.23a
25	595.47 ± 16.23B	595.47 ± 16.23A	595.47 ± 16.23B	—

TABLE 5 Fecundity of *Z. tau* adults exposed to different high-temperature treatments for 12 h.

Temperature (°C)	Fecundity per females			
	Treated♀-control♂	Control♀-treated♂	Treated♀-treated♂	Control♀-control♂
34	411.25 ± 62.97ABb	1,004.11 ± 77.80Aa	541.33 ± 69.62Ab	545.29 ± 35.48b
38	385.80 ± 38.80Bb	1,016.75 ± 116.53Aa	538.60 ± 41.84Ab	545.29 ± 35.48b
40	293.25 ± 45.62Bb	373.50 ± 52.70Bb	299.50 ± 55.98Bb	545.29 ± 35.48a
25	545.29 ± 35.48A	545.29 ± 35.48B	545.29 ± 35.48A	—

combinations, treated♀-treated♂ had the shortest pre-mating period in all treated groups ($F_{3,15} = 8.3580$, $p = 0.0002$) (Table 3).

3.2.3 Duration of copulation in *Z. tau* adults exposed to different short-term high-temperature treatments

The duration of copulation increased after treatment in *Z. tau* adults. Copulation duration was significantly longer after 38 °C exposure than in the control ($F_{3,15} = 4.380$, $p = 0.0069$). The longest durations of copulation for the treated♀-control♂ and treated♀-treated♂ combinations were 648.07 min and 678.0 min, respectively, both of which were treated after 38 °C exposure (treated♀-control♂: $F_{3,15} = 2.3110$, $p = 0.0436$; treated♀-treated♂: $F_{3,15} = 4.8960$, $p = 0.0051$). The longest duration of copulation for the control♀-treated♂ combination was 640.0 min which occurred after treatment after 34 °C exposure ($F_{3,15} = 2.1810$, $p = 0.0981$) (Table 4).

3.2.4 Fecundity of *Z. tau* adults exposed to different short-term high-temperature treatments

Mating of *Z. tau* adults after short-term high-temperature exposure affected subsequent fecundity. After 34 °C and 38 °C exposure, the fecundity of control♀-treated♂ was the highest, with the values of 1,004.11 eggs and 1,016.75 eggs, respectively (34 °C: $F_{3,15} = 16.0720$, $p = 0.0001$; 38 °C: $F_{3,15} = 5.6660$, $p = 0.0044$). After 40 °C exposure, fecundity decreased significantly ($F_{3,15} = 6.3760$, $p = 0.0036$). The fecundity of treated♀-control♂ reached the minimum level of 293.25 eggs after 40 °C exposure ($F_{3,15} = 3.3450$, $p = 0.0345$) (Table 5).

3.2.5 Hatching rate of the eggs of *Z. tau* individuals exposed to different short-term high-temperature treatments

Mating of *Z. tau* adults after short-term high-temperature exposure affected subsequent hatching rate of eggs. The hatching rate decreased to different degrees in different treated groups, among which the hatching rate of the eggs of treated♀-control♂ was the lowest (34 °C: $F_{3,15} = 3.0090$, $p = 0.0456$; 38 °C: $F_{3,15} = 0.9680$, $p = 0.4205$; 40 °C: $F_{3,15} = 9.9470$, $p = 0.0003$). The lowest hatching rate of the eggs of treated♀-control♂ was only 25.71% after 40 °C exposure ($F_{3,15} = 7.0480$, $p = 0.0010$). The hatching rate of control♀-treated♂ eggs increased with treatment temperature, reaching a maximum of 82.25% after 40 °C exposure, which was close to the control ($F_{3,15} = 2.8630$, $p =$

TABLE 6 The hatching rate of the eggs of *Z. tau* adults exposed to different high-temperature treatments for 12 h.

Temperature (°C)	Hatching rate (%)			
	Treated♀-control♂	Control♀-treated♂	Treated♀-treated♂	Control♀-control♂
34	58.07 ± 7.59Bb	61.62 ± 5.19Bb	72.09 ± 5.86Aab	82.98 ± 3.77a
38	68.26 ± 6.27ABa	74.05 ± 7.49Aba	68.99 ± 4.41Aa	82.98 ± 3.77a
40	25.71 ± 2.97Cb	82.25 ± 5.21Aa	65.78 ± 9.92Aa	82.98 ± 3.77a
25	82.98 ± 3.77A	82.98 ± 3.77A	82.98 ± 3.77A	—

0.0453). The hatching rate of treated♀-treated♂ eggs decreased with increasing treatment temperature ($F_{3,15}$ = 1.1530, p = 0.3491). (Table 6).

3.3 Effect of short-term exposure to high temperatures on the physiological enzyme activities of *Z. tau* individuals

3.3.1 Antioxidant enzyme activities in *Z. tau* individuals exposed to different short-term high-temperature treatments

The antioxidant enzyme activities of *Z. tau* individuals were affected by short-term exposure to high temperatures, and the enzyme activities of females and males differed (Figure 2). The SOD activity of both females and males increased and then decreased as the treatment temperature increased. The highest SOD activity was observed after 38°C exposure, SOD activity increased by 2.64 and 2.10 times in females and males in the treated group, respectively, compared to the SOD activity in the control group (females: $F_{3.11}$ = 202.3730, p = 0.0001; males: $F_{3.11}$ = 210.920, p = 0.0001). After 40 °C exposure, the SOD activity in males was lower than that in the individuals in the control group and significantly lower than that in females ($F_{1,5}$ = 19.6660, p = 0.0114) (Figure 2A). The highest POD activity was observed after 40 °C exposure. After this temperature exposure, the POD activity of females and males increased by 0.88 times and 0.24 times, respectively, compared to the activity in the control group (females: $F_{3,11}$ = 56.4710, p = 0.0001; males: $F_{3,11}$ = 16.7520, p = 0.0008) (Figure 2B). The CAT activity in females was the highest after 40 °C exposure, and after this temperature exposure, the activity increased by 0.44 times compared to the control ($F_{3,11}$ = 27.2690, p = 0.0001). In males, CAT activity decreased as treatment temperature increased ($F_{3,11}$ = 18.2520, p = 0.0001) (Figure 2C).

3.3.2 Activities of detoxifying enzymes in *Z. tau* individuals exposed to different short-term high-temperature treatments

As the treatment temperature increased, the activity of the detoxifying enzymes in *Z. tau* individuals first increased and then decreased, with differences between females and males (Figure 3). The AchE activity of females and males was the highest after 38°C and 34°C exposure, respectively. The activities in females and males increased by 1.04 and 1.25 times, respectively, when compared to the control group (females: $F_{3,15}$ = 161.3250, p = 0.0001; males: $F_{3,15}$ = 181.6750, p = 0.0001). (Figure 3A). CarE activity was higher in the short-term high-temperature treated groups than in the control group, with the highest activity recorded after 38°C exposure. Females' and males' CarE activities after 38 °C exposure increased 7.81 times and 1.69 times, respectively, compared to the control group (females: $F_{3.11}$ = 83.3130, p = 0.0010; males: $F_{3,11}$ = 101.2170, p = 0.0001) (Figure 3B). The GST activity in females and males was the highest after 38 °C and 34 °C, respectively. After these temperatures exposure, the GST activity in females and males increased by 1.75 times and 1.29 times, respectively, compared to the activities in the control group (females: $F_{3,15}$ = 8.7750, p = 0.0038; males: $F_{3,15}$ = 14.4580, p = 0.0014). The GST activity in males was higher than that in females after 25°C and 34°C exposure, while the activity in females was higher than that in males after 38°C and 40°C exposure (25°C: $F_{1,5}$ = 0.9160, p = 0.3926; 34°C: $F_{1,7}$ = 8.6110, p = 0.0261; 38°C: $F_{1,7}$ = 30.9230, p = 0.0051; 40°C: $F_{1,7}$ = 59.9920, p = 0.0015) (Figure 3C).

4 Discussion

This study's findings highlighted three key points. First, mating of *Z. tau* adults was promoted after short-term high-temperature exposure after 34°C and 38°C exposure. In addition, the pre-mating period was shorter, and copulation lasted longer. Second, mating of *Z. tau* adults after short-term high-temperature exposure affected subsequent oviposition. Female fecundity and hatching rate decreased after short-term high-temperature stress. In contrast, mating with males who previously had a brief exposure to 34°C and 38°C significantly increased female fecundity. Third, short-term exposure to high temperatures affected the physiological metabolism of *Z. tau* adults; the individuals responded to this stress using their antioxidant and detoxification systems.

We discovered that short-term high-temperature treatment affected mating rate in *Z. tau*. Temperature changes in the environment can influence fruit fly mating behavior (Singh et al., 2015; Singh et al., 2021; Singh et al., 2022). Behavioral adaptations in ectotherms can help them to cope with high-temperature stress (Lachenicht et al., 2010). In this study, short-term exposure to high temperatures negatively affected the survival of *Z. tau* adults, although their mating rate increased after 34°C and 38°C exposure. Therefore, we inferred that changes in the mating behavior might be a survival strategy adopted by *Z. tau* adults to cope with high-temperature stress. Other organisms have shown similar behavioral adaptation strategies for survival under environmental stress, such as hormesis and stimulated parasitic behavior in *Encarsia formosa* after exposure to sublethal concentrations of spirotetramat (Yang et al., 2021), an increase in courtship and copulation behavior in *Trichogramma chilonis* exposed to an insecticide (Wang et al., 2018), and so on. Temperature also influences the expression of many behavioral traits

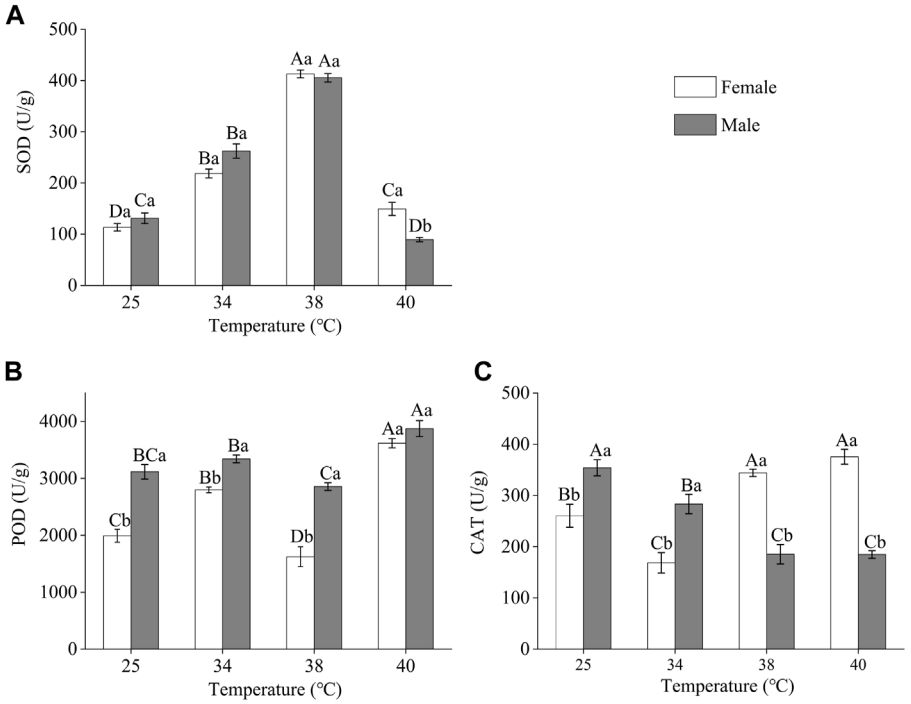

FIGURE 2
Antioxidant enzyme activities in *Z. tau* adults exposed to different high-temperature treatments for 12 h. Data are presented as the mean ± SE. Different lowercase letters above bars represent a significant difference in the antioxidant enzyme activity between females and males at the same temperature. In contrast, different uppercase letters above bars indicate a significant difference in the antioxidant enzyme activities of females/males at different temperatures ($p < 0.05$) **(A)** SOD **(B)** POD, and **(C)** CAT.

in ectotherms, including several traits involved in pair formation and mating (Singh and Prasad, 2016; Singh et al., 2017; Leith et al., 2020). Adult males exhibit a series of courtship behaviors to attract females during fruit fly mating, while a large proportion of adult females refuse to mate (Shelly, 2001; Aquino and Joachim-Bravo, 2014). In this study, the treated♀-control♂ and control♀-treated♂ combinations of *Z. tau* exhibited significantly higher mating after 34°C and 38°C exposure compared to the individuals in the control group. This finding indicated that even short-term exposure to high-temperature stress within a certain temperature range can weaken sexual selection in females, but the courtship behavior of males may not be adversely affected. Whether external stimuli can regulate the courtship behavior in fruit flies is not known. However, environmental factors and the signaling behavior of males might be involved in the regulation of courtship behavior in fruit flies (Díaz-Fleischer and Arredondo, 2011).

Short-term exposure to high-temperature stress shortened the pre-mating period and prolonged the duration of copulation in *Z. tau*. Most studies have suggested that the pre-mating period of adults is the shortest at suitable temperatures, while the duration of copulation is shortened significantly with an increase in temperature (Katsuki and Miyatake, 2008; Yang et al., 2015). In this study, we discovered disparate results. These differences occurred most likely because previous studies were conducted at constant temperatures. In mating behavior, the duration of copulation is frequently regarded as important for sex selection and has a significant impact on the adaptability of adult males and females (Linn et al., 2007; De-Lima et al., 2021). In this study, the prolonged duration of mating after exposure to short-term high-temperature treatment might be related to the mating characteristics of *Z. tau*. Fruit flies demonstrate distinct circadian rhythms during mating behavior (Fletcher, 1987). Unlike many species that mate several times a day, individuals of *Z. tau* mate only once a day. Furthermore, despite the fact that *Z. tau* females mate with multiple males, they exhibit cyclic receptivity, which means that after each mating event, females resist mating for a period of time before regaining the ability to accept mates (Chinajariyawong et al., 2009). Therefore, when mating after short periods of heat stress, *Z. tau* may prefer to extend the mating time to ensure reproductive success.

Aside from directly causing mortality, high temperatures may have an indirect effect on population development by reducing reproductive adaptability (Tao et al., 2018; Zhou et al., 2020). This study looked into the oviposition process of *Z. tau* and discovered that short-term exposure to high-temperature treatment affected fecundity and hatching rate after mating. After short-term high-temperature treatment, fecundity and the hatching rate decreased in females, which was consistent with the finding of previous studies (Liang et al., 2021). High ambient temperatures adversely affect pest reproduction, although, in most studies, this conclusion was based on the results of high-temperature treatment of females or the simultaneous treatment of females and males (Zhou et al., 2020; Takeda, 2022). In this study, the fecundity of control♀-treated♂ increased

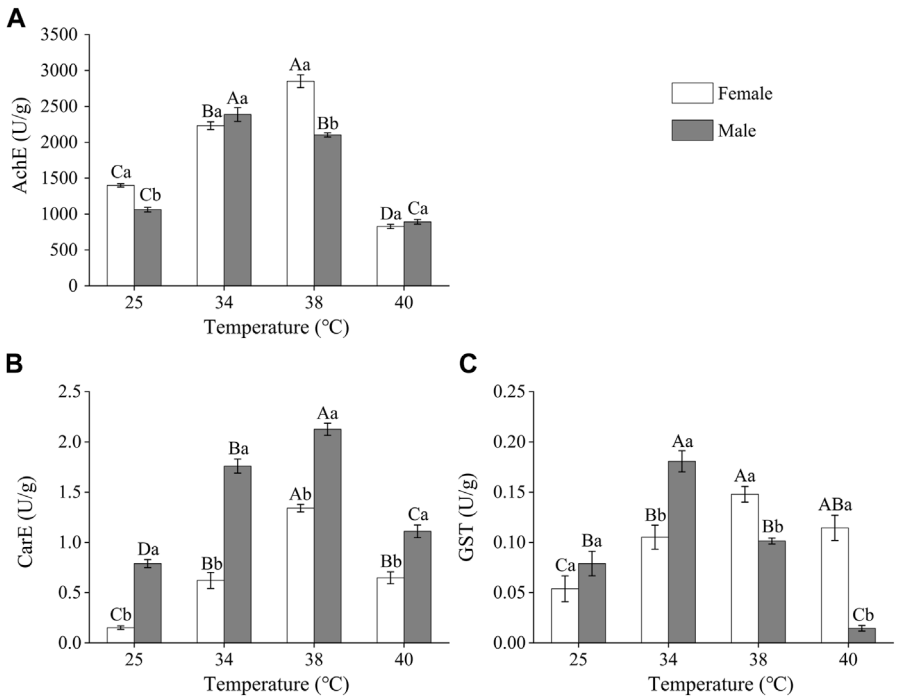

FIGURE 3
The activities of detoxifying enzymes in *Z. tau* adults exposed to different high-temperature treatments for 12 h. Data are presented as the mean ± SE. Different lowercase letters above bars represent a significant difference in the detoxifying enzyme activity between females and males at the same temperature, while different uppercase letters above bars indicate a significant difference in the detoxifying enzyme activities of females/males at different temperatures ($p < 0.05$) **(A)** AchE **(B)** CarE, and **(C)** GST.

significantly after 34°C and 38°C exposure, while the hatching rate increased with the increase in treatment temperature. Heat stress affects reproduction in adult males, and this has also been demonstrated in other species. For example, female *Bicyclus anynana*, after mating with heat-stressed males exhibited an increase in early fertilization (Janowitz and Fischer, 2011). Another study reported that short-term exposure to high temperatures was detrimental to the reproduction of male *Grapholita molesta* (Bao et al., 2019). This finding was different from the results of our study. Our findings on oviposition in the control♀-treated♂ combination, combined with the results of prolonged copulation, suggested that short-term exposure to high-temperature treatment significantly affected the fecundity and fertility of *Z. tau* males. This indicated an increase in the investment of adult males in subsequent reproduction following high-temperature stress. According to some studies, the presence of sperm in the reproductive tract of females can directly stimulate oviposition and increase fertility (Gromko et al., 1984; Tom and Nina 1998). Therefore, we speculated that the heat-stressed males produced greater quantities of sperm, which was then delivered to the females. These females consequently exhibited higher fecundity and hatching rate. In some studies, mating negatively affected females; even the secretions from male appendages reduced the number of eggs laid by the females and shortened their lifespan (Chapman et al., 1995; Siva-Jothy et al., 1998). In conclusion, mating of *Z. tau* adults after short-term exposure to high temperatures may be both advantageous and disadvantageous to their reproductive fitness.

The response of antioxidant enzymes to stress is an important strategy adopted by fruit flies to cope with temperature-related stress (Jia et al., 2011). In this study, the activities of the SOD, POD, and CAT enzymes in *Z. tau* adults were altered to varying degrees under short-term high-temperature treatment, indicating oxidative stress and physical damage to *Z. tau* adults due to high-temperature stress. After high-temperature treatment, these three antioxidant enzymes, particularly SOD, showed significant changes. SOD catalyzes the oxidation of superoxide to produce hydrogen peroxide (H_2O_2) (Larisa et al., 2021). It is an important enzyme that helps organisms resist oxidative stress. SOD activity increased significantly after 34 °C and 38 °C exposure in our study. Therefore, we inferred that high-temperature stress induced SOD activity in *Z. tau* adults, which led to effective scavenging of the oxygen free radicals and protected them from the damage caused by these reactive oxygen species. However, when the treatment temperature increased to 40°C, the high-temperature stress was beyond the tolerance range of *Z. tau* adults and the SOD activity decreased. These findings matched those of other studies on *Empoasca onukii* and *Frankliniella occidentalis* (Qiao et al., 2015; Yuan et al., 2021). After 40 °C exposure, the activity of oxidoreductase was higher in females than in males, implying that the oxidoreductase system was more efficient in females. This could be one of the reasons why males die at a higher rate than females under short-term high-temperature stress.

In fruit flies, the action of the detoxification enzyme system is important for coping with various environmental pressures (Wang et al., 2016). In this study, the activities of the three detoxifying enzymes AchE, CarE, and GST in *Z. tau* first increased and then decreased with the increase in the treatment temperature. The main factors associated with an increase in the activity of detoxification

enzymes may include oxidative stress and increased metabolic waste at high temperatures. The variation in the activity of the detoxifying enzymes was similar to that reported in a study on *Tetrarcychus urticae* exposed to high-temperature stress (Wang et al., 2021). The differences in the changes in detoxification enzymes and their levels in male and female flies exposed to the same high temperature reflected the pest's sex-specific adaptive capability. Short-term high temperatures were found to interfere with the behavioral and physiological processes of *Z. tau*, and it is speculated that metabolic differences between males and females may be one of the important factors causing the behavioral differences. There is little information on the relationship between enzyme activity and behavior in invertebrates. AChE activity can be used as a biomarker to evaluate changes in neurotoxicity and can affect related physiological and behavioral processes (Schweizer et al., 2019). The relationships between AChE inhibition and impairment of physiological and behavioral processes, particularly in vertebrate species, have been well explored (Bonansea et al., 2016; Pour et al., 2022). In *Gammarus fossarum*, for example, AChE inhibition impairs both feeding and locomotor behavior (Xuereb et al., 2009). In this study, some short-term high temperatures did increase AChE activity in *Z. tau* and changed its reproductive behavior. The persistent response of AChE may be the main mechanism of mating in *Z. tau* after short-term high temperature exposure. This study, however, does not confirm that there is a robust relationship between behavioral changes and AChE activity in *Z. tau*, and more research is needed to determine the quantitative relationship between them.

The findings of this study confirmed that the in response to short-term high-temperature environmental stress, the mechanisms of mating behavior, antioxidant defense, and detoxifying enzymes in *Z. tau* alter to cope with temperature changes and high-temperature stress, and that these mechanisms are sex-specific. Our findings may have important ecological implications for the reproduction and survival of *Z. tau* under global warming scenarios, and they provide a theoretical basis for predicting the population and range of distribution of this species under climate variability. We only evaluated and analyzed the mating process and the associated changes in *Z. tau* adults after short-term exposure to high-temperature conditions in this study; however, the mechanism underlying the regulation of the reproductive behavior of *Z. tau* and the associated gene expression pattern remains unknown. Additionally, increased ambient temperatures are generally accompanied by changes in carbon dioxide and humidity (Piotr et al., 2017). Therefore, evaluating the response and the underlying molecular mechanism in *Z. tau* individuals under the action of multiple factors is necessary to formulate novel strategies and approaches for dealing with such circumstances.

Data availability statement

The original contributions presented in the study are included in the article/supplementary material, further inquiries can be directed to the corresponding author.

Author contributions

ML, X-MZ, and G-HC conceived and designed research. ML, X-MW, JL, and S-MW conducted experiments. ML and J-LZ analyzed data. ML wrote the manuscript. X-MZ and G-HC reviewed and edited the document. All authors read and approved the manuscript.

Funding

The present research work was supported by Major Science and Technology Special Projects in Yunnan Province (202102AE090006), Reserve Talents of Young and Middle-aged Academic and Technological Leaders in Yunnan Province (202105AC160071), the Young Top Talents of "High-level Talents Training Support Program in Yunnan Province" (YNWRQNBJ2020291), and the National Fund for Studying Abroad [LJX (2021) No. 15].

Acknowledgments

We thank Prof. Bin Chen (Yunnan Agricultural University) for help in determining activities of physiological enzymes. We are also grateful to Mr. Rui Xue, Shaowu Yang, Yuyu Huang and Qian Chen (Yunnan Agricultural University) for their suggestions and help in the experiments.

Conflict of interest

The authors declare that the research was conducted in the absence of any commercial or financial relationships that could be construed as a potential conflict of interest.

Publisher's note

All claims expressed in this article are solely those of the authors and do not necessarily represent those of their affiliated organizations, or those of the publisher, the editors and the reviewers. Any product that may be evaluated in this article, or claim that may be made by its manufacturer, is not guaranteed or endorsed by the publisher.

References

Abraham, S., Contreras-Navarro, Y., and Pérez-Staples, D. (2016). Female age determines remating behavior in wild Mexican fruit flies. *J. Insect Behav.* 29, 340–354. doi:10.1007/s10905–016–9562–4

Aquino, J. C., and Joachim-Bravo, I. S. (2014). Relevance of male size to female mate choice in *Ceratitis capitata* (Diptera: Tephritidae): Investigations with wild and laboratory-reared flies. *J. Insect Behav.* 27, 162–176. doi:10.1007/s10905–013–9410–8

Baimai, V., Phinchongsakuldit, J., Sumrandee, C., and Tigvattananont, S. (2000). Cytological evidence for a complex of species within the taxon *Bactrocera tau* (Diptera: Tephritidae) in Thailand. *Biol. J. Linn. Soc. Lond.* 69, 399–409. doi:10.1111/j.1095-8312.2000.tb01213.x

Bao, X. W., Fang, A. S., Wu, J. X., and Xu, X. L. (2019). Effects of short-term heat treatment on adult's reproduction and longevity of oriental fruit moth, *Grapholita molesta* Busck. *J. Fruit. Sci.* 36, 486–492. (in Chinses). doi:10.13925/j.cnki.gsxb.20180382

Bonansea, R. I., Wunderlin, D. A., and Amé, M. V. (2016). Behavioral swimming effects and acetylcholinesterase activity changes in *Jenynsia multidentata* exposed to chlorpyrifos and cypermethrin individually and in mixtures. *Ecotoxicol. Environ. Saf.* 129, 311–319. doi:10.1016/j.ecoenv.2016.03.043

Brandt, E. E., Kelley, J. P., and Elias, D. O. (2018). Temperature alters multimodal signaling and mating success in an ectotherm. *Behav. Ecol. Sociobiol.* 72, 191. doi:10.1007/s00265–018–2620–5

Cai, P. M., Hong, J. F., Wang, C., Yang, Y. C., Yi, C. D., Chen, J. H., et al. (2018). Effects of Co-60 radiation on the activities of three main antioxidant enzymes in *Bactrocera dorsalis* (Hendel) (Diptera: Tephritidae). *J. Asia. Pac. Entomol.* 21, 345–351. doi:10.1016/j.aspen.2018.01.006

Cai, Y. B., Dou, T., Gao, F. T., Wang, G. H., Dong, Y. C., Song, N., et al. (2022). Sublethal effects of thiamethoxam on biological traits and detoxification enzyme activities in the small Brown flanthopper, *Laodelphax striatellus* (Fallén). *J. Econ. Entomol.* 115, 2051–2060. doi:10.1093/JEE/TOAC178

Canhanga, L., De-Meyer, M., Cugala, D., Massimiliano, V., and Maulid, M. (2020). Economic injury level of the oriental fruit fly, *Bactrocera dorsalis* (Diptera: Tephritidae), on commercial mango farms in manica province, Mozambique. *Afr. Entomol.* 28, 278–289. doi:10.4001/003.028.0278

Cao, Y., Yang, H., Gao, Y. L., Wang, L. J., Li, J., Wang, C., et al. (2020). Effect of elevated CO_2 on the population development of the invasive species *Frankliniella occidentalis* and native species *Thrips hawaiiensis* and activities of their detoxifying enzymes. *J. Pest Sci.* 94, 29–42. doi:10.1007/s10340–020–01224–8

Chapman, T., Liddle, L. F., Kalb, J. M., Wolfner, M. F., and amd Partridge, L. (1995). Cost of mating in *Drosophila melanogaster* females is mediated by male accessory gland products. *Nature* 373, 241–244. doi:10.1038/373241a0

Chinajariyawong, A., Drew, R. A. I., Meats, A., Balagawi, S., and Vijaysegaran, S. (2009). Multiple mating by females of two *Bactrocera* species (Diptera: Tephritidae: Dacinae). *Bull. Entomol. Res.* 100, 325–330. doi:10.1017/S0007485309990320

De-Lima, C. H. M., NÓbrega, R. L., Ferraz, M. L., and Pontes, W. J. T. (2021). Mating duration and spermatophore transfer in *Cryptolaemus montrouzieri* (Coccinellidae). *Biologia* 77, 149–155. doi:10.1007/S11756–021–00907–6

Dev, K., Chahal, J., and Parkash, R. (2013). Seasonal variations in the mating-related traits of *Drosophila melanogaster*. *J. Ethol.* 31, 165–174. doi:10.1007/s10164–013–0364–2

Díaz-Fleischer, F., and Arredondo, J. (2011). Light conditions affect sexual performance in a lekking tephritid fruit fly. *J. Exp. Biol.* 214, 2595–2602. doi:10.1242/jeb.055004

Enos, A. N., and Kozak, G. M. (2021). Elevated temperature increases reproductive investment in less preferred mates in the invasive European corn borer moth. *Ecol. Evol.* 11, 12064–12074. doi:10.1002/ECE3.7972

Fletcher, B. S. (1987). The biology of dacine fruit flies. *Annu. Rev. Entomol.* 32, 115–144. doi:10.1146/annurev.en.32.010187.000555

García-Robledo, C., Kuprewicz, E. K., Staines, C. L., Erwin, T. L., and Kress, W. J. (2016). Limited tolerance by insects to high temperatures across tropical elevational gradients and the implications of global warming for extinction. *Proc. Natl. Acad. Sci. USA.* 113, 680–685. doi:10.1073/pnas.1507681113

Gromko, M. H., Newport, M. E. A., and Kortier, M. G. (1984). Sperm dependence of female receptivity to remating in *Drosophila melanogaster*. *Evolution* 38, 1273–1282. doi:10.1111/j.1558–5646.1984.tb05649.x

Guo, L., Su, M. M., Liang, P., Li, S., and Chu, D. (2018). Effects of high temperature on insecticide tolerance in whitefly *Bemisia tabaci* (Gennadius) Q biotype. *Pestic. Biochem. Physiol.* 150, 97–104. doi:10.1016/j.pestbp.2018.07.007

Han, J., Won, E. J., Lee, B. Y., Hwang, U. K., Kim, I. C., Yim, J. H., et al. (2014). Gamma rays induce DNA damage and oxidative stress associated with impaired growth and reproduction in the copepod Tigriopus japonicus. *Tigriopus Jpn. Aquat. Toxicol.* 152, 264–272. doi:10.1016/j.aquatox.2014.04.005

Huang, Y. Y., Gu, X. P., Peng, X. Q., Tao, M., Chen, G. H., and Zhang, X. M. (2020). Effect of short-term high-temperatures on the growth, development and reproduction in the fruit fly, *Bactrocera tau* (Diptera: Tephritidae). *Sci. Rep.* 10, 6418–6427. doi:10.1038/s41598–020–63502-w

Jaleel, W., Lu, L. R., and He, Y. R. (2018). Biology, taxonomy, and IPM strategies of *Bactrocera tau* walker and complex species (Diptera: Tephritidae) in Asia: A comprehensive review. *Environ. Sci. Pollut. Res.* 20, 19346–19361. doi:10.1007/s11356–018–2306–6

Janowitz, S. M., and Fischer, K. (2011). Opposing effects of heat stress on male versus female reproductive success in *Bicyclus anynana* butterflies. *J. Therm. Biol.* 36, 283–287. doi:10.1016/j.jtherbio.2011.04.001

Jia, F. X., Dou, W., Hu, F., and Wang, J. J. (2011). Effects of thermal stress on lipid peroxidation and antioxidant enzyme activities of oriental fruit fly, *Bactrocera dorsalis* (Diptera: Tephritidae). *Fla. Entomol.* 94, 956–963. doi:10.1653/024.094.0432

Katsuki, M., and Miyatake, T. (2008). Effects of temperature on mating duration, sperm transfer and remating frequency in *Callosobruchus chinensis*. *J. Insect Physiol.* 55, 112–115. doi:10.1016/j.jinsphys.2008.10.012

Kitthawee, S., and Julsirikul, D. (2019). Population genetic structure of *Zeugodacus tau* species complex in Thailand. *Agric. For. Entomol.* 21, 265–275. doi:10.1111/afe.12328

Lachenicht, M. W., Clusella-Trullas, S., Boardman, L., Roux, C. L., and Terblanche, J. S. (2010). Effects of acclimation temperature on thermal tolerance, locomotion performance and respiratory metabolism in *Acheta domesticus* L. (Orthoptera: Gryllidae). *J. Insect Physiol.* 56, 822–830. doi:10.1016/j.jinsphys.2010.02.010

Larisa, I., Anja, G., Marija, M., Milena, V., Aleksandra, F., Dragana, M., et al. (2021). Tissue-specific responses of *Lymantria dispar* L. (Lepidoptera: Erebidae) larvae from unpolluted and polluted forests to thermal stress. *J. Therm. Biol.* 96, 102836. doi:10.1016/J.JTHERBIO.2021.102836

Leith, N. T., Jocson, D. I., and Fowler-Finn, K. D. (2020). Temperature-related breakdowns in the coordination of mating in *Enchenopa binotata* treehoppers (Hemiptera: Membracidae). *Ethology* 126, 870–882. doi:10.1111/eth.13033

Li, X. L., Qi, Y. X., and Lu, Y. Y. (2022). Advances for the metabolic detoxification genes in major Tephritidae species. *J. Plant Prot.* 49, 351–365. (in Chinese). doi:10.13802/j.cnki.zwbhxb.2022.2022832

Liang, F. F., Wang, Z. Y., He, K. L., Bai, S. X., and Zhang, T. T. (2021). Effects of brief exposure to high temperatures on the survival and fecundity of *Athetis lepigone* (Lepidoptera: Noctuidae). *J. Therm. Biol.* 100, 103066. doi:10.1016/J.JTHERBIO.2021.103066

Linn, C. D., Molina, Y., Difatta, J., and Christenson, T. E. (2007). The adaptive advantage of prolonged mating: A test of alternative hypotheses. *Anim. Behav.* 74, 481–485. doi:10.1016/j.anbehav.2007.02.004

Liu, Y., Zhang, J. L., Zhao, H. Y., Cai, J., Sultan, Y., Fang, H. Y., et al. (2022). Effects of polyvinyl chloride microplastics on reproduction, oxidative stress and reproduction and detoxification-related genes in. *Daphnia magna. Comp. biochem. Physiol. Part C Toxicol. Pharmacol.* 245, 109269. doi:10.1016/J.CBPC.2022.109269

Ma, C. S., Ma, G., and Pincebourde, S. (2021). Survive a warming climate: Insect responses to extreme high temperatures. *Annu. Rev. Entomol.* 66, 163–184. doi:10.1146/annurev-ento-041520–074454

Macchiano, A., Sasson, D. A., Leith, N. T., and Fowler-Finn, K. D. (2019). Patterns of thermal sensitivity and sex-specificity of courtship behavior differs between two sympatric species of *Enchenopa* Treehopper. *Front. Ecol. Evol.* 7, 361. doi:10.3389/fevo.2019.00361

Paweł, C., and Grzegorz, C. (2021). The effect of *Santolina chamaecyparissus* and *Tagetes patula* essential oils on biochemical markers of oxidative stress in aphids. *Insects* 12, 360. doi:10.3390/INSECTS12040360

Piotr, T., Beatriz, D., Simone, V., and Alberto, F. (2017). Insect-plant-pathogen interactions as shaped by future climate: Effects on biology, distribution, and implications for agriculture. *Insect Sci.* 24, 975–989. doi:10.1111/1744–7917.12531

Pour, S. A., Shahriari, M., Zibaee, A., Mojarab-Mahboubkar, M., Sahebzadeh, N., and Hoda, H. (2022). Toxicity, antifeedant and physiological effects of trans-anethole against *Hyphantria cunea* Drury (Lep: Arctiidae). *Pestic. Biochem. Physiol.* 185, 105135. doi:10.1016/J.PESTBP.2022.105135

Qiao, L., Qin, D. Z., Lu, Z. C., Liu, X. C., Lv, L. Z., and Wu, J. X. (2015). Effects of temperature on survival rate and protection enzymes of *Empoasca onukii* Matsuda. *J. Plant Prot.* 42, 223–228. (in Chinese). doi:10.13802/j.cnki.zwbhxb.2015.02.012

Roma, D., Malgorzata, J., Beata, C., Jan, D., Katarzyna, W., and Beata, B. S. (2021). Mild abiotic stress affects development and stimulates hormesis of hemp aphid *Phorodon cannabis*. *Phorodon cannabis. Insects* 12, 420. doi:10.3390/INSECTS12050420

Santana, P. A., Kumar, L., Silva, R. S., and Picanço, M. C. (2019). Global geographic distribution of *Tuta absoluta* as affected by climate change. *J. Pest Sci.* 92, 1373–1385. doi:10.1007/s10340–018–1057-y

Schweizer, M., Miksch, L., Köhler, H. R., and Triebskorn, R. (2019). Does Bti (*Bacillus thuringiensis* var. *israelensis*) affect *Rana temporaria* tadpoles? *Ecotoxicol. Environ. Saf.* 181, 121–129. doi:10.1016/j.ecoenv.2019.05.080

Shamshir, R. A., and Wee, S. L. (2019). Zingerone improves mating performance of *Zeugodacus tau* (Diptera: Tephritidae) through enhancement of male courtship activity and sexual signaling. *J. Insect Physiol.* 119, 103949. doi:10.1016/j.jinsphys.2019.103949

Shankarganesh, K., Rameash, K., Selvi, C., and Bagyaraj, S. (2022). Antioxidant enzymes in cotton mealy bug *Phenacoccus Solenopsis* Tinsley exeposed to high temperature. *J. Entomol.* 84, 101–104. doi:10.55446/IJE.2021.330

Shelly, T. E. (2001). Lek size and female visitation in two species of Tephritid fruit flies. *Anim. Behav.* 62, 33–40. doi:10.1006/anbe.2000.1723

Singh, K., Kochar, E., Gahlot, P., Bhatt, K., and Prasad, N. G. (2021). Evolution of reproductive traits have no apparent life-history associated cost in populations of *Drosophila melanogaster* selected for cold shock resistance. *Bmc. Ecol. Evol.* 21, 219. doi:10.1186/S12862–021–01934–2

Singh, K., Kochar, E., and Prasad, N. G. (2015). Egg viability, mating frequency and male mating ability evolve in populations of *Drosophila melanogaster* selected for resistance to cold shock. *PloS one* 10, e0129992. doi:10.1371/journal.pone.0129992

Singh, K., and Prasad, N. G. (2016). Evolution of pre- and post-copulatory traits in female *Drosophila melanogaster* as a correlated response to selection for resistance to cold stress. *J. Insect Physiol.* 91–92, 26–33. doi:10.1016/j.jinsphys.2016.06.005

Singh, K., Samant, M. A., and Prasad, N. G. (2022). Evolution of cross-tolerance in *Drosophila melanogaster* as a result of increased resistance to cold stress. *Sci. Rep.* 12, 19536. doi:10.1038/S41598–022–23674-Z

Singh, K., Samant, M. A., Tom, M. T., and Prasad, N. G. (2017). Evolution of pre- and post-copulatory traits in male *Drosophila melanogaster* as a correlated response to selection for resistance to cold stress. *PloS one* 11, e0153629. doi:10.1371/journal.pone.0153629

Siva-Jothy, M. T., Tsubaki, Y., and Hooper, R. E. (1998). Decreased immune response as a proximate cost of copulation and oviposition in a damselfly. *Physiol. Entomol.* 23, 274–277. doi:10.1046/j.1365–3032.1998.233090.x

Stazione, L., Norry, F. M., and Sambucetti, P. (2019). Heat-hardening effects on mating success at high temperature in *Drosophila melanogaster*. *J. Therm. Biol.* 80, 172–177. doi:10.1016/j.jtherbio.2019.02.001

Stazione, L., Norry, F. N., and Sambucetti, P. (2021). Do longevity and fecundity change by selection on mating success at elevated temperature? Correlated selection responses in *Drosophila buzzatii*. *Evol. Biol.* 48, 312–320. doi:10.1007/S11692–021–09540–2

Takeda, M. (2022). Effect of changing temperatures from the spawning and egg stages to the emerging adult stage on the induction of reproductive diapause in females of *Pseudaulacaspis pentagona* (Hemiptera: Diaspididae). *Appl. Entomol. Zool.* 57, 15–25. doi:10.1007/S13355–021–00757–3

Tang, W. C., Xiao, Y. Y., Yang, C. F., Guo, D. D., and Zhu, Y. (2016). Reproductive damage and oxidative stress caused by fluoride in the silkworm. *Bombyx Mori. Acta Entomol. Sin.* 59, 1308–1316. (in Chinses). doi:10.16380/j.kcxb.2016.12.003

Tao, W., Anthony, K. M., and Katja, H. (2018). The effects of temperature on the development, fecundity and mortality of *Eretmocerus warrae*: Is *Eretmocerus warrae* better adapted to high temperatures than *Encarsia formosa*? *Pest Manag. Sci.* 75, 702–707. doi:10.1002/ps.5169

Tom, T., and Nina, W. (1998). Benefits of multiple mates in the cricket *Gryllus bimaculatus*. *Evolution* 52, 1726–1730. doi:10.1111/j.1558–5646.1998.tb02252.x

Wang, C. Q., Han, Y. J., Cao, J. G., Zhang, J., and Shang, S. Q. (2021). The response of physiological of *Tetrarcychus urticae* to heat stress. *J. Environ. Entomol.* 43, 181–190. (in Chinese). doi:10.3969/j.issn.1674–0858.2021.01.18

Wang, D. S., Lü, L. H., and He, Y. R. (2018). Effects of insecticides on sex pheromone communication and mating behavior in *Trichogramma chilonis*. *J. Pest Sci.* 91, 65–78. doi:10.1007/s10340-017-0864-x

Wang, L. L., Feng, Z. J., Li, T., Lu, X. P., Zhao, J. J., Niu, J. Z., et al. (2016). Inheritance, realized heritability, and biochemical mechanisms of malathion resistance in *Bactrocera dorsalis* (Diptera: Tephritidae). *J. Econ. Entomol.* 109, 299–306. doi:10.1093/jee/tov276

Xiang, Y. Y., Liu, T. X., and Zhang, S. Z. (2018). Effects of temperature, humidity, photoperiod and host plants on the calling and mating behavior of female moths of black cutworm *Agrotis ipsilon* (Hüfnagel). *J. Plant Prot.* 45, 235–242. (in Chinese). doi:10.13802/j.cnki.zwbhxb.2018.2016150

Xuereb, B., Lefèvre, E., Garric, J., and Geffard, O. (2009). Acetylcholinesterase activity in *Gammarus fossarum* (Crustacea Amphipoda): Linking AChE inhibition and behavioural alteration. *Aquat. Toxicol.* 94, 114–122. doi:10.1016/j.aquatox.2009.06.010

Yang, H., Zhang, K. S., Yang, W., and Yang, C. P. (2015). Laboratory and field studies on the reproductive ecology of *Parocneria orienta* (Lepidoptera: Lymantriidae) in China. *Entomol. Res.* 45, 77–83. doi:10.1111/1748–5967.12096

Yang, S. W., Li, M. J., Shang, H. P., Liu, Y. H., Li, X. X., Jiang, Z. X., et al. (2021). Effect of sublethal spirotetramat on host locating and parasitic behavior of *Encarsia formosa* Gahan. *Pest Manag. Sci.* 78, 329–335. doi:10.1002/PS.6638

Yuan, J. W., Zheng, Y., Chang, Y. W., Bai, J., Qin, J., and Du, Y. Z. (2021). Differential regulation of antioxidant enzymes in *Frankliniella occidentalis* (Thysanoptera: Thripidae) exposed to thermal stress. *PeerJ* 9, e12089. doi:10.7717/PEERJ.12089

Zaelor, J., and Kitthawee, S. (2018). *CNKI:SUN:DWFL.0.2018–01–003*, 43, 27–36.Geometric morphometric and molecular evidence suggest a new fruit fly species in *Bactrocera(Zeugodacus) tau* complex (Diptera: Tephritidae)*Zool. Syst.*

Zeng, B., Zhu, W. J., Fu, Y. G., and Zhou, S. H. (2018). Influence of high-temperature exposure on the mating, oviposition and thermotaxis of *Bactrocera cucurbitae* (Coquillet) (Diptera:Tephritidae). *PloS one* 13, e0204065. doi:10.1371/journal.pone.0204065

Zhang, X. M., Li, R., Hu, C. X., Chen, G. H., Xu, H. Y., Chen, Z. X., et al. (2020). Population numbers and physiological response of an invasive and native thrip species following repeated exposure to imidacloprid. *Front. Physiol.* 11, 216. doi:10.3389/fphys.2020.00216

Zheng, S. N., and Wei, W. (2019). Assessment of the economic losses caused by four important species of fruit fly pests in Fujian Province. *Chin. J. Biol. Control.* 35, 209–216. (in Chinese). doi:10.16409/j.cnki.2095–039x.2019.02.019

Zhou, S. H., Li, L., Zeng, B., and Fu, Y. G. (2020). Effects of short-term high-temperature conditions on oviposition and differential gene expression of *Bactrocera cucurbitae* (Coquillett) (Diptera: Tephritidae). *Int. J. Pest Manag.* 66, 332–340. doi:10.1080/09670874.2019.1647370

Zhou, Z. S., Guo, J. Y., Min, L., and Wan, F. H. (2011). Effect of short-term high temperature stress on the development and fecundity of *Ophraella communa* (Coleoptera: Chrysomelidae). *Biocontrol Sci. Technol.* 21, 809–819. doi:10.1080/09583157.2011.584611

Frontiers in Physiology

Understanding how an organism's components work together to maintain a healthy state

The second most-cited physiology journal, promoting a multidisciplinary approach to the physiology of living systems - from the subcellular and molecular domains to the intact organism and its interaction with the environment.

Discover the latest Research Topics

See more →

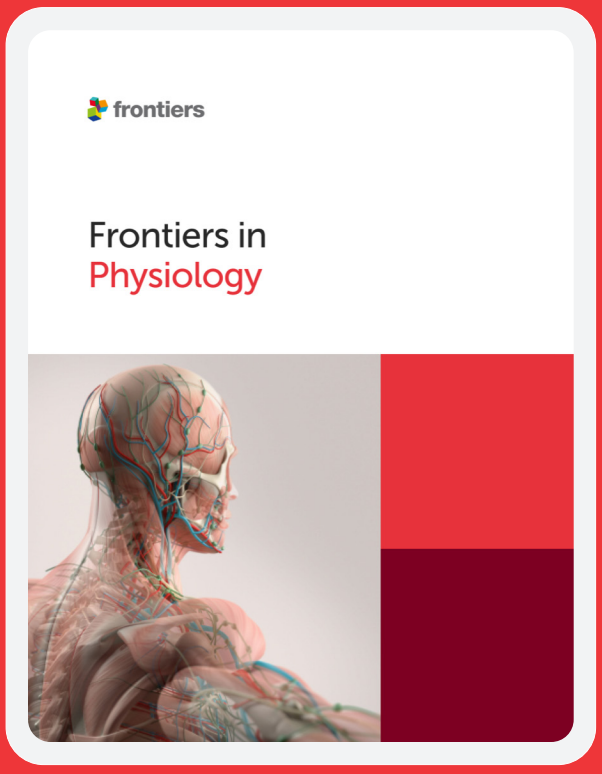

Frontiers

Avenue du Tribunal-Fédéral 34
1005 Lausanne, Switzerland
frontiersin.org

Contact us

+41 (0)21 510 17 00
frontiersin.org/about/contact